Investigating GLUT4 Trafficking in Muscle

Fazakerley, Daniel

Award date:
2010

Awarding institution:
University of Bath

Investigating GLUT4 Trafficking in Muscle

Daniel John Fazakerley

A thesis submitted for the degree of Doctor of Philosophy

University of Bath

Department of Biology and Biochemistry

January 2010

Abstract

GLUT4 trafficking in muscle cells has been studied to determine how distinct signalling pathways induce GLUT4 translocation. Two different cell models were adopted for these investigations; cardiomyocytes isolated from a transgenic mouse line expressing HA-GLUT4-GFP in muscle and L6 myotubes retrovirally expressing HA-GLUT4.

The GLUT4 constructs were largely excluded from the external membrane under basal conditions in both cell models. GLUT4 was trafficked to the external membrane in to response all stimuli studied in cardiomyocytes (insulin, contraction and hypoxia) and L6 myotubes (insulin, AICAR and A-769662). By comparing the anti-HA and GFP signals at the sarcolemma and transverse tubules in cardiomyocytes, it has also be possible to observe an enhancement of GSV fusion with the sarcolemma following stimulation with insulin and contraction. This effect was specific to these stimuli and to the sarcolemma.

Insulin-stimulation of GLUT4 exocytosis was not detected under steady-state conditions in L6 myotubes. Here, the major effect of insulin-stimulation and AMPK-activation was on GLUT4 internalisation. The rate constant for GLUT4 internalisation was very rapid in basal cells and was decreased during the steady-state responses to insulin and the AMPK-activators AICAR and A-769662. In cardiomyocytes, internalising GLUT4 colocalised with clathrin at puncta at the sarcolemma. This indicates that GLUT4 is internalised via a clathrin-mediated route.

Investigations into the amount of GLUT4 recycling in L6 cells under steady-state conditions revealed that a large proportion of cellular GLUT4 recycles with the cell surface under basal conditions. Insulin-stimulation and AMPK-activation additively mobilised GLUT4 in L6 cells. This implies a non-convergent mobilisation of GLUT4 in response to activation of the PKB/Akt and AMPK signalling pathways.

Data obtained from an *in vitro* kinase assay confirmed that serine 237 of TBC1D1 is a *bone fide* AMPK phosphorylation site. Furthermore, phosphorylation of this site in L6 myotubes incubated with AMPK activators has been confirmed using a novel antibody specific to TBC1D1 phosphorylated at serine 237.

This thesis discusses the consequences and importance of multiple controls impinging on GLUT4 traffic and highlights the advantages and limitations of kinetic studies of these processes.

Acknowledgements

I would like to thank Professor Geoff Holman for the opportunity to study for my PhD in his laboratory and for all the supervision and guidance he has given me over the last three years. His advice on all aspects of my experimental and written work has been greatly appreciated. I would also like to thank my co-supervisor Françoise Koumanov for always finding time for me to discuss my work and offer advice.

Anna Marley at AstraZeneca and Professor David James at the Garvan Institute have also acted in a supervisory capacity during my PhD. I am indebted to Anna Marley for her support, valued input and perspective on my project throughout my time at Bath. In particular, Anna commissioned the production of the TBC1D1 antibodies used in Chapter 5 of this thesis. I am very thankful to David James for the opportunity to advance my investigations into GLUT4 trafficking in L6 cells (Chapter 4) by spending time in his laboratory at the Garvan Institute in Sydney and for his enthusiastic guidance and discussion over my time there and throughout our subsequent correspondence.

I have been fortunate to have worked closely with a number of scientists from different institutions over the last 3 years. Each of these collaborations has been invaluable for the development and completion of the studies presented in this thesis. The data for Chapter 3 was obtained from transgenic mice kindly provided by Sam Cushman at the NIH in Bethesda. In addition to Sam's valued input, I am also thankful to Vlad Lizunov who kindly helped me with the analysis of the fluorescent images. I would also like to extend my gratitude to Scott Lawrence for his patience in teaching me the procedure to isolate primary cardiomyocytes used in this study. I must thank Jacky Stöckli and Cordula Hohnen-Behrens in David James' group for their help with the setting up of GLUT4 trafficking assay in L6 cells and offer special thanks to Adelle Coster for her expertise and patience in working with me on the mathematical analysis of the trafficking data. In addition, Jo Peel at AstraZeneca kindly helped me to obtain the confocal and wide-field epifluorescent images of L6 myotubes presented in this thesis. I must also extend my gratitude to the BBSRC and to AstraZeneca for funding me throughout my PhD.

Finally, I would also like to thank all the members of the Holman and James laboratories for their input to my PhD and for making the last three years such a rich and enjoyable experience, namely Françoise Koumanov, Scott Lawrence, Judith Richardson, Paul Whitley, Joe

Dukes III, Ying Feng, Lucy Roche, Remy Martin, Jennifer Tyler, Jacky Stöckli, Adelle Coster, Kyle Hoehn and Georg Ramm.

Abbreviations

α-MEM	α - Minimum essential medium
ACC	Acetyl-CoA carboxylase
AEBSF	[4-(2-Aminoethyl)benzenesulfonylflouride, HCl]
AICAR	5-Aminoimidazole-4-carboxyamide-1-β-D-ribofuranoside
Akti	PKB/Akt inhibitor
AMP	Adenosine 5'-monophosphate
AMPK	AMP-activated protein kinase
AP-1	Adaptor protein 1
AP-2	Adaptor protein 2
APS	Adaptor protein with a PH and Src homology 2 domains
APS	Ammonium persulphate
AS160	(PKB)/Akt substrate of 160 kDa
ATP	Adenosine 5'-triphosphate
BAPTA-AM	1,2-Bis(2-aminophenoxy)ethane-N,N,N′,N′-tetraacetic acid tetrakis (acetoxymethyl ester)
BSA	Bovine serum albumin
CaM	Calmodulin
CAMK	Ca^{2+}/calmodulin-dependent protein kinase
CAMKK	Ca^{2+}/calmodulin-dependent protein kinase kinase
CAP	c-Cbl-associated protein

CBD	Calmodulin binding domain
cDNA	Complementary DNA
CHX	Cycloheximide
Ci	Curies
CIP	Cdc42-interacting protein
CREB	Cyclic AMP response element binding
C-terminus	Carboxy-terminus
Da	Daltons
DAG	Diacylglycerol
ddH_2O	Double distilled water
DMEM	Dulbecco's modified eagles medium
DMSO	Dimethyl sulfoxide
DNP	2,4-Dinitrophenol
DTT	Dithiothreitol
E. coli	Escherichia coli
ECL	Enhanced chemiluminescence
EDL	Extensor digitorum longus
EDTA	Diaminoethanetetra-acetic acid disodium salt
EEA1	Early endosome antigen 1
EGF	Epidermal growth factor
EHD	Eps-15 homology domain

EV	Empty vector
FATP	Fatty-acid transport protein
FCS	Foetal calf serum
FOXO	Forkhead box O
g	Gram
GAP	GTPase activating protein
GDP	Guanosine diphosphate
GEF	Guanosine nucleotide exchange factor
GFP	Green fluorescent protein
GGA	Golgi localised γ-adaptin ear homology domain, Arf binding proteins
GLUT	Glucose transporter
GLUT4	Glucose transporter 4
GlpT	Glycerol-3-phosphate transporter
GSK3	Glycogen synthase kinase 3
GSV	GLUT4 storage vesicle
GTP	Guanosine triphosphate
h	Hour
HA	Haemagglutinin
HEPES	(N-[2-Hydroxyethyl]piperazine-N'-[2-ethenesulfonic acid])
HMIT	H^+-coupled myo-inositol transporter
HRP	Horseradish peroxidise

IgG	Immunoglobulin G
IL2-R	Interleukin 2 receptor
IR	Insulin receptor
IRAP	Insulin-responsive aminopeptidase
IRS	Insulin receptor substrate
IPTG	Isopropyl β-D-1-thiogalactopyranoside
JNK	c-Jun N-terminal kinase
kDa	KiloDaltons
k_{ex}	Rate constant for exocytosis
k_{in}	Rate constant for internalisation
KRH	Krebs-Ringer-HEPES
LB	Luria broth
LRP	Lipoprotein receptor-related protein 1
MAPK	Mitogen-activated protein kinase
MARCKS	Myristoylated alanine-rich C-kinase substrate
Min	Minutes
MMP	Membrane metallo-protease
MPR	Mannose-6-phosphate receptor
mRNA	Messenger ribonucleic acid
mTOR	Mammalian target of rapamycin
mTORC2	mTOR-Rictor complex 2

Myo1c	Unconventional myosin 1C
NSF	N-ethylmaleimide sensitive factor
N-terminus	Amino-terminus
PALM	Photo-activated localisation microscopy
PAS	Phospho-(PKB)/Akt substrate
PBS	Phosphate buffered saline
PDK1	3'-Phosphoinositide-dependent kinase-1
PFA	Paraformaldehyde
PDGF	Platelet-derived growth factor
PI	Phosphatidylinositol
PI-3-K	Phosphatidylinositol 3-kinase
PH domain	Pleckstrin-homology domain
PKB	Protein kinase B
PKC	Protein kinase C
PKD	Protein kinase D
PM	Plasma membrane
PS	Phosphatidylserine
PTB domain	Phosphotyrosine binding domain
PTEN	Phosphatase and tensin homologue
PTP1B	Protein tyrosine phosphatase 1 B
ROIs	Regions of interest

RNAi	RNA interference
SA	Serine to alanine mutation
SDS	Sodium dodecyl sulphate
SDS-PAGE	Sodium dodecyl sulphate-polyacrylamide gel electrophoresis
Sec	Seconds
SH2	Src homology 2
SH3	Src homology 3
SHIP-2	SH2-containing 5'-inositol phosphatase
SHP-2	Src homology 2-containing tyrosine phosphatase
siRNA	Small interfering RNA
SGK1	Serum/Glucocorticoid regulated kinase 1
SNAP	Soluble NSF attachment proteins
SNARE	SNAP receptors
SNARK	Sucrose, non-fermenting 1/AMP-activated protein kinase-related kinase
STORM	Stochastic optical reconstruction microscopy
SOCS	Suppressor of cytokine signalling
SOS	Son-of-Sevenless
TA	Tibialis anterior
TBS	Tris-buffered saline
TBS-T	Tris-buffered saline containing Tween-20
TEMED	N,N,N,N’-tetramethylethylenediamine

TGN	Trans-Golgi network
TIRF	Total internal reflection fluorescence microscopy
Tris	Tris(hydroxymethyl)methylamine
TT	Transverse tubules
TUG	Tether, containing an UBX domain, for GLUT4
t-SNARE	SNARE proteins present on the target membrane
Tween-20	Polyoxyethylene sorbitan monolaureate
U	Units
VAMP	Vesicle-associated membrane protein
v-SNARE	SNARE proteins present on the vesicle membrane
WGA	Wheat-germ agglutinin
WM	Wortmannin
WT	Wild type

Contents

1 Introduction

The biological questions addressed in this thesis primarily concern glucose transporter trafficking in response to stimuli that enhance glucose transport in muscle cells. As will be discussed below, there is a close relationship between the subcellular localisation of glucose transporters and whole-body glucose disposal and utilisation. Indeed, a comprehensive knowledge of the molecular and cellular processes that control glucose uptake is vital for understanding how blood glucose levels are regulated in healthy individuals and for identifying potential drug targets for the treatment of disorders, such as diabetes, where this regulation is compromised.

1.1 Glucose homeostasis

Glucose is the fundamental energy source for all eukaryotic cells. In humans, glucose is delivered to cells throughout the body via the circulatory system. Once within the cell, glucose can be processed through glycolysis and the citric acid cycle to yield the energy-storage molecule adenosine-5'-triphosphate (ATP). The concentration of glucose in blood is strictly maintained at approximately 5 mM (Reaven et al., 1988). This tight control is necessary to avoid complications associated with large fluctuations in glucose levels (hyper- and hypoglycaemia). Glucose homeostasis is primarily achieved through the antagonistic actions of two pancreatic hormones, insulin and glucagon. These hormones orchestrate the balance between the uptake, catabolism, storage, production and release of glucose.

When the concentration of glucose in the blood rises above 5 mM, for example in the post-prandial state, insulin is secreted from pancreatic β-cells. Insulin reduces circulating glucose levels by promoting glucose uptake and storage in insulin-sensitive tissues such as the liver, fat and skeletal muscle. The major site of glucose disposal under these conditions is skeletal muscle, which accounts for up to 90% of glucose uptake (DeFronzo et al., 1981). This tissue both catabolises glucose to yield ATP and, in cases of excess glucose, converts monomeric glucose into a storage polymer, glycogen. Excess glucose in the liver is also converted to glycogen, whilst in adipose tissue it is stored as triglycerides. Enhanced glucose uptake in response to insulin is accompanied by a reduction in glucose production and release. This is achieved by the inhibition

of *de novo* synthesis of glucose (gluconeogensis) and glycogen catabolism (glycogenolysis) in the liver. Together, these actions force a reduction in circulating glucose levels.

If low glucose levels are detected, for example during starvation, pancreatic α-cells release glucagon. This hormone acts to stimulate glucose production and release from the liver in order to raise circulating glucose levels. Glucagon stimulates both glycogenolysis and gluconeogenesis.

1.2 Diabetes

Diabetes is a disease state defined by the failure to control blood glucose levels. There are two types of diabetes. Type 1 diabetes is characterised by a failure to produce insulin in response to elevated blood glucose levels. This defect is caused by an auto-immune destruction of pancreatic β-cells. This sub-type of the disease can be effectively treated by administration of exogenous insulin by injection.

Type 2 diabetes has a more complex causality. An early indication of type 2 diabetes is the onset of insulin-resistance. This is where previously insulin responsive cells no longer respond to insulin. Type 2 diabetics also exhibit impaired β-cell function and insulin secretion as a consequence of prolonged hyperglycaemia (Permutt et al., 1984). The most common treatment for sufferers of type 2 diabetes is strict dietary control, although drugs such as metformin are available (Stumvoll et al., 1995). Metformin is thought to act by increasing glucose disposal via an insulin-independent pathway. Type 2 diabetes is a growing world-wide health problem and it is reported that the number of cases of type 2 diabetes will reach 300 million by the year 2025 (Zimmet and Alberti, 2008). Although classically associated with older patients, a rapid and accelerated increase in obesity has been associated with an increase in cases of type 2 diabetes in younger patients.

Type 1 and type 2 diabetes both lead to additional health complications. These include eye, nerve and kidney disease. Furthermore, recent studies have revealed that reduced insulin-sensitivity is a risk factor for mortality in individuals with coronary heart failure (Doehner et al., 2008; Doehner et al., 2005). As a result, diabetes and associated secondary health complications exert considerable strain on healthcare services. Investigations into potential drug targets and treatments for type 2 diabetes represent an important area of research.

1.3 The glucose transporter family

The transport of glucose from the bloodstream into cells for utilisation or storage occurs through the GLUT family of ATP-independent facilitative transporters. GLUTs act as a shuttle to mediate the bidirectional delivery of polar hexose molecules across the plasma membrane lipid bilayer down a concentration gradient. This transport step is the rate-limiting step in glucose utilisation/storage and so is a major focus of diabetes research.

The 14 members of the GLUT family are divided into three subclasses. GLUTs 1-4 and 14 are class I GLUTs. The fructose transporters GLUT5, 7, 9 and 11 belong to class II. Class III transporters (GLUTs 6, 8, 10, 12 and HMIT) are defined by an atypical structure, as described below. All GLUTs are unique in terms of their tissue expression, kinetics and/or substrate specificities (the properties of some of the major GLUTs have been reviewed in (Gould and Holman, 1993)). Each GLUT is adapted for its specific role by optimising these variables along with their localisation and trafficking itineraries.

Figure 1.1 depicts the predicted structure of class 1 GLUTs, although the overall structure is thought to be conserved throughout the family. GLUTs are predicted to have twelve transmembrane helices with cytosolic N- and C-termini (Joost and Thorens, 2001; Mueckler et al., 1985). In addition, they contain a highly hydrophilic domain between helices 6 and 7. The classical GLUTs (class I) have two large loop regions. The first of these is extracellular, and sits between the first and second transmembrane domains. This loop contains a glycosylation site. There is a second larger loop between transmembrane domains 6 and 7. Signal sequences within this intracellular loop, as well as within the cytosolic N- and C- terminal regions, are thought to mediate the specific intracellular trafficking itineraries for each GLUT. Although all GLUTs have a similar structure, Class III GLUTs have a smaller extracellular loop between the transmembrane helices 1 and 2 so that there is no glycosylation in this region. Rather class 3 GLUTs have a glycosylation site within a large extracellular loop between transmembrane domains 9 and 10 (Joost and Thorens, 2001; Scheepers et al., 2004).

The structure of glucose transporters is yet to be confirmed by crystallisation. The structure of lactose permease (Abramson et al., 2003) and the glycerol-3-phosphate transporter (GlpT) from *Escherichia coli* (*E. coli*) have been solved (Lemieux et al., 2003). These proteins are structurally-related to GLUTs and therefore this data has been quoted as confirmation of the

predicted GLUT structure. Attempts to crystallise members of the GLUT family are ongoing. In addition to providing information on GLUT structure, these studies may provide an insight into the mechanism by which these transporters shuttle glucose across the plasma membrane.

The adaptation of GLUTs to their precise role can be illustrated by focusing on GLUTs 1, 2 and 4. GLUT1 was the first GLUT to be characterised and as such is best-studied member of this family. It was isolated from human erythrocyte membranes and subsequently characterised and cloned (Mueckler et al., 1985). mRNA-probes and antibodies generated following these initial characterisation studies have revealed the almost ubiquitous expression of GLUT1 (Flier et al., 1987), including expression in insulin-responsive tissues, and its localisation to the cell surface and endosomal compartments (Calderhead and Lienhard, 1988). The expression of GLUT1 has been reported to be increased under conditions of glucose starvation and during cell culture transformation (Merrall et al., 1993a; Merrall et al., 1993b). The k_m for glucose influx through GLUT1 is reported to be lower than the k_m for glucose efflux (Gould et al., 1991). Therefore, GLUT1 preferentially binds to and transports glucose into the cell and the expression of this transporter could convey an advantage under conditions where the intracellular glucose concentration is low and almost unidirectional transport is required (Gould and Holman, 1993).

The kinetics of glucose transport into liver tissue is very different from that of erythrocytes (Axelrod and Pilch, 1983) and despite the wide-ranging expression of GLUT1, it is not present in liver tissue. Therefore, glucose uptake into liver is not mediated by GLUT1. GLUT2 is highly expressed in liver tissue, pancreatic β-cells, the small intestine and on the basolateral surface of the kidney (Thorens et al., 1988; Thorens et al., 1990; Orci et al., 1989; Fukumoto et al., 1988). In these tissues, GLUT2 primarily localises to the plasma membrane (Thorens et al., 1993). The high K_m value for this transporter allows for rapid glucose efflux into the bloodstream during periods of gluconeogenesis. In addition, GLUT2 has a high transport capacity compared to other GLUTs (Colville et al., 1993) meaning that this transporter is less susceptible to saturation in cases of high glucose concentrations (Gould et al., 1991). This is particularly advantageous for transepithelial glucose uptake in the kidney and the small intestine. These features of GLUT2 kinetics demonstrate the adaptations of GLUTs depending on their specific physiological role.

In addition to kinetic considerations, GLUT localisation can also regulate glucose transport activity. Tissues with a high glucose requirement such as the brain, which is responsible for up to 80% of whole-body glucose consumption in resting conditions, express GLUTs such as

GLUT1, 2 and 3 which are constitutively localised to the cell surface. The most specialised GLUT in terms of subcellular localisation is GLUT4. The subcellular trafficking of this glucose transporter can be modified to increase (or decrease) glucose uptake. GLUT4 is highly expressed in the insulin-responsive tissues muscle and fat. GLUT4 has also been reported to be expressed in some regions of the brain such as the hypothalamus (Leloup et al., 1996), where GLUT4 is thought to play a role in glucose sensing and metabolic regulation. In muscle fibres and adipose cells, GLUT4 translocates from an intracellular location to the cell surface in response to insulin. In this way, GLUT4 is the primary mediator of insulin-stimulated glucose uptake.

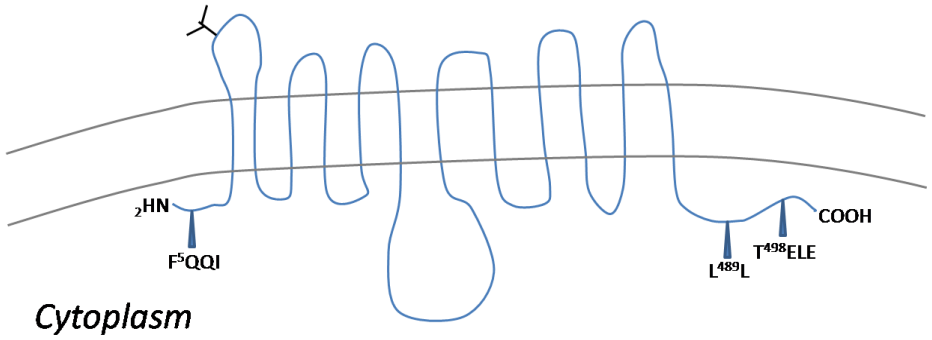

Figure 1.1. Predicted structure of Class I GLUTs. GLUTs are predicted to contain twelve membrane spanning domains. Class I GLUTs are glycosylated in the primary exofacial loop and contain a large cytosolic loop between transmembrane domain six and seven. The trafficking motifs depicted are those present in GLUT4. Adapted from (Joost and Thorens, 2001).

1.3.1 The insulin responsive glucose transporter

The isolation of insulin and identification of its ability to enhance glucose transport into adipose and muscle was reported in the mid-twentieth century (Park and Johnson, 1955) . However, the mechanism by which insulin enhances glucose uptake into responsive tissues was not deduced until 1980. In this year, two groups separately reported an increase in glucose transport activity at the plasma membrane of adipocytes in response to insulin (Suzuki and Kono, 1980; Cushman and Wardzala, 1980). Cushman's and Wardzela's experiments took advantage of radiolabelled

cytochalasin B, which binds to and inhibits glucose transporters. By studying cytochalasin B binding to subcellular fractions from primary adipocytes it was found that glucose transporters move from a low density microsome fraction (small vesicles) to the plasma membrane upon insulin stimulation. More detailed analysis of the kinetics of cytochalasin B binding revealed that more than one glucose transporter was responsible for glucose uptake into adipocytes. As described above, later studies identified GLUT1 expression in adipocytes; however this transporter could not be responsible for the full insulin-stimulated increase in glucose uptake (Joost et al., 1988). Therefore, an unidentified insulin-responsive glucose transporter was present in primary adipocytes.

This unidentified glucose insulin-responsive transporter was GLUT4. This glucose transporter was first described and cloned by James *et al.* in 1989 (James et al., 1989). This finding was supported by data from a number of laboratories at this time (Charron et al., 1989; Birnbaum, 1989; Kaestner et al., 1989). Other GLUTs expressed in insulin-responsive tissues include GLUT8, GLUT12 and HMIT in adipocytes and GLUT5 and GLUT12 in skeletal muscle. However, only GLUT4 has the special trafficking characteristics required to be designated the insulin-responsive glucose transporter. This has recently been challenged by reports that GLUT12 also translocates to the cell surface in muscle tissue in response to insulin-stimulation (Stuart et al., 2009).

GLUT4 has a high sequence identity to GLUT1 (65%). The major differences in amino acid sequence between GLUT4 and GLUT1 occur at the N- and C-termini and in the large cytosolic loop between transmembrane domains 6 and 7 (Kaestner et al., 1989). These regions only have a 40% sequence similarity and therefore may confer the differences in intracellular trafficking itineraries between these GLUTs. This is contrary to the putative membrane spanning regions which have a reported 73% homology (Birnbaum, 1989).

The glucose transport activity of a cell is determined by both the kinetics of individual transporters and by the concentration of GLUTs in the plasma membrane. The amount of GLUT4 expressed within the cell is not changed by acute exposure to insulin. As such, there are two possible explanations for the increase in the number of active transporters at the cell surface. Firstly, insulin-stimulation could convert plasma membrane localised GLUT4 molecules from an inactive to active form. The second hypothesis, termed the ‘translocation hypothesis’, states that

insulin-induces the translocation of active glucose transporters from an intracellular location to the plasma membrane.

Since the identification of GLUT4, GLUT4 trafficking has been extensively studied by various methods. These include subcellular fractionation, electron and fluorescence-based microscopy techniques, bis-mannose photolabelling and the use of GLUT4 fusion proteins, for example HA-GLUT4-GFP. The findings from GLUT4 trafficking studies are discussed extensively below. These studies have provided data in support of the 'translocation hypothesis' in both adipocytes and muscle cells. Under basal conditions, a small proportion (5 – 10%) of GLUT4 is at the cell surface. The amount of GLUT4 at this location is increased to ~50% of cellular GLUT4 in insulin-stimulated cells (Holman et al., 1990).

The translocation mechanism by which GLUT4 enhances glucose uptake allows for a large, rapid and reversible increase in glucose uptake. These changes in glucose uptake enable enhanced glucose storage and prevent large fluctuations in blood glucose levels when necessary, for example in the post-prandial state. In addition, GLUT4 is trafficked to the cell surface of muscle cells in response to contraction (discussed below). Under these conditions, a quick increase in glucose transport is important to meet the large increase in the metabolic demands of muscle during exercise.

The importance of GLUT4 expression in peripheral tissues in whole body glucose homeostasis has been revealed by studies on transgenic mouse lines. Heterozygous GLUT4 (+/-) knockout mice, where GLUT4 levels are severely reduced in adipose and muscle tissues, exhibit insulin resistance as would be expected (Li et al., 2000; Stenbit et al., 1997; Rossetti et al., 1997). Equally, tissue-specific deletion of GLUT4 in muscle or adipose tissue results in an insulin-resistant phenotype (Abel et al., 2001; Kim et al., 2001). Correspondingly, transgenic mice which express high levels of GLUT4 in muscle or adipocytes are very insulin sensitive and glucose tolerant (Shepherd et al., 1993; Tsao et al., 1996; Tsao et al., 2001).

1.3.1.1 Intracellular localisation of GLUT4

Given that insulin-stimulation increases glucose uptake by modifying the subcellular localisation of GLUT4, the intracellular localisation of GLUT4 under basal conditions is of interest. This

information is the first step in identifying how GLUT4 is excluded from the plasma membrane under basal conditions and may shed light on the mechanism by which insulin-stimulation enhances cell surface levels.

Newly synthesised and glycosylated GLUT4 enters a recycling pathway which concentrates the majority of GLUT4 at intracellular locations. It has been reported that GLUT4 localises to several subcellular sites including the plasma membrane, early/sorting endosomes, recycling endosomes, the trans-Golgi network (TGN) and peripheral vesicles, but not to lysosomes, late endosomes or mutivesicular bodies. These locations form the complex intracellular trafficking itinerary of GLUT4 which is depicted in Figure 1.2. Early investigations into GLUT4 localisation were conducted using electron microscopy. This analysis was performed in a wide range of insulin-responsive tissues including white and brown adipose, skeletal muscle and cardiac muscle (Ploug et al., 1998; Slot et al., 1991b; Friedman et al., 1991; Smith et al., 1991; Malide et al., 2000; Robinson et al., 1992; Ralston and Ploug, 1996; Rodnick et al., 1992b). This technique identified that GLUT4 localised to tubulo-vesicular structures including dispersed small vesicles in the periphery in basal cells. In addition, GLUT4 was observed in clathrin-coated pits at the cell surface. Small amounts of GLUT4 was localised to the cell surface (plasma membrane in adipocytes or sarcolemma and transverse tubules in muscle) under basal conditions, but GLUT4 was enriched in this domain after insulin stimulation. This corresponded with a 40 – 50% decrease in GLUT4 within tubulo-vesicular structures. The fold increase in plasma membrane GLUT4 levels strongly correlates with data from GLUT4 translocation studies described by Holman *et al.* (Holman et al., 1990) and further supports the translocation hypothesis.

The transferrin receptor (TfR) is an extensively characterised recycling protein with a well defined subcellular trafficking routine between the cell surface and the endosomal compartment. Therefore, TfR can provide a useful comparative tool for investigating the endosomal recycling and localisation of GLUT4. Insulin-stimulation results in increased GLUT4 not only at the plasma membrane but also in endosomes (Ploug et al., 1998; Slot et al., 1991b). This provides evidence that GLUT4 recycles from the plasma membrane through the continuously recycling endosomal system.

In addition to these microscopy-based techniques, GLUT4 localisation to the endosomal compartment has been studied using a TfR-HRP construct which can be used to chemically ablate the endosomal compartment (Livingstone et al., 1996; Martin et al., 1996; Karylowski et al.,

2004). This technique does not completely inhibit insulin-stimulated GLUT4 translocation, but has revealed that as much as 40 – 50% of GLUT4 resides in the endosomal compartment in 3T3-L1 adipocytes. In a recent review, Larance *et al.* point out that since this ablation technique is enzyme based, any mis-trafficking of TfR-HRP (even one molecule) to a non-endosomal compartment will result in ablation of this compartment (Larance et al., 2008). This would result in an overestimation of the amount of GLUT4 in the endosomal compartment. In addition, this assay was performed in rapidly differentiated and replated 3T3-L1 adipocytes, which have distinct protein trafficking characteristics from fully differentiated 3T3-L1 (Muretta et al., 2008). Therefore, the data obtained from this cell model may be misleading when investigating GLUT4 localisation and trafficking. Indeed, defining the exact nature of GLUT4 trafficking through endosomal compartments is difficult because this compartment is made up of many subcompartments. Furthermore, assessing the importance of endosomal GLUT4 trafficking is challenging since the amount of GLUT4 present in the endosomal pool varies between cell systems (~10% in primary adipocytes (Slot et al., 1991b; Malide et al., 1997) compared to 50% in 3T3-L1 adipocytes (Karylowski et al., 2004)). Despite these difficulties, by comparing the trafficking of TfR and GLUT4 it is possible to distinguish between insulin's effect on the general recycling pathway and the specialised GLUT4 compartment. Insulin-stimulation has a modest effect on endosomal recycling. In this way insulin-induces a small (2-fold) increase in cell surface TfR and GLUT1 (Tanner and Lienhard, 1987; Holman et al., 1990). This is a significantly lower enhancement of cell surface levels than occurs for GLUT4, implying that the endosomal compartment is not the primary insulin-responsive compartment.

Investigations into GLUT4 localisation using the chemical ablation method and electron microscopy have revealed that the majority of GLUT4 is trafficked to a subcellular location where it can be sequestered from TfR. Additionally, the rate of GLUT4 exocytosis in non-stimulated adipocytes is 10-times slower than the TfR (Tanner and Lienhard, 1987; Holman et al., 1994). It is therefore proposed that in unstimulated cells, GLUT4 primarily resides in specialised GLUT4-storage vesicles (GSV). The sequestration of GLUT4 into an insulin-responsive GSV compartment is an important process in insulin-responsive cells. This compartment permits the rapid increase in glucose uptake required in fat and muscle tissue in response to insulin and in muscle tissue in response to exercise. The trafficking route for GLUT4 entry into the GSV compartment and the constituent proteins of GSVs has been studied and the findings are discussed below.

1.3.1.2 The GLUT4 storage compartment

As GLUT4 is localised to several distinct locations throughout the cell a large research effort has aimed to define the properties of the GSV compartment. It is thought that this compartment corresponds to the small peripheral vesicular compartment identified in the original electron microscopy experiments. These vesicles are proposed to have trafficking characteristics that promote the sequestration of GLUT4 in this compartment. For example, the vesicles may be static or recycle very slowly under basal conditions, or form part of a dynamic recycling loop that excludes GLUT4 from the plasma membrane (the model for GLUT4 retention is discussed in detail below (1.7)). The relationship between the tubular and vesicular compartments containing GLUT4 may be analogous to the compartments responsible for insulin storage and release in pancreatic β-cells. This hypothesis implies that a fraction of the GLUT4 storage compartment, the vesicular portion, is readily available for fusion with the cell surface upon insulin-stimulation. Following this initial release of GLUT4, there is a second, slower release phase during which more fusion-competent vesicles are released from the tubular GLUT4 storage compartment.

The enhanced insulin-responsiveness observed in 3T3-L1 cells as they undergo differentiation from fibroblasts into adipocytes correlates with increased sequestration of GLUT4 into the specialised GSV compartment. In fibroblasts, most GLUT4 colocalises with TfR in the endosomal compartment (Ross et al., 1998). This may explain the relatively small insulin-stimulated increase in plasma membrane GLUT4 in these cells compared to fully differentiated cells (Govers et al., 2004).

1.3.1.3 The formation of GSVs

GLUT4 trafficking into the GSV compartment is of interest as it may represent a site of insulin action. McGraw's laboratory has studied the trafficking of GLUT4 from the PM back into the GSV compartment via the endosomes using the Tf-HRP ablation technique. Using this method, the time-course for GLUT4 to escape ablation has been determined. Data from these studies have led to the conclusion that GLUT4 is sorted into GSVs from endosomes. However, these studies were limited as GLUT4 trafficking events after leaving the endosomes were not examined in detail. TGN38, a marker for the TGN, localises poorly with internalised GLUT4 (Karylowski et al., 2004; Martin et al., 1994). However, the organisation of TGN subdomains is complex. Therefore,

the limited colocalisation observed between TGN38 with internalised GLUT4 does not provide definitive evidence that GLUT4 does not traffic through the TGN into GSVs.

A proportion of GLUT4 is present in the TGN of fat and muscle cells (Slot et al., 1991b; Slot et al., 1991a; Malide et al., 2000). Furthermore, GLUT4 entry into GSVs from the TGN is not blocked by protein synthesis inhibitors (Slot et al., 1997). From these data, it is likely that recycling GLUT4 enters GSVs by trafficking from endosomes via the TGN. In addition, studies monitoring GLUT4 internalising from the cell surface have identified that GLUT4 traffics through endosomes to a peri-nuclear compartment. This compartment is distinct from recycling endosomes (Palacios et al., 2001), and is proposed by Shewan *et al.* to be a subdomain the TGN enriched in syntaxin 6 and 16 (Shewan et al., 2003). These data support a role for the TGN in the sorting of recycling GLUT4 into the GSV compartment. Therefore, the accumulation of GLUT4 in the GSV compartment can occur via an endocytic route (via endosomes and TGN) and more directly via the biosynthetic pathway from the TGN as depicted in figure 1.2.

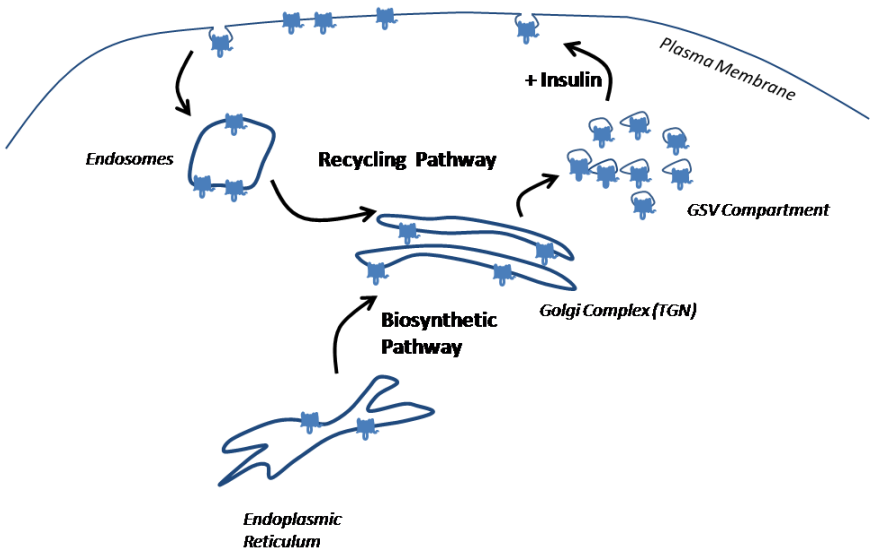

Figure 1.2. GLUT4 entry into the GSV compartment. GLUT4 is trafficked into the GSV compartment via two routes. Newly synthesised GLUT4 enters via the endoplasmic reticulum and Golgi complex (Biosynthetic Pathway). Recycling GLUT4 re-enters the GSV compartment from the endosomal compartment, via the trans-Golgi network (TGN) (Recycling Pathway).

The mechanism for sorting GLUT4 from other proteins into the GSVs is also of interest. Several proteins have been proposed to fulfil this role. GLUT4 localises to Adaptor protein-1 (AP-1) clathrin-coated vesicles trafficking from the TGN (Martin et al., 2000; Gillingham et al., 1999). The recruitment of GLUT4 to these vesicles may permit the sorting of GLUT4 from other proteins in the trafficking of GLUT4 from the TGN to the storage compartment. Investigations assessing the insulin-responsiveness of newly synthesised GLUT4-GFP have identified a role for Golgi localised γ-adaptin ear homology domain, Arf binding proteins (GGAs) in sorting GLUT4 (Watson et al., 2004). In support of a role for GGAs, these proteins have been reported to interact with cargo containing dileucine (LL) motifs. This motif is present in both GLUT4 and the GSV localised protein insulin-responsive aminopeptidase (IRAP) (Shiba et al., 2002). GGAs are known to play a role in clathrin coat assembly and in sorting other proteins such as the MPR. However, MPR is not present in GSVs, which implies a further sorting step downstream of GGAs in selecting proteins to traffic to GSVs. Sortillin binds to the lumenal domains of GSV proteins such as GLUT4 and IRAP and has been proposed to fulfil this additional sorting step (Shi and Kandror, 2007). However, sortillin cannot offer a full explanation as substitution of the lumenal domains of GLUT4 or IRAP with non-GSV protein lumenal domains does not perturb their trafficking to GSVs.

Eps15 Homology (EH) domain containing proteins have also been proposed to play a role in the formation of GSVs. These proteins are involved in membrane sorting and trafficking events in the cell, particularly the recycling of receptors to the plasma membrane via the recycling endosome (Naslavsky and Caplan, 2005). EHD2 resides on GLUT4 containing vesicles in primary adipocytes (Park et al., 2004). Expression of a dominant-negative construct of EHD1 (missing the EH domain) resulted in enlarged endosomes, dispersed perinuclear GLUT4-containing membranes, and inhibited insulin-stimulated GLUT4 translocation in 3T3-L1 adipocytes (Guilherme et al., 2004). EHD1 has been reported to interact with the Rab11 effector Rab11-FIP2 (Naslavsky et al., 2006). This is of interest since Rab11 is thought to be necessary for sorting GLUT4 from endosomes and into the GSV (Zeigerer et al., 2002).

Since GLUT4 and other GSV resident proteins are selectively sorted into GSVs, they must contain specific signals to mediate this trafficking. GLUT4 contains N- and C-terminal sorting motifs (Figure 1.1) (Bernhardt et al., 2009; Blot and McGraw, 2008; Shewan et al., 2000). These motifs (FQQI and LL) resemble adaptor protein (AP) binding motifs and therefore are thought to be important for GLUT4 internalisation through an interaction with AP-2 (discussed below). However, sorting motifs have been reported to be required for GLUT4 trafficking away from the

recycling endosomes and into the GSV compartment. For instance, the N-terminal FQQI motif is also recognised by the intracellular adaptor protein AP-1 (Al Hasani et al., 2002; Bernhardt et al., 2009). In addition to these classic trafficking motifs GLUT4 and IRAP contain a C-terminal TELEY motif, which has also been implicated in GLUT4 trafficking to the GSV compartment (Shewan et al., 2003; Blot and McGraw, 2008). The FQQI and TELEY motifs are involved in the sorting of GLUT4 out of recycling endosomes to the GSV compartment (Blot and McGraw, 2008). The exact role for each of these motifs and the predominant point at which they act in GLUT4 trafficking to the specialised compartment remains to be determined.

1.3.1.4 GSV-component and associated proteins

The protein content of the GSV compartment has been examined by the use of an immuno-adsorption method to isolate GLUT4 containing membrane compartments (Kandror and Pilch, 1996; Kupriyanova et al., 2002; Hashiramoto and James, 2000; Larance et al., 2005). This purification procedure can be used in conjunction with proteomic methods to identify the proteins present in the vesicle population.

Such studies have led to the identification of both proteins specific to GSVs and proteins within the GLUT4 trafficking itinerary. For example, these include endosomal proteins that partly colocalise with GLUT4 such as TfR and the MPR (Kandror and Pilch, 1998; Kandror, 1999). However, the majority of GLUT4 localises away from TfR in non-endosomal compartments when assessed by subfractionation protocols. As such, GSVs are biochemically distinct from endosomal (Hashiramoto and James, 2000) and TGN membranes. GSVs can be further segregated into insulin-responsive and non-insulin-responsive immuno-isolated GSVs, which have been characterised as cellugyrin-negative and cellugyrin-positive compartments, respectively (Kupriyanova and Kandror, 2000). Cellugyrin is a ubiquitously expressed homologue of synaptogyrin. The insulin-responsive GSV population is enriched with GLUT4, VAMP2 and IRAP (Kupriyanova and Kandror, 2000; Larance et al., 2005). These proteins exhibit very similar trafficking behaviours to GLUT4 and translocate to the plasma membrane to a similar extent as GLUT4. VAMP2 is the vesicle SNARE protein required for GLUT4 exocytosis (Cheatham et al., 1996). IRAP knock-out animals exhibit reduced GLUT4 expression (Keller et al., 2002), and IRAP knock-down by siRNA results in impaired GLUT4 translocation (Yeh et al., 2007). From these

data, it is thought that IRAP is required for the formation and retention of GSVs in fat and muscle cells (Yeh et al., 2007). Lipoprotein receptor-related protein 1 (LRP1) protein, another GSV-resident protein, has also been reported to be required for the stability for GSVs (Jedrychowski et al., 2009).

In addition to proteins resident within GSVs, these studies have also identified GSV associated proteins. These include proteins such as TUG (tether, contain a UBX domain, for GLUT4) (Bogan et al., 2003) and p115 (Hosaka et al., 2005), which are of interest since they may offer a means by which GSVs are retained at an intracellular location. Other proteins associated with GSVs include the Rab-GAPs TBC1D4/AS160 and TBC1D1. A putative role for these Rab-GAPs in GLUT4 trafficking will be addressed in more detail below. In addition, Rabs 2, 4, 8, 10, 11,12 and 14 have been identified on immuno-isolated GSVs (Larance et al., 2005; Kessler et al., 2000; Aledo et al., 1995).

Investigations into the roles of GSV-resident and -associated proteins are vital to reveal the mechanisms that mediate GSV retention and insulin-regulated translocation.

1.4 The insulin signalling pathway

The binding of insulin to its receptor at the cell surface of responsive cells activates a complex and extensive signalling cascade. Downstream effects of insulin signalling are varied and include metabolic, anabolic and transcriptional changes. The most relevant aspect of the insulin response to research into type 2 diabetes is the increase in glucose uptake from the circulation into target cells. As described above, enhanced glucose transport is achieved by an increase in the amount of glucose transporters at the cell surface. Insulin resistance is caused by the disruption of insulin signalling and/or glucose transporter trafficking. There has been extensive research to characterise the insulin signalling pathway leading to GLUT4 translocation. Indeed, investigations are continuing into the downstream targets of insulin signalling and are vital in order to identify novel drug targets to treat insulin-resistance and type 2 diabetes.

The initial steps of the classical insulin signalling pathway, which operates via phosphatidylinositol-3-kinase (PI-3-K), have been well characterised (Figure 1.3). There is currently much interest in identifying and characterising novel molecules involved in the latter

stages of this pathway, particularly those directly linking insulin-signalling to membrane trafficking events. A second, PI-3-K-independent pathway has been reported to be involved in insulin-mediated glucose transport. However, the evidence for the involvement of this pathway in insulin-mediated glucose uptake remains controversial.

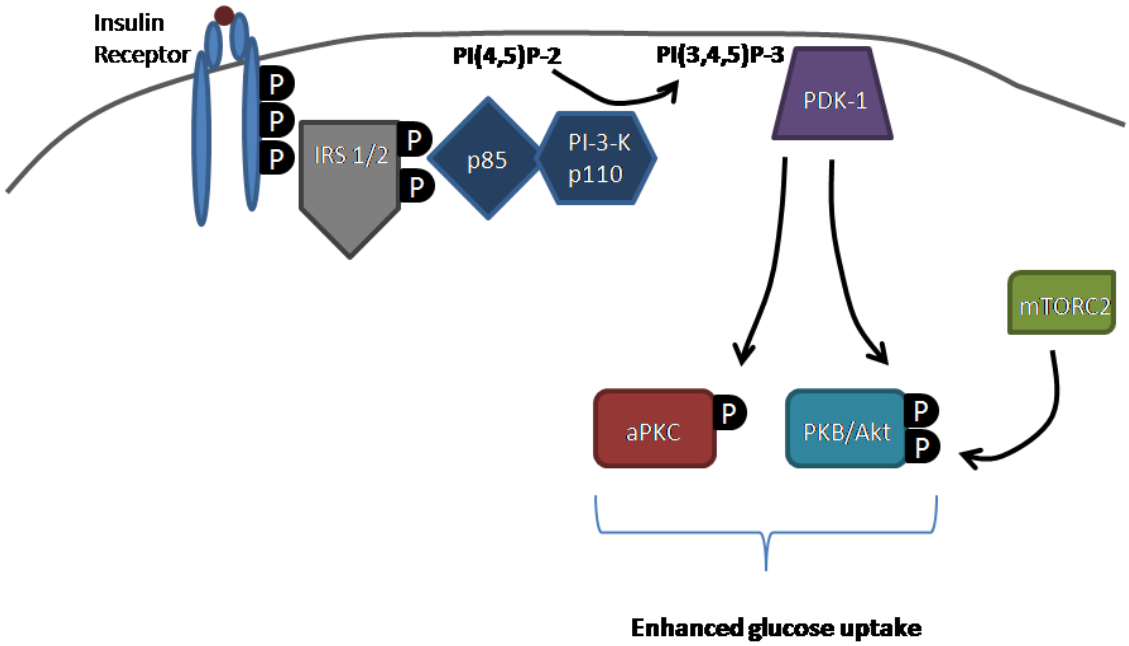

Figure 1.3 – The classical PI-3-K-dependent insulin signalling cascade. Activation of the insulin receptor results in the recruitment of PI-3-K to the plasma membrane through an interaction with phosphorylated IRS1/2. PI-3-K converts PI(4,5)P-2 to PI(3,4,5)P-3 at the inner leaflet of the plasma membrane. This lipid recruits PDK-1, PKB/Akt and PKC to the plasma membrane. PKB/Akt and PKC are activated by phosphorylation and mediate insulin's effects on cellular processes such as enhanced glucose uptake.

1.1.1. The insulin receptor

The insulin receptor (IR) is a member of the receptor tyrosine kinase family. The IR comprises two extracellular regulatory α-subunits and two transmembrane catalytic β-subunits, forming a

$\alpha_2\beta_2$-heterotetramer (Kasuga et al., 1982a). Each β-subunit is bound to its partner α-subunit via a disulphide bond. In the absence of insulin, the tyrosine kinase activity of the β-subunit is inhibited. Insulin binding to the α-subunit confers a conformational change that activates β-subunit catalytic activity. Subsequently, tyrosine kinase activity is further enhanced by the trans-phosphorylation of one of the β-subunits by the other at several specific tyrosine residues (Kasuga et al., 1982c; Kasuga et al., 1982b).

Activation of the β-subunit tyrosine kinase domains translates insulin binding into intracellular signalling events through the targeting of substrates to the IR and subsequent phosphorylation of these substrates. The most studied of these substrates are the insulin receptor substrates.

1.4.1 Insulin receptor substrates

The IR does not directly interact with downstream effector proteins. Rather, its activation results in the recruitment and tyrosine phosphorylation of scaffolds through which the IR indirectly recruits effector proteins (Lee and Pilch, 1994). These scaffolds are known as insulin receptor substrate (IRS) proteins, and the major IR substrates have been classified into the IRS protein family. Other IR substrates have been identified but not annotated as members of the IRS family. These include Shc adaptor proteins, signal regulatory protein (SIRP) family members, Grb-1 and adaptor protein with a pleckstrin homology (PH) and Src homology 2 (SH2) domains (APS).

Six proteins (IRS1-6) have been classified into the IRS family based on structural motif and domain similarity rather than by sequence homology. The domain similarities between members of this family include a lipid-binding PH domain and a phosphotyrosine binding (PTB) domain at the N-terminus. These domains are required for IRS targeting to the IR. The PTB domain interacts with a phosphorylated NPEY motif in the juxtamembrane region of the IR (He et al., 1995; Wolf et al., 1995). There is an additional interaction between IRS-2 and the IR via a central region between amino acids 591 and 786. The PH domain interacts with phosphoinositides at the cell surface (Voliovitch 1995, Yenush 1996). Furthermore, the C-terminal portion contains up to 20 IR kinase consensus motifs (YMXM or YXXM) (Shoelson et al., 1992). As such, IRS proteins can be tyrosine phosphorylated on several sites following recruitment to the IR (Paz et al., 1996; Sun et al., 1992). These sites are recognised by effector

proteins containing Src homology 2 (SH2) domains. IRS proteins also contain proline rich regions which may interact with SH3 or WW domain containing proteins. In addition to these interaction sites, IRS proteins can be phosphorylated on serine and threonine resides. Phosphorylation at these sites is thought to be involved in the desensitisation of the insulin-signalling pathway (discussed below) (Shepherd et al., 1998; White and Yenush, 1998).

IRS family members have been studied for their expression profile and for their role in insulin signalling leading to glucose transport. IRS-1 and -2 are more widely and highly expressed than the other members of the IRS family. IRS-3 expression is limited to brain and adipocytes and IRS-4 is only expressed in the pituitary and thyroid glands. Two new members of the IRS family were identified in 2003. IRS-5 is widely expressed although enriched in the liver and kidney, whilst IRS-6 is highly expressed in skeletal muscle (Cai et al., 2003).

IRS-1, -2, -5 (in liver) and -6 are the putative IRS proteins involved in insulin signalling leading to glucose uptake. Due to its expression profile, it is possible to rule out an involvement for IRS-4 in insulin signalling. Furthermore, a role for IRS-3 in this regard is unlikely since the knockout mouse exhibits no abnormalities in glucose homeostasis (Liu et al., 1999) and it is not expressed in humans (Bjornholm et al., 2002). Therefore the IRS-3 and IRS-4 isoforms, despite being implicated in negative regulation of insulin signalling, are unlikely to be involved in maintenance of glucose homeostasis.

IRS-1 and IRS-2 are the most studied IRS isoforms in the context of insulin-stimulated glucose uptake. These isoforms are highly homologous and seem to serve a complimentary rather than redundant role in signalling. Data from knockout mouse models and siRNA experiments support the conclusion that the predominant isoform of IRS involved in insulin signalling to glucose uptake is IRS-1 (Withers et al., 1998; Kaburagi et al., 1997; Tamemoto et al., 1998; Huang et al., 2005). Although IRS-1 and IRS-2 are the major isoforms involved in insulin-mediate glucose uptake, IRS-6 may also play an important role. Insulin-stimulated phosphorylation of IRS-6 is slow (compared to IRS-1 and IRS-2) and so might be involved in the maintenance of the insulin signal over prolonged stimulations. In addition to this, it has been reported that IRS-6 does not bind SH2-domain containing proteins. Therefore, IRS-6 may have distinct downstream interactors from IRS-1 and IRS-2 (Cai et al., 2003).

In addition to the activation of PKB/Akt, which is described below, insulin-stimulation also leads to MAPK activation. Grb-2 associates with IRS proteins via its SH-2 domain. Grb2 interacts with Son-of-Sevenless (SOS) to activate the Ras-MAP kinase signalling cascade (Virkamaki et al., 1999). This pathway is required to insulin's effects on cellular growth and differentiation, but is not involved in insulin-mediated glucose uptake.

1.4.2 Negative regulation of IR and IRS

The mechanisms by which the IR and IRS proteins are negatively regulated are similar. These include dephosphorylation by protein tyrosine phosphatases, phosphorylation by serine/threonine kinases and ligand-induced down-regulation.

The best studied tyrosine phosphatase involved in negatively regulating insulin signalling is PTP1B. This enzyme directly interacts with the IR and reduces IR kinase activity by dephosphorylating tyrosine residues (Elchebly et al., 1999). IRS proteins are regulated by dephosphorylation by protein tyrosine phosphatases such as SHP2, which binds to phospho-tyrosine residues within IRS proteins in order to act on phosphorylated tyrosine residues at other locations which mediate PI-3-K and Grb2 binding (Myers, Jr. et al., 1994).

Other negative regulators of IR activity, such as SOCS1, SOCS3, Grb10 and PC1, act by sterically hindering the interaction between the IR and IRS proteins (Emanuelli et al., 2001; Ueki et al., 2004).

As mentioned above, serine phosphorylation of IRS proteins has been identified as a mechanism by which insulin signalling is negatively regulated. There a large number (~70) of potential serine phosphorylation sites on IRS proteins (Gual et al., 2005). Insulin stimulation results in the activation of several serine/threonine kinases such as PKB/Akt, ERK, S6 kinase, and JNK. Therefore serine phosphorylation may be part of a negative feedback loop. Increased serine phosphorylation of IRS proteins has been reported in insulin resistant states, which may indicate a role for serine phosphorylation in the induction of insulin resistance (Boura-Halfon and Zick, 2009). However, the exact mechanism by which this phosphorylation influences the function of IRS proteins is unclear.

1.4.3 Phosphatidylinositol-3-kinase

A role for phosphatidylinositol-3-kinase (PI-3-K) in insulin-regulated glucose transport was first identified though studies using a PI-3-K inhibitor, wortmannin (Okada et al., 1994; Clarke et al., 1994; Kanai et al., 1993). This inhibitor completely abolished insulin-stimulated glucose transport. Further studies into the role of PI-3-K using wortmannin, other PI-3-K inhibitors or dominant negative constructs have reported that reducing PI-3-K activity completely inhibited all metabolic actions stimulated by insulin including enhancement of glucose transport. Therefore, PI-3-K plays a pivotal role in mediating the activation of downstream signalling pathways following the binding of insulin to its receptor.

This family of enzymes catalyses the phosphorylation of phosphatidylinositol (PI) at the 3' position of the inositol ring. There are 3 classes of PI-3-Ks; classes I, II and III. Each class is defined by its structure, binding partners and lipid substrate specificity. Class I enzymes have a broad specificity, but preferentially phosphorylate phosphatidylinositol-(4,5)-bisphosphate (PI(4,5)P-2) to produce phosphatidylinositol-(3,4,5)-trisphosphate (PI(3,4,5)P-3). Class I PI-3-Ks are further classified into class I_A and I_B, determined by their adaptor or regulatory subunit. Class 1_A PI-3-Ks bind to adaptor proteins containing SH2 domains, whilst class I_B PI-3-Ks interact with the βγ subunits of G-proteins. Class II PI-3-Ks phosphorylate PI and PI(4)P, whilst PI3K from class III only act on PI (Vanhaesebroeck et al., 1997).

There is substantial evidence that class I_A PI-3-Ks are the most important subclass when studying insulin signalling, although a role for other subclasses cannot be discounted. Class I_A PI-3-Ks are heterodimers comprising a regulatory p85 subunit and a catalytic p110 subunit. The p110 subunit is almost always in complex with its regulatory partner since p110 is unstable when outside of this complex. There are three different p110 subunits (α, β and γ), and over-expression studies have identified p110β as the most important isoform in insulin-stimulated glucose uptake (Asano et al., 2000).

Following insulin-stimulation PI-3-K is recruited to the plasma membrane via an interaction between the SH2 domain of the p85 subunit and phosphorylated YMXM motifs within IRS proteins. The binding of the p85 subunit to phosphorylated tyrosine residues releases the p110 subunit from inhibition by p85. The catalytic subunit then converts PI(4,5)P-2 to PI(3,4,5)P-3 at the inner leaflet of the plasma membrane.

This transient increase in PI(3,4,5)P-3 leads to the recruitment of proteins containing PH domains with high affinity for PI(3,4,5)P-3 to the plasma membrane. 3'-Phosphoinositide-Dependent Kinase-1 (PDK-1) and PKB/Akt are key proteins in the propagation of insulin signalling that are recruited in this way.

The action of PI-3-K is negatively regulated by phospholipid phosphatases which act to reduce PI(3,4,5)P-3 levels. These include phosphatase and tensin homlogue (PTEN) and SH2-containing inositol 5'-phosphatase-2 (SHIP2) which dephosphorylate PI(3,4,5)P-3. Deletion of PTEN and knockout of SHIP2 have been reported to increase insulin-sensitivity and protect against insulin resistance respectively (Wijesekara et al., 2005; Sasaoka et al., 2005). These results support a role for these phosphatases in the negative regulation of PI-3-K.

1.4.4 3'-Phosphoinositide-dependent kinase-1 and the mTOR-Rictor complex 2

PDK-1 contains an N-terminal serine/threonine kinase domain and a C-terminal PH domain. The PH domain is required for the recruitment of PDK-1 to the cell surface following insulin-stimulated generation of PI(3,4,5)P-3. In this way, PDK-1 provides the link between the production of PI(3,4,5)P-3 following PI-3-K activation and activation of PKB/Akt (Vanhaesebroeck and Alessi, 2000). The recruitment of PDK-1 results in the phosphorylation and activation of downstream serine/threonine kinases. The most important of these proteins in terms of insulin-stimulated glucose transport are PKB/Akt and the atypical PKC isoforms ζ and λ. PDK-1 activates PKB/Akt via phosphorylation at threonine 308 which resides within the activation loop of PKB/Akt (Alessi et al., 1997). PDK-1 knockout mice have provided genetic evidence for the importance of PDK-1 in insulin-mediated glucose uptake (Mora et al., 2005b; Mora et al., 2005a).

The full activation of PKB/Akt requires phosphorylation of both threonine 308 and serine 473. The kinase that phosphorylates PKB/Akt at Serine 473 has been identified as the mammalian target of rapamycin (mTOR) kinase in complex with the regulatory protein RICTOR (mTORC2) (Sarbassov et al., 2005; Hresko and Mueckler, 2005). mTORC2 activation in response to growth and mitogen activation is promoted by the TSC1/TSC2 complex, although the mechanism of activation is unclear (Huang and Manning, 2008).

1.4.5 Protein kinase B/Akt

Three isoforms of PKB/Akt have been identified. These are PKBα/Akt1, PKBβ/Akt2 and PKBγ/Akt3. Structurally, all PKB/Akt isoforms comprise an N-terminal PH domain, a catalytic domain and a C-terminal regulatory domain. Knockout mice and studies utilising siRNA directed toward the different isoforms of PKB/Akt indicate that these different isoforms play distinct biological roles. Deletion of PKBα/Akt1 results in growth retardation and reduced lifespan but no metabolic abnormalities (Chen et al., 2001). This contrasts to PKBβ/Akt2 knockout mice which suffer from insulin-resistance and diabetes due to reduced glucose disposal and inability to control hepatic glucose output (Cho et al., 2001). Although PKBα/Akt1 and PKBβ/Akt2 are both widely expressed, PKBβ/Akt2 is enriched in insulin-sensitive tissues. PKBγ/Akt3 has been reported to play a role in neuronal development and brain size (Easton et al., 2005). Appropriately, PKBγ/Akt3 is predominantly expressed in the nervous system. The main structural difference between PKB/Akt isoforms is in the PH domain. This may be how PKB/Akt isoforms mediate their different effects when expressed in the same cells (Masure et al., 1999; Gonzalez and McGraw, 2009).

In unstimulated cells, PKB/Akt is localised in the cytosol. Following insulin stimulation, PKB/Akt is recruited to the plasma membrane through the interaction between its PH domain and PI(3,4,5)P-3. This interaction also induces a conformational change, following which PKB/Akt is activated by phosphorylation at threonine 308 by PDK-1 and at serine 473 by mTORC2. Threonine 308 is within the catalytic domain of PKB/Akt and the serine 473 phosphorylation site is within the regulatory domain. Following activation, PKB/Akt phosphorylates downstream targets containing a PKB/Akt consensus (RXRXXS/T) motif (Alessi et al., 1996; Obata et al., 2000).

There is a large body of evidence for PKB/Akt playing an important role in insulin-mediated glucose uptake and GLUT4 translocation. These data are from a wide range of experimental techniques including those using constitutively active PKB/Akt (myr-PKB/Akt), dominant negative constructs, knock-out mice and pharmacological inhibition of PKB/Akt. Expression of constitutively active myristoylated PKB/Akt leads to a high level of glucose uptake through increased plasma membrane GLUT4 content (Kohn et al., 1998). Conversely, both expression of a dominant negative form of PKB/Akt and knock-down of PKBβ/Akt2 using siRNA greatly reduced glucose uptake in response to insulin in muscle and adipose cells (Wang et al., 1999; Jiang et al., 2003). This knock-down technique resulted in a 70% reduction in PKBβ/Akt2

levels and reduced insulin-induced glucose uptake by 50%. Knock-down of PKBα/Akt1 by a similar technique only slightly reduced insulin-induced glucose uptake. However this isoform may be responsible for some compensation in Akt2/PKBβ knockdown cells. A small but significant role for PKBα/Akt1 is further supported by data from combined depletions of PKBα/Akt1 and PKBβ/Akt2. This double knock-down further attenuates the action of insulin on GLUT4 translocation. These data identify PKBβ/Akt2 as the most important isoform for mediating insulin-mediated glucose uptake. This has been confirmed in Akt2/PKBβ knock-out mice, which have severe insulin resistance in primary muscle tissue and isolated adipocytes (Bae et al., 2003). This implies that in these transgenic animals PKBα/Akt1 is unable to play a compensatory role in mediating insulin-stimulating glucose uptake. PKBα/Akt1 is a major focus of cancer research as it acts to inhibit apoptosis and its deregulation is implicated in a number of cancer subtypes (Lindsley et al., 2008).

The data obtained from the studies described above may be misleading. In each of these methods the cells are lacking the relevant isoform of PKB/Akt for long periods. This may permit the induction of compensatory mechanisms. This criticism has been answered in recent studies by two separate techniques. Ng *et al.* have described an elegant method for acute and direct activation of PKBβ/Akt2 in 3T3-L1 adipocytes (Ng et al., 2008). Activation of PKBβ/Akt2 using this method rapidly induced GLUT4 translocation and glucose uptake to a similar level as stimulation with a maximal dose of insulin. This provides further evidence that insulin-induced glucose uptake is primarily mediated by activated PKBβ/Akt2.

In addition, a specific PKB/Akt pharmacological inhibitor has been recently described and characterised (Lindsley et al., 2005). This inhibitor, which is known as Akt1/2 or Akti, acutely targets PKB-α/Akt1 and PKB-β/Akt2. Incubation of L6 myotubes with submicromolar concentrations of Akti inhibits insulin induced glucose and amino acid uptake (Green et al., 2008). Importantly, this inhibitor did not inhibit DNP-stimulated glucose transport in L6 cells, which occurs in a PKB/Akt-independent manner. Inhibition of PKB/Akt activity following insulin-stimulation was found to be dependent on tryptophan 80, which resides in the PH domain. These studies have provided different models for PKB/Akt inhibition by Akti depending on whether the studies are performed *in vitro* or *in vivo*. In *in vitro* experiments, PKB/Akt activity is inhibited by Akti despite the phosphorylation of threonine 308 and serine 473. Akti binding to tryptophan 80 sterically hinders the access of PKB/Akt substrates to the active site of the kinase domain. *In vivo*, Akti binds to the PH domain in the same way. However this binding prevents the conformational

change in PKB/Akt that is required to permit phosphorylation at serine 473 and threonine 308. This initial characterisation provided evidence that this inhibitor is extremely effective at almost completely inhibiting PKB/Akt activity and downstream effects in response to insulin. However, this complete inhibition has not been achieved in subsequent studies (Gonzalez and McGraw, 2006). However, these studies were conducted in different cell lines and the origin and therefore the structure and efficacy of the inhibitor may differ .

A large number of PKB/Akt substrates have been identified including glycogen synthase kinase 3 (GSK3), Rac1, Bad and CREB and FOXO transcription factors (reviewed in (Manning and Cantley, 2007)). These substrates mediate the downstream effects of PKB/Akt activation such as promoting glycogen synthesis, cytoskeletal rearrangements inhibition of apoptosis, and cell proliferation. Despite the identification of a plethora of substrates, a PKB/Akt substrate directly responsible for mediating insulin-stimulated glucose transport and GLUT4 translocation remained elusive as recently as 2002. Despite this, it had been reported that PKB/Akt is localised to GSVs following insulin-stimulation, implying that PKB/Akt acts directly upon proteins associated with vesicles containing GLUT4. (Calera et al., 1998). Ducluzeau *et al* (Ducluzeau et al., 2002) and Chen *et al.* (Chen et al., 2003) further investigated the role for PKB/Akt at the GSVs through the expression of a PKB/Akt-GLUT4 fusion protein containing either kinase-dead, wildtype or constitutively active PKB/Akt. Using these constructs, Ducluzeau *et al* reported that that PKB/Akt activation at, or close to, the GLUT4 vesicle was necessary, but not sufficient, to induce GLUT4 vesicle translocation to the plasma membrane. Using a PKBβ/Akt2-GLUT4 fusion protein, Chen *et al.* reported similar results, although expression of wildtype PKBβ/Akt2-GLUT4 was sufficient to stimulate GLUT4 translocation to a similar level to insulin-stimulation. The reason for these different observations is unclear, but both sets of data imply a role for activated PKB/Akt at, or near, GSVs.

1.4.6 PKB/Akt substrates linking insulin signalling to GLUT4 trafficking

A major focus in the field at the beginning of the twenty-first century was to identify PKB/Akt substrates implicated in glucose uptake. A particular aim was to link insulin signalling downstream of PKB/Akt to the membrane trafficking events leading to GLUT4 translocation. The identification of the PKB/Akt consensus phosphorylation motif (Alessi et al., 1996; Obata et al.,

2000) permitted the development of an antibody that recognises the phosphorylated PKB/Akt consensus motif (Arg-X-Arg-X-X-pSer/pThr; X = any amino acid). By using this antibody in combination with tandem mass-spectrometry based analysis techniques, Kane *et al.* identified an PKB /Akt substrate of 160 kDa (AS160) (Kane et al., 2002). In addition to this well characterised Rab-GAP, a related Rab-GAP TBC1D1 and PIKfyve have also been identified to be PKB/Akt substrates and are discussed below (Stone et al., 2006; Berwick et al., 2004). Despite the identification of these substrates, there is still a need to identify further PKB/Akt substrates. It is likely that recent advances in quantitative mass-spectrometry techniques will help to achieve this aim (Larance et al., 2008).

1.4.6.1 Rab-GAP proteins; TBC1D4/AS160 and TBC1D1

1.4.6.1.1 TBC1D4/AS160

Domain analysis of AS160 (also known as TBC1D4) revealed two phosphotyrosine binding (PTB) domains, a calmodulin binding domain and a GAP (GTPase activating protein) or TBC domain (Kane et al., 2002). The presence of a GAP domain implied that TBC1D4/AS160 is able to modulate the activity of Rab proteins, which themselves are known to be involved in membrane trafficking specificity. Therefore, TBC1D4/AS160 offered a potential link between signal transduction and GLUT4 trafficking. Mass spectrometry analysis of phosphopeptides derived from basal or insulin-stimulated 3T3-L1 adipocytes insulin revealed that insulin-stimulation increased phosphorylation at five PKB/Akt consensus motif sites (serine 318, serine 570, serine 588, threonine 642, and threonine 751) (Sano et al., 2003). These correspond to five of seven computationally predicted PKB/Akt phosphorylation sites. Although serine 588 is a predicted PKB/Akt phosphorylation site it has recently been experimentally deduced to be a PKCζ phosphorylation site (Ng et al., 2009).

TBC1D4/AS160 has now been extensively studied and its role in insulin-mediated GLUT4 trafficking more fully elucidated. TBC1D4/AS160 mutants have been key tools in these studies. These include a 4-P mutant, in which four PKB/Akt consensus phosphorylation motifs (serine 318, serine 588, threonine 642 and serine 751) have been mutated to alanine, and a 4P - R/K mutant which also has impaired GAP activity (arginine 973 lysine) (Sano et al., 2003). Over-expression of the 4P mutant, but not wild-type TBC1D4/AS160, inhibits insulin-stimulated GLUT4

translocation in 3T3-L1 adipocytes. Experiments in which single phosphorylation sites of AS160/TBC1D4 have been mutated have indicated that serine 588 and threonine 642 are the key residues involved in insulin-stimulated GLUT4 translocation.

Simultaneous abolition of GAP activity results in a loss of inhibition by the 4P mutant. Therefore, TBC1D4/AS160 mediated GLUT4 retention is dependent on the function of the GAP domain. Data from RNAi knockdown experiments performed on TBC1D4/AS160 in 3T3-L1 adipocytes support a role for the TBC1D4/AS160 Rab-GAP in retaining GLUT4 intracellularly. RNAi-mediated reduction in TBC1D4/AS160 protein levels resulted in a partial redistribution of GLUT4 from an intracellular location to the cell-surface GLUT4 under basal conditions (Eguez et al., 2005; Larance et al., 2005). TBC1D4/AS160 is therefore thought to act as a negative regulator of GLUT4 translocation.

It might be expected that over-expression of wild-type TBC1D4/AS160 would inhibit insulin-stimulated GLUT4 translocation if TBC1D4/AS160 is a negative regulator of GLUT4 translocation. The fact that over-expression of wild-type TBC1D4/AS160 did not inhibit GLUT4 translocation may indicate that insulin is able to fully phosphorylate all endogenous and over-expressed TBC1D4/AS160 in these cells. In addition, the increase in basal GLUT4 cell surface levels under conditions where TBC1D4/AS160 levels are depleted by siRNA is small (Larance et al., 2005). This may be explained by the fact that other proteins are able to compensate for the loss of TBC1D4/AS160. In support of this, the inhibition of GLUT4 translocation and glucose transport shown by the TBC1D4/AS160 phosphorylation mutants is not complete (Stockli et al., 2008; Sano et al., 2003; Kramer et al., 2006a). It should be noted that the partial nature of the TBC1D4/AS160-RNAi phenotype could also be explained if only a small proportion of total cellular TBC1D4/AS160 is required for GLUT4 retention.

From these early characterisation studies and more recent reports it is currently thought that in the absence of insulin TBC1D4/AS160 resides on specialised GSVs. Proteomic analysis of immuno-isolated GLUT4 vesicles has identified TBC1D4/AS160 as a component of this subcellular compartment in 3T3-L1 adipocytes (Larance et al., 2005). Of the two N-terminal PTB domains, the most C-terminal of which has been reported to associate the N-terminus of IRAP (Peck et al., 2006). This interaction may confer the localisation of TBC1D4/AS160 to GSVs. Stöckli *et al.* have reported that modification of serine 588 and threonine 642 to alanine or aspartic acid in TBC1D4/AS160 has no effect on IRAP binding in basal and insulin-stimulated cells (Stockli et al.,

2008; Peck et al., 2006). Therefore the interaction between TBC1D4/AS160 and IRAP is not modulated by insulin-stimulation and TBC1D4/AS160 phosphorylation by PKB/Akt.

The current model of TBC1D4/AS160 involvement in insulin signalling is outlined in Figure 1.4. Phosphorylation by PKB/Akt leads to repression of TBC1D4/AS160 GAP activity, allowing relevant Rab proteins to mediate GSV trafficking to the cell surface. The mechanism for inactivation of TBC1D4/AS160 GAP activity is unclear. There is currently no evidence to suggest that phosphorylation *per se* can reduce TBC1D4/AS160 GAP activity. Changing the localisation of TBC1D4/AS160 and thereby preventing access to Rabs on GSVs would be another mechanism of indirectly 'inactivating' GAP activity. However, there is contradictory evidence as to whether TBC1D4/AS160 is removed from GSVs upon insulin stimulation. TBC1D4/AS160 has been reported to translocate to the cytosol in response to insulin (Larance et al., 2005; Stockli et al., 2008). This translocation was not observed with the 4P mutant, suggesting that the role of phosphorylation is to mediate TBC1D4/AS160 dissociation from GSV membranes. However, through the use of a GLUT4-TBC1D4/AS160 fusion protein, Stöckli *et al* have reported that insulin-stimulated GLUT4 translocation in adipocytes does not require TBC1D4/AS160 translocation to the cytosol, but does require TBC1D4/AS160 phosphorylation (Stockli et al., 2008). In support of this, the same study reported that agonists other than insulin (including AMP-activated protein kinase (AMPK) activators) that stimulated GLUT4 translocation in the L6 muscle cell line (discussed below) resulted in phosphorylation of TBC1D4/AS160 at threonine 642, but not TBC1D4/AS160 translocation to the cytosol. However, data obtained from studies using L6 cells may be misleading as another Rab-GAP, TBC1D1, has been identified and may be more relevant than TBC1D4/AS160 when studying the action of AMPK activators in mediating GLUT4 trafficking in muscle cells.

A role for 14-3-3 binding to TBC1D4/AS160 in response to insulin has also been investigated. PKB/Akt induced phosphorylation of TBC1D4/AS160 at threonine 642 results in increased 14-3-3 association (Chen et al., 2008). Furthermore, introduction of a constitutive 14-3-3 binding site in the 4P mutant reversed its inhibition of GLUT4 translocation (Ramm et al., 2006). This is similar to the reversal of 4P inhibition by the GAP inactive version of TBC1D4/AS160 4P (4P-R/K). These data support an important role for 14-3-3 binding to TBC1D4/AS160 in insulin-regulated GLUT4 translocation in 3T3-L1 adipocytes. The exact role of phosphorylation and 14-3-3 binding in inhibiting TBC1D4/AS160 GAP activity remains

unresolved, although both are required for insulin-stimulated GLUT4 translocation to the plasma membrane.

Inhibiting TBC1D4/AS160 GAP function permits Rab proteins present on GSVs to be converted to their active (GTP bound) form, and allows them to mediate GLUT4 translocation to the plasma membrane. In this way, TBC1D4/AS160 is involved in insulin-mediated effects on the exocytosis limb of the GLUT4 trafficking pathway. A role for insulin-signalling to TBC1D4/AS160 in GLUT4 exocytosis has been supported by work using an assay measuring the kinetics of GLUT4 trafficking (Gonzalez and McGraw, 2006). Methods to investigate GLUT4 trafficking and the results obtained from such studies are discussed in detail below. The recent development of total internal reflectance fluorescence (TIRF) microscopy has further enabled the dissection of the role of TBC1D4/AS160 in insulin-signalling to GLUT4 translocation. Over-expression of the 4P mutant reduced GLUT4 translocation into the TIRF zone, whilst having no effect on the rate of GSV fusion with the cell surface (Gonzalez and McGraw, 2006). These data led to the conclusion that TBC1D4/AS160 has a role in pre-fusion trafficking of GLUT4-containing vesicles to an area close to the cell surface, and may be involved in GSV docking with the plasma membrane. Additional studies in Xu's laboratory have revealed that TBC1D4/AS160 plays a role in GSV docking with the cell surface, and not the fusion of GLUT4-containing vesicles (Jiang et al., 2008). However, these data suggest this distal role in GLUT4 trafficking is the primary site of TBC1D4/AS160 action, and that expression of a 4P mutant does not inhibit GSV trafficking to the cell surface. This is contrary to the data presented by Gonzalez and McGraw. Although the exact site of TBC1D4/AS160 action needs to be resolved, these data all support a role for this Rab-GAP in negatively regulating GLUT4 translocation by inhibiting the access of GSVs to the cell surface.

1.4.6.1.2 TBC1D1

TBC1D1, a protein with sequence and structural similarity to TBC1D4/AS160 as illustrated in Figure 1.4, has been recently identified in a study which investigated genetic predisposition to obesity. A genetic variation of TBC1D1 (arginine 125 tryptophan) was reported to be significantly associated with severe obesity in females (Stone et al., 2006). This association has been confirmed in a similar study based in France (Meyre et al., 2008). Therefore, TBC1D1 is implicated in predisposition to obesity in humans. This could be due to signalling or trafficking

defects associated with glucose uptake if TBC1D1 is playing a similar role in insulin-mediated GLUT4 translocation as TBC1D4/AS160. However the presence of TBC1D1 in the hypothalamus means that an appetite related effect cannot be discounted (Chadt et al., 2008).

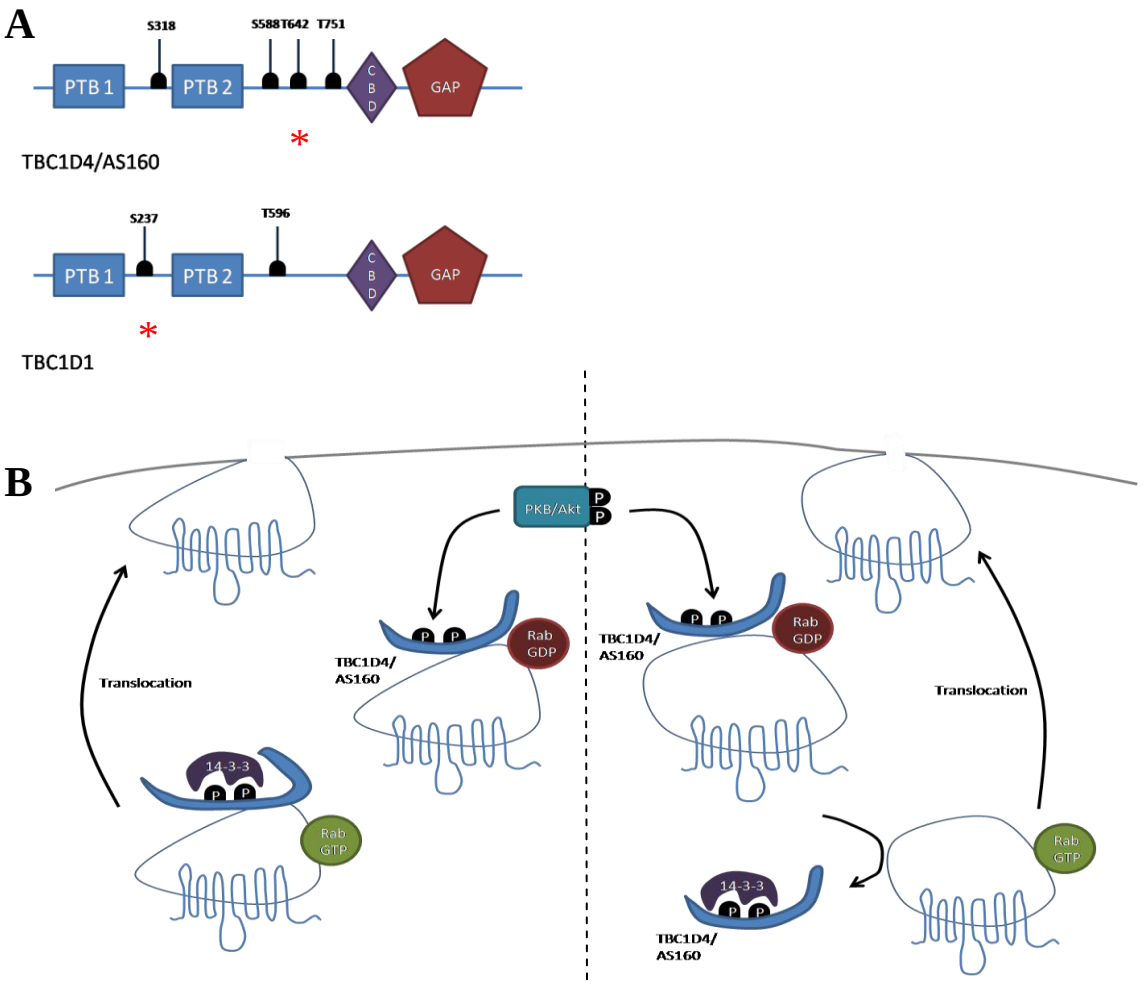

Figure 1.4. A, The domain structure of TBC1D4/AS160 and TBC1D1. Both Rab-GAPs contain two phosphotyrosine binding domain (PTB), a calmodulin binding domain (CBD) and a GAP domain. The PKB/Akt phosphorylation sites mutated in the 4P-mutant are depicted on TBC1D4/AS160. The phosphorylation sites in TBC1D1 represented are the PKB/Akt site at threonine 596 and the AMPK site at serine 237 (serine 231 in rat). Additional AMPK phosphorylation sites have been identified by mass spectrometry. The important phosphorylation sites for 14-3-3 binding are highlighted (*). B, Two potential mechanisms of TBC1D4/AS160 deactivation leading to GSV translocation. Phosphorylation of TBC1D4/AS160 induced 14-3-3 association and resultant inhibition of TBC1D4/AS160 GAP activity (left). Alternatively, phosphorylation of TBC1D4/AS160 alone, or in conjunction with 14-3-3 binding, induces TBC1D4/AS160 translocation from GSVs to the cytosol (right). Both mechanisms permit the GTP-loading of the TBC1D4/AS160 partner Rab and subsequent Rab-mediated GSV trafficking to the cell surface.

TBC1D1's GAP domain has been reported to display a similar Rab specificity profile to the TBC1D4/AS160 GAP domain (Roach et al., 2007). Furthermore, TBC1D1 has conserved PKB/Akt consensus phosphorylation motifs. PKB/Akt phosphorylation motifs in TBC1D4/AS160 (serine 570 and threonine 642) are also present in TBC1D1 (serine 507 and threonine 596) (Stone et al., 2006). PKB/Akt is reported to primarily phosphorylate Threonine 596 (Roach et al., 2007). Phosphorylation of endogenous TBC1D1 following AICAR-stimulation of the C2C12 mouse muscle line analysed by mass spectrometry identified a large number of AMPK-sensitive phosphorylation sites (serine 145/6, serine 231, serine 489, serine 497, threonine 499, serine 501, serine 521, serine 559/560, serine 565, threonine 590, serine 608, serine 621, serine 660, serine 661, serine 697/8/9, serine 700, tyrosine 1039 and threonine 1218). On comparison of these motifs to the AMPK consensus sequence, only seven of these sites were considered to be AMPK phosphorylation sites (serine 231, serine 559, threonine 590, serine 621, serine 660, serine 697 and serine 700) (Peck et al., 2009). The fact that TBC1D1 is phosphorylated by both PKB/Akt and AMPK is of interest since muscle tissues respond to both insulin-stimulation and AMPK-activation by increasing glucose uptake.

14-3-3 binding to TBC1D1 has also been investigated. In contrast to TBC1D4/AS160, PKB/Akt-mediated phosphorylation of TBC1D1 did not induce 14-3-3 binding. This is surprising given the homology between the PKB/Akt consensus motifs between TBC1D1 and TBC1D4/AS160. Activation of AMPK and subsequent phosphorylation at serine 237 resulted in 14-3-3 binding to TBC1D1 (Chen et al., 2008; Pehmoller et al., 2009). In addition to these differences in kinase specificity and 14-3-3 binding, there is also a difference in the location and sequences of the two N-terminal PTB domains present in each protein. These variations between TBC1D4/AS160 and TBC1D1 are likely to yield important functional differences *in vivo*.

In the first investigations into the action of TBC1D1 in cells, Roach *et al.* and Chavez *et al.* over-expressed the short splice variant of wild-type TBC1D1 in 3T3-L1 adipocytes. This reduced GLUT4 plasma membrane levels in insulin stimulated cells (Roach et al., 2007; Chavez et al., 2008). This contrasts to over-expression of wild-type TBC1D4/AS160, which had no effect on GLUT4 translocation in 3T3-L1 adipocytes. Abolition of TBC1D1 GAP activity (R/K) reversed TBC1D1 inhibition of GLUT4 translocation. TBC1D1-mediated retention of GLUT4 is dependent its GAP activity in a similar way to TBC1D4/AS160.

In a recent study, Peck *et al.* have conducted similar experiments with the long splice variant of TBC1D1 and have concluded that insulin-stimulated phosphorylation of TBC1D1 relieves its inhibition on GLUT4 translocation (Peck et al., 2009). In this way, it is currently thought that TBC1D1 regulates glucose uptake and GLUT4 translocation via an analogous mechanism to TBC1D4/AS160 as described above (Figure 1.4). Furthermore, it was found that AMPK-induced phosphorylation of TBC1D1 is able to partially relieve TBC1D1-mediated inhibition of GLUT4 trafficking. The potential relevance of this dual regulation will be more fully addressed below. Peck *et al.* also studied the effect on the arginine 125 to tryptophan mutant (as found in the genetic screen for predisposition to obesity in humans) on TBC1D1 inhibition of GLUT4 trafficking. This mutant expressed in 3T3-L1 adipocytes inhibited GLUT4 translocation to a similar level as the wild-type protein. This result does not shed any light on how this mutant influences TBC1D1 activity *in vivo*. The lack of any obvious effect may be due to the expression of the construct in a cell type (3T3-L1 adipocytes) that expresses TBC1D1 at very low levels. Indeed, the study of TBC1D1 action may be more appropriate in a cell type that normally expresses higher levels of TBC1D1.

A knock-out mouse model for TBC1D1 has been described. SJL mice have a truncated TBC1D1 gene, which is not translated into protein because of nonsense-mediated RNA decay (Chadt et al., 2008). However, it has been pointed out in a recent review that if a truncated version of the protein without GAP activity is expressed then the conclusions drawn from the data may need to be reinterpreted (Leney and Tavare, 2009). These mice were lean and resistant to diet-induced obesity. The main finding from this study was that in the absence of TBC1D1 fatty acid uptake and oxidation was increased, whilst glucose uptake was reduced in EDL muscle (glycolytic muscle). Commensurate with expression levels of TBC1D1 between fibre types, the loss of TBC1D1 had no effect on fatty acid uptake and oxidation or glucose uptake in soleus muscle (oxidative muscle).

The data from EDL muscle described above is contrary to what would be expected given the proposed role for TBC1D1 as a negative regulator of glucose uptake. Instead, the authors propose that TBC1D1 may in fact have a yet to be defined role in whole-body energy homeostasis through regulating fatty-acid oxidation in skeletal muscle. This study highlights the need to investigate the role of TBC1D4/AS160 and TBC1D1 *in vivo*. One interpretation of the data is that TBC1D1 acts to regulate the translocation of fatty acid transporters (CD36, FATP1) to the cell surface in an analogous fashion to TBC1D4/AS160 regulation of glucose transport

translocation. This hypothesis was not considered by the authors and has not yet been investigated. As well as increasing phosphorylation of TBC1D1, AMPK activation has been reported to increase fatty acid uptake into muscle by enhancing cells surface levels of fatty acid transporters such as CD36 (van Oort et al., 2009; Habets et al., 2009; Habets et al., 2007).

Given the similarities and differences between TBC1D4/AS160 and TBC1D1 structure and phosphorylation motifs, their expression profile is of particular interest. TBC1D4/AS160 expression is highest in adipose tissue, the heart and oxidative muscle fibres (such as soleus muscle). TBC1D1 expression is correspondingly low in these tissues. TBC1D1 is highly expressed in glycolytic muscle fibres (including the tibialis anterior (TA) and plantaris muscles), in which TBC1D4/AS160 is present as much lower levels (Taylor et al., 2008). In addition to these expression differences, each Rab-GAP can be expressed as either a long or short splice variant. Functional differences between these splice variants are yet to be discovered and the significance of the differential expression profile of the Rab-GAPs and their splice variants is yet to be determined (Taylor et al., 2008).

1.4.6.1.3 Downstream targets of TBC1D4/AS160 and TBC1D1

The proposed mechanism of action for TBC1D4/AS160 and TBC1D1 requires a partner Rab(s) to orchestrate GLUT4 translocation to the cell surface once the Rab-GAP is inactivated. Miinea *et al.* have performed an *in vitro* screen using the GAP domain of TBC1D4/AS160 with all known Rabs and reported that this GAP domain is active towards Rab2B, 8A, 10 and 14 (Miinea et al., 2005). TBC1D1 GAP domain has the same Rab specificity (Roach et al., 2007). Of these Rabs, only siRNA-mediated knockdown of Rab10 inhibited GLUT4 translocation (Sano et al., 2007; Sano et al., 2008). A role for Rabs 10 and 14 is further supported by reports identifying these Rabs to be associated with GLUT4 vesicles in 3T3-L1 adipocytes. However, this analysis also identified Rab11a and Rab11b on this vesicle population (Larance et al., 2005). This is of interest since Rip11, a Rab11-interacting protein, also binds to TBC1D4/AS160 (Welsh et al., 2007). Therefore, Rip11 may be involved in coordinating the link between insulin-signalling and trafficking machinery leading to GLUT4 translocation. There is currently a major focus in the field to verify whether these Rabs are regulated by TBC1D4/AS160 and TBC1D1 *in vivo*.

1.4.6.2 PIKfyve

Following the identification of TBC1D4/AS160 in 2002, Berwick *et al.* identified a FYVE domain-containing phosphatidylinositol-3-phosphate (PI(3)P) 5' kinase (PIKfyve) as a PKB/Akt substrate in 2004 (Berwick et al., 2004). PIKfyve binds to its lipid substrate PI(3)P via its FYVE domain phosphorylates the inositol ring at the 5-position to produce PI(3-5)P-2. Berwick *et al.* reported that PIKfyve is phosphorylated by PKB/Akt at serine 318 (Berwick et al., 2004). *In vitro* studies have suggested that phosphorylation of PIKfyve may moderately enhance its 5-kinase activity (Berwick et al., 2004). The PKB/Akt phosphorylation site is in close proximity to the FYVE domain of PIKfyve. Therefore, it is possible that enhanced PIKfyve kinase activity is achieved by increased binding to its substrate (PI(3)P), rather than by direct activation of PIKfyve's catalytic activity.

It has been reported that serine 318 of PIKfyve is phosphorylated by Serum/Glucocorticoid regulated kinase 1 (SGK1). SGK1 and PKB/Akt have similar consensus phosphorylation motifs. Phosphorylation of PIKfyve at serine 318 has now been implicated in SGK1 mediated regulation of the Na(+)/ glucose cotransporter SGLT1 (SLC5A1) and the creatine transporter CreaT (SLC6A8) (Shojaiefard et al., 2007; Strutz-Seebohm et al., 2007).

The phosphorylation of PIKfyve seems to have a functional role since expression of a serine 318 to alanine mutant potentiated insulin-induced GLUT4 translocation in 3T3-L1 adipocytes (Berwick et al., 2004). Consistent with this data, pharmacological inhibition of PIKfyve with YM201636 (Jefferies et al., 2008) and siRNA knock-down of PIKfyve potentiates secretory granule exocytosis in PC12 cells (Osborne et al., 2008). This is perhaps counter-intuitive as these data indicate that insulin-induced phosphorylation of PIKfyve acts to increase the amount of PI(3,5)P-2 and as a result to reduce the level of GLUT4 at the cell surface. However, Tavaré and colleagues propose that PKB/Akt phosphorylation of PIKfyve links the production of PI(3,4,5)P-3 at the cell surface with PI(3,5)P-2 production on endosomes. PIKfyve is localised to endosomes, and has been implicated in the trafficking of mannose-6-phosphate receptor from endosomes to the TGN (Rutherford et al., 2006). Therefore, PIKfyve may play a role in mediating GLUT4 trafficking between endosomal compartments and the TGN. As discussed, specialised GLUT4 storage vesicles have been postulated to originate from the TGN. Therefore, insulin-stimulated phosphorylation and activation of PIKfyve may be required to enhance GLUT4 sorting back into the GSV compartment.

Contrary to the data described above, Shisheva's group state that over expression of a kinase-dead version of the PIKfyve and siRNA-mediated knock-down of PIKfyve both inhibit insulin-stimulated GLUT4 translocation in adipocytes (Ikonomov et al., 2002; Ikonomov et al., 2007). Data generated from investigations into the role of PIKfyve using techniques such as siRNA, over-expression of a kinase dead version, or use of an inhibitor (YM201636) should be interpreted with care since these techniques can lead to severe vacuolation of intracellular membranes. This could lead to inhibition of GLUT4 translocation or mistargetting of GLUT4 via a non-specific mechanism, as a result of global trafficking defects (Jefferies et al., 2008; Shisheva et al., 2001). Further work is needed to establish the role for PIKfyve in insulin-mediated glucose transport.

1.4.7 Protein kinase C

Insulin stimulation activates members of the protein kinase C serine/threonine kinase family as well as PKB/Akt. There is a large body of evidence that suggests that PKC is important in insulin-stimulated glucose transport. Twelve PKC isoforms have been identified in mammalian cells, and have been classified depending on their mode of activation and sequence homology. The conventional PKCs (cPKCs α, β1, β2 and γ) are activated in the presence of phosphatidylserine (PS), calcium (Ca^{2+}) and diacylglycerol (DAG). Novel PKCs (nPKCs δ, ε, θ, and η) are activated by PS and DAG, whilst atypical PKCs (aPKCs ζ and λ) are activated by mechanisms independent of both Ca^{2+} and DAG, but still require PS.

The aPKCs (ζ and λ) are thought to be the predominant PKC isoforms involved in insulin-stimulated glucose transport. For example, defective aPKC activation is proposed to contribute to the pathophysiology of diabetes since aPKC activation is diminished in muscles in a large number of type 2 diabetic models (Kanoh et al., 2003; Standaert et al., 2004; Vollenweider et al., 2002; Beeson et al., 2003). PKCλ is the main aPKC in muscle and adipose of mice, whereas PKCζ is predominant in rat and human tissues (Farese, 2002). These isoforms may act interchangeably to support insulin-stimulated glucose transport. The exact role of PKC isoforms in insulin-stimulation glucose transport has not yet been determined, although PKC has recently been reported to phosphorylate TBC1D4/AS160 at serine 588 (Ng et al., 2009). This implies that PKC may have similar downstream targets to PKB/Akt.

The mechanism of aPKC activation in response to insulin is analogous to the activation of PKB/Akt. There is a requirement for the recruitment of IRS-1 and IRS-2 to the IR, production of PI(3,4,5)P-3 and phosphorylation of aPKCs, which are recruited to the membrane through binding to PS and PI(3,4,5)P-3, by PDK-1 (Standaert et al., 2001).

A number of studies in different cell types have provided data supporting a role for aPKCs in insulin-mediated glucose transport. Insulin-stimulated glucose transport was inhibited in L6 cells expressing a myristoylated PKC-ζ pseudo-substrate and following incubation with general PKC inhibitors (Bandyopadhyay et al., 1997). Conversely, expression of constitutively active PKC-λ resulted in glucose uptake and GLUT4 translocation to a similar extent as insulin in L6 cells (Bandyopadhyay et al., 2000). In cardiomyocytes, PKC-ζ is required for insulin stimulated GLUT4 and fatty acid transporter (CD36) translocation. Interestingly, insulin does not increase PKC-ζ activity in cardiomyocytes, implying although PKC-ζ is required for insulin-mediated-GLUT4 translocation, may only play a permissive rather than regulatory role (Luiken et al., 2009). A role for aPKC in insulin-mediated glucose transport has also been identified in cultured adipocytes (Bandyopadhyay 2002, 2004).

Despite the data supporting a role for aPKCs in insulin-mediated glucose transport, a recent publication has provided evidence for a role for PKC-βII in L6 cells (Chappell 2009). Insulin-stimulation resulted in phosphorylation of PKC- βII in a PI-3-K-dependent manner. PKC-βII phosphorylates myristoylated alanine-rich C-kinase substrate (MARCKS), which provides a link between insulin signalling and the cytoskeleton. Further evidence for a role for PKCs in modulating the actin cytoskeleton, has been provided by the finding that PKCζ activation induces actin rearrangements in L6 cells (Liu et al., 2006). Despite these correlative findings, the exact role of PKCs in insulin-stimulated glucose uptake remains unresolved.

1.4.8 PI-3-K independent insulin signalling pathways

The activation of PI-3-K following insulin-stimulation is central to the signalling pathway leading to enhanced glucose uptake. However, there is also evidence that a PI-3-K-independent pathway plays a role in insulin-induced GLUT4 translocation and glucose uptake. Circumstantial evidence supporting the presence of this alternative pathway comes from two different experimental approaches. Firstly, exogenous administration of cell permeable PI(3,4,5)P-3 is unable to fully

recapitulate the effect of insulin stimulation in adipocytes (Sweeney et al., 2004). Secondly, stimulation of cells with other growth factors such as PDGF, which stimulate PI-3-K activity in a similar manner and to a similar extent to insulin, only result in a minor increase in glucose uptake (Isakoff et al., 1995; Guilherme and Czech, 1998).

Therefore, a PI-3-K-independent pathway has been proposed to be activated alongside the classical PI-3-K-dependent signalling pathway following insulin-stimulation. This pathway involves the recruitment of the proto-oncogenes c-Cbl and Cbl-b to caveolin-enriched domains at the cell surface through an interaction with the IR via the adaptor proteins CAP (c-Cbl-associated protein) and APS (Baumann et al., 2000). The CAP adaptor protein contains three C-terminal SH3 domains which binds to the proline-rich domains within Cbl. CAP also contains an N-terminal SoHo domain, which is so named because of the homology of the region to the gut peptide sorbin. This domain of CAP interacts with the lipid raft protein flotillin (Baumann et al., 2000; Kimura et al., 2001).

The second adaptor protein, APS, interacts with the insulin receptor via a SH2 domain. APS is tyrosine phosphorylated by the activated IR and interacts with c-Cbl via this phosphorylation site. Following its recruitment to the IR c-Cbl is tyrosine phosphorylated at three residues by the β-subunit of the IR (Ribon and Saltiel, 1997). The APS/CAP/Cbl complex dissociates from the IR once c-Cbl has been phosphorylated.

Phosphorylated c-Cbl recruits CrkII. CrkII contains a SH3 domain, through which it associates with a guanylnucleotide exchange factor (GEF) called C3G. C3G activates TC10 (a Rho family protein) by promoting the exchange of GDP to GTP (Chiang et al., 2001). Both TC10α and TC10β are activated following insulin stimulation and both these isoforms have reported to be localised to lipid raft domains in adipocytes.

The reported downstream effects of this pathway are defined by TC10 interacting partners. These partners include CIP4/2 (Chang et al., 2002), N-WASp (Jiang et al., 2002) and Exo70 (Inoue et al., 2003). As such, the PI-3-K-independent pathway has been implicated in a variety of insulin-regulated processes such as influencing GLUT4 internalisation (Hartig et al., 2009), cortical actin arrangements, recruitment of the exocyst complex to the cell surface (Inoue et al., 2003), PI(3)P formation at the plasma membrane and inactivation of Rab31 (Lodhi et al., 2007).

The role of this pathway in insulin stimulated glucose uptake remains controversial. Studies using transgenic knock-out mice or siRNA knock-down techniques have reported conflicting or surprising results. For example, siRNA-mediated knock-down of c-Cbl, CAP and CrkII did not have any effect of glucose uptake into 3T3-L1 cells (Mitra et al., 2004; Zhou et al., 2004). This result is in direct contradiction to data from a publication from the same year which reported that siRNA-mediated depletion of APS or Cbl resulted in inhibition of insulin-stimulated glucose transport (Ahn et al., 2004). Knockout mice models have yielded counter-intuitive results. Given the hypothesis that this PI-3-Kinase-independent pathway is involved in positively regulating glucose uptake, c-Cbl and APS knockout mice would be expected to exhibit reduced insulin sensitivity. In contrast, both c-Cbl and APS knock-out have increased peripheral insulin-sensitivity. In addition, it has been reported that TC10 is not involved in cortical actin rearrangements in muscle. Therefore, this PI-3-K-independent pathway is not relevant in muscle tissue (JeBailey et al., 2004) and plays a role in insulin signalling only in adipocytes. Additional studies into the involvement and requirement for this pathway in insulin-mediated GLUT4 translocation and glucose uptake are necessary.

1.4.9 Insulin signalling to the cytoskeleton and its role in GLUT4 trafficking

Insulin signalling exerts a control over cytoskeletal elements to facilitate insulin-dependent GLUT4 translocation and glucose uptake. Immuno-electron microscopy studies have identified GSV association with microtubules and intermediate filaments (Guilherme et al., 2000). Disruption of these cytoskeletal structures in 3T3-L1 adipocytes resulted in redistribution of GLUT4 from a peri-nuclear region to the cell periphery (Guilherme et al., 2000).

Microtubules offer a route by which GSVs can traffic to the cell surface. Disruption of the microtubule network results in a 40% reduction in GLUT4 redistribution to the plasma membrane (Fletcher et al., 2000). Insulin signalling effects on the microtubule network are reported to be mediated by targetting motor proteins. For example, Huang *et al.* have reported that insulin-stimulation inhibited Dynein (a motor protein) association with microtubules and that this resulted in inhibition of GLUT4 endocytosis from the cell surface (Huang et al., 2001). A role for kinesin motors in GLUT4 translocation in 3T3-L1 adipocytes has also been reported (Emoto et al., 2001). The exact role of microtubules in GSV trafficking is not fully understood. It

has been proposed that these cytoskeletal elements may be more important in GLUT4 sorting from endosomes to the GSV, than in insulin-regulated translocation (Molero et al., 2001; Shigematsu et al., 2002).

The requirement for microtubules in GLUT4 translocation needs to be investigated in primary cells. In basal 3T3-L1 adipocytes GLUT4 is localised to the peri-nuclear region in the centre of the cell. Therefore, relatively long translocation events may have to occur to translocate GSVs from this region to the cell periphery. TIRF microscopy has identified a role for microtubules in long-range GSV trafficking (Xu et al., 2007). In contrast, the intracellular volume of primary adipocytes is primarily comprised of a single large lipid droplet (90% of cell volume) and as such intracellular GLUT4 is forced to localise in close proximity to the plasma membrane. Considering these morphological differences, it is clear that microtubule mediated vesicle trafficking may play a more important role in GLUT4 translocation in 3T3-L1 adipoctyes than in primary adipocytes.

In contrast to the major changes in GLUT4 localisation in response to microtubule depolymerisation, similar disruption of actin filaments does not redistribute GLUT4 in the basal state. Insulin-stimulation induces a rapid remodelling of actin filaments into a cortical mesh in muscle cells and adipocytes (JeBailey et al., 2004; Lopez et al., 2009; Brozinick, Jr. et al., 2004). If this mesh formation is inhibited by administration of excess PI(3,4,5)P-3 (Patel et al., 2003) or by the G-actin polymerisation inhibitor latrunculin-B (Omata et al., 2000; Lopez et al., 2009), then insulin induced GLUT4 translocation is inhibited. The exact role of cortical actin is unclear, although several possibilities have been proposed. Remodelled actin could facilitate GLUT4 translocation by promoting GLUT4 sorting, localising signalling complexes or PI(3,4,5)P-3, by guiding myosin motors on the GSVs or by positioning GLUT4 near the plasma membrane and aiding GSV docking with the plasma membrane (Patel et al., 2003).

The role of actin in GLUT4 appearance at the cell surface has been studied using TIRF microscopy and probes that can distinguish between transport to the plasma membrane and fusion with the membrane. Disruption of cortical action by latrunculin-B resulted in a normal redistribution of GLUT4 to the evanescent field (close to the plasma membrane), but inhibited GSV fusion with the plasma membrane (Lopez et al., 2009). These data support a role for cortical actin in facilitating the fusion of GLUT4-containing vesicles but not the translocation of GSVs to a region close to the plasma membrane. It has also been proposed that the cortical actin network

is required for short distance GSV movement (Xu et al., 2007). Therefore another interpretation of these results is that although cortical actin is not required for GSV trafficking to the evanescent field, it is required for the short-distance delivery of GSVs to the plasma membrane.

Disruption of the cortical actin network also inhibited GLUT4 appearance at the plasma membrane in L6 cells (Randhawa et al., 2008). However, cortical actin was also required for GLUT4 trafficking to, or accumulation in, a region close to the cell surface. This conflicts with the observations from TIRF microscopy in 3T3-L1 adipocytes. The data from L6 cells implies that the actin cytoskeletal network close to the plasma membrane is required to retain GSVs in this location. Without this actin mesh, GSVs trafficked to this point are not retained (Randhawa et al., 2008). This model relies on GSV association with actin. α-Actinin4 may provide this link as it is co-immunoprecipitated with GLUT4 in an insulin-dependent manner (Talior-Volodarsky et al., 2008). The contradictory results obtained from these TIRF and confocal microscopy studies may be attributed to the different cell type used for the studies, and studying GLUT4 trafficking in L6 myoblasts or myotubes by TIRF microscopy may address this discrepancy.

Several signalling molecules have been implicated in insulin-stimulated actin rearrangements. One such protein is TC10, which along with local PI(3,4,5)P-3 production at the cell surface has been proposed to recruit N-WASP and arp-3 to initiate actin polymerisation. However, TC10 is not present in muscle which implies an alternate mechanism for achieving the required actin reorganisation. In muscle, the Rho GTPase family member Rac1 may initiate actin polymerisation (JeBailey et al., 2004; Marcusohn et al., 1995). Another Rho family GTPase, Cdc42, has been reported to be activated following insulin-stimulation in 3T3-L1 adipocytes (Usui et al., 2003).

The identification of new insulin-regulated cytoskeletal effector proteins is an on-going process. For example, Myo1c, a motor protein that mediates movement along actin filaments, has recently been reported by Yip *et al.* to be phosphorylated in response to insulin-stimulation on a previously unreported site (Yip et al., 2008). This protein has been previously identified in proteomic analysis of GSVs isolated from 3T3-L1 adipocytes (Bose et al., 2002) and therefore may act to direct GSV trafficking to the cell surface.

The importance of understanding the exact role of the cytoskeleton and its regulators in insulin-regulated GLUT4 trafficking is highlighted by the finding that cortical actin filaments are

lost in insulin-resistant L6 muscle cells (McCarthy et al., 2006). Therefore, disruption of these filaments likely contributes to the insulin-resistant phenotype.

1.4.10 GSV docking and fusion and insulin action at the plasma membrane

Following their translocation to the cell surface, GSVs dock and fuse with the plasma membrane. At this point GLUT4 is present at the cell surface and is able to bind and transport glucose into the cell. The importance of insulin signalling events at the plasma membrane has been best demonstrated by data derived from an *in vitro* fusion assay. In this assay, the different constituent parts (plasma membrane, GSVs and cytosol) of the assay can be obtained from either basal or insulin-stimulated cells. Considering this, insulin-stimulated increase in fusion is observed in assays containing basal cytosol and GSVs, with only the plasma membrane derived from stimulated cells (Koumanov et al., 2005). Therefore, there must be an import insulin-regulated step at the plasma membrane to enhance the rate of GSV fusion at this site.

The process of membrane fusion is evolutionarily conserved and requires N-ethylmaleimide sensitive factor (NSF), soluble NSF attachment proteins (SNAPs), SNAP receptors (SNARE) proteins and small Rab GTPases. A SNARE complex is formed between the vesicle SNARE on GSVs, VAMP2 (Cain et al., 1992), and the plasma membrane (target membrane) SNAREs syntaxin-4 (Timmers et al., 1996) and SNAP23 (Rea et al., 1998). The formation of this stable ternary complex of coiled coil domain interactions is thought to bring the vesicle and target membrane into close proximity, facilitating fusion.

The formation of this SNARE complex is regulated by insulin signalling. In basal cells, Munc-18c interacts with syntaxin-4 and prevents syntaxin-4 association with SNAP23 and VAMP2. Similarly, pantophysin is thought to bind to VAMP2 (Brooks et al., 2000). Insulin-stimulation promotes dissociation of Munc-18c from syntaxin-4. This dissociation may be promoted by the phosphorylation of Munc-18c at tyrosine 219 (Jewell et al., 2008). At this point, the SNARE complex between VAMP2, syntaxin-4 and SNAP23 can form. In addition to the insulin-sensitive phosphorylation of Munc-18c, PKB/Akt and PKCζ mediated phosphorylation of VAMP2 has been reported. The role of this phosphorylation is yet to be determined (Kupriyanova and Kandror, 1999; Braiman et al., 2001). The importance of the formation of the SNARE complex has

been examined by inhibition of VAMP2 function through cleavage by botulinum toxin. This treatment inhibits GLUT4 appearance at the cell surface (Randhawa et al., 2000).

Using adipocytes derived from embryonic fibroblasts from knockout mice, Zhao *et al.* have investigated the requirement for VAMP2, 3 and 8 in insulin-stimulated GLUT4 translocation (Zhao et al., 2009). Only knocking out all three of these v-SNARE isoforms completely inhibits insulin-stimulated GLUT4 translocation. Re-expression of either of these isoforms rescues this phenotype. This study highlights the plasticity in the requirement for v-SNAREs in insulin-stimulated GLUT4-vesicle fusion with the plasma membrane. Other VAMPs have been implicated in GLUT4 translocation to the cell surface. For example, VAMPs 2,3 5 and 7 have been identified on GSVs in skeletal muscle (Rose et al., 2009).

Other proteins have been identified to be involved in the regulation of SNARE complex formation. These include Doc2β, which is a positive regulator of vesicle fusion in adipocytes (Ke et al., 2007). Additional negative regulators of SNARE complex assembly through syntaxin-4 binding include synip, which is specifically phosphorylated by PKBβ/Akt2 (Yamada et al., 2005), and Tomosyn (Widberg et al., 2003). The majority of these studies into proteins involved in GSV fusion have been carried out in adipocytes, however the fusion machinery and its regulation is thought to be analogous in muscle tissues.

The investigation of insulin action at this site has been greatly aided by the relatively new technique of TIRF microscopy. TIRF microscopy allows high resolution imaging of events within 100 to 250 nm of the cell surface. In depth analysis of live-cell images using this technique has identified that GLUT4 vesicle tethering/docking times are increased by insulin. Furthermore, individual fusion events can be monitored using fluorescently tagged-GLUT4 molecule or a pH sensitive IRAP-pHluorin molecule.

There is contradictory evidence for the role of PI-3-Kinase and PKB/Akt in GSV trafficking to the cell surface, docking and fusion. The docking and fusion of GSVs are reported to be PI-3-K-dependent as both events are blocked by wortmannin. In these TIRF-based experiments, stable docking of GSVs at the cell surface were completely inhibited (Bai et al., 2007). Koumanov *et al* have presented data from an *in vitro* fusion assay that supports a role for PI-3-K in the fusion process, since use of plasma membrane derived from wortmannin-treated cells inhibited fusion (Koumanov et al., 2005). Interestingly, Munc-18c knockout mice are insensitive to wortmannin

treatment, which implicates Munc-18c as the PI-3-K-mediated fusion step. Further data from this fusion assay has supported a role for PKB/Akt in mediating GSV fusion. A low temperature block ($19^{o}C$), which inhibits PKB/Akt activation but not PI(3,4,5)P-3 production, causes an accumulation of GSVs beneath the cell surface. This data implies that PKB/Akt, not PI-3-K, is the key mediator of GSV fusion events (van Dam et al., 2005). Therefore, the requirement of PI-3-K for GSV docking and fusion with the cell surface may be because PI-3-K is upstream of PKB/Akt.

This question has been addressed in recent studies using the PKB/Akt inhibitor Akti. Gonzalez and McGraw (Gonzalez and McGraw, 2006) observed that pharmacological inhibition of PKB/Akt did not reduce the fusion competency of GSVs, but rather reduced the amount of GSVs recruited to the TIRF zone. This data has been replicated by another, more recent, TIRF microscopy-based study (Lopez et al., 2009) and points to a role for PKB/Akt in the recruitment of GSVs to the plasma membrane rather than in GSV fusion with the plasma membrane. However, inhibition of an upstream process is likely to influence downstream events. For example, a reduction in GSV translocation to the cell surface will cause a reduction in observed fusion events.

These data taken together generally support a model by which insulin stimulates GSV translocation to a region in close proximity to the cell surface. This is achieved via a PKB/Akt-dependent mechanism. GSV docking and fusion at the plasma membrane then occur in a PI-3-K-dependent, PKB/Akt-independent manner. Contrary to this hypothesis, it has been reported that inhibition of PI-3-K using wortmannin did not inhibit GSV trafficking to the cell surface (Kawaguchi et al., 2008). This indicates that GLUT4 translocation is a PI-3-K-independent process. This is supported by data from an independent method (van Dam et al., 2005). In addition, a role for PKB/Akt at the plasma membrane has been implied by mathematical clustering analysis of data from an investigation into the kinetics of PKB/Akt activation and substrate phosphorylation (Ng et al., 2009). Here, PKB/Akt activation at the plasma membrane (rather than whole cell PKB/Akt activation) highly correlated with PKB/Akt substrate phosphorylation and GLUT4 translocation. The discrepancies described here need to be addressed to in order to fully understand the role of PI-3-K and PKB/Akt in GLUT4 translocation and GSV docking and fusion.

Over-expression of the 4P-TBC1D4/AS160 mutant in L6 cells reported only a partial inhibition of GLUT4 accumulation beneath the cell surface (Randhawa et al., 2008). Therefore, the inhibition of GLUT4 translocation by the 4P mutant cannot be purely attributed to inhibition

of GLUT4 trafficking from an intracellular location to the plasma membrane. This implies a role for TBC1D4/AS160 in GSV interaction with the cell surface. This has been supported by data from another study, where TBC1D4/AS160 has been identified to play a role in the docking of GLUT4 vesicles, although not involved in vesicle fusion (Jiang et al., 2008). These data suggest that the primary role for TBC1D4/AS160 maybe in regulating the interaction between GSVs and the cell surface (Bai et al., 2007).

A protein complex essential for the tethering and docking of membrane vesicles in budding yeast, known as the exocyst complex, has been shown to be required for GLUT4 insertion into the cell surface membrane (Inoue et al., 2003; Inoue et al., 2006; Ewart et al., 2005). However, there is conflicting data as to the importance of the exocyst in insulin-stimulated GLUT4 translocation. For example, expression of an Exo70 mutant in 3T3-L1 adipocytes inhibited GLUT4 accumulation at the cell surface (Inoue et al., 2003). This same mutant expressed in primary adipocytes has been reported to enhanced GLUT4 docking with the plasma membrane and did not reduce GSV fusion with the cell surface (Lizunov et al., 2009).

Further work into the specific effects of insulin-stimulation at the plasma membrane in modulating GSV docking and fusion will be required to further understanding of insulin action at this site. This will be aided by taking advantage of the *in vitro* fusion assay (Koumanov et al., 2005) and through the development and advancement of TIRF microscopy and analysis programmes.

1.4.11 Role of calcium in GLUT4 vesicle translocation and fusion

It is generally considered that changes in intracellular Ca^{2+} levels are not involved in insulin-mediated glucose uptake (reviewed in (Lanner et al., 2008)). However the observation that global Ca^{2+} levels do not change in response to insulin may not be as illuminating as information on localised Ca^{2+} ion fluxes at the cell surface. For instance, it has been reported that insulin-stimulation increases the amount of free Ca^{2+} just beneath the plasma membrane in skeletal muscle fibres (Bruton et al., 2001). This increase is achieved by an influx of Ca^{2+} into the cell. The channel responsible for this influx has not yet been identified. In addition, the Ca^{2+}-chelator BAPTA-AM has been used to study the requirement for Ca^{2+} in GLUT4 translocation and GSV fusion. BAPTA-AM strongly inhibits GLUT4 trafficking to the cell periphery and insertion into the

cell surface (Lopez et al., 2009). However, this method does not differentiate between an overall requirement for Ca^{2+} in GLUT4 translocation and an insulin mediated change in Ca^{2+} levels at the cell surface. In addition, BAPTA-AM has been reported to have several off-target effects and so is not the ideal method for investigating the requirement for Ca^{2+} in GLUT4 translocation.

The Ca^{2+} sensor required for insulin-stimulated GLUT4 translocation has not yet been identified. A recent study in synaptotagmin-VII-knockout mice revealed a requirement for this Ca^{2+}-dependent protein in insulin-mediated GLUT4 translocation in adipocytes, but not skeletal muscle (Li et al., 2007). Doc2β and Rip11, which translocate to the plasma membrane upon insulin-stimulation (Fukuda et al., 2009; Welsh et al., 2007), contain C2 domains which bind Ca^{2+} in order to coordinate lipid binding (Lindsay and McCaffrey, 2004; Kojima et al., 1996). Although a requirement for Ca^{2+} in Rip11 binding to phospholipids has not been identified, it has been established that Doc2β is recruited to the cell surface in a Ca^{2+}-dependent manner (Kojima et al., 1996).

As described above, Myo1c activity has been reported to be increased following insulin stimulation. The proposed model for this activation is that insulin-stimulation results in a localised increase in Ca^{2+} at the plasma membrane. Subsequent activation of the Ca^{2+}/calmodulin-dependent protein kinase II (CamKII) results in phosphorylation of Myo1c. This phosphorylation increases the ATPase activity of Myo1c, which may enhance GSV trafficking along cortical actin filaments beneath the cell surface. Since this increase in Myo1c ATPase activity is regulated by Ca^{2+}, this provides indirect evidence that Ca^{2+} levels are modulated at localised sites to activate specific processes in response to insulin-stimulation. With the advancement in imaging techniques and TIRF microscopy, it will be important to try and identify localised changes in Ca^{2+} ion concentration.

1.5 Insulin-independent pathways linked to glucose transport

In skeletal muscle, contraction and exercise also enhance glucose transport. The signalling pathways involved in contraction- and exercise-mediated glucose transport have been extensively studied. In response to these stimuli, an acute increase in glucose uptake is achieved through redistribution of GLUT4 to the plasma membrane. This is the same mechanism by which insulin enhances glucose uptake. There is a wealth of experimental evidence that contraction

operates via distinct signalling cascades to insulin in skeletal muscle. For example, insulin-stimulation and contraction are additive in enhancing glucose transport (Lund et al., 1995). In addition, although there are some contradictory reports, contraction-mediated glucose uptake in skeletal muscle is generally held to be insensitive to the PI-3-K inhibitor wortmannin (Lund et al., 1995; Hayashi et al., 1998; Wojtaszewski et al., 1996). In contrast, contraction-stimulated glucose uptake and GLUT4 translocation in cardiomyocytes is sensitive to wortmannin (Yang and Holman, 2005). Considering this, there may be subtle differences in how contraction signals to enhance glucose uptake between muscle sub- and fibre-types. Figure 1.5 illustrates several distinct signalling molecules implicated in contraction-stimulated glucose uptake and GLUT4 translocation. Importantly, contraction-, exercise-, hypoxia- and direct AMPK-activation-mediated mechanisms leading to glucose uptake remain intact in insulin-resistant individuals (Kennedy et al., 1999; Thorell et al., 1999; Azevedo, Jr. et al., 1995; Ryder et al., 2000; Koistinen et al., 2003). Therefore, further characterisation of these signalling pathways uptake may reveal therapeutic targets for bypassing insulin resistance.

A further consideration is the adaptations that take place in muscle in response to prolonged contraction or exercise resulting in increased insulin-independent glucose uptake and increased insulin-sensitivity. This is an active area of research driven by the known therapeutic benefits of exercise to type 2 diabetics.

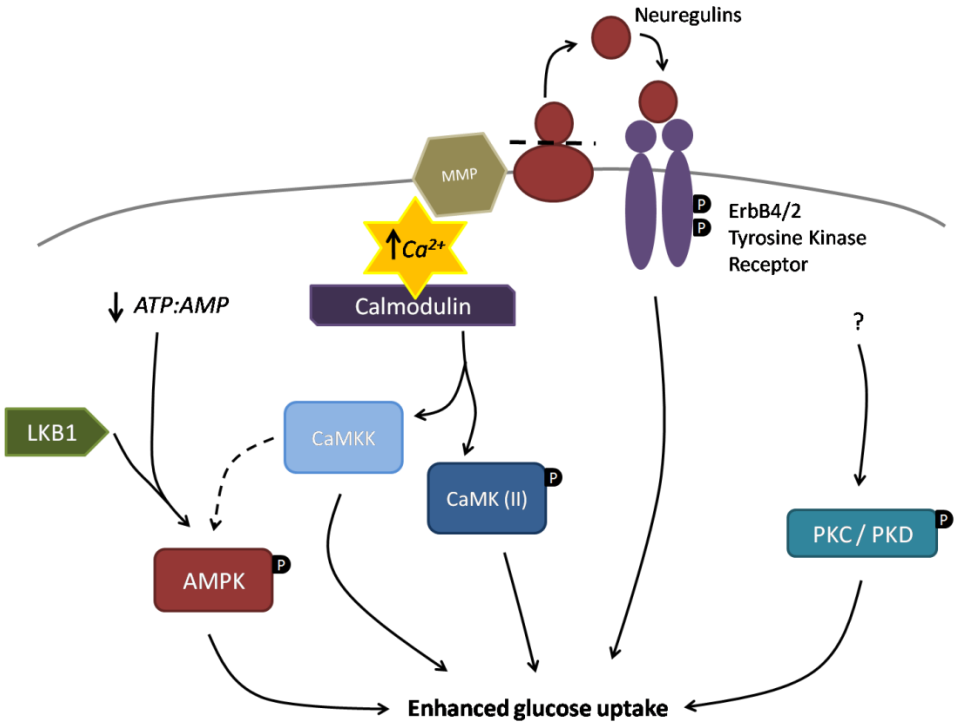

Figure 1.5. Insulin-independent pathways leading to enhanced glucose uptake. A change in the cellular energy-status during exercise or contraction lowers the ATP:AMP ratio and activates AMPK. AMPK activation by phosphorylation is mediated by LKB1. Increased intracellular calcium levels in muscle during contraction results in activation of Ca^{2+}/calmodulin-dependent proteins kinases and in the cleavage of neuregulin receptors by membrane metallo-proteases (MMP). Neuregulins activate ErbB4/2 tyrosine kinase receptors which can stimulate glucose transport into muscle cells. Ca^{2+}/calmodulin-dependent proteins kinases can signal more directly to enhance glucose uptake (CaMKII) or may signal to AMPK via CaMKK. Atypical PKCs or PKD are also activated by contraction, although the mechanism of activation is not known.

1.5.1 AMP-activated protein kinase (AMPK)

AMPK is activated by changes in the cellular energy status, as would occur in muscle during periods of high contractile activity (i.e. during exercise). AMPK is the most studied kinase in the context of insulin-independent glucose uptake in muscle. This kinase acts to maintain or elevate ATP levels within the cell and, as such, plays a role in regulating whole-body energy homeostasis

(Kahn et al., 2005; Leff, 2003; Kim and Lee, 2005). Accordingly, AMPK is activated in response to a drop in the ATP:AMP ratio, the glycogen content of the cell or as a result of hormonal signalling (reviewed in (Carling, 2004)). Activation of AMPK switches metabolism from an anabolic to a catabolic state. This is achieved though the acute regulation of metabolic enzymes and longer term regulation of gene expression.

AMPK is a heterotrimeric protein consisting of a catalytic subunit (α1 or α2) and two regulatory subunits (β1 or β2 and γ1, γ2 or γ3). 12 different AMPK complexes have been identified. The most abundant heterotrimers present in a particular muscle-type is both fibre-type- and strain/species-dependent. For example, Chen *et al.* state that rat soleus muscle (an oxidative muscle-type) contains only α2β1 whereas in rat EDL muscle (a glycolytic muscle-type) α2 associates with both β1 and β2 (Chen et al., 1999). In contrast, Trebek *et al.* have published that α2β2γ1 is by far the most abundant trimer of AMPK in the soleus and EDL muscle of 129S6/sv and C57BL/b mice (Treebak et al., 2009a). In addition to these differences in subunit expression, differential AMPK subunit activation in response to exercise in different muscle fibre-types has been reported (Lee-Young et al., 2009).

There are several levels of regulation of AMPK activity. As with its yeast homologue SNF1, AMPK kinase activity is enhanced over 100-fold by phosphorylation of the threonine 172 residue in the T-loop region of the α-subunit (Suter et al., 2006). This phosphorylation site is the target of upstream kinases. LKB-1 was the first AMPK kinase identified (Hawley et al., 2003; Woods et al., 2003a). Subsequently, additional kinases such as Ca2+/calmodulin-dependent protein kinase kinase β (CaMKKβ) (Hawley et al., 2005; Woods et al., 2005; Hurley et al., 2005) and transforming growth factor-β-activated kinase (Tak1) (Momcilovic et al., 2006) have been discovered. There are additional phosphorylation and auto-phosphorylation sites in the α- and β-subunits which may further regulate AMPK activity and localisation (Warden et al., 2001; Woods et al., 2003b).

AMPK kinase activity is also regulated by AMP binding. The γ-subunit is able to bind three AMP molecules via 'Bateman domains'. The effect of AMP binding is two-fold. Firstly, AMP binding allosterically activates AMPK (Suter et al., 2006). Secondly, AMP binding indirectly inhibits dephosphorylation of threonine 172 (Sanders et al., 2007). This two-pronged effect makes AMPK extremely sensitive to changes in the cellular ATP:AMP ratio. The kinase is therefore a very effective cellular energy-status sensor. In accordance with this role, AMPK

activity is also regulated by glycogen. The β-subunit has a glycogen binding domain which results in inhibition of AMPK activity under conditions were cellular glycogen content is high.

AMPK activation by the AMP analogue 5-aminoimidazole-4-carboxamide ribonucleoside (AICAR) or by hypoxia in skeletal muscle correlates with enhanced glucose uptake. AICAR- or hypoxia-stimulation and muscle contraction do not additively enhance glucose transport, which indicates that AMPK is involved in contraction signalling to glucose uptake (Azevedo, Jr. et al., 1995; Cartee et al., 1991). AMPK activation has also been reported to increase glucose transport in other muscle cell types or models. Activation of AMPK by hypoxia and by mitochondrial toxins such as oligomycin increase glucose uptake into cardiomyocytes (Yang and Holman, 2005; Yang and Holman, 2006). GLUT4 translocation following AMPK activation has also been studied in the L6 cell culture model. In this model, several AMPK activators including AICAR, the mitochondrial inhibitor DNP, IL-6 and adiponectin have been reported to increase cell surface GLUT4 levels (Stockli et al., 2008). In addition, the recently described small molecule AMPK activator A-769662 enhances glucose uptake in L6 cells (Guigas et al., 2009).

Despite these data, there is convincing evidence from transgenic mice that AMPK is not the sole mediator of contraction-stimulated glucose transport. For example, inhibition of AMPK activity in both glycolytic and oxidative muscle fibres by transgenic disruption of the α2-subunit or γ3-subunit of AMPK resulted in complete inhibition of AICAR-stimulated glucose uptake (Mu et al., 2001; Barnes et al., 2004; Jorgensen et al., 2004). However, these transgenic mouse models still exhibit enhanced, albeit slightly attenuated, glucose transport into skeletal muscle in response to contraction. Any modest reduction in contraction-mediated glucose transport in these transgenic mice may be a result of these transgenic mice generating less force during contraction than wild-type mice, rather than a direct effect of reducing AMPK levels (Fujii et al., 2005).

Interestingly, LKB-1 knockout mice have a more profound decrease in contraction-stimulated glucose uptake (Sakamoto et al., 2005). Reduction of muscle LKB-1 levels to 10% of normal level largely blocked contraction-induced glucose uptake in EDL muscle. These data imply that a LKB-1-dependent kinase other than AMPK may play a role in contraction signalling to increase glucose uptake. Investigations into other AMPK kinases such as Fyn kinase (Vatish et al., 2009) and LKB-1 substrates such as SNARK (Rune et al., 2009) are currently ongoing.

In addition to the varying expression of AMPK subunit isoforms in different muscle types, distinct stimuli that activate AMPK and glucose transport may do so through different AMPK subunit isoforms. For example, AMPK γ3-subunit is highly expressed in glycolytic muscle fibres (Mahlapuu et al., 2004) and is required for AICAR- and hypoxia- but not contraction-stimulated glucose transport (Barnes et al., 2004; Deshmukh et al., 2009). This is surprising given that α2β2γ3 is the complex most activated by exercise in humans (Birk and Wojtaszewski, 2006). The diverse requirement for the AMPKγ3 isoform in contraction-, AICAR- and hypoxia-stimulated glucose transport exemplifies the complexity in signalling pathways that stimulate glucose uptake into skeletal muscle.

Since AMPK plays a role in regulating energy (e.g. glucose) intake, utilisation and storage, it is a prime target for treatment of metabolic syndromes such as type 2 diabetes (Winder and Hardie, 1999). Administration of the AMPK activator AICAR to mouse models of obesity and insulin-resistance reverses many of their metabolic abnormalities (Song et al., 2002; Bergeron et al., 2001; Iglesias et al., 2002). The commonly prescribed anti-diabetic drug metformin is thought to act by reducing circulating glucose levels in insulin-resistant patients through activation of AMPK. Despite the role of AMPK in promoting glucose uptake and storage in muscle, the beneficial effects of metformin can be primarily attributed to its inhibition of gluconeogensis in the liver (Shaw et al., 2005; Owen et al., 2000). Additional activation of AMPK at peripheral sites may provide further beneficial effects.

As described above, hypoxic conditions, metformin, DNP, oligomycin and other mitochondrial inhibitors are used experimentally to activate AMPK by inhibiting ATP production (El Mir et al., 2000; Owen et al., 2000). This has the net result of decreasing the ATP:AMP ratio. The most commonly used pharamcological AMPK activator is AICAR. AICAR artificially decreases the ATP:AMP ratio through its conversion to an AMP analogue, ZMP. In this way, AICAR is extremely effective at activating AMPK. However, AICAR, and other molecules that activate AMPK by altering the ATP:AMP ratio, activate AMPK indirectly and as a result may have off-target effects. For example, AICAR has been reported to also have an effect on the activity of other enzymes modulated by AMP binding such as glycogen phosphorylase (Longnus et al., 2003) and fructose-1,6-bisphosphatase (Vincent et al., 1996).

A more direct and specific activator of AMPK has recently been described (Cool et al., 2006). The AMPK activator A-769662 was optimised from a lead generated from an initial screen

of over 700,000 compounds. Administration of A-769662 to ob/ob mice resulted in similar metabolic improvements as observed following treatment with AICAR, such as reduced body weight and lower plasma glucose and triglyceride levels. A-769662 activates AMPK independently of AMP binding, and shows some similarities to the mechanism of activation of AMPK by AMP. Goransson *et al.* report that A-769622 binding to AMPK causes both an allosteric activation of AMPK and an inhibition of threonine 172 dephosphorylation (Goransson et al., 2007). These effects are dependent on A769662 binding to the β1 subunit of the heterotrimeric complex. As such this activator exclusively activates AMPK heterotrimers containing the β1 subunit (Scott et al., 2008).

A-769662-stimulated glucose transport has been reported in L6 myotubes (Guigas et al., 2009). The AMPK-specificity of this effect has been questioned by a study in isolated skeletal muscle (Treebak et al., 2009a). In this study, wortmannin inhibited A-769662-induced glucose uptake. Therefore, it was concluded that A-769662 may enhance glucose transport via the PI-3-K pathway. This is clearly an off-target effect. A key difference between these studies is the concentration of A-769662 used. The maximum concentration used in L6 calls was 100 μM, whereas 500 μM – 1 mM was used to stimulate the isolated skeletal muscle. It may be that AMPK activation by A-769662 is less efficient in isolated skeletal muscle than in cultured cells. Therefore, the higher concentration of A-769662 required for AMPK activation may result in some off-target effects. Further characterisation of A-769662-induced AMPK activation may provide important data to aid the design of novel molecules to activate AMPK in patients with metabolic disorders such as type II diabetes.

1.5.2 Calcium-mediated signalling

During muscle contraction there is a large increase the cytosolic Ca^{2+} concentration due to Ca^{2+} release from the sarcoplasmic reticulum. It has been proposed that this increase in intracellular Ca^{2+} activates Ca^{2+}/calmodulin (CaM) sensitive pathways and kinases which stimulate glucose uptake. In particular, Ca^{2+}/calmodulin-dependent protein kinase II (CaMKII) is activated by contraction (Rose et al., 2007) and has been implicated in contraction-stimulated glucose transport (Wright et al., 2005).

A role for CaM-sensitive pathways in contraction-stimulated glucose uptake is supported by evidence from rat epitrochlearis muscle where the Ca^{2+}/calmodulin competitive inhibitor KN-93 decreased contraction-induced glucose uptake by inhibiting CaMK phosphorylation and activation. In oxidative muscle types, contraction-stimulated glucose uptake has been identified to be completely dependent on Ca^{2+}-mediated pathways (Wright et al., 2005). In contrast, contraction-stimulated glucose transport is dependent on both AMPK- and Ca^{2+}-dependent pathways in glycolytic muscle fibres (Wright et al., 2004).

It has been proposed that CaMK or CaMKK may be an upstream kinase for AMPK. This hypothesis has been derived from work in cell lines were Ca^{2+}/calmodulin have been reported to activate AMPK via CAMKKα and β (Hurley et al., 2005; Hawley et al., 2005). There is evidence both for and against this hypothesis. Inhibition of Ca^{2+}/calmodulin by KN-93 or the direct CaMK kinase inhibitor STO-609 in mouse EDL and soleus muscle inhibited contraction-mediated glucose uptake by blocking AMPK activation (Jensen et al., 2007). This implies a link between increasing Ca^{2+} concentration and AMPK activation. In contrast, other studies have reported that KN-93-mediated inhibition of contraction-stimulated glucose uptake occurred in the absence of any effect on AMPK activation. Therefore contraction activates and signals via CaMK independently of AMPK (Wright et al., 2004; Witczak et al., 2007). The use of an inhibitor of Ca^{2+} release from the sarcoplasmic reticulum (Dantrolene) (Cartee et al., 1991; Wright et al., 2004) has also revealed an important role for Ca^{2+} in hypoxia-stimulated glucose transport. Therefore, in addition to AMPK pathways, Ca^{2+}-dependent pathways regulate glucose transport in response to hypoxia. The muscle fibre types used in these studies described above differed, and this may provide a reason for the contrasting results.

An increase in Ca^{2+} levels following contraction activates neuregulin receptors. This family of receptors are related to EGF and act as autocrine factors. Neuroregulins activate ErbB receptors, which are tyrosine kinase receptors (Citri et al., 2003; Tzahar et al., 1996). Blocking the activation of ErbB4 using an ErbB4 blocking antibody in oxidative muscle, which has limited AMPK signalling, impairs contraction-induced glucose uptake (Canto et al., 2006). The inhibition is less pronounced in glycolytic EDL fibres. These findings support the hypothesis that oxidative fibres are more reliant on Ca^{2+} mediated signalling in their contraction response than glycolytic fibres. The finding that neuregulins can stimulate glucose uptake into muscle is supported by work in L6 cells (Canto et al., 2004).

1.5.3 Protein kinase C

PKC and, more recently, Protein Kinase D (PKD) have also been implicated in contraction-stimulated glucose uptake. PKC has also been reported to be involved in insulin-mediated GLUT4 translocation in adipocytes as described above (1.4.7). The involvement of cPKCs and nPKCs in contraction-stimulated glucose uptake is supported by pharmacological inhibitors of these PKC isoforms. However, only aPKCs have been shown to be activated by contraction stimulus. This is surprising given that this subfamily of PKCs is not dependent on Ca^{2+} for activation. Indeed, contraction-stimulated glucose uptake is unaffected in muscle lacking PKCα (which accounts for 97% of muscle cPKCs) (Jensen et al., 2009). This indicates that results gained using pharmacological inhibitors of cPKCs are likely to be a result of non-specific effects on contraction signalling. A study in EDL muscle and L6 cells has reported a link between aPKC activation and AMPK activation (Chen et al., 2002). Further investigation of this putative interaction is required. In addition, depolarisation (mimicking contraction) of L6 cells resulted in increased cell surface GLUT4 levels by a mechanism dependent on PKC. The isoform specificity of this effect however remains to be elucidated (Wijesekara et al., 2006).

One study in cardiomyocytes has identified that PKD (also known as PKCμ) is activated following electrically-induced contraction (Luiken et al., 2008). This study determined that PKD is required for contraction- and oligomycin stimulated GLUT4 translocation. The activation of PKD is independent of the activation of AMPK and cardiac PKC isoforms. The fact that PKD is known to phosphorylate cardiac-troponin-I may link enhanced contractile activity to increased glucose uptake. The mechanism by which PKC isoforms and PKD are activated by contraction-stimulation has not yet been elucidated.

1.5.4 Potential convergence of signalling pathways leading to glucose uptake in muscle

The presence of distinct signalling pathways leading to glucose uptake and GLUT4 translocation raises the question as to whether these initially distinct pathways are convergent. Investigations into molecules at which insulin- and exercise/contraction-stimulated signalling pathways converge may have pathophysiological relevance in attempting to bypass the point of failure in

insulin-mediated GLUT4 translocation in insulin-resistant patients. Recently, a large number of publications have focussed on the Rab-GAPs TBC1D4/AS160 and TBC1D1 as the point of convergence for insulin- and exercise/contraction-stimulated signalling. These proteins are thought to act to bridge signalling and membrane trafficking events and are therefore a logical convergence point.

TBC1D4/AS160 is phosphorylated in response to insulin-, contraction- and AICAR-stimulation (Kramer et al., 2006a; Jessen and Goodyear, 2005; Treebak et al., 2006; Kramer et al., 2006b; Geraghty et al., 2007; Treebak et al., 2009b). Studies into the phosphorylation status of TBC1D4/AS160 have primarily been conducted using the anti-phospho PKB/Akt substrate antibody (PAS), which recognises phosphorylated forms of the PKB/Akt consensus motif. Investigations into the phosphorylation status of both TBC1D4/AS160 and TBC1D1 in response to insulin and contraction have been studied by Cartee's laboratory using the PAS antibody. An increase in immuno-reactivity of TBC1D4/AS160 and TBC1D1 with the PAS antibody has been reported in response to contraction stimulation in an AMPK-dependent manner (Bruss et al., 2005; Funai and Cartee, 2009). This is surprising given that PKB/Akt is not required for this phosphorylation. Although not yet fully addressed in the literature, the reason that AMPK activation enhances TBC1D4/AS160 PAS-reactivity may be that the main PKB/Akt phosphorylation site (threonine 642) also has some similarity to an AMPK consensus motif. Another explanation is that the PAS-antibody recognises phosphorylated serine 588. This site has been reported to be phosphorylated following treatment with AICAR (Geraghty et al., 2007), although this site does not strictly resemble an AMPK consensus site. In either case, the observation that AMPK phosphorylates TBC1D4/AS160 using the PAS antibody was serendipitous, given that it would not have been made if AMPK-mediated phosphorylation had occurred at a more stringent AMPK consensus site (or a site less similar to a PKB/Akt consensus site). Having raised this point, it should also be considered that the threonine 642 (or serine 588) site may have evolved to act as both a PKB/Akt and AMPK phosphorylation site in order to allow convergence of signalling from these kinases. Therefore, although these studies have yielded some interesting results, the use of the PAS antibody to investigate AMPK (or other kinase) mediated phosphorylation of TBC1D4/AS160 and TBC1D1 is not ideal as it is biased towards phosphorylation sites that are similar to the PKB/Akt consensus motif. In addition, the PAS antibody exhibits preferential binding to some PKB/Akt phosphorylation sites, for example threonine 596 in TBC1D1 (Pehmoller et al., 2009).

More recently, a study of TBC1D1 phosphorylation status in response to contraction in AMPK knockout mice has used site-specific antibodies (Pehmoller et al., 2009). The use of such antibodies will be vital in characterising the role of TBC1D4/AS160 and TBC1D1 phosphorylation in agonist-stimulated glucose transport. They will also be a useful tool in establishing to what extent distinct signalling pathways converge at these Rab-GAPs.

Pharmacological inhibition of PKB/Akt or AMPK by wortmannin or Compound C, respectively, has revealed differential regulation of TBC1D1 and TBC1D4/AS160 phosphorylation in response to contraction as measured by PAS antibody reactivity in rat epitrochlearis muscle (Funai and Cartee, 2009). Inhibition of AMPK completely inhibited contraction-stimulation TBC1D1 PAS-reactivity. Wortmannin inhibited contraction-mediated TBC1D4/AS160 PAS-reactivity, implying that this phosphorylation is mediated by PKB/Akt and not AMPK. Both TBC1D1 and TBC1D4/AS160 are phosphorylated by PKB/Akt in response to insulin in this muscle type. These data imply that, although TBC1D4/AS160 and TBC1D1 are phosphorylated following both insulin- and contraction-stimulation in this muscle type, only TBC1D1 is a true candidate to be considered as a site of convergence for distinct (PKB/Akt and AMPK) signalling pathways.

In addition to TBC1D4/AS160 acting as a substrate for the distinct kinases activated by insulin- and contraction-stimulation, this Rab-GAP also binds to calmodulin in a Ca^{2+}-dependent manner (Kane and Lienhard, 2005). The identification of the calmodulin binding domain (CDB) in close proximity to the GAP domain offered another potential level of TBC1D4/AS160 regulation. The role of calmodulin binding in contraction-stimulated glucose transport has been studied in mouse TA muscle (Kramer et al., 2006a). Over-expression of TBC1D4/AS160 without the CBD did not inhibit insulin-stimulated glucose transport. However, contraction-stimulated glucose transport was inhibited to a similar level as seen with the TBC1D4/AS160-4P mutant. In agreement with this comparison, over-expression of a mutant without a CBD and without GAP activity relieved this inhibition. This inhibition occurred despite normal contraction-induced phosphorylation of TBC1D4/AS160. Therefore, contraction-mediated glucose uptake requires both contraction-induced phosphorylation of, and calmodulin binding to, TBC1D4/AS160. Although this study revealed additional sites of regulation of TBC1D4/AS160 the muscle fibre type used in the study (TA) has now been reported to express low levels of TBC1D4/AS160. TBC1D1 is the major Rab-GAP expressed in this muscle type. Therefore, although it is desirable that over-expression of TBC1D4/AS160 will have a dominant effect over endogenous TBC1D4/AS160, the dominance of the electroporated constructs over endogenous TBC1D1 is an

important consideration and may influence interpretation of the data. TBC1D1 also contains a CBD (Roach et al., 2007), although It remains to be determined if there is a similar calmodulin-dependent regulation of TBC1D1. In addition to this Ca^{2+}/calmodulin-mediated effect on TBC1D4/AS160, a correlation between the kinetics of CaMK II activation and TBC1D1 and TBC1D4/AS160 phosphorylation in response to contraction has been reported (Funai and Cartee, 2008). A role for this kinase in the direct phosphorylation of these Rab-GAP proteins is yet to be determined. The relative importance of Ca^{2+}-/calmodulin-mediated regulation of TBC1D4/AS160 and TBC1D1 compared to phosphorylation of these Rab-GAPs needs to be established. If TBC1D4/AS160 and TBC1D1 are preferentially targeted by different (PKB/Akt vs. AMPK) kinases, it may be that contraction is able to effectively signal through changes in intracellular Ca^{2+} levels to regulate the activity of both Rab-GAPs.

Despite the evidence that AMPK phosphorylates TBC1D4/AS160, sequence scanning of this Rab-GAP in ScanSite (scansite.mit.edu) does not reveal any high stringency AMPK phosphorylation motifs. In contrast, similar scanning of TBC1D1 reveals several AMPK sites. As discussed previously, a multitude of sites of TBC1D1 have been reported to be phosphorylated in response to AMPK activation both *in vitro* and *in vivo*. Activation of AMPK and subsequent phosphorylation at serine 237 (the most stringent AMPK consensus motif) enhances 14-3-3 binding to TBC1D1 (Chen et al., 2008). The differential phosphorylation and 14-3-3 binding to TBC1D4/AS160 and TBC1D1 (described in detail above) in response to insulin-stimulation and AMPK-activation suggest that TBC1D1 and TBC1D4/AS160 may serve complementary rather than redundant roles in regulating GSV trafficking.

Further characterisation of the role of AMPK in contraction-mediated phosphorylation of TBC1D1 has been carried out in mice overexpressing an inactive form of the AMPK α2 subunit (Pehmoller et al., 2009). This study investigated individual AMPK phosphorylation sites using antibodies specific to phosphorylated serine 237 or threonine 596. In EDL muscle, contraction and AICAR induced the phosphorylation of serine 237 and threonine 596 in an AMPK-dependent manner. This was accompanied by an increase in 14-3-3 binding to TBC1D1. In support of data obtained in L6 cells (Chen et al., 2008), insulin-stimulation of EDL muscle did not result in phosphorylation of serine 237. Surprisingly, insulin-stimulated phosphorylation of threonine 596 was abolished in mice overexpressing catalytically inactive AMPK. This may indicate that TBC1D1 is primarily regulated by AMPK and that phosphorylation of sites other than threonine 596 by AMPK is required to prime TBC1D1 for insulin-stimulated phosphorylation of threonine 596.

In a study investigating the role of TBC1D4/AS160 translocation to the cytosol in mediating GLUT4 translocation, it was reported that insulin-stimulation results in TBC1D4/AS160 translocation to the cytosolic fraction (from GSVs). In contrast, other stimuli leading to GLUT4 translocation such as the AMPK activators Berberine and AICAR did not result in TBC1D4/AS160 translocation to the cytosol (Stockli et al., 2008). Although this data is presented as evidence that TBC1D4/AS160 translocation to the cytosol is not required for GLUT4 translocation to occur, another explanation is that these AMPK-activators mediate GLUT4 translocation through targeting TBC1D1 rather than TBC1D4/AS160. Therefore, TBC1D1 may translocate to the cytosol in response to AMPK activation. The fact that this study and others have reported inhibition of AMPK-stimulated GLUT4 translocation by the TBC1D4/AS160-4P may indicate that this over-expression of this construct has a dominant negative effect on both TBC1D4/AS160 and TBC1D1.

A more thorough investigation into a role for TBC1D4/AS160 in GLUT4 translocation in response to a range of agonists in L6 cells revealed a differential requirement or TBC1D4/AS160 between agonists (Thong et al., 2007). Over-expression of TBC1D4/AS160 inhibited GLUT4 translocation in response to insulin-, PDGF-, AICAR-stimulation and K^+-induced depolarisation. Again, the interpretation of these data may be complicated by the possibility that this TBC1D4/AS160 construct may be dominant over endogenous TBC1D4/AS160 and TBC1D1. In contrast, DNP- and hypertonicity-stimulated cell surface GLUT4 enhancement was not inhibited by over-expression of the mutant construct. Since these agonists have been reported to increase cell surface GLUT4 by inhibiting GLUT4 internalisation, this data supports a role for TBC1D4/AS160 in regulating GLUT4 exocytosis. It should also be noted that although DNP is a mitochondrial inhibitor and therefore activates AMPK, DNP-stimulated increase in cell surface GLUT4 is proposed to be independent of AMPK (Thong et al., 2007). These studies in L6 cells have revealed an important role for TBC1D4/AS160 (and/or TBC1D1) in a number of agonists leading to increased GLUT4 at the cell surface. The relative contribution of these different Rab-GAPs in distinct signalling pathways leading to GLUT4 translocation needs to be more fully resolved (Thong et al., 2007).

Stimuli enhancing cell surface GLUT4 levels do so by utilising downstream targets other than TBC1D4/AS160 and TBC1D1. A recent study in AMPKγ3 knockout mice has revealed that TBC1D4/AS160 / TBC1D1-independent mechanisms may contribute to glucose transport in skeletal muscle (Deshmukh et al., 2009). The possibility of the presence of TBC1D4/AS160 / TBC1D1-independent mechanisms is further supported the observation that insulin- and AMPK-

activation differentially affect GLUT4 trafficking kinetics in muscle (Karlsson et al., 2009; Yang and Holman, 2005; Antonescu et al., 2008). In rat and human skeletal muscle, insulin-stimulation enhanced GLUT4 exocytosis whereas AMPK-activation inhibited GLUT4 internalisation (Karlsson et al., 2009). This clearly raises questions over whether both these agonists similarly signal to TBC1D4/AS160 or TBC1D1 (or both). The TBC1D4/AS160 and TBC1D1 Rab-GAPs are implicated in regulating GLUT4 exocytosis. Given that AMPK phosphorylates TBC1D1 and AS160/TBC1D4, AICAR would therefore be expected to modulate GLUT4 exocytosis. Since this study identifies distinct affects of insulin- and AICAR-stimulation on GLUT4 trafficking, it is unlikely that these stimuli converge upon TBC1D4/AS160 or TBC1D1. It would be of interest to extend the study to identify the changes in GLUT4 trafficking induced by contraction-stimulation and to investigate how the phosphorylation status of TBC1D4/AS160 and TBC1D1 relates to changes in GLUT4 trafficking parameters.

From the data described above, it appears that TBC1D4/AS160 acts primarily as a target for activated PKB/Akt, and therefore may regulate insulin-stimulated GLUT4 translocation. In contrast, TBC1D1 is phosphorylated in response to AMPK activation during contraction. Therefore, rather than TBC1D4/AS160 and TBC1D1 acting as points of converge for distinct signalling pathways in a redundant manner, these Rab-GAPs are complementary. However, insulin-stimulation is able to relieve wildtype TBC1D1-induced inhibition of GLUT4 translocation in 3T3-L1 adipocytes (Peck et al., 2009) implying that TBC1D1 may act as a point of convergence between insulin- and AMPK-signalling. Nevertheless, this hypothesis may be supported by the variation in expression levels of the different Rab-GAPs between tissue types and muscle fibre types. For example, adipocytes highly express TBC1D4/AS160 as their primary role is to respond to insulin. The differences in TBC1D4/AS160 and TBC1D1 expression in muscle subtypes may represent the difference in metabolic demands of these fibres. For example, glycolytic fibres, which have a high level of TBC1D1 expression, may fatigue more rapidly in response to contraction than oxidative fibres and therefore may require a Rab-GAP more sensitive to changes in the cellular energy levels. The role of Ca^{2+}/calmodulin regulation of TBC1D4/AS160 and TBC1D1 activity following increases in intracellular Ca^{2+} levels may provide a mechanism by which both oxidative (highly expressing TBC1D4/AS160) and glycolytic (highly expressing TBC1D1) fibres increase glucose uptake rapidly in response to contraction. A recent study in 3T3-L1 adipocytes has revealed that phosphorylation of serine 588 in TBC1D4/AS160 in response to insulin-stimulation is mediated by atypical PKC (Ng et al., 2009). Since these PKCs are also

activated following contraction, this site may be phosphorylated in response to contraction-stimulation.

In addition to TBC1D4/AS160 and TBC1D1, the PKB/Akt substrate PIKfyve may act as mediator of GLUT4 translocation in response to insulin and other stimulators of glucose transport. PIKfyve has been observed to be phosphorylated in CHO-T cells under hyperosmotic stress via a PI-3-K-independent kinase (E. Hill and J.Tavaré, unpublished observations revealed in (Leney and Tavare, 2009)). Hyperosmotic stress has been reported to induce GLUT4 translocation in both 3T3-L1 adipocytes and L6 muscle cells. Therefore, PIKfyve may act as point of convergence for these stimulators of GLUT4 translocation. This hypothesis requires further investigation.

1.6 GLUT4 trafficking studies

Enhanced glucose transport is dependent on GLUT4 translocation to the cell surface. This explains the interest in identifying proteins such as the Rab-GAP proteins TBC1D4/AS160 and TBC1D1 which offer a putative link between signalling pathways and GLUT4 trafficking events. In addition, GLUT4 trafficking itself has been extensively studied. GLUT4 is effectively retained at intracellular sites in unstimulated cells. This sequestration is highly regulated and redistribution or translocation of GLUT4 to the cell surface of insulin-responsive cells is necessary for whole-body glucose homeostasis. Furthermore, under insulin resistant conditions, the amount of GLUT4 within tissues is unchanged (Bjornholm and Zierath, 2005). Therefore, reduced glucose uptake is a result of faulty GLUT4 translocation. This could be caused by disrupted signalling or a more direct affect on GLUT4 trafficking. In some models of insulin resistance, no signalling defect has been identified (Hoehn et al., 2008). By studying GLUT4 trafficking, it may be possible to identify the mechanism of insulin-resistance in these models.

There are a number of eventsin the intracellular trafficking itinerary of GLUT4 which may be regulated by insulin-signalling (Figure 1.6). Larance *et al.* listed these to include the biogenesis of a specialised GSV compartment; delivery of newly synthesised GLUT4 from the TGN to the GSVs, release of GSVs from sequestration; GSV translocation to the cell surface (exocytosis), transport of GSVs; GSV trafficking to the plasma membrane through interaction with cytoskeletal elements (microtubules and actin), tethering; the low affinity interaction

between GSVs and the cell surface, docking; the high affinity binding of GSVs to the plasma membrane through SNARE complex formation and fusion of bilayers, endocytosis; removal of GLUT4 from the cell surface and trafficking to endosomes, resequestration of GLUT4; delivery of internalised GLUT4 from the endosomal system back into a sequestered GSV compartment (Larance et al., 2008; Bryant et al., 2002; Holman and Cushman, 1994).

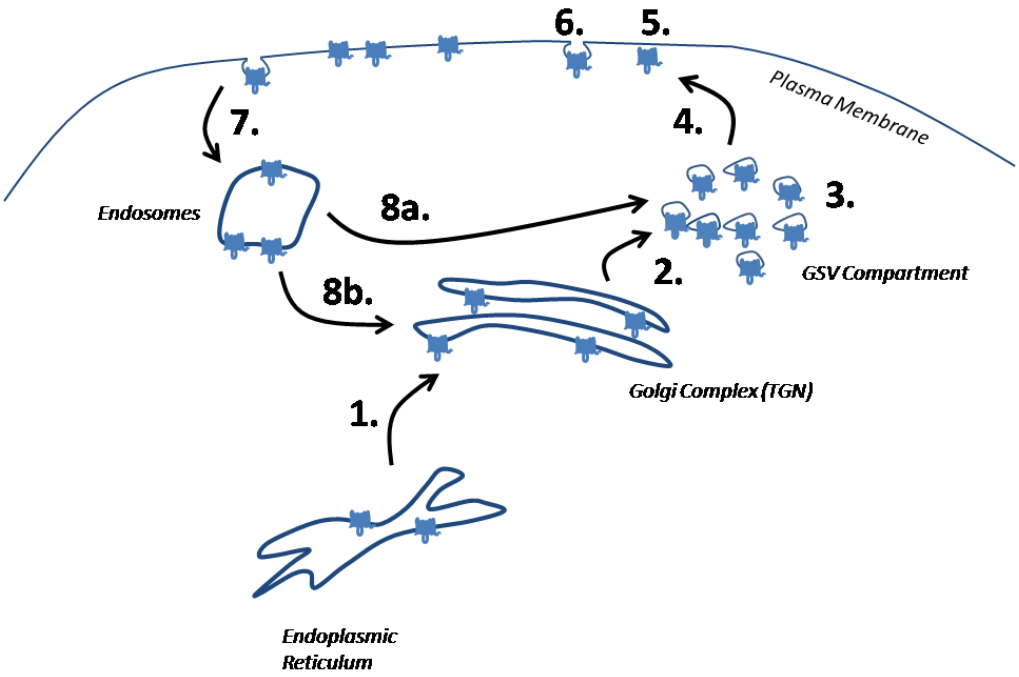

Figure 1.6. GLUT4 trafficking and possible points of insulin-regulation. These include; 1) and 2) delivery of newly synthesised GLUT4 from the TGN to the GSVs, 3) release of GSVs from sequestration 4) GSV translocation to the cell surface (exocytosis), 5) low affinity interaction between GSVs and the cell surface, 6) high affinity docking of GSVs and GSV fusion with the plasma membrane, 7) GLUT4 endocytosis, 8 a and b) resequestration of GLUT4; delivery of internalised GLUT4 from the endosomal system back into a sequestered GSV compartment.

GLUT4 has complex trafficking itinerary. However, when considering a simplified view of GLUT4 trafficking there are three overall mechanisms by which stimuli could modulate GLUT4 trafficking kinetics to enhance GLUT4 cell surface levels. This is a very simplified view of GLUT4 trafficking. Firstly, stimuli could increase GLUT4 exocytosis to increase the rate of its appearance at the plasma membrane. Secondly, insulin-stimulation could release 'static' GSVs to the cell surface and increase the amount of GLUT4 in the general recycling pool. In this model, GLUT4 in

the static GSV compartment must be effectively sequestered from general recycling under basal conditions. Finally, stimuli may act to inhibit the internalisation of GLUT4 from the plasma membrane, thereby enhancing the cell surface GLUT4 content.

Translocation of GLUT4 to the cell surface in response to insulin-stimulation enhances glucose uptake. Therefore, a change in the rate of glucose transport into the cell is related to the amount of GLUT4 at the cell surface. However, although investigating changes in glucose uptake is an important endpoint measurement for investigations into downstream effects of insulin-signalling, measuring this parameter does not explicitly measure GLUT4 relocation to the cell surface. This is because other glucose transporters may contribute to the increase in glucose uptake. For example, increased glucose uptake into 3T3-L1 adipocyte cells in response to insulin-stimulation is not purely mediated by GLUT4 since these cells also express high levels of GLUT1. It has been reported that insulin-stimulation results in a 2-fold increase in cell surface levels of GLUT1, which is localised to recycling endosomes (Foran et al., 1999). Therefore, to specifically measure the characteristics GLUT4 trafficking, a more targeted method is required.

Advances in both reagents and methods have permitted the in depth analysis of GLUT4 trafficking under basal and insulin-stimulated conditions. Such studies can measure two types of trafficking kinetics. These are the kinetics of transition between the GLUT4 distribution in the basal and stimulated state (or vice versa), or the kinetics of GLUT4 trafficking in the steady-state, where GLUT4 recycles between an intracellular location and cell surface but the amount of GLUT4 at each location remains constant. Classical techniques such as subfractionation and western blotting can give information on GLUT4 translocation (transition kinetics), but are limited by the number of time points that can be sampled. In addition, subfractionation is inadequate for steady-state analysis since it is not possible to distinguish between GLUT4 in recycling compartments and GLUT4 in other pathways such as the biosynthetic and degradation pathways.

The development of an impermeant photoreactive glucose molecule that covalently labels GLUTs at the plasma membrane enabled the first targeted studies of GLUT4 transition-state and steady-state trafficking (Jhun et al., 1992; Yang and Holman, 1993; Satoh et al., 1993). These glucose analogues were originally radiolabelled, but more recently have contained a biotin moiety which enables photolabelled GLUTs to be purified (Yang and Holman, 2006; Yang and Holman, 2005). This photolabelling technique is able to bind to both GLUT1 and GLUT4 (or other

glucose transports at the cell surface). Therefore, antibodies are required to distinguish between these different GLUTs by western blotting, and specifically monitor GLUT4 trafficking. GLUT4 exocytosis, endocytosis and recycling has been studied using this photoreactive label. Endpoint measurements of trafficking processes are often difficult to interpret kinetically as they are a combination of both exocytic and endocytic events. For example, GLUT4 translocation to the plasma membrane in response to insulin-stimulation (transition state kinetics) is dependent on both the rate of GLUT4 exocytosis and endocytosis. A further advantage of using these photoreactive labels is that methods can be modified to measure unidirectional GLUT4 trafficking, for example GLUT4 exocytosis in transition state experiments (Karlsson et al., 2009).

Photolabelling experiments designed to investigate changes in GLUT4 trafficking in response to stimulation have been performed in several cell types. Initial steady-state studies in 3T3-L1 adipocytes identified that GLUT4 continuously recycles under basal conditions, and that the major effect of insulin was to increase the rate constant for GLUT4 exocytosis (k_{ex}). Two separate studies identified a similar 3-fold increase in k_{ex} (Jhun et al., 1992; Yang and Holman, 1993). However, these studies reported a very different insulin-induced change in the rate constant for GLUT4 internalisation (k_{in}). Jhun *et al.* reported 3-fold decrease in k_{in}, whilst Yang and Holman noted only a ~30% decrease in k_{in}. Since these initial studies, this photolabelling technique has been used to monitor GLUT4 trafficking in primary adipocytes, cardiomyocytes and skeletal muscle (Satoh et al., 1993; Yang et al., 2002; Karlsson et al., 2009). The controversies in insulin-stimulated changes in k_{in} and findings from GLUT4 trafficking studies in muscle are addressed in detail in subsequent sections (1.6.1 and 1.7).

In 1994, Holman *et al.* modelled prevailing GLUT4 trafficking data from glucose uptake, photolabelling and subfractionation studies (Holman et al., 1994). This modelling process identified that an inhibition of endocytosis alone could not account for the rapid increase in glucose uptake measured in adipocytes. In addition, this study indicated that GLUT4 trafficking behaviour is inconsistent with of GLUT4 trafficking between 2 compartments (plasma membrane and intracellular pool). The addition of a further intracellular compartment to the model (3-compartment model) simulated the properties of GLUT4 trafficking. This extra compartment is required to more readily explain the slow basal exocytosis of GLUT4. This additional pool may refer to the specialised GSV compartment. In addition to modelling basal exocytosis,this extra compartment in which GLUT4 is sequestered can also model the large rapid initial stimulation of GLUT4 translocation to the plasma membrane in response to insulin-stimulation.

Although the photolabelling methods have permitted a significant advancement in understanding GLUT4 trafficking, there are problems associated with this method such as photolabel synthesis and the need for additional purification steps and western blotting. GLUT4 reporter constructs have been developed to bypass these problems. Investigations into GLUT4 trafficking has been greatly aided by these GLUT4 fusion proteins. Despite this, the photolabelling technique is still the best method for investigating the trafficking of endogenous GLUT4.

GLUT4 reporter constructs have been designed to contain a Haemagglutinin (HA) or Myc tag in the first exofacial loop, and can have a C-terminal Green Fluorescent Protein (GFP) tag (HA/Myc-GLUT4-GFP). Variations of this construct exist with only one of the tags described present (HA/Myc-GLUT4, GLUT4-GFP) (Dawson et al., 2001). The GFP tag allows the detection of all cellular GLUT4. However, the exofacial tag enables antibody labelling of only those GLUT4 molecules inserted into the cell surface, exposing the epitope to the extracellular milieu. Therefore these exofacial epitopes label a population of GLUT4 that is presumably in the correct orientation to transport glucose into the cell. Exofacial labelling in this manner is analogous to the labelling obtained with the photoreactive label. However, this antibody labelling is direct and requires no further purification as is necessary with photolabelling. The exofacial epitope-containing fusion proteins have been particularly useful for antibody uptake assays. These fusion proteins have been investigated and are reported to traffic in a similar manner to endogenous GLUT4 (Martin et al., 2006). More recently, transgenic mouse models Myc-GLUT4-GFP and HA-GLUT4-GFP have been developed. Data from our study into GLUT4 trafficking in cardiomyocytes isolated from HA-GLUT4-GFP mice are presented in this thesis (Fazakerley et al., 2009). These transgenic models will be enable the investigation of GLUT4 trafficking in both adipocytes and muscle fibres *in vivo* (Schertzer et al., 2009).

Several studies have taken advantage of HA-epitope containing GLUT4-fusion proteins to investigate steady-state GLUT4 trafficking in 3T3-L1 adipocytes (Martin et al., 2006; Karylowski et al., 2004; Govers et al., 2004; Muretta et al., 2008). These studies have investigated GLUT4 trafficking by incubating cells in the continuous presence of a saturating concentration of anti-HA antibody. In this assay, the high concentration of anti-HA antibody in the extracellular media means that all HA-GLUT4 that appears at the cell surface is labelled with antibody. Antibody uptake is therefore a direct measurement of the appearance of the HA-epitope at the membrane, and so GLUT4 exocytosis. The amount of antibody-bound GLUT4 reaches a plateau

when all GLUT4 available to recycle to the plasma membrane has reached the plasma membrane. The size of the recycling pool is an important measurement as it distinguishes between a static GSV compartment and a continuously recycling compartment. Both Govers *et al.* and Karylowski *et al.* have reported a similar increase in steady-state k_{ex} for GLUT4 following stimulation with insulin. The 3-fold changes in k_{ex} are also similar to those measured by the photolabelling techniques. However, the data obtained from these groups supported different models of GLUT4 retention.

McGraw's group have presented data that supports a dynamic exchange retention mechanism (Karylowski et al., 2004; Martin et al., 2006). The change in k_{ex} for GLUT4 was coupled with a two-fold reduction in the k_{in}. An important observation was that these changes in GLUT4 trafficking rate constants in response to insulin-stimulation occurred in the absence of any change in the amount of GLUT4 in the recycling pathway. In McGraw's model for GLUT4 trafficking in basal cells, GLUT4 exocytosis to the cell surface is slow and GLUT4 is rapidly internalised from the cell surface. This is supported by previous data obtained in rat adipocytes using the photoreactive label (Jhun et al., 1992). Therefore, GLUT4 is dynamically retained at an intracellular location by slow exocytosis, rapid internalisation and potentially via a futile cycle of intracellular vesicle fusion between the GSVs and endosomes (Karylowski et al., 2004; Martin et al., 2006). Insulin-stimulation increases surface GLUT4 following insulin-stimulation by enhancing GLUT4 exocytosis and reducing GLUT4 internalisation. The amount of futile recycling between the GSV compartment and endosomes is presumably also reduced. A key feature of this model is that all cellular GLUT4 is available to recycle to the plasma membrane under basal conditions.

The presence of an intracellular vesicle fusion cycle for GLUT4 included in the dynamic retention model has also been suggested by Bryant *et al*. (Bryant et al., 2002). Crucially, in this hypothesis, futile cycling does not result in GLUT4 insertion into the endosomal recycling system. This means that GLUT4 is not exposed to the rapid trafficking to the plasma membrane as occurs for endosomal recycling proteins. Rather, Bryant *et al.* proposed that GLUT4 traffics between the GSVs and TGN and this pathway may further promote GLUT4 sequestration.

In contrast to the model proposed by Karylowski *et al.* and Martin *et al.*, Govers *et al.* reported that only a small proportion of GLUT4 had access to the plasma membrane under basal conditions (less than 10%), and that the size of this recycling pool was increased in a dose dependent manner by insulin-stimulation (Govers et al., 2004). The model derived from this data

was termed the 'static retention' model and proposed that there are sequestered pools of GLUT4 that do not traffic to the cell surface under basal conditions, but are released in response to insulin-stimulation. Furthermore, amount of GLUT4 released is dependent on the concentration of insulin, termed 'quantal release'. In this way, GLUT4 trafficking and GSV sequestration is akin to exocytosis of synaptic vesicles leading to neurotransmitter release. By measuring the amount of labelled GLUT4 as a percentage of total cellular GLUT4 in their investigation, Govers *et al.* identify a latent pool of GLUT4 that does not traffic to the cell surface even under insulin-stimulation. Another possibility is that this latent pool is comprised of newly synthesised GLUT4 which has not yet been trafficked into the recycling pathway. Since the data from experiments supporting the dynamic retention model were normalised to the insulin-stimulated level of antibody uptake, these studies have not indicated whether a latent pool exists in this system. Whereas Karylowski *et al.* and Govers *et al.* reported a similar insulin-induced increase in k_{ex}, Govers *et al.* did not note a change in k_{in} in insulin-stimulated cells.

These studies were performed under steady-state conditions and k_{ex} and k_{in} values determined as 'bulk' rate constants for the trafficking of GLUT4 to, and from, the plasma membrane. These rate constants do not refer to a specific process, but rather are defined by the rate limiting step in GLUT4 trafficking. This limiting step for k_{ex} and k_{in} may be different in basal and insulin stimulated cells. For example, in the static retention model, the overall k_{ex} for GLUT4 may reflect both the movement of GLUT4 from the endosomal pool and from the specialised pool to the cell surface. In this case, the observed increase in k_{ex} following insulin-stimulation may be due solely to an increase in GLUT4 exocytosis trafficking from GSVs. In support of this possibility, over-expression of a constitutively active version of PKB/Akt induces GSV translocation, but does not increase GLUT4 trafficking to the cell surface from the endosomal pool (Foran et al., 1999). However, a specific targeting of GSVs by insulin-signalling is inconsistent with the fact that cell surface TfR is also enhanced by insulin-stimulation. This highlights the importance of investigating the trafficking of other recycling proteins when analysing GLUT4 trafficking kinetics to determine the effect of insulin and other stimuli on membrane trafficking from different cellular compartments to the cell surface.

The discrepancy in the trafficking data described above has underpinned one of the major questions in the field; how GLUT4 is retained at an intracellular site under basal conditions? It is important to distinguish between these models since it may shed light on the point at which insulin-signalling acts to increase cell surface GLUT4. A recent study by Muretta *et*

al. aimed to investigate the reason for the disagreement between the two trafficking models (Muretta et al., 2008). The different results could not be explained by differences in the constructs, expression systems or cell line used (Martin et al., 2006). Other possible reasons included the clonal cell background and GLUT4-reporter expression levels (Dugani and Klip, 2005). By focusing on technical differences between the studies, it has been found that the truncated differentiation procedure used by Karylowski *et al*. and Martin *et al.* along with the replating of 3T3-L1 adipocytes (as part of an electroporation procedure) disrupts the static GSV compartment. This is perhaps supported by data presented by Govers *et al.*, which indicated that the process of differentiation of 3T3-L1 cells from fibroblasts to adipocytes increased the proportion of GLUT4 within the static compartment (Govers et al., 2004).

Interestingly, Muretta *et al.* reported that in cells returning to a basal state, the sequestration of GLUT4 into GSVs remained slow, but the removal of GLUT4 from the cell surface was quite rapid. Modelling of GLUT4 trafficking indicates that this bipartite mechanism is able to account for many of the features of GLUT4 trafficking (Muretta et al., 2008). This data implies that both the dynamic retention and static retention models may be important *in vivo*, and may be part of the same retention system.

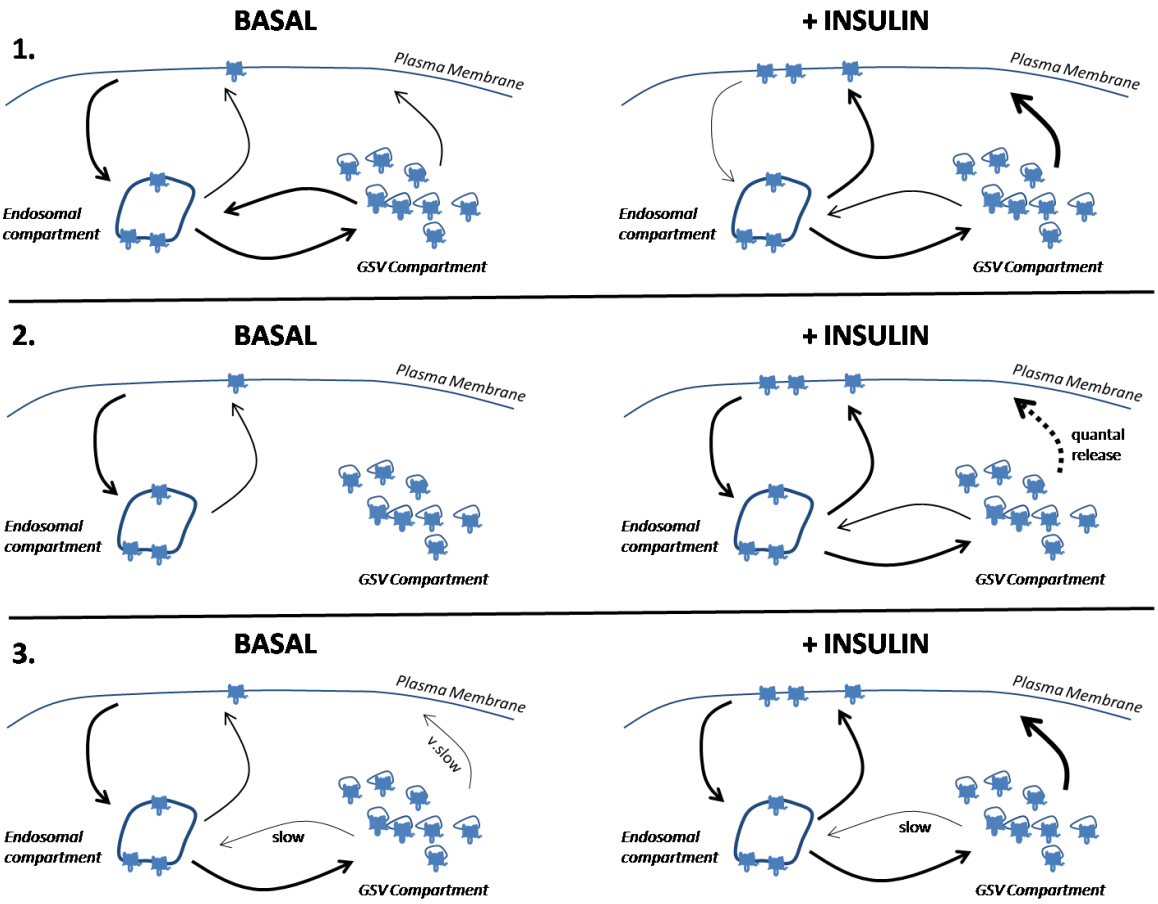

Figure 1.7. Models of GLUT4 retention under basal conditions and redistribution to the cell surface upon insulin-stimulation. 1) Dynamic retention: under basal conditions, GLUT4 slowly exocytoses to the plasma membrane. This GLUT4 is rapidly endocytosed. A futile cycle between the endosomal compartment and GSVs retains GLUT4; insulin-stimulation enhances GLUT4 exocytosis and reduces GLUT4 internalisation. 2) Static retention: A small proportion of cellular GLUT4 recycling under basal conditions. Insulin-stimulation releases GLUT4 from a static compartment by a quantal mechanism. The released GLUT4 either cycles via the endosomal compartment with enhanced exocytosis or continues to translocate to the plasma membrane via the GSV compartment. 3) 3-pool model – a combination of dynamic and static retention models; very slow trafficking from the GSV compartment under basal conditions results in accumulation of GLUT4 in this compartment. Insulin-stimulation enhances GLUT4 exocytosis from the endosomal and, more significantly, the GSV compartment.

A three-pool model presented by Holman *et al.* is illustrated in Figure 1.7 alongside the dynamic and static retention models (Holman et al., 1994). It is interesting that this earlier model effectively represents a combination of these newer models. It states that in basal cells, the release from the storage compartment is rate limiting and so GLUT4 accumulates in this compartment. Insulin increases GLUT4 levels at the plasma membrane primarily through enhancing GLUT4 exocytosis from the slowly recycling storage pool. Therefore, insulin-stimulation increases the rate at which GLUT4 leaves the storage compartment to a rate faster than GLUT4 enters this compartment. This results in GLUT4 accumulation at the plasma membrane and in the endosomal pool. At this point the rate of GLUT4 transfer into the storage pool is rate limiting. Although the 3-compartment model predicts a recycling, not static, storage compartment, the rate of GLUT4 release from this compartment is very slow. Therefore, GLUT4 accumulates in this compartment and may mean that GLUT4 appears to be completely sequestered from the plasma membrane in experimental data-sets that only span a few hours.

Just as TIRF microscopy has been a very useful technique in identifying signalling events regulating GSV fusion at the cell surface, when coupled with appropriate advances in the software programs used for data analysis it has also given significant information on GSV movements and trafficking events in close proximity to the plasma membrane. Studies in isolated adipocytes and 3T3-L1 cells have identified key GSV trafficking features. In basal cells, GSVs are highly motile, and move over relatively long distances at the cell surface. This movement is punctuated by short stops, which is interpreted as GSV docking at the plasma membrane. Insulin acts to increase the number of docked GSVs that go on to fuse with the plasma membrane (Jiang et al., 2008). Therefore, insulin-stimulation decreases the mobility of GSVs in the TIRF zone and enhances fusion. A recent study calculated that insulin-stimulation enhanced GSV fusion by 42-fold as measured by the pH sensitive reporter dye IRAP-pHluorin (Jiang et al., 2008). From these studies, it seems that GSVs are constantly trafficked to, and docked with, the plasma membrane even under basal conditions; however, the fusion-competency of the membrane is enhanced following treatment with insulin.

A recent investigation identified subpopulations of GSVs with distinct trafficking patterns in 3T3-L1 adipocytes (Wang et al., 2009). This study defined three types of GSVs defined by the extent of, and direction of, their movement. As such, these distinct vesicle populations have been termed static, lateral and vertical. The vertically moving vesicles were found to be the only vesicle population that responded to insulin-stimulation. In addition, these vesicles excluded the

transferrin receptor. These vertically mobile vesicles may correspond to the specialised GLUT4 storage vesicles.

TIRF microscopy is an exciting technology through which events leading to GSV fusion with, and internalisation of GLUT4 from, the plasma membrane can be investigated. However, there are caveats. For example, as described above the techniques 3T3-L1 cells are subjected to can result in changes in GLUT4 trafficking and therefore may influence the behaviour of GSVs in the TIRF zone. Furthermore, GLUT4 is localised differently in isolated primary adipocytes and 3T3-L1 adipocytes. As described, GLUT4 is localised to a peri-nuclear region in the centre of the cell in the cell culture line, but is more peripherally located in primary adipocytes due to the presence of a single large lipid droplet. This may influence the interpretation of data. For instance, GSV trafficking into the TIRF zone may be a more important event in 3T3-L1 adipocytes. A final caveat is that GSVs have been reported to be 50-60 nm in diameter and these very small vesicles may not be easily distinguished from larger GLUT4-containing membrane compartments in TIRF studies since these vesicles are below the resolution of conventional fluorescence microscopy. In addition, these small GSVs may not contain enough GFP to be visualised. This is particularly relevant in experiments where constitutively fluorescent tags such as GFP, which result in high background fluorescence, are used. Indeed, it has been proposed that a large majority of the membrane fusion events identified using GLUT-GFP reporter proteins may be the fusion of small endosomal membranes with the cell membrane (Leney and Tavare, 2009). The pH-sensitive dyes are more appropriate for identifying these small vesicles since they have a very low background fluorescence and can therefore reveal fusion events even if vesicles contain very few reporter constructs.

Methods to computationally enhance the resolution of fluorescence microscopy have recently been described (Henriques and Mhlanga, 2009). By using techniques such as photo-activated localisation microscopy (PALM) or stochastic optical reconstruction microscopy (STORM) it is possible to achieve single molecule (super) resolution. Therefore, by utilising these methods to enhance resolution within live cell imaging it may be possible the observe trafficking of individual GLUT4 molecules.

1.6.1 GLUT4 trafficking in muscle

GLUT4 trafficking is thought to be regulated by similar machinery in both adipocytes and muscle fibres. However, a key difference between these tissues is that GLUT4 trafficking kinetics in muscle can be modified by insulin-stimulation, contraction, and AMPK-activation. In addition, muscle fibres have distinct regions of the cell surface. These are the sarcolemma and transverse tubules. Therefore, investigations into GLUT4 trafficking in muscle aims to answer three principal questions. How do different agonists such as insulin and contraction alter GLUT4 trafficking rate constants? Does activation of distinct signalling pathways recruit distinct pools of GLUT4 to the cells surface? Is GLUT4 similarly targeted to both the sarcolemma and transverse tubules in response to distinct stimuli?

GLUT4 trafficking has been much more extensively studied in adipocytes than muscle. This includes both isolated adipocytes and cultured cell lines such as 3T3-L1 cells. The reasons for this bias relates to the ease of isolation of cells from the tissue of interest, the appropriateness of cell culture lines and the appropriateness of methods used to investigate GLUT4 trafficking. Isolation procedures are well established for adipose cells and yield a large number of cells. These adipose cells, although fragile, retain their insulin responsiveness for a significant period of time following isolation. This is not the case for cardiac and skeletal muscle. The isolation of individual muscle fibres is technically challenging, and it has been reported that the dissociation of muscle fibres from tendons and neuromuscular innervation results in a rapid loss of insulin-responsiveness (Lauritzen et al., 2008b).

The technical issues in primary muscle fibre isolation are matched by problems in subfractionating muscle tissue. Muscle tissue contains an abundance of contractile myofibrils. Subcellular organelles and membranes of interest containing GLUT4 can be lost during subfractionation procedure due to their association with these myofibrils. As such, data from these studies can be difficult to interpret. Historically, subfractionation was the primary method for determining GLUT4 subcellular localisation and investigating GLUT4 translocation. As a result, GLUT4 trafficking has been less studied in muscle tissue.

In a study utilising a subfractionation protocol in muscle, Lemieux *et al.* identified the presence of distinct intracellular pools of GLUT4 in rat skeletal muscle which are differentially mobilised depending on the signalling pathway activated (Lemieux et al., 2000). These studies

have reported the presence of a TfR-positive (presumably endosomal) and a TfR-negative pool (GSVs) within muscle fibres. Insulin-simulation preferentially reduced the amount of GLUT4 within the TfR-negative pool, whilst contraction-stimulation caused the translocation of GLUT4 from both pools. This data is supported by electron microscopy data (Ploug et al., 1998). In addition, whereas the TfR-positive pool is only trafficked to the sarcolemma, the GLUT4 from the TfR-negative pool is translocated to the sarcolemma and the transverse tubules.

The data from these studies and from electron microscopy (Ploug et al., 1998) support a role for the transverse tubules in increasing glucose transport into muscle tissue (Dohm and Dudek, 1998; Dohm et al., 1993). Indeed, GLUT4 insertion into transverse tubule potentially contributes extremely significantly to glucose transport into muscle since this membrane compartment has a surface area 2-3 times greater than the sarcolemma (Knudson and Campbell, 1989).

The study by Lemieux *et al.* also reported additivity between insulin- and contraction-stimulation in inducing GLUT4 translocation (Ploug et al., 1998; Lund et al., 1995; Kolter et al., 1992). As reported above, such additivity has been quoted as evidence that different stimuli operate via distinct signalling pathways. Taken further, this additivity could be a result of these stimuli targeting distinct populations of GLUT4 within the muscle (Coderre et al., 1995).

More recently, the identification of more appropriate muscle cell lines, advancements in muscle isolation and in imaging techniques have permitted detailed studies into GLUT4 trafficking in muscle. However, insulin-responsive cell culture muscle cells lines such C2C12 and L6 are not as insulin responsive as muscle *in vivo*. A possible reason for this discrepancy and a potential flaw in using these cell lines is that there is loss of muscle architecture and a lack of neuron-muscle interaction in culture conditions. For example, these cells do not have transverse tubules. In addition, primary cardiomyocytes maintained in cell culture conditions rapidly lose their transverse tubule network (Mitcheson et al., 1996). This external membrane may be responsible for a large proportion of glucose transport into muscle. Therefore, these cells are likely to be missing a key GLUT4 trafficking route that exists *in vivo*.

Trafficking studies have been performed in L6 myoblasts and myotubes (Patel et al., 2003; Wijesekara et al., 2006). In this cell system, insulin-stimulation enhances exocytosis of GLUT4 without changing GLUT4 internalisation. This data has been obtained by taking advantage

of a Myc-epitope tagged GLUT4 reporter construct in an antibody uptake assay and an assay that directly measures Myc-GLUT4 internalisation (described below). Despite the generation of this data, it was not analysed to determine the kinetic rate constants (k_{ex} and k_{in}). The antibody uptake assay also revealed that all Myc-GLUT4 recycles to the cell surface under basal conditions. This is similar to the data obtained by Karylowski *et al*. in 3T3-L1 adipocytes and supports the dynamic retention model for GLUT4 intracellular retention. These assays have also been used to determine how different agonists modulate GLUT4 trafficking parameters. Contraction-stimulation (mimicked by K^+) enhanced GLUT4 cell surface levels by inhibiting GLUT4 internalisation. A similar result was found in DNP-stimulated L6 cells. Both these stimuli inhibited internalisation in an AMPK-independent, PKC-dependent manner. The mode of contraction- and DNP-induced inhibition of GLUT4 internalisation will be discussed below. As previously stated, the L6 cell line does not represent the ideal system for investigating GLUT4 trafficking kinetics. Despite the disadvantages, GLUT4 trafficking can be more readily investigated in such models and any findings subsequently tested in models that more accurately mimic muscle *in vivo*.

Analysis of GLUT4 trafficking in fully differentiated muscle has been enabled by photolabelling methods in isolated muscle fibres and by advances in *in vivo* imaging techniques (Lauritzen et al., 2002; Lauritzen et al., 2006; Lauritzen et al., 2008b; Lauritzen et al., 2008a; Karlsson et al., 2009; Schertzer et al., 2009; Fazakerley et al., 2009). GLUT4 trafficking in primary muscle has been investigated using the photolabelling reagent. Studies in both primary cardiomyocytes and isolated muscle fibres have investigated the effect of different stimuli on GLUT4 trafficking kinetics. In cardiomyocytes, insulin- and contraction-stimulation enhanced GLUT4 exocytosis, whilst not influencing GLUT4 internalisation (Yang and Holman, 2005). In contrast, activation of AMPK by induction of hypoxia or incubation with oligomycin or metformin enhanced cell surface GLUT4 by inhibiting GLUT4 internalisation rather than affecting exocytosis. These observations have recently been confirmed in rat epitrochlearis and human vastus lateralis muscle. Again, these trafficking studies were performed using a GLUT4 photolabelling technique. Of specific interest is the measurement of GLUT4 trafficking in human muscle. In this study, insulin-stimulation resulted in a 7-fold increase in k_{ex} in both muscle preparations. In contrast, AICAR-stimulation did not enhance GLUT4 exocytosis, but rather decreased GLUT4 internalisation (Karlsson et al., 2009).

In 2002, Lauritzen *et al.* reported a new method for investigating GLUT4 trafficking in muscle *in vivo* (Lauritzen et al., 2002). *In vivo* confocal imaging of GLUT4-GFP trafficking in live

mouse skeletal muscles has revealed that GLUT4 translocation to both the sarcolemma and transverse tubules in response to insulin. The recruitment of GLUT4 to the transverse tubules was delayed by approximately 10 minutes compared to the sarcolemma, which correlated exactly with the delay in insulin diffusion into the transverse tubule network.

More detailed analysis of data from live imaging of muscle fibres *in vivo* has indicated that GLUT4 storage structures do not traffic over large distances, but rather large storage vesicles remain stationary and are locally depleted to either the sarcolemma or transverse tubules (Lauritzen et al., 2008a). This mechanism for GLUT4 delivery to the cell surface membranes is practical since the interior of muscle fibres is densely packed with the contractile machinery. Gradual GLUT4 internalisation to internal stores following removal of insulin was observed from both cell surface domains. Internalisation of GLUT4 from the transverse tubule membrane was delayed, which is most likely due to a delayed clearance of insulin from the transverse tubule network. Further work in insulin-resistant muscle has indicated that impaired insulin signalling and GLUT4 translocation is primarily localised to the transverse tubules and not the sarcolemma (Lauritzen et al., 2008b).

The development of this *in vivo* imaging method enables GLUT4 trafficking within muscle fibres to be intimately observed. It has yielded interesting results, and further studies will need to focus on other stimuli leading to GLUT4 translocation in muscle such as AICAR. Due to the nature of real-time microscopy, studying GLUT4 trafficking in response to contraction will be extremely challenging. In addition, it is unlikely that this technique in its current form would be able to identify whether GLUT4 traffics from distinct pools in response different stimuli.

1.7 Internalisation of GLUT4

When studying GLUT4 trafficking, the exocytosis rate constant is often easier to obtain than the internalisation rate constant. For example, the antibody uptake assay described above allows the measurement of GLUT4 exocytosis in a unidirectional manner. The rate constant for GLUT4 internalisation is difficult to determine because internalisation is a net process; comprising endocytosis and re-exocytosis. During measurements of internalising GLUT4 some recycling of GLUT4 will inevitably occur. These difficulties may account for some of the controversies that surround the issue of whether insulin-stimulation is able to markedly reduce GLUT4 endocytosis

(Muretta and Mastick, 2009). For example, Jhun *et al*. and Blot *et al.* have reported that the k_{in} was reduced in 3T3-L1 adipocytes by ~3-fold and ~2-fold respectively (Jhun et al., 1992; Blot and McGraw, 2006). However, Yang and Holman report only a small reduction in k_{in} (30%) in this cell line (Yang et al., 1992), whilst Satoh *et al.* found no effect on GLUT4 endocyotosis in rat primary adipocytes (Satoh et al., 1993). In general, GLUT4 and IRAP are both reported to be quite rapidly endocytosed from the cell surface in both basal and stimulated cells. The exact reported rate constants for internalisation differ depending on the cell type and the method adopted for the measurement of internalisation.

As mentioned above, Blot *et al.* have provided evidence that GLUT4 internalisation is slowed in response to insulin-stimulation. A criticism of the data presented in this study is that k_{in} was calculated from antibody uptake experiments with the assumption that at early time-points, GLUT4 internalisation is a unidirectional process. However, as described in a recent review by Muretta and Mastick, this is an inappropriate assumption. Whilst it seems intuitive, it is mathematically incorrect as the data obtained from these experiments is a function of k_{ex} and k_{in} even at early time points (Muretta and Mastick, 2009). This can be proven in modelling programs where changes in k_{ex} can dramatically change the slope of internalisation data even at early points in the data. It is therefore more desirable to measure internalisation at short and long time points and fit the data taking into account the contribution of both k_{in} and k_{ex}.

The inhibition of GLUT4 internalisation reported by McGraw's group has been investigated and reported to be a PKB/Akt-independent action. This was determined through the use of the PKB/Akt inhibitor Akti. Wortmannin completely inhibited enhanced cell surface GLUT4 levels in response to insulin-stimulation, whereas the inhibition by Akti inhibition was only partial. Gonzalez *et al.* attribute this partial inhibition of GLUT4 translocation by Akti to a failure of Akti to prevent insulin-mediated inhibition of GLUT4 internalisation (Gonzalez and McGraw, 2006). However, it is not clear whether the concentration of Akti used in this study completely inhibited PKB/Akt activity.

Studies into the mechanism of GLUT4 internalisation have been carried out in 3T3-L1 and L6 cells (Blot and McGraw, 2006; Antonescu et al., 2008). Blot *et al.* reported that in unstimulated 3T3-L1 adipocytes GLUT4 was mostly internalised from the plasma membrane via a very rapid non-clathrin dependent mechanism. This route of endocytosis was shown to be cholesterol-dependent, since the cholesterol aggregating drug nystatin inhibited GLUT4

internalisation in basal cells. This observation is consistent with reports that GLUT4 colocalises with caveolin in 3T3-L1 cells and isolated adipocytes (Karlsson et al., 2002). Studies using TIRF microscopy have reported that GLUT4 localises to clathrin coated pits at the cell surface in basal cells, and this localisation in enhanced under insulin stimulation (Huang et al., 2007). Although the majority of GLUT4 internalisation is carried out via this cholesterol-dependent mechanism under basal conditions, a small proportion is internalised through a clathrin mediated route. In support of the TIRF microscopy data, Blot *et al.* reported that GLUT4 internalisation in insulin-stimulated cells occured predominantly via clathrin-mediated endocytosis. The insulin-induced inhibition of cholesterol-mediated endocytosis and redirection of GLUT4 to a slower clathrin-mediated route caused an approximately 2-fold reduction in the GLUT4 internalisation rate constant. This is not achieved by a specific effect on GLUT4, but by a general inhibition of the internalisation of cargo internalising by a clathrin-independent route, such as cholera toxin B. Consistent with these data, knock-down of AP-2 in 3T3-L1 adipocytes reduced the rate of GLUT4 internalisation in insulin-stimulated cells, but not in basal cells (Blot and McGraw, 2006).

In addition to these data, electron and fluorescent microscopy and gene silencing techniques have provided evidence for GLUT4 endocytosis via a clathrin-mediated process in skeletal muscle, cardiomyocytes, adipocytes, 3T3-L1 and L6 cells (Ploug et al., 1998; Blot and McGraw, 2006; Robinson et al., 1992; Antonescu et al., 2008; Rodnick et al., 1992b). There is also evidence for the involvement of dynamin in GLUT4 internalisation. Inhibition of dynamin (Volchuk et al., 1998) or expression of dynamin mutants (Al Hasani et al., 1998; Kao et al., 1998) inhibits GLUT4 internalisation. Dynamin is a GTPase and is an important protein in the formation of clathrin-coated vesicles (van der Bliek et al., 1993). This protein forms oligomeric rings around the neck of the budding vesicle and GTP hydrolysis is required for vesicle scission (Takei and Haucke, 2001).

Despite evidence that GLUT4 internalises via a clathrin mediated route, it does not internalise at the same rate as TfR, which is known to internalise in a clathrin-dependent manner. Measurements of TfR and GLUT4 internalisation rates imply that these proteins undergo distinct endocytic routes. TfR internalisation (half-time of 1.6-2 min) is much faster in adipocytes than GLUT4 (half-time of 8 min) (Tanner and Lienhard, 1987). Although GLUT4 may undergo a distinct internalisation route, it is likely that this route still includes the endosomal compartment due to the large body of evidence that GLUT4 partially colocalises with TfR, especially in stimulated cells.

Rab5 has also been implicated in GLUT4 trafficking from the cell surface in 3T3-L1 adipocytes (Huang et al., 2001). Rab5 is known to be involved in directing vesicle transport and endosomal fusion in the early endocytic pathway. Insulin has been reported to inhibit Rab5 activation. This may provide a mechanism by which insulin-stimulation inhibits GLUT4 internalisation (Huang et al., 2001).

Although there are contradictory reports as to whether insulin-signalling is able to affect GLUT4 internalisation in adipocytes, insulin-stimulation does not signal to influence GLUT4 internalisation in muscle. This has been reported in L6 myoblasts, myotubes and in primary cardiomyocytes and skeletal muscle (Karlsson et al., 2009; Antonescu et al., 2008; Wijesekara et al., 2006; Yang and Holman, 2005). However, GLUT4 internalisation is reduced by other insulin-independent signals, such as AMPK-activation, leading to increased glucose uptake in muscle tissue. A characterisation of the mechanisms by which GLUT4 is internalised in muscle has been performed in L6 cells (Antonescu et al., 2008). As in 3T3-L1 adipocytes, GLUT4 is internalised via both a clathrin-dependent and clathrin-independent route. Aggregation of cholesterol by nystatin and other drugs such a β-methyl-cyclodextrin inhibits GLUT4 internalisation in L6 cells. However, in contrast to 3T3-L1 adipocytes, in these cells clathrin-independent endocytosisis does not occur via caveolae (Antonescu et al., 2008). Therefore, the nature of the cholesterol-dependent (clathrin-independent) endocytosis is not clear. IL2Rβ has been reported to be internalised via a dynamin-dependent route which is independent of both clathrin and caveolin (Lamaze et al., 2001). Therefore, GLUT4 may internalise via a similar mechanism to IL2Rβ. In support of this hypothesis, electron microscopy images indicate colocalisation between GLUT4 and IL2Rβ at the cell surface of L6 cells.

These data from adipocytes and muscle cell lines taken together imply that GLUT4 is internalised by a clathrin-mediated and clathrin-independent/cholesterol-dependent endocytoic route. However, the type of non-clathrin mediated endocytosis and the relative contribution of each of these endocytic mechanisms is different in each cell type. The reason for the discrepancy in the route of non-clathrin dependent internalisation between 3T3-L1 and L6 cells and whether these differences between fat and muscle tissue exist *in vivo* has not yet been elucidated.

As mentioned above, insulin-stimulation does not inhibit GLUT4 internalisation in L6 myoblasts and myotubes. However, GLUT4 internalisation in L6 cells has been reported to be inhibited by a high K^+ concentration (mimicking contraction) and by the mitochondrial inhibitor

DNP which acts to transiently reduced ATP levels and activate AMPK (Antonescu et al., 2008; Wijesekara et al., 2006). The rate of GLUT4 internalisation is also reduced in cardiomyocytes and skeletal muscle in response to AMPK activation (Yang and Holman, 2005; Yang and Holman, 2006; Karlsson et al., 2009). In L6 cells, this effect has been reported to be due to an inhibition of the non-clathrin mediated route of endocytosis. This is analogous to the effect of insulin-stimulation in adipocytes, where the clathrin-independent route of internalisation is inhibited following insulin-stimulation.

Recently, the Cdc42 interacting protein-4 (CIP4a) has been implicated in mediating GLUT4 internalisation in insulin-stimulated primary adipocytes and L6 cells (Hartig et al., 2009; Feng et al., 2009). CIP4 is an F-BAR domain containing protein. These domains drive membrane deformation and can therefore modulate endocytic processes. Interestingly, adipocytes isolated from CIP4-null mice exhibit enhanced insulin-stimulated glucose uptake compared to adipocytes from wild-type mice and siRNA-mediated knockdown of CIP4a resulted in increased glucose transport into basal L6 cells. These data imply a role for CIP4 in regulating GLUT4 internalisation and more specifically a role for CIP4 in enhancing GLUT4 internalisation under insulin stimulation. It is thought that CIP4 may mediate its effects on internalisation via insulin-dependent interactions with N-WASP and dynamin-2. Increasing GLUT4 endocytosis in response to insulin-stimulation appears counter-intuitive. The role of CIP4 in GLUT4 endocytosis requires further examination.

As described above, GLUT4 contains FQQI and LL motifs in its cytoplasmic tails which resemble AP-2 binding motifs. Mutation of these motifs results an increased levels of GLUT4 at the cell surface under steady-state conditions presumably due to reduced interaction with AP-2 and therefore decreased GLUT4 internalisation. For example mutation of FQQI to AQQI abolishes GLUT4 localisation to clathrin coated pits through disruption of this GLUT4-AP-2 interaction (Blot and McGraw, 2006). It has more recently been discovered that these motifs are also recognised by the intracellular adaptor protein AP-1 (Bernhardt et al., 2009). Therefore, any interpretation of results gained from GLUT4 with mutated FQQI or LL motifs could be due to disruption of intracellular trafficking of GLUT4. Assays directly measuring GLUT4 endocytosis have reported a requirement for only the FQQI motif for GLUT4 internalisation in 3T3-L1 adipocytes (Watson et al., 2008; Blot and McGraw, 2008). Therefore the dileucine motif may be act as a general endocytosis signal in non-insulin responsive cells, but may not perform this function in mature insulin-responsive cells. Taken further, it has been proposed that both of these motifs have been

conserved in GLUT4 primarily to fulfil a role in the intracellular sorting of GLUT4 rather than mediating GLUT4 internalisation.

1.8 Aims of experimental work described in this thesis

The studies described in this thesis were performed to advance our understanding of GLUT4 trafficking responses in muscle following the activation of distinct signalling pathways. To achieve this aim, I have investigated the kinetics and specificity of GLUT4 trafficking in primary cardiomyocytes and in the L6 muscle cell line. Each of these cell types has permitted the investigation of certain aspects of GLUT4 trafficking as determined by the experimental advantages of the particular model. For example, primary cardiomyocytes retain important features of muscle architecture which are not present in L6 myotubes, such as transverse tubules. However, cell culture models can be more readily manipulated to allow rigorous kinetic studies through the analysis of a large population of cells at a sufficient number of time-points.

Two aspects of GLUT4 trafficking have been investigated in isolated cardiomyocytes from a transgenic mouse line expressing HA-GLUT4-GFP. The first of these was GLUT4 translocation to the limiting membrane in response to insulin, contraction and hypoxia. This part of the study addressed the question of whether these agonists, which operate through distinct signalling pathways, preferentially translocate GLUT4 to the sarcolemma or transverse tubules. Secondly, I have interrogated GLUT4 trafficking in cells returning to the basal state. Through interpreting data from these experiments, I have determined whether GLUT4 is internalised to distinct compartments in cells initially treated with different stimuli and have been able to comment on the possibility that insulin-, contraction- and hypoxia-stimulation release GLUT4 to the cell surface from physically distinct storage locations.

It has been reported in both cardiomyocytes and skeletal muscle that insulin and AMPK may impinge at different points in GLUT4 trafficking. In order to more fully investigate changes in GLUT4 trafficking kinetics in response to different agonists than was possible in the cardiomyocyte model, trafficking assays were developed in the L6 muscle cell line. Using this cell line, I have been able to determine changes in GLUT4 trafficking rate constants and the size of the recycling GLUT4 pool following stimulation with insulin and/or an AMPK activator. These

studies have revealed the mechanism by which insulin-stimulation and AMPK-activation are able to increase the amount of GLUT4 at the cell surface, and maintain these elevated levels.

Furthermore, I have performed the preliminary characterisation of novel TBC1D1 antibodies. These experiments were performed with the longer term aim of investigating the role of phosphorylation of serine 237 of TBC1D1 in AMPK- and contraction-stimulation of glucose uptake.

Contraction- and AMPK-stimulated glucose uptake remains intact in insulin-resistant individuals. Therefore, characterisation of insulin-independent signalling pathways leading to GLUT4 translocation and glucose uptake is an important process in identifying novel drug targets for bypassing insulin-resistance. The investigations detailed in this thesis are primarily focussed on the details of GLUT4 trafficking in muscle cells. In addition, the TBC1D1 antibodies described here will form a part of future investigations into the signalling molecules which regulate GLUT4 trafficking in muscle. By combining data from signalling and trafficking studies, such as those described here, it will be possible to identify the role of specific signalling components in controlling aspects of GLUT4 trafficking.

2 Materials and Experimental Procedures

2.1 Materials

2.1.1 Sources of Laboratory Chemicals and Reagents

Table 2.1 provides a list of companies from which reagents were purchased along with an abbreviation for use in the text.

Company	Address	Abbreviation
Abcam	Cambridge, MA, USA	[A]
Acros Organics	Geel, Belgium	[ACR]
Adobe	San Jose, CA, USA	[ADO]
Amersham Biosciences	Little Chalfont, UK	[AB]
Atto Corporation	Tokyo, Japan	[AT]
Bachem UK Ltd	St.Helens, UK	[B]
BD Biosciences	Oxford, UK	[BD]
Beckman Coulter	High Wycombe, UK	[BC]
BMG Labtechnologies	Offenburg, Germnay	[BMG]
Biostatus	Shepshed, UK	[BSS]
Bio-Rad	Hemel Hempstead, UK	[BR]
Calbiochem	Nottingham, UK	[CAL]

Carl Zeiss, Ltd	Welwyn Garden City, UK	[Z]
CBS Scientific	Del Mar, CA, USA	[CBS]
Celluliance	Toronto, Canada	[CEL]
Cell Signaling	Danvers, MA, USA	[CS]
Clontech	Palo Alto, CA, USA	[C]
Covance Research Products, Inc	Berkeley, CA, USA	[COV]
Definiens	Munich, Germnay	[DEF]
Eurogentech	Southampton, UK	[E]
Fisher Thermo Scientific UK Ltd.	Loughborough, UK	[FTS]
Fujifilm (Raytek)	Sheffield, UK	[FU]
Greiner Bio-One	Stonehouse, UK	[G-BO]
Hyclone - Fisher Thermo Scientific UK Ltd.	Loughborough, UK	[H-FTS]
Invitrogen - Molecular Probes	Paisley, UK	[I-MP]
Invitrogen - Gibco	Paisley, UK	[I-G]
Lonza	Slough, UK	[L]

Melford	Ipswich, UK	[MEL]
Merial Animal Health Ltd	Harlow, UK	[MER]
MicroCal Inc. GE Healthcare	Piscataway, NJ, USA	[M-GE]
Millipore	Watford, UK	[M]
Molecular Devices	Sunnyvale, CA, USA	[MD]
National Diagnostics, Flowgen Bioscience Ltd	Nottingham, UK	[ND-F]
Novagen – Merck Biosciences	Nottingham, UK	[N-MB]
Novo Nordisk	Bagsværd, Denmark	[NN]
Perkin Elmer	Waltham, MA, USA	[PE]
Pierce	Rockford, Il, USA	[P]
Promega	Madison, WI, USA	[PRO]
Roche Molecular Biochemical	Mannheim, Germany	[RMB]
Science Services	Munich, Germany	[SS]
Sigma-Aldrich	Poole, UK	[S]
Stratagene	La Jolla, Ca, USA	[ST]
Tecan	Männedorf, Switzerland	[TE]
Upstate	Dundee, UK	[U]

UVP	Cambridge, UK	[UVP]
Vector Laboratories UK	Burlingame, CA, USA	[VL]
Worthington Biochemical Corporation	Lakewood, NJ, USA	[WB]

Table 2.1. The address of each of the suppliers along with the abbreviation used to denote each company in the text

2.1.2 Buffers

The buffers referred to in the Experimental Procedures are listed in alphabetical order below.

Agar plates*:* 1% (w/v) Bacto™ Tryptone [BD], 0.5% (w/v) Bacto™ Yeast Extract [BD], 0.5% NaCl [TFS], 1.5% (w/v) Agar [TFS], pH 7.5 (autoclaved)

AMPK kinase assay reaction buffer: 50 mM Tris-HCl pH 7.4 [S], 0.02% Brij-35 [S], 100 µM DTT [TFS], 192 µM ATP (Mg^{2+} salt) [S], 4.8 mM $MgCl_2$ [TFS], 10 µM AMP [S] and 0.5 µCi ^{32}P-ATP [PE]

BCA reagent B: 4% (w/v) $CuSO_4.5H_2O$. [S]

Blocking buffer: 3% (v/v) goat serum [S] and 1% (w/v) BSA [CEL] in PBS

Cardiomyocyte basal media: Perfusion buffer supplemented with 0.5% (w/v) fatty acid-free BSA [RMB] and 1 mM $CaCl_2$ [S]

Cardiomyocyte calcium-resistance buffer: Perfusion buffer supplemented with 15mM BMD [S], 2% (w/v) BSA [CEL] and 200 µM $CaCl_2$ [S]

Cardiomyocyte digestion buffer: Perfusion buffer supplemented with 0.7% (w/v) bovine serum albumin (BSA) [CEL], 15 mM 2,3-butanedione monoxine (BMD) [S], 1.1 mg/mL collagenase [WB] and 2.65 mg/mL hyaluronidase [S]

Cardiomyocyte perfusion buffer: KRH buffer containing 2mM inosine [S], 2mM pyruvate [S] and 5.5 mM glucose [S]

Coomassie Blue destain: 30% methanol [TFS], 10% glacial acetic acid [TFS], made up in ddH_2O

Coomassie Blue stain: 0.2% Brilliant Blue R [S] made up in Coomassie Blue destain solution (Filter before use)

Electrophoresis running buffer: 25 mM Tris-HCl pH 6.3 [S], 0.1% (w/v) SDS, 0.2 M glycine [TFS]

HEK-293 growth medium: Dulbecco's Modified Essential Medium (DMEM) [L] supplemented with 10% heat-inactivated Foetal Calf Serum [L] and 100 IU/ml penicillin [L], 100 µg/ml streptomycin [L], 2 mM glycine [L]

IgG binding buffer: 50 mM Tris-HCl pH 7.4 [S]

IgG elution buffer: 1M glycine pH 1.7 [TFS]

Krebs-Ringer-HEPES (KRH) buffer: 6 mM KCl [S], 1 mM Na_2HPO_4 [TFS], 0.2 mM $NaHPO_4$ [TFS], 1.4 mM $MgSO_4$ [S], 1 mM $CaCl_2$ [S], 128 mM NaCl [TFS], 10 mM HEPES [S] pH 7.4

L6 cells basal medium – Alpha Modified Eagles Medium (α-MEM) without bicarbonate: Alpha-Modified Eagles Medium without bicarbonate [I-G], 20 mM HEPES [TFS] and 0.2% BSA [CEL]

L6 cells differentiation medium – Alpha Modified Eagles Medium (α-MEM) with bicarbonate: Alpha-Modified Eagles Medium [L], 1% Antibiotic/Antimycotic [I-G] and 2% Foetal Calf Serum [H-TFS]

L6 cells normal growth medium – Alpha-Modified Eagles Medium (α-MEM) with bicarbonate: Alpha-Modified Eagles Medium [L], 1% Antibiotic/Antimycotic [I-G] and 10% Foetal Calf Serum [L]

L6 cells (HA-GLUT4) normal growth medium – Alpha-Modified Eagles Medium (α-MEM) with bicarbonate: Alpha-Modified Eagles Medium [L], 1% Antibiotic/Antimycotic [I-G] and 10% Foetal Calf Serum [L] containing 2 μg/mL puromycin [S]

Luria broth (LB): 1% (w/v) Bacto™ Tryptone [BD], 0.5% (w/v) Bacto™ Yeast Extract [BD], 0.5% NaCl [TFS], pH 7.5 (autoclaved)

Phosphate buffered saline (PBS): 12.5 mM Na_2HPO_4 [TFS], 154 mM NaCl [TFS], pH 7.2

Plat-E growth media: Dulbecco's Modified Essential Medium (DMEM) [L] supplemented with 10% heat-inactivated Foetal Calf Serum [L], 100 IU/ml penicillin [L], 100 μg/ml streptomycin [L], 2 mM glycine [L], 10 μg/mL blastocidin [S] and 1 μg/mL puromycin [S]

Ponceau S stain*:* 0.1% (w/v) Ponceau S [S], 3% (w/v) trichloroacetic acid [TFS]

Resolving gel buffer: 1.5 M Tris-HCl ph 8.8 [S], 0.4 % (w/v) SDS [TFS]

Resuspension buffer: 50 mM sodium phosphate, 300 mM NaCl [TFS], 1% (v/v) Triton-x100 [S], 5 mM β-mercaptoethanol [TFS], 10 mM imidazole containing protease inhibitors (aprotinin, antipain, pepstatin A, and leupeptin; each at 1 μg/mL, 100 μM 4-(2-aminoethyl)benzenesulfonyl fluoride (AEBSF) [S])

Sample buffer: 2% (w/v) SDS [TFS], 62.5 mM Tris-HCl (ph 6.8) [S], 0.01% (w/v) bromophenol blue [TFS], 10% (w/v) glycerol [TFS], 100 mM Dithiothreitol (DTT) [TFS]

SDS lysis buffer – 2% Sodium Dodecyl Sulphate (SDS) buffer: 2% (w/v) SDS [TFS] in PBS, containing protease inhibitors (aprotinin, antipain, pepstatin A, and leupeptin; each at 1 µg/mL [S], 100 µM 4-(2-aminoethyl)benzenesulfonyl fluoride (AEBSF) [S]), and phosphatase inhibitors (10 mM sodium fluoride, 1 mM $NaMO_4$, 200 µM Na_3VO_4, 58 nM cypermethrin, 5 µM dephostain, 100 nM okadaic acid, and 10 pM nuclear inhibitor of protein phosphatase-1 [CAL])

Sodium phosphate buffer: 50 mM Na_2HPO_4 [TFS], 300 mM NaCl [TFS]

Stacking gel buffer: 0.5 M Tris-HCl ph 6.8 [S], 0.4 % (w/v) SDS [TFS]

Transfer buffer: 39 mM glycine [TFS], 49 mM Tris-HCl [S], 0.0375% (w/v) SDS [TFS], 20% (v/v) methanol [TFS]

Tris-buffered saline containing Tween-20 (TBS-T): 10 mM Tris-HCl pH 7.4 [S], 154 mM NaCl [TFS], 0.1% (v/v) Tween [S]

2.1.3 Insulin

Monocomponent porcine insulin, kindly provided by Dr. G. Daniellson [NN] was used for all experimental procedures involving cardiomyocytes. Recombinant human insulin [CAL] was used for all experimental procedures using L6 myotubes. Insulin was dissolved in 30 mM HCl and was subsequently diluted in Phosphate Buffered Saline (PBS) to give the required concentration, aliquoted and stored at -20°C.

2.1.4 Heparin

Heparin Grade 1A [S] isolated from porcine intestinal mucosa was reconstituted in 0.9% (w/v) NaCl [TFS] (2000 Units/ml) and filter sterilised through a 0.2 μm filter [M]. Aliquots were stored at 4 °C.

2.2 Experimental Procedures

2.2.1 Transgenic mice

As detailed in a manuscript in preparation (Ivonne Lisinski, Vladimir A. Lizunov, Dena R. Yver, Oksana Gavrilova, Hadi Al-Hasani, and Samuel W. Cushman), lines of C57Bl/6 mice were prepared homozygously expressing an HA-GLUT4-GFP transgene under the control of the creatine kinase promoter. cDNA for HA-GLUT4-GFP (Dawson et al., 2001) was cloned into the pBSMCK-polyA vector which contains the muscle creatine kinase promoter (Bruning et al., 1998). The transgene was injected into fertilised eggs of FVB/N mice. These were implanted into C57B1/6 foster mothers. These mice exhibit normal growth, feeding behaviour, glucose homeostasis and reproduction. All procedures used in transgenic mouse generation were conducted in accordance with National Institutes of Health guidelines as approved by the Animal Care and Use Committee of the National Institute of Diabetes and Digestive and Kidney Diseases. The procedures for cardiomyocytes isolation conformed to UK Home Office Guidance on the Operation of the Animals (Scientific Procedures) Act and were approved by the University of Bath Animal Care and Use Committee.

2.2.2 Glucose uptake and GLUT4 trafficking in cardiomyocytes

2.2.2.1 Isolation of cardiomyocytes

Calcium resistant cardiomyocytes from adult (5-6 weeks, 22- 25 g) male wild-type mice (CD-1 Swiss albino) and transgenic mice expressing HA-GLUT4-GFP were prepared by collagenase digestion by use of a method previously described for rat cardiomyocytes (Eckel and Reinauer, 1980; Fischer et al., 1996) but with the inclusion of 2 mM inosine [S] in the media. Mice were terminally anaesthetised by intraperitoneal injection of 0.10 mg/g Euthatal (pentobarbital) [MER]. Heparin [S] (100 U) was injected at the same time to prevent blood clotting. 5-10 min after this injection, the heart was removed and rapidly cooled in ice-cold cardiomyocyte perfusion buffer. All buffers were pre-oxygenated and maintained in an oxygen atmosphere. The heart was mounted via the aorta onto a cannula and perfused with perfusion buffer at 37^{o}C. After 5 min, the buffer was exchanged for digestion buffer. Perfusion was maintained at 37^{o}C for 25 min by a peristaltic pump. During the final 5 min of digestion, the calcium concentration of digestion buffer was raised to 200 µM (in 100 µM increments) by the addition of calcium chloride to the circulating digestion buffer.

Cardiac tissue was manually dissociated in a 1:1 mix (20 mL final volume) of digestion buffer and calcium-resistance buffer. Once dissociated, the cells were incubated at 37^{o}C for 6 minutes and the calcium concentration of the media was increased to 800 µM (in 200 µM increments). The cell suspension was then passed through nylon gauze (250 µm^2) and cells were allowed to settle for 2-3 minutes.

Once cells had settled, they were washed through 30 mL perfusion buffer supplemented with 2% (w/v) BSA [CEL] and 1mM $CaCl_2$ to remove any remaining collagenase and hyaluronidase. Cells were washed a final time in 50 mL basal media and allowed to recover for 25 min at room temperature. The quality of the cardiomyocyte preparation was assessed by light microscopy.

2.2.2.2 Stimulation of cardiomyocytes

Cell suspensions were adjusted to approximately 10% cytocrit (approximately 1 mL) and maintained under basal conditions or stimulated with insulin, contraction or hypoxia. Cardiomyocytes were stimulated with insulin at 30 nM for 30 min. Stimulation by hypoxia was induced by incubation of cells in 20 mL of basal media that had been deoxygenated for 60 min and pre-gassed with nitrogen for a further 30 min. The nitrogen atmosphere was maintained throughout subsequent incubations. For electrical induction of contraction, 1 mL aliquots of cell suspensions at 37°C, ~10% cytocrit, were placed in 19-mm diameter polystyrene dishes [GBO]. A dish lid with attached electrodes was dipped into the cell suspension. Cells were stimulated at exercise levels of contraction for 5 min at 100 V, with pulse duration of 1 ms and frequency of 10 Hz. Contraction was monitored under a light microscope.

2.2.2.3 2-Deoxy-D-glucose uptake into mouse cardiomyocytes

Following stimulation and 5 minutes prior to the addition of radiolabelled 2-deoxy-D-glucose, cells were transferred into new basal media without glucose. The transport assay was initiated by the addition of 2-deoxy-D-glucose [S] (100 µM final concentration) containing 0.5 µCi 2-deoxy-D-[^{3}H] glucose [AB]. 2-Deoxy-D-glucose uptake was terminated after 10 min by transferring the cell suspension to microfuge tubes containing phloretin [S] (400 µM final concentration) in KRH buffer. Background radioactivity was determined by premixing cells with phloretin prior to adding 2-deoxy-D-glucose. The samples were immediately centrifuged at 3,500 x *g* for 1 min. The supernatants were removed, and cells washed three times with 1 mL of KRH buffer containing 400 µM phloretin. Cells were lysed with 1 mL of 0.1 M NaOH [TFS], and aliquots were taken for determination of radioactivity by scintillation counting and protein levels by the bicinchoninic acid (BCA) assay [P] as described below (section 2.2.5.3).

2.2.2.4 Selective immunofluorescent labeling of sarcolemma GLUT4

Stimulated cardiomyocytes were washed through 15 mL KRH buffer, transferred to miscrofuge tubes to be fixed in 1 mL of 4% (w/v) paraformaldehyde (PFA) [S] for 20 min at room

temperature and incubated in 1 mL of blocking buffer in PBS for 30 min at room temperature. All subsequent incubations were carried out in microfuge tubes. For detection of HA-GLUT4-GFP at the sarcolemma surface, cells were labelled overnight at 4°C with 1 μg/mL whole anti-HA antibody [COV] in blocking buffer. Cells were washed to remove unbound antibody and then incubated for 60 min at room temperature with Alexa-633 conjugated goat anti-mouse IgG secondary antibody [I-MP] at 4 μg/mL in blocking buffer. Finally cells were washed three times with PBS and mounted in Vectashield mounting solution [VL].

2.2.2.5 Immunofluorescent labelling of sacrolemma and transverse-tubule GLUT4

To label HA-GLUT4 at both the sarcolemma and the transverse-tubules 5 μg/mL anti-HA antibody Fab fragment or non-specific Fab fragment was added to the cell suspension for 15 min at 37°C (the method for the generation of Fab fragments is described in section 2.2.3.2). For insulin- and hypoxia-stimulated cells, Fab fragments were added during the stimulus. For contraction-stimulated cells, cells were first stimulated, and then labeled with Fab fragment for 15 min at 37°C. After stimulation and labelling, cells were washed with 15 mL KRH buffer, transferred to microfuge tubes to be fixed in 1 mL of 4% (w/v) PFA for 20 min at room temperature and incubated in 1 mL of blocking buffer containing 0.1% (w/v) saponin [S] for 30 min at room temperature. Saponin permeabilised cells were then incubated for 60 min at room temperature with Alexa-633 conjugated goat anti-mouse secondary antibody [I-MP] at 4 μg/mL in blocking buffer. This permeabilisation step allowed association of the secondary antibody with the Fab fragments bound to HA-GLUT4-GFP at the transverse tubules. Finally, cells were washed three times with PBS and mounted in Vectashield mounting medium.

2.2.2.6 Pulse labelling and internalisation of GLUT4

Cells were stimulated and subsequently pulse labelled with 5 μg/mL whole anti-HA antibody for 15 min at 37°C. For insulin and hypoxia stimulated cells, antibody was added during the stimulus. For contraction stimulated cells, cells were first stimulated, and then exposed to anti-HA antibody. For removal of the initial stimulus, insulin-stimulated cells were washed through KRH buffer pH 6.0 to strip insulin from its receptor. Contraction- and hypoxia-stimulated cells were transferred to basal oxygenated buffer. Unbound antibody was removed from all cells by washing with basal media. Cardiomyocytes were incubated to return to a basal state in basal

media at 37°C for specific times (0, 5, 10, 15 and 30 min). Internalisation was considered complete after 40 min.

Following the internalisation incubations, cells were washed with 15 mL KRH buffer, transferred to microfuge tubes to be fixed in 1 mL of 4% (w/v) PFA for 20 min at room temperature and incubated in 1 mL of blocking buffer containing 0.1% (w/v) saponin for 30 min at room temperaturePermeabilised cells were then incubated for 60 min at room temperature with Alexa-633 conjugated goat anti-mouse IgG secondary antibody at 4 µg/mL in blocking buffer. For immunofluorescent labeling of clathrin, cells were washed to remove unbound secondary antibody and then incubated overnight at 4°C with anti-clathrin antibody [S] (diluted 1/40) in blocking buffer containing 0.1% (w/v) saponin. Cells were subsequently incubated with Alexa-546 conjugated donkey anti-goat IgG secondary antibody [I-MP]. The same procedure was carried out with another anti-clathrin antibody [CS] (2.5 µg/mL) but using Alexa-546 conjugated goat anti-rabbit secondary antibody [I-MP]. Finally cells were washed in PBS and mounted in Vectashield mounting medium.

2.2.2.7 Confocal microscopy and image analysis for cardiomyocytes

Confocal microscopy was performed on a Zeiss LSM 510 META microscope [Z] with 63x 1.4 NA oil-immersion objective. GFP, anti-Clathrin (Alexa-546) and anti-HA (Alexa- 633) fluorophores were excited at 488 nm, 543 nm, and 633 nm, respectively, and detected with corresponding channels 505-530 nm, 560-615 and 657-753 nm. The pinhole was set at one Airy disc, images were digitised at 16 bit with pixel size of 0.07 µm. Gain and offset were optimised to fill the dynamic range and were kept constant for all images acquired for quantitative fluorescence measurements. Images were exported from a Zeiss LSM Data server [Z] for analysis with ImageJ software (National Institutes of Health).

To determine the extent of colocalisation, GFP and anti-HA signals were correlated and Pearson's coefficients determined for cells labelled with anti-HA and non-specific Fab fragments. Regions of Interest (ROIs) at the transverse-tubules were selected to include intracellular areas of the cardiomyocyte, excluding sarcolemma and perinuclear regions. ROIs at the sarcolemma were carefully selected in order to exclude signals from adjacent transverse-tubules. Single pixel noise was removed with ImageJ despeckle filter, and intensities of GFP and anti-HA signals were

analysed and correlated using the Red-Green Correlator plugin. Pearson's coefficients were measured for 1-3 regions of 5-7 cells for each condition.

The relative amounts of HA-GLUT4-GFP exposed at transverse-tubules and sarcolemma was estimated from measurements of GFP and anti-HA fluorescence signals. Profiles were calculated for regions of transverse-tubule and sarcolemma and averaged along the corresponding membrane (~100 lines/profiles per ROI) to increase signal-to-noise ratio. Sarcolemma ROIs were rotated such that membrane was parallel to the y-axis of the profile. Membrane regions were selected such that peak width corresponded to a diffraction limited image of a membrane. This was estimated from the full width half maximum of a point spread function (~7 pixels = 0.5 µm). Profiles data were exported to Origin [M-GE] and peak intensity and peak integrals (the area under the peak) were automatically measured using a peak analysis subroutine. Peaks of a width significantly larger than 0.5 µm were excluded from analysis since they were likely to represent membrane regions with associated large intracellular GLUT4-containing compartments. Peak intensity and integral value were adjusted for non-specific background, which was measured as a baseline level within the cell. For sarcolemma regions, peaks were adjusted for background difference inside and outside of the cell. For transverse-tubules peak values were averaged for 10-20 individual tubules within 3 ROIs per cell. For sarcolemma regions peaks were averaged for 3-5 ROIs per cell. At least 10 cells were processed for each condition. All data presented as a mean value ± standard error.

2.2.3 Anti-HA antibody purification and Fab fragment generation

2.2.3.1 Purification of anti-HA antibody from ascites fluid

For antibody uptake experiments, anti-HA antibody was purified from ascites fluid to remove any potential stimuli present in the ascites fluid. Ascites fluid was diluted 1/10 in IgG binding buffer before being passed through a 5 mL column of Protein A- or G- conjugated amylose resin beads [P]. The beads were then washed with 50 mL binding buffer to remove any non-IgG proteins. Bound antibody was eluted in elution buffer. The eluant was immediately neutralised in 1 M Tris-HCl pH 8. Finally, the buffer was exchanged to PBS using centrifugal filtration columns [M] and the antibody solution concentrated to 5-7 mg/mL.

2.2.3.2 Production of anti-HA antibody Fab fragments

Fab fragments were generated using the ImmunoPure® Fab Preparation Kit [P], following the manufacturer's instructions. Briefly, Anti-HA antibody and Mouse IgG isotype control [A] were subjected to papain digestion for 5 h at 37^{o}C. Fab fragments were subsequently purified by binding undigested antibody and Fc fragments to a Protein A column [P] as described above. Collected fractions were pooled, concentrated and the buffer exchanged to PBS using centrifugal filtration columns [M]. The concentration of Fab fragment in solution determined by absorbance at 280 nm before BSA was added to a final concentration of 0.1% (w/v) BSA [CEL].

2.2.4 GLUT4 trafficking in L6 cells

2.2.4.1 L6 cell culture

L6 cells (Professor David James (The Garvan Institute, Sydney)) (up to passage 25) were cultured in normal growth media (α-minimal essential medium supplemented with 10% heat-inactivated foetal calf serum (FCS) and 1% antibiotic/antimycotic (A/A) solution) at 37°C in 10% CO_2. Cells were seeded in 96 well plates [GBO] and for differentiation into myotubes were cultured in differentiation media (α-minimal essential medium supplemented with 2% heat-inactivated FCS and 1% A/A solution) at 37 °C in 10% CO_2. Myotubes were maintained in this medium post differentiation and were used for experiments 5–9 days after the initiation of differentiation.

2.2.4.2 Manipulation of pBabe HA-GLUT4 plasmid

HA-GLUT4 cloned into the retroviral vector pBabe was provided by Professor David James. This construct was transformed into competent XL-1 blue *E.coli* (*recA1 endA1 gyrA96 thi-1 hsdR17 supE44 relA1 lac* [F´ *proAB lacI*qZΔ*M15* Tn*10* (Tetr)] (Genes listed signify mutant alleles. Genes on the F´ episome, however, are wild-type unless indicated otherwise) [ST] by adding 2 µL miniprep product to 50 µL of the cells on ice for 30 min. XL-1 Blue cells were subsequently heat-shocked for 45 sec at 42^{o}C before returning to ice for 2 min. Luria Broth (200 µL) was added to the cells

and they were outgrown for 30-45 min at 37°C. All cells were then transferred to agar plates containing 50 µg/mL Ampicillin [S], and incubated at 37°C overnight.

Plasmid DNA was purified from 10 mL XL-1 Blue cultures using the Wizard Plus SV miniprep DNA purification system [PRO] according to the manufacturer's instructions.

2.2.4.3 Platinum-E packaging cell line cell culture

Platinum-E (Plat-E) cells (provided by Professor David James) were cultured in Plat-E growth media (Dulbecco's Modified Essential Medium (DMEM) supplemented with 10% heat-inactivated FCS, penicillin/streptomycin/glycine, 10 µg/mL blastocidin [S] and 1 µg/mL puromycin [S]) at 37°C in 10% CO_2. Cells were maintained at less than 90% confluence and passaged every 3 days.

2.2.4.4 Generation of HA-GLUT4 retrovirus

The Plat-E packaging cell line (modified HEK-293 cells) (Morita et al., 2000) was used for retrovirus production essentially as previously described (Shewan et al., 2003). These cells were transfected with HA-GLUT4 pBabe retroviral vector (containing the *gag* retrovirus gene) at 70% confluence using lipofectamine 2000 reagent [I-G] following the manufacturer's instructions. Cells were maintained at 37°C for 48 h post transfection, before being moved to 30°C for 24 h. The media containing retrovirus was collected, filtered to remove cellular debris and stored at -80°C.

2.2.4.5 Stable expression of HA-GLUT4 in L6 myotubes

L6 myoblasts at approximately 30% confluence were incubated with 1 mL (virus amount varied for viral titration experiments) HA-GLUT4 retrovirus in the presence of 8 µg/mL polybrene [S] for 5 h at 37°C, 10% CO_2. Following an overnight recovery period to allow to HA-GLUT4 and selection marker expression, cells were passaged in L6 normal growth media supplemented with 2 µg/mL puromycin to select for infected cells. L6 cells to be used as a background control were infected

with 1 mL of retrovirus containing the empty pBabe vector. Myoblasts were differentiated into myotubes in 96 well plates as described above.

2.2.4.6 Measuring GLUT4 plasma membrane levels; transition state assay

Measurement of cell surface HA-GLUT4 as a percentage of total cellular HA-GLUT4 was performed as previously described (Govers et al., 2004). L6 myotubes cultured in 96 well plates were serum-starved for 16 hrs in α-minimal essential medium (without bicarbonate) with 20 mM HEPES and 0.2% BSA [CEL] and maintained in this medium throughout subsequent incubations. Where stated, L6 myotubes were incubated with 100 nM wortmannin [CAL] or 10 μM Akti (Professor Peter Shepherd (Auckland, NZ)) for 15 min prior to stimulation. Cells were stimulated with 200 nM insulin [CAL], 2 mM AICAR [S] or 100 μM A-769662 (Dr. Kei Sakamoto (Dundee, UK)) for stated times. To investigate additivity between insulin plus AICAR, insulin plus A-769662 and AICAR plus A-769662, agonists were added simultaneously. All inhibitors or agonists were added to basal media so that the final volume was 100 μL per well. Following treatment, cells were moved to 4^{o}C to arrest GLUT4 trafficking. Cells were washed three times with 200 μL ice-cold PBS and fixed with 100 μL 3% PFA [SS]. Cells were blocked and wells being used to determine total HA-GLUT4 levels were also permeabilised (50 μL blocking buffer ± 0.1% (w/v) saponin) before being incubated with 30 μL of blocking buffer containing anti-HA antibody (approx. 4 μg/mL) for 60 min at 25^{o}C (room temperature). Following extensive washing with PBS, myotubes were re-blocked (presence of saponin was vice versa to the first blocking step) before an incubation with 30 μL blocking buffer containing Alexa 488-conjugated goat anti-mouse secondary antibody (20 μg/mL) for 45 min at room temperature. After washing three times with 200 μL PBS, fluorescence (emm 485 nm/exc 520 nm) was measured with the bottom reading mode in a fluorescence microtitre plate reader (FLUOstar Galaxy; [BMG]). All incubations with agonists, inhibitors and antibodies were also performed on L6 cells stably expressing the empty pBabe vector and therefore not expressing HA-GLUT4. The fluorescent signal obtained from these wells was considered to be background and was subtracted from the signal detected from similarly treated wells containing L6 cells expressing HA-GLUT4. All data were expressed as a percentage of total HA-GLUT4.

2.2.4.7 Determination of recycling HA-GLUT4 as a percentage total HA-GLUT4

L6 myotubes cultured in 96 well plates were serum-starved as described above (section 2.2.4.6). 200 nM insulin and/or 2 mM AICAR was added to cells 30 min before anti-HA antibody so that the volume buffer in each well was 100 µL. To measure GLUT4 recycling with the cell surface, basal or stimulated myotubes were labelled with a saturating concentration of purified anti-HA antibody for 180 min. The saturating concentration of antibody was experimentally determined as 50 µg/mL. Wells being used to measure total cellular GLUT4 were not labelled with antibody. Cells were moved to 4^{o}C, washed three times with 200 µL ice-cold PBS and fixed with 100 µL 3% PFA. All cells were blocked and permeabilised (50 µL blocking buffer with 0.1% (w/v) saponin). To determine total GLUT4 levels, unlabelled cells were labelled with anti-HA antibody for 60 min at room temperature. Cells pre-labelled with anti-HA antibody did not receive additional antibody. Finally, cells were incubated with Alexa 488-conjugated goat anti-mouse secondary antibody (20 µg/mL) overnight at 4^{o}C. After washing three times with 200 µL PBS, fluorescence (emm 485 nm/exc 520 nm) was measured with the bottom reading mode in a fluorescence microtitre plate reader (FLUOstar Galaxy; [BMG]). All incubations with agonists, inhibitors and antibodies were also performed on L6 cells stably expressing the empty pBabe vector and therefore not expressing HA-GLUT4. The fluorescent signal obtained from these wells was considered to be background and was subtracted from the signal detected from similarly treated wells containing L6 cells expressing HA-GLUT4. Antibody-bound HA-GLUT4 was expressed as a percentage of total cellular HA-GLUT4, as measured by antibody labelling of cells post-fixation.

2.2.4.8 HA-GLUT4 recycling assay; anti-HA antibody uptake

L6 myotubes cultured in 96 well plates were serum-starved as described (2.2.4.6). For measurement of steady-state trafficking of HA-GLUT4 cells were left in basal media, or stimulated with 200 nM insulin, 100µM A-769662 or 2 mM AICAR, or a combination of these stimuli for 30 min before addition of anti-HA antibody. For inhibition of protein synthesis, cells were incubated with 15 µM cycloheximide [S] for 60 min prior to the addition of insulin. For wortmannin and Akti experiments, 100 nM wortmannin or 10 µM Akti was added 15 minutes prior to stimulation. In the case of basal cells, inhibitors were added 45 minutes before the addition of antibody. The final volume of buffer within each well was 100 µL prior to the addition

of anti-HA antibody. Basal or stimulated myotubes were labelled with a saturating concentration of anti-HA antibody for indicated times. Cells were moved to 4°C, washed extensively with ice-cold PBS and fixed with 3% PFA. Cells were blocked and permeabilised (blocking buffer with 0.1% (w/v) saponin) before being incubated with goat anti-mouse Alexa 488-conjugated secondary antibody (20 μg/mL) overnight at 4°C. After washing, fluorescence (emm 485 nm/exc 520 nm) was measured as described above. All incubations with agonists, inhibitors and antibodies were also performed on L6 cells stably expressing the empty pBabe vector and therefore not expressing HA-GLUT4. The fluorescent signal obtained from these wells was considered to be background and was subtracted from the signal detected from similarly treated wells containing L6 cells expressing HA-GLUT4. All values were normalised to fluorescence of insulin-stimulated samples which were incubated with antibody for 3 h.

Wide-field epifluorescent images (40x) of cells in 96 well plates were automatically obtained on the ImageXpress™ 5000 inverted epifluorescent imaging system, software and robotics [MD]. Prior to imaging, nuclei were labelled with Hoechst fluorescent dye (1/10,000 dilution) [I-MP]. Hoechst dye and Alexa-488 (Anti-HA antibody) fluorophores were excited at 360 (+/- 20) nm and 480 (+/-20) nm, respectively, and detected with corresponding channels 460 (+/-25) nm and 535 (+/- 25) nm. For presentation, images were exported to Photoshop 6.0 [ADO].

For comparison, 125-iodine labelled antibody was used to measure HA-GLUT4 trafficking. This was performed as above with an anti-HA antibody previously labelled with ^{125}I [PE]. After moving to ice and washing with PBS, cells were dissolved in 1M NaOH and transferred to vials. The uptake of ^{125}I labelled anti-HA antibody was determined by Gamma counting.

2.2.4.9 Subcellular localisation of anti-HA antibody labelled HA-GLUT4

L6 myotubes were processed as for the anti-HA uptake assay. Staining for anti-HA antibody labelled HA-GLUT4 was performed as described above (section 2.2.4.8).

To investigate the subcellular location of anti-HA antibody labelled GLUT4, antibodies to a range of subcellular markers were chosen, and individually incubated with anti-HA antibody labelled cells. These included markers for the endoplasmic reticulum (anti-PDI [CS] diluted 1/12.5), TGN (Syntaxin-6 [CS], 1/25), lyosomes (LAMP-2 [I-MP], 1/100) and early endosomes (EEA1 [CS], 1/100). In addition an antibody raised to the C-terminus of GLUT4 (in house) was used to ensure that all anti-HA antibody was associated with GLUT4. For all conditions, cells were

incubated with 30 µL of antibody diluted in blocking buffer. All antibodies were then labelled with goat anti-rabbit Alexa 633-conjugated secondary antibody. In addition to these antibodies, other markers used included Alexa-568 tagged wheat germ agglutinin (WGA) (TGN marker) [I-MP] and the nuclear dye DRAQ-5 [BSS].

Confocal microscopy was performed on 96 well plates on a Zeiss LSM710 confocal microscope with a 63x 1.4 NA oil-immersion objective. Alexa-488 (Anti-HA antibody), Alexa-568 (WGA) and Alexa-633 (subcellular markers or DRAQ-5) fluorophores were excited at 488 nm, 543 nm, and 633 nm, respectively, and detected with corresponding channels 505-530 nm, 560-615 and 657-753 nm. Pinhole was set at one Airy disc. Gain and offset were optimised to fill the dynamic range. For presentation, images were exported from a Zeiss LSM Data server [Z] to Photoshop 6.0 [ADO].

2.2.4.10 HA-GLUT4 internalisation assay

L6 myotubes cultured in 96 well plates were serum starved and stimulated as described above (2.2.4.6) and surface HA-GLUT4 was pulse-labelled with 50 µL of anti-HA antibody (50 µg/mL) diluted in α-minimal essential medium (without bicarbonate) with 20 mM HEPES and 0.2% BSA containing the relevant stimulus at 4^{o}C for 60 min. Following extensive washes to remove unbound antibody, myotubes were returned to 37^{o}C for designated periods of time. Cells were subsequently moved to 4^{o}C, washed with ice cold PBS and fixed with 3% PFA. Cells were incubated with blocking buffer for 20 min before surface antibody was detected using Alexa 488-conjugated goat anti-mouse secondary antibody, and fluorescence detected as described. All incubations with agonists, inhibitors and antibodies were also performed on L6 cells stably expressing the empty pBabe vector and therefore not expressing HA-GLUT4. The fluorescent signal obtained from these wells was considered to be background and was subtracted from the signal detected from similarly treated wells containing L6 cells expressing HA-GLUT4. Data normalised to give values as a percentage of the original (0 min) cell surface signal.

2.2.4.11 Measuring GLUT4 plasma membrane levels; transition from the stimulated to inhibited steady-state

L6 myotubes cultured in 96 well plates were serum-starved for 16 hrs as described above (2.2.4.6) and stimulated with 200 nM insulin for 30 min prior to incubation with 100 nM wortmannin for stated time periods. The assay was performed at either 37°C or 25°C. Following treatment, cells were moved to 4°C, washed with ice-cold PBS and fixed with 3% PFA. Cells surface and total levels of HA-GLUT4 were determined as described above (2.2.4.6). All data expressed as a percentage of total HA-GLUT4.

This assay was modified to investigate whether antibody binding to HA-GLUT4 altered the kinetics for HA-GLUT4 internalisation. The data obtained from the method described above was compared to data obtained from an assay where antibody was pre-bound to GLUT4. The assay was performed as above, except that 50 µg/mL anti-HA antibody was added to cells for which surface levels of GLUT4 were to be determined 30 min prior to stimulation with insulin. Cells pre-incubated with antibody were not incubated with anti-HA antibody post-fixation. Total cellular GLUT4 was determined by exposure of permeabilised L6 myotubes to anti-HA antibody as described above.

2.2.4.12 Kinetic analysis of GLUT4 trafficking in L6 cells

2.2.4.12.1 Kinetic analysis of transition state experiments

The time constant and half time for the translocation of GLUT4 was determined from transition state assays. This assay measures the translocation of GLUT4 to the plasma membrane following stimulation, the data from which was fitted to

$$L(t) = (P_0 - P_1)e^{-t/\tau} + P_1 \qquad \text{(Eq. 1)}$$

where $L(t)$ is the amount of GLUT4 at the plasma membrane at time, t, P_0 is the initial amount of GLUT4 at the plasma membrane in the absence of the perturbing agent, P_1 is the level of GLUT4 at the plasma membrane after long treatment with agonist(s), and τ is the time constant for the transition.

The half-time, $t_{1/2}$ for the transition is given by $t_{1/2} = \tau \ln 2$. However, this does not mean that the rate at which GLUT4 arrives at the plasma membrane is constant during this transition from the basal steady-state to the stimulated steady-state. This could be due to differing amounts of GLUT4 available for transport to the surface and/or varying exocytosis and endocytosis rate constants for GLUT4 which only become constant once the system is in steady-state.

2.2.4.12.2 Kinetic analysis of steady-state experiments

For the purposes of this analysis only the overall exocytosis and endocytosis rate constants to and from the plasma membrane were considered. These rate constants could be (and are highly likely to be) a combination of several processes. Overall measures of the exocytosis and endocytosis rate constants for GLUT4 to and from the plasma membrane were determined for the system using a two-compartmental model outlined previously (Coster et al., 2004), and described below (Figure 2.1).

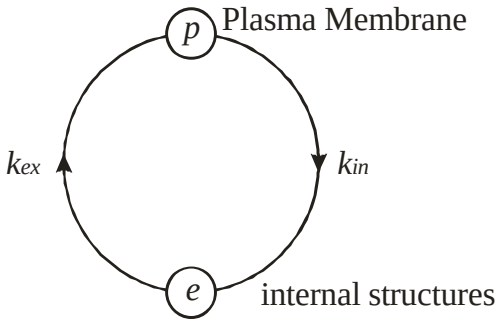

Figure 2.1. Representation of the two compartment model. GLUT4 is considered to be present either at the plasma membrane (P) or at internal structures (e). Only the overall rate constants for GLUT4 trafficking to (k_{ex}) and from (k_{in}) the plasma membrane are considered by this model.

As previously reported (Coster et al., 2004; Govers et al., 2004), it was assumed that all unlabelled HA-GLUT4 was immediately labelled with antibody upon GSV insertion into the plasma membrane. The increase in fluorescently labelled GLUT4 as a function of time is given by

$$L(t) = (P - T)e^{-k_{ex}t} + T \quad \text{(Eq.2)}$$

where $L(t)$ is the measured fluorescence as a function of time, t, k_{ex} is the overall exocytosis rate constant of GLUT4 to the plasma membrane, P is the amount of GLUT4 at the plasma membrane, and T is the total amount of GLUT4 recycling from internal structures to the plasma membrane, which includes both labelled GLUT4 at the plasma membrane and at internal sites.

The endocytosis rate constant, k_{in}, can be inferred from these 3 steady-state parameters as

$$k_{in} = \frac{k_{ex}(T - P)}{P} \quad \text{(Eq.3)}$$

In order to directly relate these parameters to the rate of GLUT4 trafficking, a combined parameter, R, defined as

$$R = k_{in}P = k_{ex}(T - P) \quad \text{(Eq.4)}$$

was determined, which is a measure of the GLUT4 transport rate from the plasma membrane. As the system is in steady-state, this is equivalent to the total transport rate to the plasma membrane.

2.2.4.12.3 Kinetic analysis of internalisation assays

The internalisation of GLUT4 is controlled by the overall internalisation rate constant, k_{in}. However, once the labelled GLUT4 molecules are internalised they then become part of the pool which can be exocytosed, at an overall rate k_{ex}. The amount of antibody-labelled GLUT4 is equal to the amount of GLUT4 present at the plasma membrane in the steady-state, and is initially all localised at the cell surface. This is distributed with time between the plasma membrane and the internal recycling structures. The model for this is

$$L(t) = \frac{P_0}{k_{ex} + k_{in}}\left(k_{ex} + k_{in}e^{-(k_{ex}+k_{in})t}\right) \quad \text{(Eq.5)}$$

where $L(t)$ is the measured fluorescence at the plasma membrane as a function of time, t, P_0 is the initial level at the plasma membrane, and k_{in} and k_{ex} are the overall exocytosis and endocytosis rate constants of GLUT4 to and from the plasma membrane respectively.

2.2.4.12.4 Error determination

The 95% confidence intervals for the parameters were determined as part of the non-linear regression fitting to the data. These confidence intervals were used to calculate the standard error for the parameters. The number of standard errors spanning the interval was determined using the Student's t inverse cumulative distribution function. The standard error is then the confidence interval divided by the number of standard errors. Data is presented as ± standard error.

2.2.4.12.5 Significance

Given that the standard errors were determined from the confidence interval, it was not possible to perform normal tests of significance. Statistical significance was tested by comparing the overlap of the confidence intervals of the parameters. In the case of no overlap then the difference in the values was statistically significant. An overlap of confidence intervals, however, does not imply the converse, but rather that there may or may not be statistical significance. All the data presented was analysed for statistical significance, and only those changes that were significant are discussed in the text.

2.2.5 Investigating insulin and AMPK signalling in L6 myotubes

2.2.5.1 Investigating the levels of phosphorylated PKB/Akt by fluorescent microscopy

L6 myotubes cultured in 96 well plates were serum-starved for 16 hrs in α-minimal essential medium (without bicarbonate) with 20 mM HEPES and 0.2% BSA [CEL]. Cells were stimulated with 200 nM insulin for stated times, and fixed as described above (2.2.4.6). Surface HA-GLUT4

was labelled in non-permeabilised cells with anti-HA antibody and Alexa 488-conjugated goat anti-mouse secondary antibody as described above (2.2.4.6). Cells were permeabilised with blocking buffer containing saponin and and labelled with anti-phospho-serine 473 Akt antibody [CS] diluted 1/50 in blocking buffer for 60 min. This was followed by incubation with 20 µg/mL Alexa 568-conjugated goat anti-rabbit secondary antibody for 30 min. Before imaging, nuclei were labelled with Hoechst fluorescent dye (1/10,000 dilution) [I-MP].

Wide-field epifluorescent images of cells in 96 well plates were automatically obtained on the ImageXpress™ 5000 inverted epifluorescent imaging system, software and robotics [MD]. Hoechst (nuclei), Alexa-488 (Anti-HA antibody) and Alexa-568 (phospho-serine 473 Akt) and fluorophores were excited at 360 (+/- 20) nm, 480 (+/-20) nm and 570 (+/-10) nm, respectively, and detected with corresponding channels 460 (+/-25) nm, 535 (+/- 25) nm and 620 (+/- 30) nm. Analysis of images was performed by Definiens software [DEF]. This software uses an object-orientated programming language permitting in-house rule sets to be written. This allows fully automated classification and quantification of any biological feature such as nuclei or whole cells. Specifically designed rule sets (Jo Peel (AstraZeneca, Loughborough, UK)) were used to analyse 20x images of L6 myotubes to determine the number of nuclei, the total area of nuclei, a quantification of Alexa-488 and Alexa-568 fluorescent signals and the area covered by Alexa-488 and Alexa-568 fluorescent signals.

2.2.5.2 Production of L6 whole cell lysates

L6 myoblasts were differentiated into myotubes in 96 well plates as described above (section 2.2.4.1). Cells were serum-starved for 16 hrs in α-minimal essential medium (without bicarbonate) with 20 mM HEPES and 0.2% BSA. Where indicated, cells were incubated with 100 nM wortmannin or 10 µM Akti for 15 min prior to stimulation. Cells were stimulated with previously indicated concentrations of agonists for stipulated time periods. Myotubes were washed three times with 200 µL PBS, and lysed with 50 µL lysis buffer per well for 10 min. Cells were lysed in SDS lysis buffer containing protease inhibitors (aprotinin, antipain, pepstatin A, and leupeptin; each at 1 µg/mL, 100 µM 4-(2-aminoethyl)benzenesulfonyl fluoride (AEBSF) [S]), and phosphatase inhibitors (10 mM sodium fluoride, 1 mM $NaMO_4$, 200 µM Na_3VO_4, 58 nM cypermethrin, 5 µM dephostain, 100 nM okadaic acid, and 10 pM nuclear inhibitor of protein

phosphatase-1 [CAL]). Wells containing similarly treated cells were combined and sonicated at 10 microns for 6 x 1 seconds. Cells were centrifuged at 17,000 x g for 30 min at 15^{o}C to pellet any non-soluble material. The protein concentration of cleared lysates was determined by the BCA assay.

2.2.5.3 BCA protein assay

The bicinchoninic acid (BCA) protein assay [P] was used to determine protein concentrations. A standard curve of BSA (0 – 1 mg/mL BSA in 0.1 M NaOH) was prepared. 10 μL of the BSA standard curve was added to a microtitre plate [G] in duplicate. 10 μL of sample was also added to the plate, either undiluted or diluted in 0.1 M NaOH. The BCA working solution was prepared by adding Reagent A [P] and Reagent B [P] together in a ratio of 50:1. 200 μL of this was then added to each of the wells containing standard and sample. The plate was incubated at 37^{o}C for 30 min, allowed to cool and then read on a Tecan Spectra Rainbow Thermo microplate spectrophotometer at 565 nm [T].

2.2.5.4 SDS-PAGE electrophoresis

Electrophoresis was carried out using the Laemmli discontinuous buffer system (Laemmli, 1970) in electrophoresis running buffer. 1.5 mm thick slab gels were prepared using either the Bio-Rad mini-Protean II apparatus [BR], CBS system apparatus [CBS] or Atto Dual Mini Vertical PAGE cell system [ATT]. Gels were prepared using acrylamide/bis-acrylamide (30% (w/v) acrylamide) [ND-F] and resolving gel buffer or stacking gel buffer. Gel polymerisation was initiated by addition of 10% (w/v) ammonium persulphate (APS) [TFS] and N,N,N,N'-tetramethylethylenediamine (TEMED) [S]. The acrylamide composition of the resolving and stacking gels varied depending on the protein of interest. Prior to electrophoresis, lysates were further solubilised by the addition of sample buffer and boiled for 5 min. Samples were loaded onto the gels alongside Novex sharp prestained markers [I]. The gels were run at 200 V in electrophoresis buffer until the dye front had run out of the gel (approximately 1 h).

2.2.5.5 Electrophoretic transfer of proteins to nitrocellulose membranes

Following SDS-PAGE, proteins were transferred onto a nitrocellulose membrane using the Multiphor II NovaBlot electrophoretic transfer apparatus [A]. Gels were briefly washed in transfer buffer to remove the electrophoresis running buffer. The electrode paper and nitrocellulose were also briefly immersed in transfer buffer. Nine pieces of NovaBlot electrode paper [A] cut to the size of the gel were placed on the anode, followed by a piece of nitrocellulose membrane with a 45 μM pore size [GE]. The resolving gel was then placed on top followed by another nine pieces of electrode paper and then the cathode. It was ensured that there were no bubbles trapped between the layers. The transfer was run at (area of the gel cm^2 x 0.8) mA for 1 h 50 min or 2hr 30 min when blotting for larger proteins such as Acetyl Coenzyme A Carboxylase (ACC). Following the transfer, the nitrocellulose membrane was washed in double-distilled H_2O (dd H_2O), and incubated in Ponceau S stain for 2 min. Excess stain was washed off with ddH_2O.

2.2.5.6 Western blotting

The nitrocellulose was washed in Tris-buffered Saline containing Tween-20 (TBS-T) to remove the Ponceau S stain. The nitrocellulose was blocked in 5% (w/v) Marvel (dried skimmed milk powder) in TBS-T or 5% (w/v) BSA in TBS-T when blotting for phospho-proteins for 30 min to block non-specific protein binding sites. Membranes were briefly rinsed and primary antibody incubations were performed overnight at 4^{o}C. All antibody incubations were performed at a 1/1000 dilution unless otherwise stated. Antibodies directed towards phospho-Akt (serine 473), phospho-AMPK (threonine 172) and AMPK (alpha subunit) where from Cell Signaling [CS]. Antibodies to detect Akt2 and phospho-ACC (serine 79) where purchased from Upstate [U]. Rabbit anti-C-terminal GLUT4 antibody (used at 1/5000 dilution) was raised in-house as previously described (Holman et al., 1990). The membrane was washed 4 x 15 min in TBS-T before being incubated with appropriate secondary antibody. Secondary antibodies (goat anti-rabbit IgG HRP conjugate [P] or goat anti-mouse IgG HRP conjugate [P]) (used at 1/4000) were made up in 5% (w/v) Marvel in TBS-T and incubated with membranes for 45 min at room temperature. The membrane was then washed 5 x 10 min with TBS-T. Finally the nitrocellulose was developed by incubating the membrane with ECL SuperSignal West Dura [P] or ECL Advance [A] following the manufacturers

guidelines. The membrane was imaged using a Hamamatsu camera attached to the EPI Chemi II darkroom [UVP].

2.2.6 Characterisation of TBC1D1 antibodies

2.2.6.1 Manipulation of TBC1D1 and TBC1D4 plasmids

Full length TBC1D1 and TBC1D4 cloned into the pcDNA3 vector with a flag coding sequence so that a flag sequence fuses at the N-terminus of the protein were provided by Professor Francis Barr (Liverpool, UK).

Wild-type (WT) TBC1D1 PTB domains (amino acids 12-393) were amplified from a rat muscle cDNA library, and subsequently cloned into the pET-28a(+) vector (adding an N-terminal His-tag). A serine 231 to alanine mutation was subsequently generated in the TBC1D1 PTB domains by site directed mutagenesis (work carried out by Judith Richardson, University of Bath). These constructs were transformed into competent XL-1 blue *E.coli* (*recA1 endA1 gyrA96 thi-1 hsdR17 supE44 relA1 lac* [F´ *proAB lacI*q*ZΔM15* Tn*10* (Tetr)] (Genes listed signify mutant alleles. Genes on the F´ episome, however, are wild-type unless indicated otherwise) [ST] by adding 2 µL miniprep product to 50 µL of the cells on ice for 30 min. XL-1 Blue cells were subsequently heat-shocked for 45 sec at 42^{o}C before returning to ice for 2 min. Luria Broth (250 µL) was added to the cells and they were outgrown for 30-45 min at 37^{o}C. All cells were then transferred to agar plates containing 50 µg/mL Ampicillin [S], and incubated at 37^{o}C overnight.

Plasmid DNA was purified from 10 mL XL-1 Blue cultures using the Wizard Plus SV miniprep DNA purification system [PRO] according to the manufacturer's instructions.

2.2.6.2 Expression of recombinant His-tagged TBC1D1

Recombinant TBC1D1 PTB domain constructs were transformed into Rosetta-Gami (DE3) pLysS *E.Coli* cells (D(*ara-leu*)*7697* D*lacX74* D*phoA Pvu*II *phoR araD139 ahpC galE galK rpsL* (DE3) F′[*lac*$^{+}$ *lacI*^{q} *pro*] *gor522*::Tn*10 trxB* pRARE2 (Cam^{R}, Str^{R}, Tet^{R})) [N-MB] and grown overnight on agar plates supplemented with tetramycin, kanamycin and chloramphenicol [S]. Individual colonies were then used to inoculate large scale cultures. A test was performed to identify the best expression conditions (section 5.1). For all subsequent experiments, expression was induced with

0.5 mM isopropyl-β-D-thiogalactopyranoside (IPTG) [MEL] and incubated for 4 h at 25^{o}C. The culture was centrifuged at 5000 rpm for 10 min to pellet the bacteria.

Cells were resuspended in resuspension buffer and left on ice for 1 h. Suspensions were then sonicated 16 x 15 sec at 20 microns on ice, and soluble material pelletted by centrifugation at 12,000 x g at 4^{o}C for 15 min.

The supernatant was incubated with Ni-NTA His resin beads [N-MB] at 4^{o}C for 60 min to bind His-tagged proteins. Following washes with sodium phosphate buffer, the beads were added to a Talon column [C] and washed with resuspension buffer.

His-tagged protein was eluted with resuspension buffer supplemented with 100 mM imidazole. Fractions containing protein (as determined by spotting 2 µL on to nitrocellulose membrane and ponceau staining) were pooled and dialysed versus 50 mM Tris buffer in dialysis cassettes [P]. Protein concentration was determined by densitometry using a BSA standard curve and SDS-PAGE.

2.2.6.3 HEK-293 cell culture

HEK-293 cells were cultured in HEK-292 growth medium (Dulbecco's Modified Essential Medium (DMEM) supplemented with 10% heat-inactivated foetal calf serum and penicillin/streptomycin/glycine) at 37°C in 10% CO_2. Cells were maintained at less than 90% confluence and passaged every 3 days.

2.2.6.4 Expression of flag-tagged full-length TBC1D1 and TBC1D4 in HEK-293 cells

HEK-293 cells were seeded into 6 well plates in HEK-292 growth medium without antibiotics. The next day (at 60-70% confluence) cells were washed briefly with culture media (without antibiotics). Cells were transfected with full length flag-tagged TBC1D1 or TBC1D4 in the pcDNA 3 vector using lipofectamine LTX reagent [I-G] following the manufacturer's instructions.

24 h post-transfection, cells were washed and cell lysates were prepared for western blots in SDS lysis buffer containing protease inhibitors (aprotinin, antipain, pepstatin A, and leupeptin; each at 1 µg/mL, 100 µM 4-(2-aminoethyl)benzenesulfonyl fluoride (AEBSF) [S]), and phosphatase inhibitors (10 mM sodium fluoride, 1 mM $NaMO_4$, 200 µM Na_3VO_4, 58 nM cypermethrin, 5 µM dephostain, 100 nM okadaic acid, and 10 pM nuclear inhibitor of protein phosphatase-1 [all CAL])). Crude lysates were sonicated at 10 microns for 6 x 1 seconds, before being centrifuged at 17,000 x g for 30 min at 15^{o}C to pellet any non-soluble material. The protein concentration of cleared lysates was determined by the BCA assay. Lysates were separated by SDS-PAGE and transferred to a nitrocellulose membrane as described above (section 2.2.5.4-2.2.5.6). Recombinant proteins were detected by incubation of membranes with anti-His antibody conjugated to HRP [S] or novel rabbit polyclonal total-TBC1D1 antibodies (described below in section 2.2.6.6)

2.2.6.5 *In-vitro* AMP-activated protein kinase assay

0.5 µg of recombinant TBC1D1 PTD WT or TBC1D1 PTD S231A protein was incubated with 0.1 µg/mL human AMPK or 0.01 mU rat liver AMPK in reaction buffer (final volume 30 µL) for 15 min at 37^{o}C. The reaction was terminated by adding 15 µL 3x Laemmli sample buffer containing DTT. Samples were heated for 5 min at 95^{o}C, before being separated by 10% SDS-PAGE electrophoresis using the Atto Dual Mini Vertical PAGE cell system [ATT]. Poly-acrylamide gels were stained with Coomassie Blue stain in order to visualise and quantify recombinant TBC1D1 proteins. Gels were dried at 80^{o}C for 2-3 h under a vacuum. The dried gel was exposed to an imaging plate [F] for 1-3 days before radioactivity was measured and quantified on a Fuji FLA-5000 Fluoro Image Analyser [F].

To test the specificity of phospho-specific antibodies described below, the AMPK kinase assay was performed on both TBC1D1 PTD WT and TBC1D1 PTD S231A without radiolabelled ATP. Samples were separated by 10% SDS-PAGE and transferred to nitrocellulose membrane as described above and probed with anti-TBC1D1 antibodies.

2.2.6.6 TBC1D1 antibody generation

All TBC1D1 antibody generation was carried out by the Antibody Generation Group at AstraZeneca (Loughborough, UK). A brief overview of the generation protocol is provided below.

Peptide synthesis was performed by Bachem UK Ltd [B]. Target peptides were conjugated to BSA. All couplings were performed via a cysteine residue. Immunisation for rabbit polyclonal antibody generation was achieved via a 13 week protocol by Eurogentec [E]. The resulting antisera was affinity purified on a target peptide/antigen column (sulfolink coupling gel [P]). In the case of the phosphospecific antibodies, material bound to the phospho-peptide was further depleted by passing through the corresponding non-phospho-peptide affinity column.

2.2.6.7 TOTAL-TBC1D1 peptides for antibody generation

Three distinct immunogenic peptides from the amino acid sequence of TBC1D1 were selected for generation of an antibody to the total protein. These peptides were specifically chosen so as not to be present in the closely related Rab-GAP TBC1D4. These sequences were Glu-Pro-Asp-Leu-Arg-Lys-Ser-Gln-Pro-Trp (amino acids 76-85) (ID. 3001724), Asp-Ser-Pro-Ser-Arg-Tyr-Glu-Asp-Tyr-Ser-Glu (amino acids 766-776) (ID. 3001725) and Gln-Lys-Leu-Arg-Pro-Arg-Asn-Glu-Gln-Arg-Glu-Asn (amino acids 428-439) (ID. 3001726). Antibodies raised to total TBC1D1 were used at 1 µg/mL for western blotting procedures.

2.2.6.8 Phospho-specific TBC1D1 peptide for antibody generation

The peptide sequence surrounding serine 231 was used to raise an antibody to TBC1D1 phosphorylated at this site. The peptide corresponded to Cys-Pro-Met-Arg-Lys-Ser-Phe-Ser(phospho)-Gln-Pro-Gly-Leu-Arg-Ser (amino acids 226-235) (ID.3003377). Phospho-specific antibodies were used at 0.025 µg/mL for western blotting procedures.

2.2.7 Data analysis

GraphPad PRISM version 4.0 was used for all graphical analysis and determination of significance. Labworks version 4 [UVP] was used for densitometry analysis of western blots. The intensity of the radioactive ^{32}P-containing bands was determined using ImageGauge [F]. Analysis and error determination for kinetic experiments is described in detail above (sections 2.2.4.11.4-2.2.4.11.5).

3 Investigation of GLUT4 trafficking in cardiomyocytes in response to insulin, contraction and energy-status signalling

Glucose transport into skeletal muscle is enhanced by insulin-stimulation and in response to exercise. The signalling intermediates mediating glucose uptake in response to exercise include those activated by contraction and those activated by changes in the energy-status of the muscle such as AMP-activated protein kinase (AMPK). These stimuli activate initially distinct signalling pathways but increase glucose uptake by the same mechanism; augmenting the amount of the glucose transporter GLUT4 at the cell surface. Cardiac muscle responds to these stimuli in a similar way to skeletal muscle. In addition, cardiac tissue has experimental advantages over skeletal muscle in that it can be more readily dissociated into individual myocytes. This *ex-vivo* cardiomyocyte model permits the study of GLUT4 trafficking in cells retaining important aspects of muscle architecture such as the transverse tubules. In this study, we have isolated cardiomyocytes from a transgenic mouse line in which HA-GLUT4-GFP has been expressed under the control of a muscle specific promoter (I. Lisinski, V.A.Lizunov, D. R. Yver, O. Gavrilova, H. Al-Hasani and S.W.Cushman, unpublished). Therefore, recombinant GLUT4 is expressed only in skeletal muscle and heart muscle. Using this model system, we have investigated GLUT4 trafficking to and from the cell surface in response to activation of distinct signalling pathways which enhance glucose uptake.

3.1 Insulin, contraction and AMPK activation enhances glucose uptake into murine cardiomyocytes

Cardiomyocytes from wild-type (CD-1 Swiss albino) male mice were isolated by Langendorf perfusion and collagenase digestion. The glucose transport activity was determined by measuring 2-deoxy-D-glucose transport into cardiomyocytes stimulated by insulin, electrically-induced contraction and hypoxic conditions (Figure 3.1).

Basal cells transported 213.1 pmoles of 2-deoxyglucose/mg of protein/min, which corresponded to 20.3% of 2-deoxyglucose transported into insulin-stimulated cells. Stimulation

with 30 nM insulin resulted in a 5.0-fold increase in 2-deoxy-D-glucose uptake (p=<0.0001). Glucose uptake was stimulated less by contraction and hypoxia than by insulin. Electrically-induced contraction (p=0.0003) and hypoxia (p=0.0053) resulted in to a 3.3-fold and 2.2-fold increase in 2-deoxyglucose uptake over cardiomyocytes maintained in basal conditions, respectively.

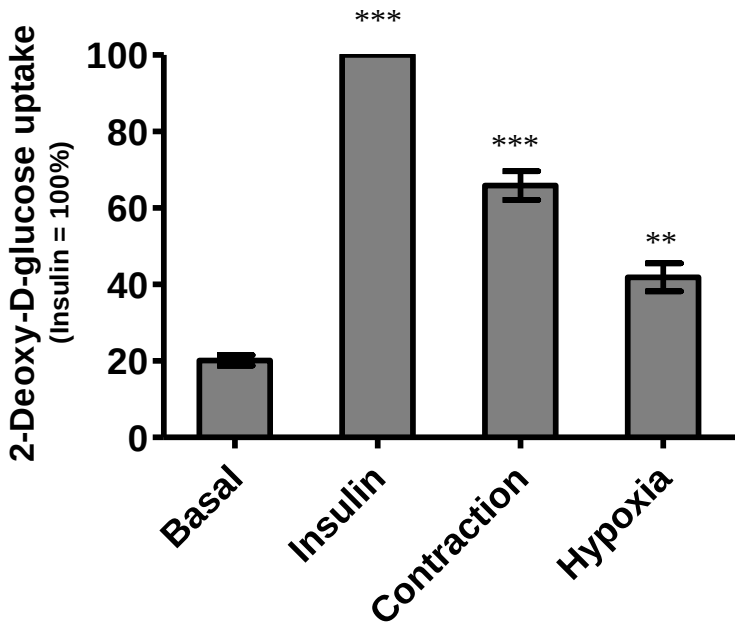

Figure 3.1. 2-Deoxy-D-glucose transport activity in insulin-, contraction- and hypoxia-stimulated cardiomyocytes. Glucose transport activities were determined in wild-type cardiomyocytes maintained in the basal unstimulated state or incubated with 30 nM insulin for 30 min, electrically induced to contract for 5 min or incubated under hypoxic conditions for 15 min. The data presented are the mean ± S.E.M. from three to six experiments. *** p = <0.005, ** p = <0.05 (unpaired t-test compared to basal).

3.2 Insulin, contraction and AMPK-activation stimulates GLUT4 translocation to the sarcolemma of murine cardiomyocytes

Stimulation with insulin, electrically-induced contraction or hypoxia enhanced 2-deoxy-D-glucose uptake in isolated cardiomyocytes. Although it is known that this is achieved by increasing GLUT4 levels at the cell surface, there is biochemical evidence that these distinct stimuli may preferentially translocate GLUT4 to the sarcolemma or transverse tubules. Using a transgenic

mouse line expressing HA-GLUT4-GFP under the control of a muscle specific promoter, we have studied GLUT4 trafficking to the sarcolemma and transverse tubules under insulin-, contraction- and hypoxia-stimulation.

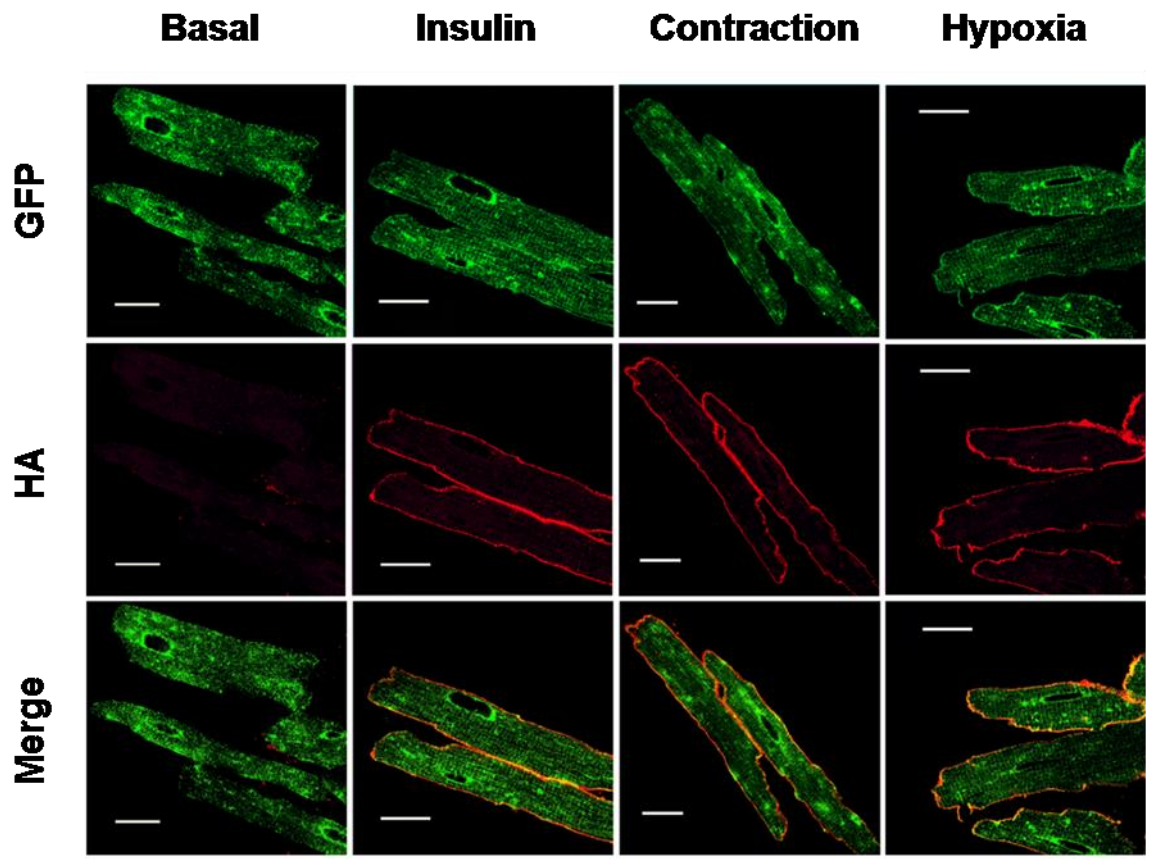

Figure 3.2. Translocation of HA-GLUT4-GFP to the sarcolemma of insulin-, contraction- and hypoxia-stimulated cardiomyocytes. Isolated cardiomyocytes expressing HA-GLUT4-GFP were maintained in a basal unstimulated state or incubated with 30 nM insulin for 30 min, electrically induced to contract for 5 min or incubated under hypoxic conditions for 15 min. After these treatments, the cells were washed with KRH buffer, fixed with 4% and blocked with 3% goat serum, 1% BSA. Cells were incubated with intact anti-HA antibody (1 µg/ml) which preferentially detects sarcolemma GLUT4. All cells were viewed in approximately the same focal plane. The size bar is 20 µm. GFP (top panels) was detected between 505 and 530 nm and anti-HA antibody labelled with Alexa-633-conjugated secondary antibody (middle panels) was detected between 657 and 753 nm. Merged images are in the bottom panels. Results shown are from representative images from approximately 25 examined cells in 5 experiments.

In unstimulated cardiomyocytes, HA-GLUT4-GFP has a punctate distribution throughout the cell interior with a particular concentration in a perinuclear region. GLUT4 is present only at very low levels at the sarcolemma (low GFP signal) and the exofacial HA- epitope is not available to bind antibody (very low Alexa-633 signal) (Figure 3.2 *middle panel*). Under these basal conditions, GLUT4 does not appear to be aligned along regions corresponding to the transverse tubules. When the cardiomyocytes were stimulated with insulin, electrically-induced contraction or by hypoxia, the GFP signal from the GLUT4 appeared to show more alignment along transverse tubules (Figure 3.2 *top panel*). The change in distribution of GFP from intracellular sites to the sarcolemma surface was hard to visualise via the GFP signal as this signal is diluted as it becomes dispersed throughout the sarcolemma. In order to detect HA-GLUT-GFP translocation to the cell sarcolemma surfaces more readily, we have taken advantage of the availability of the exofacial HA-tag. We have found that when using whole anti-HA-antibody detection in non-permeabilised cells, the HA-epitope is only detected at the sarcolemma and not at the transverse tubule membrane (Figure 3.2). The level of HA-epitope exposure at the sarcolemma was increased by all stimulating conditions studied.

3.3 Insulin, contraction and AMPK-activation stimulates GLUT4 translocation to the transverse tubules of murine cardiomyocytes

The specificity in labelling towards the sarcolemma with the anti-HA antibody was found to be due to several factors that included the relatively large size of intact anti-HA antibody and fixation of the cells before incubation with anti-HA antibody. To more readily detect the exposure of the exofacial HA-epitope at both the sarcolemma and the transverse-tubule surfaces, we generated a Fab fragment of the anti-HA-antibody. In addition, the labelling procedure was amended so that the cells were fixed after incubation with the Fab fragment.

The profile of the GFP and anti-HA signals within an intracellular region of interest (ROI) of a non-stimulated basal cell is diffuse (Figure 3.3 *A*). In addition, the anti-HA signal is very low. By contrast, the anti-HA signal is increased in cells that have been stimulated with insulin, and the GFP and anti-HA signals are clearly defined and localised transversely within the ROI (Figure 3.3 *B*). Cells stimulated by electrically-induced contraction and hypoxia (Figure 3.3 *C* and *D*

respectively) also have strong transverse alignment of the GFP with anti-HA signals that are similar to those produced following insulin-stimulation.

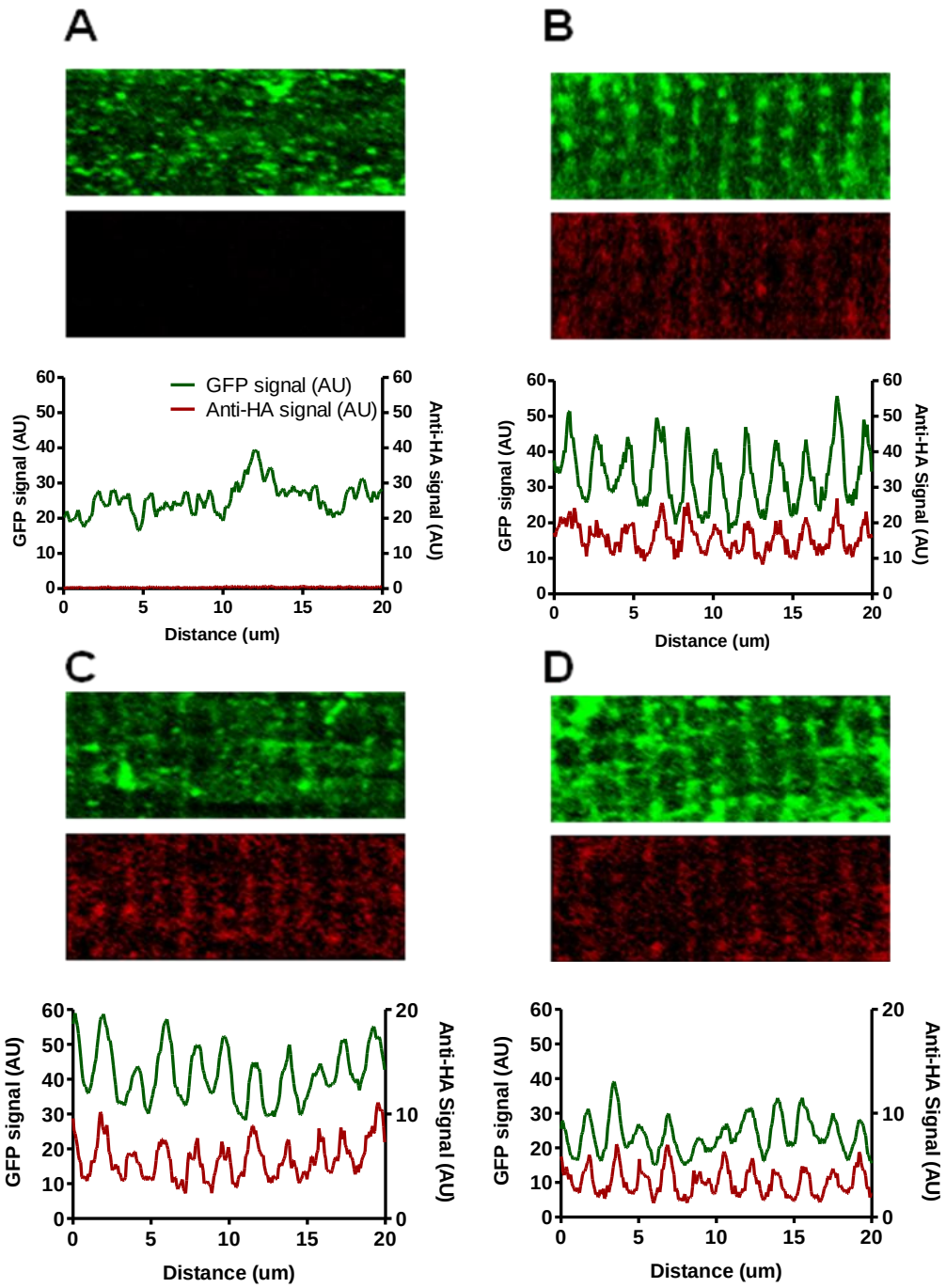

Figure 3.3. Translocation of HA-GLUT4-GFP to the transverse tubules of insulin-, contraction- and hypoxia-stimulated cardiomyocytes. *A*, Isolated cardiomyocytes expressing HA-GLUT4-GFP were either maintained in the basal unstimulated state or *B*, incubated with 30 nM insulin for 30 min, *C*, electrically induced to contract for 5 min at 100V, 10 Hz, pulse width 1 ms or *D*, incubated under hypoxic conditions for 15 min. Following stimulation, cells were incubated with anti-HA Fab fragment (5 µg/ml) for 15 min to label exposed HA-epitope at both the sarcolemma and transverse-tubules. Cells were washed, fixed in 4% PFA, permeabilised and then probed with Alexa-633-conugated secondary antibody. The GFP (top panels) and anti-HA signals (middle panels) were analysed in regions of interest (defined as described in Materials and Experimental Procedures) as transverse intensity profiles (lower panels). Results shown are from representative images from approximately 25 examined cells in 3 experiments.

The signals in ROIs were averaged along each transverse tubule (in the direction of the *y*-axis) and are presented as intensity plots below the fluorescence data (Figure 3.3). This profile averaging efficiently eliminates single-pixel noise and random peaks caused by scattered GLUT4 vesicles. It is clear from these plots that the pattern of anti-HA signal very closely matches the pattern of the GFP signal. This conclusion is supported by the calculation of Pearson's colocalisation coefficients (Figure 3.4), which were calculated for GFP and anti-HA signals for all ROIs studied. A non-specific Fab fragment was included as a negative control to ensure that the anti-HA signal was not a result of Fab fragments being 'trapped' by the fixation procedure. The colocalisation coefficients for ROIs from stimulated cells were significantly different from the nonspecific Fab fragment controls ($p = <0.005$ for all conditions). These data suggest that the anti-HA antibody Fab fragment was specifically recognising HA-epitope exposed at the transverse tubules.

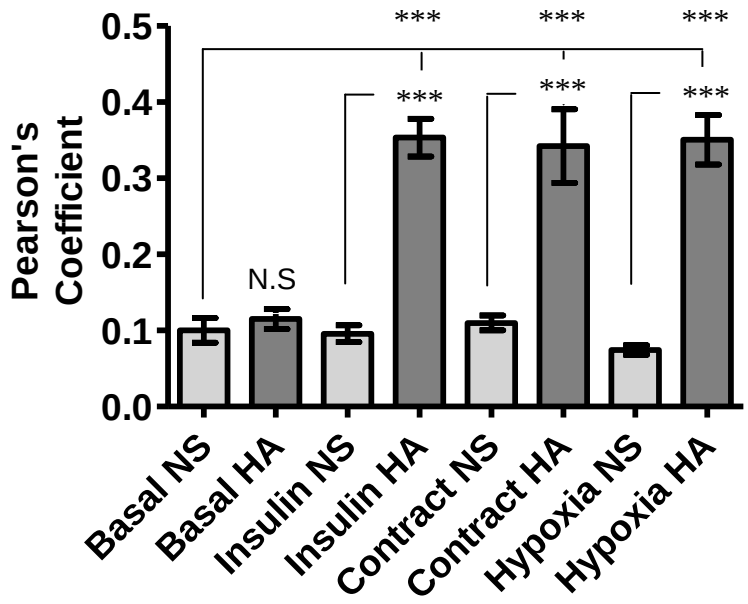

Figure 3.4. The Pearson's colocalisation coefficient for GFP and anti-HA (HA) or non-specific (NS) Fab fragment signals (as detected by goat anti-mouse IgG Alexa-633) in unstimulated cardiomyocytes and cardiomyocytes stimulated with 30 nM insulin, electrically-induced contraction or hypoxia. The data presented are the mean ± S.E.M from 25 images from three experiments. *** p = <0.005, (unpaired t-test compared to basal anti-HA Fab labelling), *** p = <0.005, N.S. p = <0.5 (unpaired t test compared to NS Fab fragment).

3.4 Quantification of GLUT4 translocation responses

Use of the anti-HA antibody Fab fragment enabled analysis and comparison of sarcolemma and transverse-tubule labelling within the same cells. The patterns of sarcolemma labelling as recorded from the GFP and Fab anti-HA signals are similar to those obtained using the intact anti-HA antibody (Figure 3.2 and Figure 3.5 *A*). In order to compare the levels of translocation of GLUT4 induced by stimulations of different signalling pathways, both the GFP and anti-HA signals at the sarcolemma and the transverse tubules were quantified (Figure 3.5). Representative ROIs from which intensity profiles were generated and fluorescence intensities calculated are presented in Figure 3.5 (*B* and *C*). For each condition studied, there was a significant increase in GFP and anti-HA signal at both the sarcolemma and transverse tubules (p= <0.005). In

comparison with the insulin response, contraction and hypoxia give rise to smaller responses at the sarcolemma (Figure 3.5 *D*) and the transverse tubules (Figure 3.5 *E*). Furthermore, no selectivity is apparent for the stimulated translocation response at the sarcolemma versus the transverse-tubules. The absolute values for the increases in the anti-HA and GFP signals at the sarcolemma and the transverse tubules cannot be directly compared. This is because there is a possibility of differential access of the Fab fragment to the exofacial surface of GLUT4 at these locations and there is a difference in the surface area of these external membrane domains. The transverse-tubule network has been estimated to make up 66% of the total external membrane area of cardiomyocytes (Soeller and Cannell, 1999).

At the sarcolemma insulin- and contraction-stimulation led to a greater increase in the anti-HA signal than the GFP signal (Figure 3.5 *D*). The fold-increase in the anti-HA signal is approximately twice the increase in the GFP signal for these stimulating conditions. The change in anti-HA signal reaches a maximum of approximately sevenfold for the insulin stimulation (Figure 3.5 *D*). However, following hypoxia stimulation, the rises in GFP and anti-HA signals at the sarcolemma are similar (both approximately threefold). This differential effect can be seen most readily by calculating the ratio of the anti-HA signal to the GFP signal (Figure 3.5 *F*). It suggests that insulin and contraction signalling may have a greater stimulatory effect on the reaction, possibly vesicle fusion, which leads to full exposure of the HA-epitope tag at the sarcolemma. This effect of insulin and contraction signalling is not evident at the transverse tubules (Figure 3.5 *E* and *F*). At this location these stimuli and hypoxia resulted in similar increases in anti-HA and GFP signals.

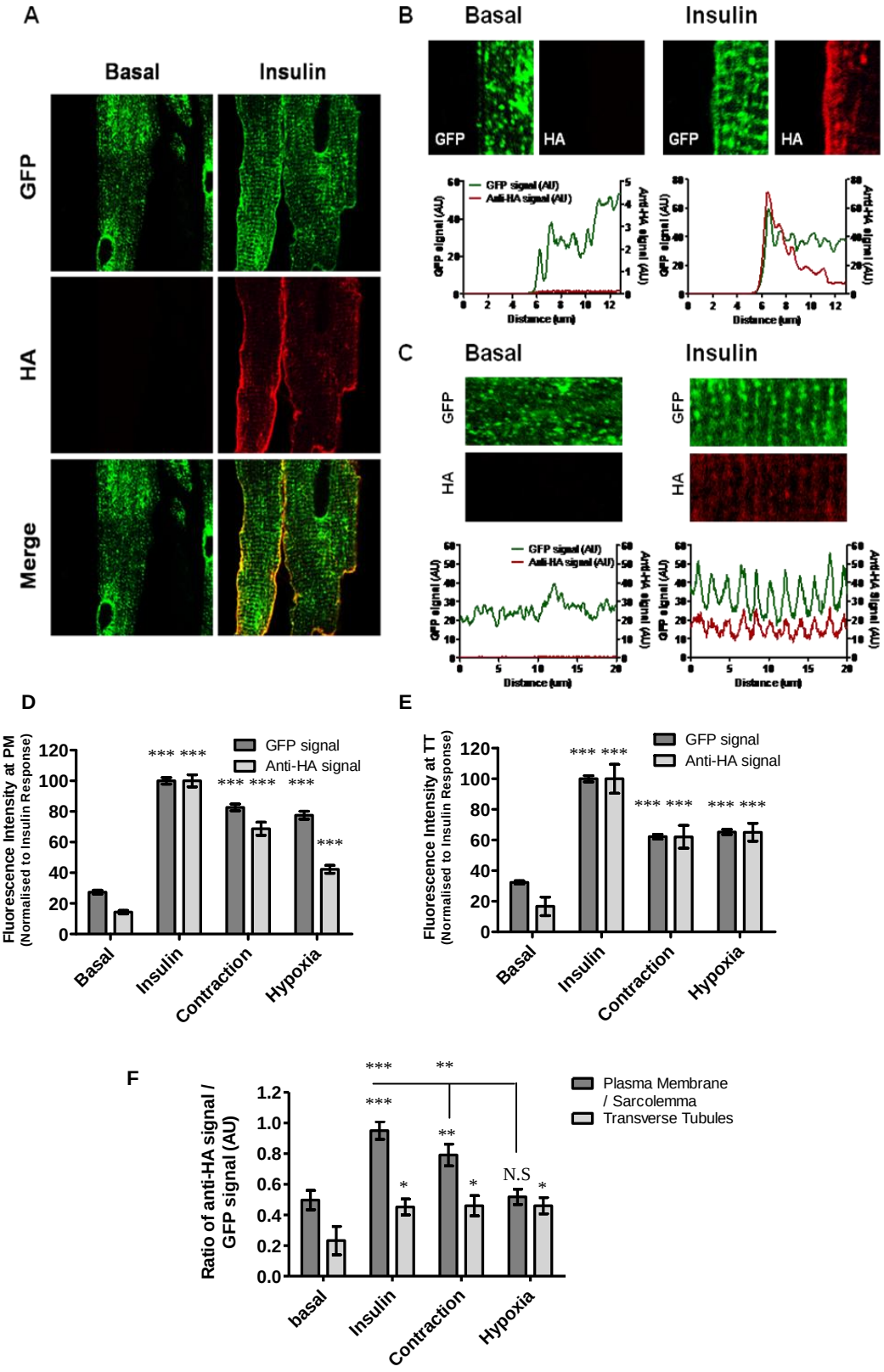
A
Basal
Insulin
GFP
HA
Merge
B
Basal
Insulin
GFP
HA
GFP signal (AU)
Anti-HA signal (AU)
Distance (um)
C
Basal
Insulin
GFP
HA
GFP signal (AU)
Anti-HA signal (AU)
Distance (um)
D
Fluorescence Intensity at PM
(Normalised to Insulin Response)
GFP signal
Anti-HA signal
Basal
Insulin
Contraction
Hypoxia
E
Fluorescence Intensity at TT
(Normalised to Insulin Response)
GFP signal
Anti-HA signal
Basal
Insulin
Contraction
Hypoxia
F
Ratio of anti-HA signal /
GFP signal (AU)
Plasma Membrane
/ Sarcolemma
Transverse Tubules
N.S
basal
Insulin
Contraction
Hypoxia

Figure 3.5. Quantitative analysis and comparison of GLUT4 translocation to sarcolemma and transverse-tubule membranes of cardiomyocytes. *A*, Isolated cardiomyocytes expressing HA-GLUT4-GFP were either maintained in the basal unstimulated state or incubated with 30 nM insulin for 30 min,. Following stimulation, cells were incubated with anti-HA Fab fragment (5 μg/ml) for 15 min to label exposed HA-epitope at both the sarcolemma and transverse-tubules. Cells were washed, fixed in 4% PFA, permeabilised and then probed with Alexa-633-conugated secondary antibody. The GFP (top panels) and anti-HA signals (middle panels) were analysed in regions of interest (as defined in Materials and Experimental Procedures). Representative ROIs and intensity profiles used to quantify the fluorescent signal at the sarcolemma (*B*) and transverse tubule (*C*) are shown for basal and insulin-stimulated cells. Average GFP and anti-HA fluorescence intensity was determined from regions representing the sarcolemma and transverse-tubule membrane (as defined in the Materials and Experimental Procedures). *D*, Sarcolemma GFP (dark bars) and anti-HA (light bars) signals measured under insulin-, contraction- and hypoxia-stimulation. All fluorescence signals were normalised to the maximum values obtained under insulin stimulation. *E*, Transverse tubules GFP (dark-grey bars) and anti-HA (light-grey bars) signals measured under insulin-, contraction- and hypoxia- stimulation. *F*, Ratio of anti-HA to GFP signals at sarcolemma and transverse tubules. Error bars are ± S.E.M. of 24-27 sarcolemma values and 40-90 transverse-tubules values from seven to ten cells per condition, from a single representative experiment. *** p= <0.0005, **p=<0.005, *p=<0.05, N.S p =>0.005 (unpaired t test compared to basal (*D* and *E*)), *** p = <0.005, ** p = <0.05 (unpaired t-test compared to sarcolemma or transverse tubule anti-HA/GFP ratio (*F*)).

3.5 Internalisation of GLUT4; return to the basal state following insulin, contraction and hypoxia stimuli

In order to investigate the process of internalisation of GLUT4 mobilised to the sarcolemma by different specific stimuli, cardiomyocytes were stimulated and live cells were incubated with anti-HA antibody. This was used to pulse-label the GLUT4 at the cell surface via the HA-epitope. From earlier studies (Figure 3.2), it is likely that this labelling procedure was selectively labelling GLUT4 at the sarcolemma. Cells were subsequently subjected to washing steps and reversal conditions to return the cells to an un-stimulated basal state. Upon removal of the stimulus, anti-HA staining at the sarcolemma became punctate, as shown clearly by the red anti-HA-antibody signal (Figure 3.6). The appearance of this punctate anti-HA staining was very rapid (within 1 min) after the removal of the stimulus. The punctate appearance of the anti-HA signal at the sarcolemma contrasts to images obtained during stimulations as in Figure 3.2, where anti-HA

staining appears as a contiguous signal at the sarcolemma. This change is associated with an increase in anti-HA antibody detected at intracellular locations, including the peri-nuclear region. When insulin-, contraction- and hypoxia-stimulated cardiomyocytes are returning to a basal state, the GLUT4 becomes co-localised with clathrin at, and adjacent to, the sarcolemma (Figure 3.6). The zoomed images (small insets in Figure 3.6) indicate colocalisation of anti-clathrin antibody (blue) with both anti-HA-antibody (red) and the GLUT4-GFP signal (green). In cardiomyocytes that are maintained in the basal state during the same labelling procedures, very little anti-HA antibody signal is detected. However, GLUT4 that colocalises with clathrin is also evident at the sarcolemma (Figure 3.6, basal panels). We have also found extensive colocalisation of GLUT4-GFP with clathrin at the sarcolemma, transverse tubules and perinuclear regions in the basal state and following the insulin, contraction and hypoxia stimulations (but using a different anti-clathrin antibody) (Figure 3.7).

Figure 3.6. Colocalisation of internalising GLUT4 with clathrin. Isolated cardiomyocytes expressing HA-GLUT4-GFP were maintained in the unstimulated, basal state (top panels), stimulated with 10 nM insulin (middle panels) or in hypoxic buffer for 15 min (bottom panels). During treatment cells were incubated with anti-HA antibody (5 µg/ml) at 37°C for 15 min. Following removal of the stimulus and washing to remove excess antibody, cells were incubated for 0 - 40 min. Images shown are from 10 min time points. For detection of the anti-HA antibody that was internalised during the incubation, permeabilised cells were probed with Alexa-633 conjugated secondary antibody. This was followed by incubation of permeabilised cells with anti-clathrin antibody overnight at 4°C. Cells were then incubated with Alexa-568 conjugated secondary antibody. Results shown are representative images. All cells were viewed in approximately the same focal plane. Size bar on large images are 10 µm, and on smaller images are 5 µm.

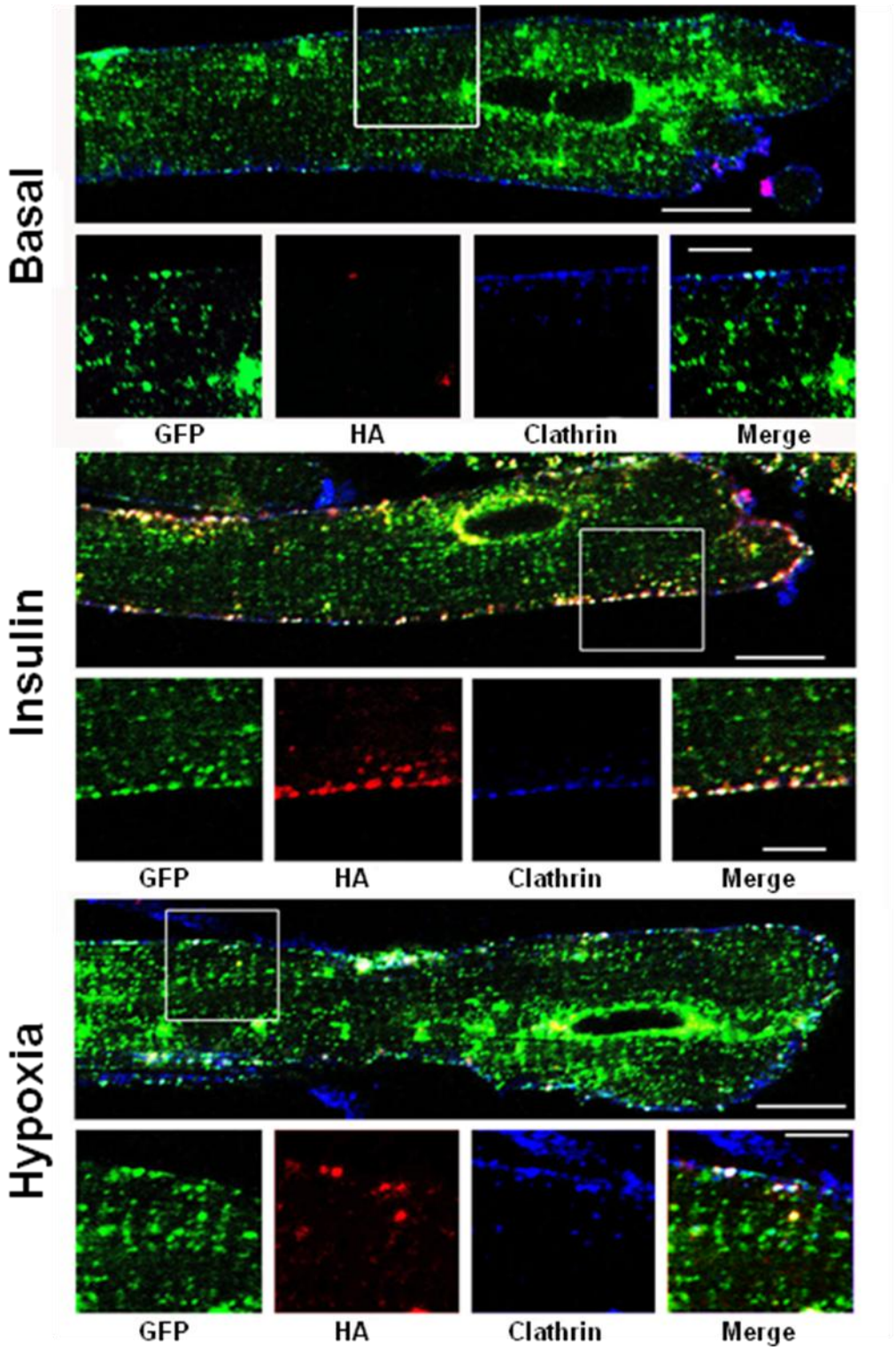
Basal
GFP
HA
Clathrin
Merge
Insulin
GFP
HA
Clathrin
Merge
Hypoxia
GFP
HA
Clathrin
Merge

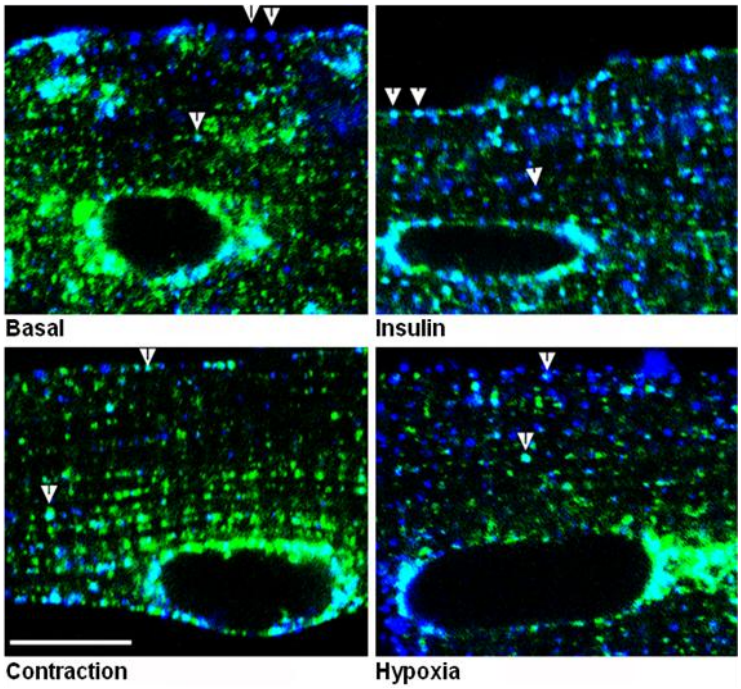

Figure 3.7. Colocalisation of internalising GLUT4 with clathrin was similarly observed with an alternative anti-clathrin antibody (Cell Signalling), which was secondarily labelled with Alexa-568 conjugated secondary antibody. Arrowheads indicate colocalisation of the GFP tag and clathrin. Results shown are representative of ~20 cells per condition examined in three experiments. All cells were viewed in approximately the same focal plane. Size bar on large images are 10 µm.

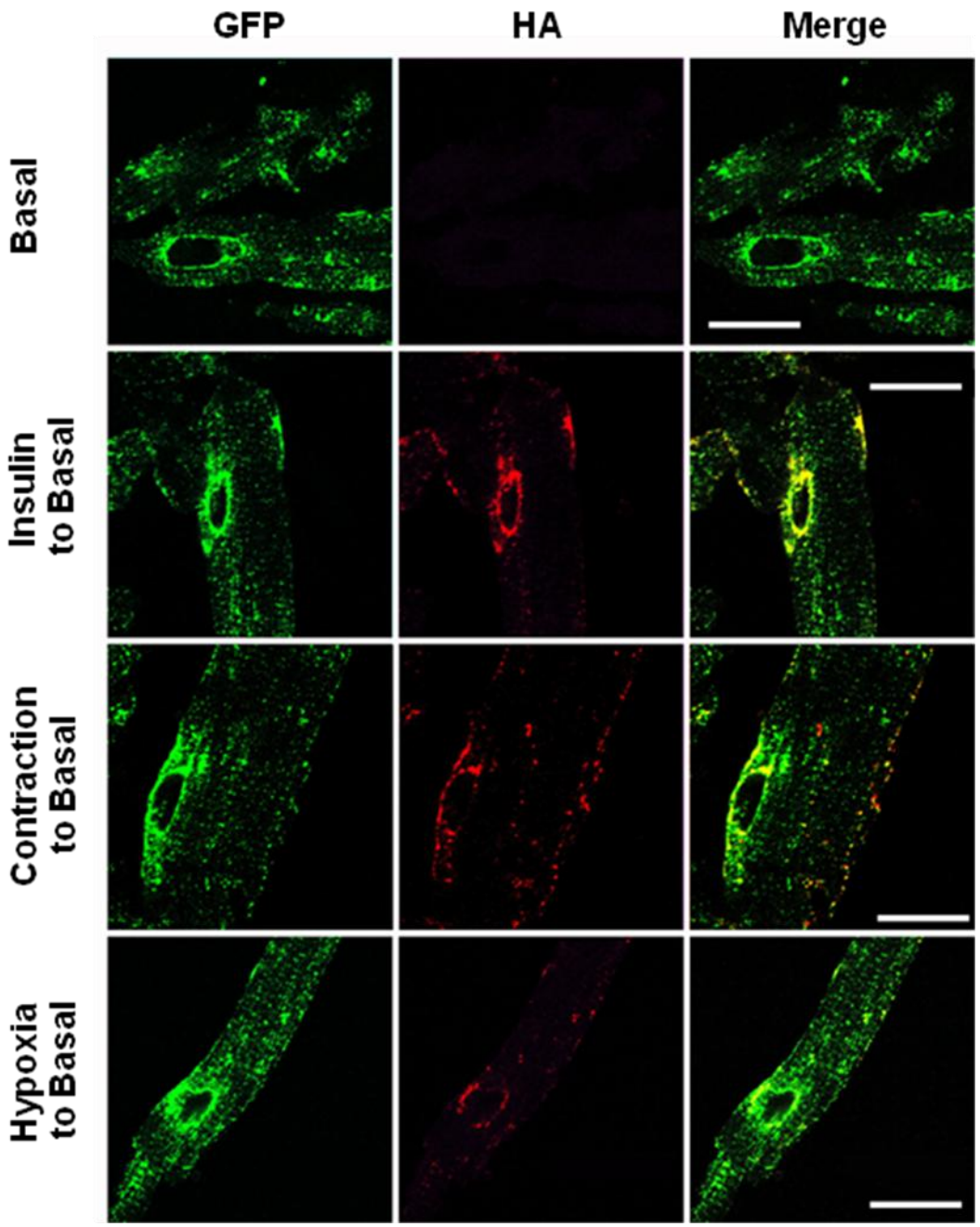
GFP
HA
Merge
Basal
Insulin to Basal
Contraction to Basal
Hypoxia to Basal

Figure 3.8. Reversal of stimulation and internalisation of sarcolemma antibody-labelled GLUT4 in cardiomyocytes. Isolated cardiomyocytes were either maintained in the unstimulated basal state (top panels), incubated with 10 nM insulin for 30 min (second row panels), electrically induced to contract (100 V, 10 Hz, pulse width 1 ms) for 5 min (third row panels) or incubated under hypoxic conditions for 15 min (bottom panels). During these treatments, cells were incubated with anti-HA antibody (5 µg/ml). Following removal of the stimulus and washing to remove excess antibody, cardiomyocytes were incubated for a further 40 min to return to the basal state. For detection of the anti-HA antibody that was internalised during the incubation, permeabilised cells were probed with an Alexa-633 conjugated secondary antibody for 60 min at room temperature. All cells were viewed in approximately the same focal plane. The size bar is 20 µm. Results shown are representative of approximately 25 cells examined in 3 experiments.

Full internalisation of anti-HA antibody labelled-GLUT4 following stimulation with insulin, contraction and hypoxia occurred with indistinguishable time courses and reversal was complete within approximately 40 min for all three stimulation conditions. In the recovered basal state, neither the anti-HA-antibody signal nor the GFP is found associated with transverse tubules. This finding is consistent with the lack of strong alignment of GFP-GLUT4 along the transverse tubules in cells that have been continuously maintained in the basal state (Figure 3.2). In all cases, the anti-HA-antibody-tagged GLUT4 becomes predominately localised to the perinuclear area (Figure 3.8). Antibody-tagged GLUT4 is also present at other locations in the cell. For example, some antibody-tagged GLUT4 remains close to the sarcolemma. However, it is not possible to distinguish between internalising GLUT4 and GLUT4 that has recycled back out to this region following processing through the peri-nuclear region.

3.6 Discussion

In this study we have used a new method to investigate the subcellular localisation and trafficking of GLUT4 in cardiomyocytes. We have studied GLUT4 trafficking responses to insulin-, contraction- and hypoxia-stimulation. These stimuli operate via distinct signalling pathways. For example, insulin-stimulation activates PKB/Akt to invoke GLUT4 translocation. Incubation of cells with hypoxic buffer has been previously reported to activate AMPK (Yang and Holman, 2005), presumably by altering the ATP:AMP ratio within cells. Although in this study hypoxia has been used as a means to activate AMPK, it has recently been reported that hypoxia-stimulated glucose uptake is inhibited by a calcium/calmodulin competitive inhibitor in skeletal muscle (Deshmukh et al., 2009). Therefore, it may be that incubation of cardiomyocytes in hypoxic conditions does not only activate the AMPK signalling pathway.

The data presented was obtained using a transgenic mouse line in which an HA-epitope and GFP tagged version of GLUT4 has been expressed under the control of a muscle specific promoter (I. Lisinski, V.A. Lizunov, D. R. Yver, O. Gavrilova, H. Al-Hasani and S.W.Cushman, unpublished). Recombinant GLUT4 is expressed in skeletal muscle and heart muscle, but not in adipose tissue. This mouse model potentially allows the GLUT4 translocation to be studied in fully differentiated muscle cells in a physiological setting. The inserted HA-epitope is located in the first exofacial loop of GLUT4 which means that it is only accessible to antibody at the external surface of non-permeabilised cells. It therefore allows a quantification of the levels of GLUT4 translocation and exposure of GLUT4 at the external surface. This HA-epitope tagged version of GLUT4 has advantages compared with GLUT4 tagged with GFP alone. When using GFP-tagged versions of GLUT4 it is difficult to distinguish between GSVs that has accumulated just beneath surface membranes and GSVs that have fused with the external membrane, exposing GLUT4 in a functional form to transport glucose into the cell. Exofacial epitope-tagged versions of GLUT4 have been previously used to study the translocation of GLUT4 in adipocyte (Lampson et al., 2000; Karylowski et al., 2004) and muscle cell lines (Wang et al., 1998; Wijesekara et al., 2006; Antonescu et al., 2008) and in primary adipose cells (Lizunov et al., 2005). The trafficking of the C-terminally GFP-tagged GLUT4 in all these studied cases appears to closely parallel the trafficking of endogenous GLUT4 (Martin et al., 2006). The localisation of HA-GLUT4-GFP in the cardiomyocytes mouse model closely parallels the localisation of endogenous GLUT4 in rat cardiomyocytes (Yang et al., 2002).

We have found that the exofacial exposure of GLUT4 at the sarcolemma of cardiomyocytes can be selectively studied if intact anti-HA antibody is used to label fixed cells. This selectivity was found to be due to the inability of the large intact antibody to penetrate the transverse tubule spaces and to the tendency of the fixation procedure to narrow or occlude these spaces. A restriction in antibody accessibility to the transverse tubules has been previously described for an antibody raised towards an exofacial epitope of the Na^+-K^+-ATPase β subunit (McDonough et al., 1996).

It is particularly clear using the whole antibody in this way that in the basal state the levels of insertion of GLUT4 into the sarcolemma membrane are extremely low and barely detectable. This technique, using a method that does not involve disruption or extensive manipulation of the cells, confirms that in cardiomyocytes very large increases in GLUT4 translocation to the sarcolemma occur in response to insulin-, contraction- and hypoxia-stimulation. As is the case in skeletal muscle cells, heart muscle cells have two distinct cell surface domains, the sarcolemma and the transverse tubule systems, at which GLUT4 can become accessible to the extracellular media. The transverse tubule system greatly extends the membranous network of the cell and provides a large surface area over which glucose transport can be facilitated. In cardiac muscle the transverse tubules have approximately twice the surface area of the sarcolemma (Clark et al., 2001; Soeller and Cannell, 1999). To measure translocation to sarcolemmal and transverse-tubule surfaces, we have used the Fab fragment of the anti-HA antibody to label non-fixed cells. Because of the unknown extent of relative labelling efficiency in these two locations, we cannot directly compare the levels of translocation. However, by normalising to the insulin signal, we can compare the effects of the different signalling initiators on the final steps of translocation to these systems. In addition, by comparing the GFP and anti-HA signals, we are able to distinguish between stimuli that result in increased accumulation of GSVs close to the sarcolemma or transverse tubule membrane and stimuli that enhance GSV fusion with external membranes. It has recently been proposed that the isolation procedure adopted in this study may cause the transverse tubules to collapse, resulting in narrowing of the transverse tubule space compared to cardiomyocytes *in vivo* (Lauritzen, 2009). This change may lead to aberrant GLUT4 trafficking. This criticism is based on the observation that while whole anti-HA antibody is not able to penetrate into the transverse tubules, albumin has been reported to present in the lumen of transverse tubule *in vivo* (Knudson and Campbell, 1989). However, the molecular weight of albumin (~68,000 Da) is closer to the size of a Fab fragment (~50,000 Da)

than of the whole anti-HA antibody (~150,000 Da). Given these size comparisons, the presence of albumin in the lumen of transverse tubules *in vivo* and the lack of whole anti-HA antibody accessibility to exposed HA-epitope in the transverse tubules does not support the conclusion that the integrity of the transverse tubules is compromised in cardiomyocytes isolated by this method.

We find that insulin- and contraction-induced signalling produce essentially indistinguishable patterns of translocation to these cell surface locations. The insulin effect is more potent and produces a greater translocation, but this may be a technical issue associated with a decline in contraction-induced signalling intermediates between the time of contraction induction and subsequent labelling with the anti-HA Fab fragment. The fold changes in translocation to the transverse-tubule system appear approximately two-fold lower than translocation to the sarcolemma under insulin- and contraction-stimulation, but estimating this fold change depends on the accuracy of recording the low basal level of translocation at these two locations.

The translocation of GLUT4 to the sarcolemma in response to hypoxia-stimulation produced a slightly but significantly different pattern of exposure of the HA-epitope tag to those produced by insulin- or contraction-induced translocation. The levels of translocation as measured by HA-epitope tag exposure are lower than those detected by alterations in the alignment of the GFP signal with this membrane (Figure 3.5 *B*). This difference is clearest when considering the anti-HA:GFP signal ratio (Figure 3.5 *C*). Here, hypoxia-stimulation has a significantly lower anti-HA:GFP signal ratio at the sarcolemma ratio than insulin- or contraction-stimulation.

Insulin- and contraction-induced GLUT4 trafficking to the sarcolemma is different to the trafficking observed to the transverse tubule membrane. Whereas insulin- and contraction-stimulation resulted in a higher fusion tendency at the sarcolemma (as measured by the anti-HA signal: GFP signal ratio), this was not the case at the transverse tubule membrane. Rather, insulin-, contraction- and hypoxia-stimulation resulted in identical anti-HA signal: GFP signal ratios. These ratios were similar to that observed for GLUT4 trafficking to the sarcolemma under hypoxic conditions. These observations suggest that, although the routes of GLUT4 vesicle trafficking are similar under insulin- or contraction- and hypoxia-stimulation, the details of the

kinetics of trafficking may differ depending on the stimulus and/or the membrane to which vesicles are trafficked.

One potential explanation for the difference between insulin- or contraction- stimulated and hypoxia-stimulated GLUT4 trafficking to the two limiting membrane systems is that insulin- and contraction-signalling acts at the sarcolemma to facilitate the fusion of GSVs at this site. In the cases of hypoxia-stimulated trafficking to the sarcolemma and insulin-, contraction- and hypoxia-stimulated trafficking to the transverse tubules there is a low anti-HA signal: GFP signal ratio. This could be explained if in these instances the stimuli are unable to enhance GSV fusion at these sites. It has previously been reported that whereas insulin action- and contraction-stimulation led to increased exocytosis of GLUT4 in cardiomyocytes, stimulation of the AMPK pathway by means of hypoxia, mitochondrial inhibition (Yang and Holman, 2005) or metformin action (Yang and Holman, 2006) led to inhibition of endocytosis. An AMPK-mediated inhibition of GLUT4 internalisation has also been reported in epitrochlaeris muscle (Karlsson et al., 2009). These different mechanisms for enhancing cell surface GLUT4 levels may explain the lower level of exposure of the HA-epitope relative to the GFP signal under hypoxic conditions at both the sarcolemma and transverse tubules. It is possible that because exocytosis and fusion are occurring at the basal or unstimulated rates in hypoxia-stimulated cardiomyocytes, non-fused vesicles at the sarcolemma accumulate to a greater extent. Taken further, insulin- and contraction-stimulated GLUT4 translocation to the transverse tubules may occur via an analogous mechanism (inhibition of GLUT4 internalisation). Therefore, while GLUT4 translocation to the sarcolemma in response insulin- and contraction-stimulation occurs via enhanced exocytosis, the increased amount of GLUT4 in the transverse tubule membrane may be achieved by inhibition of internalisation. Studies investigating GLUT4 trafficking in cardiomyocytes using a photolabelling technique have not identified an effect of insulin- or contraction-stimulation on GLUT4 internalisation (Yang and Holman, 2005; Yang and Holman, 2006). However, it may be that these studies are biased towards GLUT4 present in the sarcolemma membrane if GLUT4 in the transverse tubule network is less accessible to the photolabelling reagent.

The signalling events responsible for mediating enhanced GSV fusion with the sarcolemma following insulin- and contraction-stimulated have not been investigated in this study. Insulin- and contraction-stimulated glucose uptake is wortmannin-sensitive in cardiomyocytes (Yang and Holman, 2005). In contrast, hypoxia-stimulated glucose uptake is not

inhibited by wortmannin. Therefore, it may be that the PI-3-K-PKB/Akt signalling pathway is able to signal to facilitate GLUT4-vesicle fusion with the sarcolemma. A role for PI-3-K and PKB/Akt at the plasma membrane has been reported in adipocytes (Koumanov et al., 2005; Bai et al., 2007; Gonzalez and McGraw, 2006). This may correlate with the location of kinase activation under each of the stimulation conditions tested. PKB/Akt is recruited to the inner leaflet of the limiting membrane prior to activation by PDK-1 and therefore would be appropriately localised to modulate the fusion reaction. In contrast, it is not thought that AMPK is relocalised in this way prior to activation. As we measure a different effect on fusion at the sarcolemma and the transverse tubules, this hypothesis would require the PKB/Akt substrate(s) responsible for enhanced GSV fusion to be specifically localised to the sarcolemma and not the transverse tubule membrane.

The routes and time courses for internalisation of GLUT4 are indistinguishable following the stimulations by insulin action, electrically induced contraction or hypoxia. The internalisation has been followed using the intact anti-HA antibody that, under the conditions used in this assay, preferentially associates with GLUT4 that is exposed at the sarcolemma membrane. Following reversal of these stimuli, anti-HA antibody-labelled GLUT4 very rapidly, within 1-2 minutes, appeared just below the cell surface and became punctuate in appearance, suggesting the formation of internalising vesicles. These internalising vesicles are highly associated with clathrin and the anti-HA signal from GLUT4 colocalises with clathrin. These data are consistent with an immunogold study of GLUT4 in cardiomyocytes (Slot et al., 1991a), and with a study on GLUT4 and clathrin within a 100 nm TIRF zone at the surface of 3T3-L1 cells (Huang et al., 2007). Over longer (40 min) periods of internalisation, HA-antibody tagged GLUT4 becomes mainly associated with a perinuclear compartment, suggesting that long-range movements of GLUT4 to and from the sarcolemma occur in cardiomyocytes. The GLUT4 does not appear to relocate to localised satellite reservoirs. A recent study using time-lapse fluorescent confocal microscopy of quadriceps muscle in situ (Lauritzen et al., 2008a), led to the conclusion that translocation of GLUT4 to the sarcolemma and transverse tubules in response to insulin occurred locally and without long-range translocation of GLUT4 vesicles. Instead, localised static GLUT4 reservoirs present at the membranes are replenished as the insulin signal wanes and GLUT4 is internalised. We do not see clear evidence for such patches or satellite reservoirs of GLUT4 in basal cardiomyocytes or cardiomyocytes in which the HA antibody is internalised. This difference may be because of the relatively small size of the cardiac muscle cells compared with the long

quadriceps muscle fibres used for the gene injection technique. In skeletal muscle cells, a more localised translocation may have evolved as an adaptation in these longer multinucleate cells. Much of the GLUT4 that is present in the perinuclear storage compartment of cardiomyocytes also colocalises with clathrin. The requirement for clathrin association in this location may be associated with vesicle budding reactions at the trans-Golgi network.

We observed no difference in the overall trafficking route of GLUT4 in cardiomyocytes returning to a basal state following the stimulation of GLUT4 translocation by insulin, contraction or AMPK-activation. This conclusion is specific to GLUT4 internalising from the sarcolemma since GLUT4 was pulse labelled with whole anti-HA antibody which cannot access GLUT4 in the transverse tubules. These data imply that these stimuli mobilise GLUT4 from a similar intracellular location. This study did not address the exact trafficking itinerary and localisation of internalising GLUT4 and therefore it is unclear whether the intimate details of these trafficking routes were identical.

It has been reported that in 3T3-L1 cells that GLUT4 internalising in the basal state does not associate with clathrin-dependent internalisation, but rather is mainly associated with a non-clathrin, cholesterol-dependent, nystatin-inhibitable route (Blot and McGraw, 2006). Although we cannot rule out the possibility that a clathrin-independent route for internalisation occurs in cardiomyocytes, it is evident that a large, but difficult to quantify, proportion of GLUT4 is associated with clathrin in the basal state. This finding is supported by data from L6 cells, in which GLUT4 internalises via both a clathrin-mediated and cholesterol-dependent mechanism (Antonescu et al., 2008). These data indicate that GLUT4 internalisation routes may differ between cell types and cell lines. In the future, it will be important to determine, more quantitatively, the proportion of GLUT4 that is internalised by the clathrin-dependent and clathrin-independent cholesterol-dependent route in heart muscle cells. Furthermore, it would be of interest to pin-point the mechanism by which stimuli modulate GLUT4 internalisation in this cell-type.

A common trafficking route for GLUT4 that can be regulated by several separate signalling pathways could be considered to be consistent with the possibility that the separate signals lead to a single point of convergence with the GLUT4 trafficking pathway. Recent signalling studies in skeletal muscle have led to the postulation that the Rab-GAP proteins TBC1D4/AS160 and TBC1D1 act as points of convergence for signalling from insulin, contraction,

and energy-status signalling (reviewed by (Sakamoto and Holman, 2008)). Induction of signalling through these initially distinct pathways has been reported to increase TBC1D4/AS160 and TBC1D1 phosphorylation (Funai et al., 2009; Funai and Cartee, 2009; Kramer et al., 2006a). However, a single point of convergence cannot account for all aspects of stimulated GLUT4 translocation. Signalling via insulin and contraction in heart leads to increased exocytosis of GLUT4, whereas signalling via AMPK leads to reduced endocytosis of GLUT4. As described, these kinetic differences appear to be consistent with increased exposure of the HA-epitope tag at the sarcolemma surface in response to insulin and contraction, but not to hypoxia. We therefore propose that a common trafficking route exists for GLUT4 in cardiomyocytes that can be stimulated at different points and that these stimulatory responses produce subtle changes in the kinetics of GLUT4 movement along this route. Kinetic differences in GLUT4 translocation rates rather than differences in the translocation route per se may also account for the additivity of insulin- and hypoxia-mediated, but not insulin- and contraction-mediated, glucose transport responses observed in cardiomyocytes (Yang and Holman, 2005).

3.7 Conclusions

The HA-GLUT4-GFP mouse model that we have studied here is an important development as it has allowed analysis of GLUT4 distributions and translocations in cardiac muscle cells (Fazakerley et al., 2009). Until recently, GLUT4 trafficking to the sarcolemma and transverse tubule membranes has been extremely difficult to study quantitatively in muscle subtypes. This is because distinguishing between GLUT4 at different membranes relied on using procedures that require cell disruption and subfractionation. More recently, a Myc-epitope tagged GLUT4 transgenic mouse model has also been generated and described (Schertzer et al., 2009). The epitope tagging technique has been previously applied to cell lines and the extension of this approach to a mouse model system should greatly facilitate future studies on GLUT4 trafficking, for example in investigating responses to simultaneous stimulation of distinct signalling pathways. In addition, identifying changes in GLUT4 trafficking associated with the onset of insulin resistance in cardiac muscle would be of interest. Such studies could address whether selective changes occur in GLUT4 trafficking to distinct external membranes in insulin-resistant heart cells as has been described in skeletal muscle (Lauritzen et al., 2008b).

The cardiomyocyte model described here offers a convenient method to investigate GLUT4 trafficking in fully differentiated myocytes. These cells can be isolated relatively easily compared to skeletal muscle fibres. This *ex vivo* method has an advantage over the *in vivo* methods described by Lauritzen in that the HA-epitope can be labelled to distinguish between GLUT4 in close proximity to the membrane and GLUT4 present in the external membrane. An *in vivo* imaging method capable of tracking GLUT4 trafficking and of identifying GLUT4 present in the external membrane would be ideal. This could perhaps be achieved by *in vivo* imaging of cells expressing both GLUT-GFP and IRAP-pHluorin. Here, the GFP signal would allow GLUT4 trafficking to be monitored, whilst the pH-sensitive IRAP construct would permit analysis of GSV insertion into external membranes. In addition, recent advances in microscopy techniques will permit a more detailed analysis of GLUT4 trafficking. By combining live cell imaging with photo-activated localisation microscopy (PALM) or stochastic optical reconstruction microscopy (STORM), which can achieve single molecule (super) resolution, it may be possible the observe the trafficking of individual GLUT4 molecules.

4 GLUT4 trafficking in the L6 cell culture model

Technical challenges associated with cardiomyocyte preparation and analysis prevented this model from being used for more extensive examination of GLUT4 trafficking kinetics. Therefore assays to measure GLUT4 trafficking kinetic parameters were established in the L6 cell culture model. These assays have enabled the measurement of the rate constants for GLUT4 exocytosis and endocytosis and, importantly, the amount of GLUT4 recycling with the plasma membrane. L6 cells, extensively used and characterised by Klip and colleagues, have been reported to respond to insulin and AMPK activation by increasing glucose uptake and cell surface GLUT4 content. In this study we have performed a detailed analysis of the kinetic parameters that define GLUT4 trafficking in response to these distinct signalling pathways in L6 myotubes using the agonists insulin, AICAR and A-769662. Mechanistically, insulin stimulates GLUT4 translocation via the PI-3-K/PKB/Akt pathway while AICAR and A-769662 are thought to operate via the AMPK pathway. Commonly, contraction and AICAR have been used to study the role of AMPK activation in *in vivo*, *ex vivo* and cell culture muscle models. However, both these stimuli have been reported to also activate pathways other than AMPK (reviewed in (Guigas et al., 2009)). A more specific AMPK activator would more clearly define a role for AMPK in GLUT4 translocation. Here we have approached this problem by comparing the effects of AICAR and the direct AMPK activator A-769662, which is a currently believed to be a more specific activator of AMPK than AICAR and as a result has less AMPK-independent side-effects.

4.1 Establishing a method to investigate GLUT4 trafficking in L6 myotubes

In order to measure the steady-state GLUT4 recycling kinetics, an anti-HA antibody uptake assay was adapted from previous studies for use in L6 cells (Govers et al., 2004; Martin et al., 2006; Karylowski et al., 2004; Muretta et al., 2008; Wijesekara et al., 2006). Anti-HA antibody was purified prior to use in this study to avoid any possible stimulation of GLUT4 trafficking by constituents of ascites fluid. In the analysis of data generated from an antibody uptake assay, an important assumption is that the anti-HA antibody is present at a saturating concentration; so that the antibody concentration is sufficient that all GLUT4 trafficked to the plasma membrane is rapidly labelled. Therefore, an antibody saturation test was performed on each batch of purified

anti-HA antibody to ensure that a saturating concentration of antibody was used for all antibody uptake assays.

One of the problems associated with L6 cells is that differentiated L6 muscle cells express very little GLUT4, presumably because the cells are denervated (Henriksen et al., 1991). To overcome this problem epitope-tagged GLUT4 reporters can be expressed and used to study GLUT4 trafficking. In this study, a GLUT4 reporter protein with a HA-epitope tag in its exofacial domain was expressed in L6 myotubes to facilitate labelling of the protein in intact cells. This reporter has been used to monitor GLUT4 trafficking in both 3T3-L1 cells and isolated adipocytes (Lizunov et al., 2005; Govers et al., 2004; Karylowski et al., 2004; Martin et al., 2006). While many investigators use stably expressing L6 cell clones (Antonescu et al., 2008) this can be problematic due to the possibility for clonal selection of an aberrant cell line as well as difficulties in maintaining efficient muscle cell differentiation in stable clones. To overcome these problems we have developed a system whereby cells are infected with retrovirus expressing HA-epitope tagged GLUT4, which are then selected as pools rather than as clones.

A key consideration is the level of over-expression of GLUT4. It has been reported that over-expression of GLUT4 in adipocytes can result in inhibition of insulin-stimulated glucose uptake, presumably due to aberrant GLUT4 trafficking (Al Hasani et al., 1999). Therefore, the amount of GLUT4 expressed in the retroviral system may influence the GLUT4 kinetics measured. It is possible that there is a finite capacity for GLUT4 storage. As such, it may be that at higher levels of GLUT4 over-expression, a lower proportion of the total GLUT4 can be dynamically retained or sequestered. To investigate this possibility, a viral titration was performed, where the kinetic parameters in L6 myotubes expressing different amounts of GLUT4 where measured (Figure 4.1).

Incubation of L6 cells with increasing volumes of HA-GLUT4 retrovirus resulted in enhanced levels of HA-GLUT4 expression (Figure 4.1 *A* and *B*). The highest amount of virus used to infect L6 myoblasts (2 mL) resulted in a 38.7-fold increase in GLUT4 over cells infected with an empty-vector (EV) control. This level of over-expression was reduced to 11.4-fold in cells infected with 25 µL of virus.

Fitting antibody uptake data obtained from unstimulated and insulin stimulated L6 myotubes (Figure 4.1 *C*) to Eq. 2 and 3 (Materials and Experimental Procedures 2.2.4.12.2) allows

determination of the initial plasma membrane level of GLUT4, P, the final plateau level T and the rate constants k_{ex} and k_{in} for movement of GLUT4 out of, and back into, the single intracellular compartment. Insulin-induced changes in GLUT4 trafficking are discussed in more detail below. GLUT4 trafficking parameters in basal and insulin-stimulated cells are similar regardless of the level of GLUT4 over-expression (Figure 4.1 *D*-*G*). At each expression level, there was a ~3-fold increase in plasma membrane GLUT4 in response to insulin-stimulation (Figure 4.1 *D*). In particular, the proportion of GLUT4 recycling with the cell surface is not enhanced under higher levels of GLUT4 over-expression (Figure 4.1 *E*).

Figure 4.1. Effect of different HA-GLUT4 expression levels on the kinetics of HA-GLUT4 trafficking in L6 myotubes. *A*, HA-GLUT4 levels were determined by blotting for GLUT4, HA-epitope and β-tubulin in basal cells infected with different amounts of HA-GLUT4 retrovirus. *B*, The level of GLUT4 expression compared to cells retrovirally infected with an empty vector (EV) was determined by densitometry. The analysed data are from 3 experiments. *C*, L6 myotubes were maintained in the basal state (▲) or stimulated to steady-state with 200 nM insulin (•). Anti-HA antibody was then added and at indicated times the bound antibody was determined by incubation with an Alexa-488-conjugated secondary antibody. The analysed data are from 3 experiments. In some cases error bars are smaller than the symbol. The uptake time courses for the increase in antibody bound to HA-GLUT4 were analysed to give *D*, the plasma membrane level of HA-GLUT4 (*P*), *E*, the total available GLUT4 (*T*), *F*, the k_{ex} rate constant and *G*, the k_{in} rate constant. The analysed data are from 3 experiments. S.E.M. calculated from the confidence intervals (see Materials and Experimental Procedures) for the fits are shown.

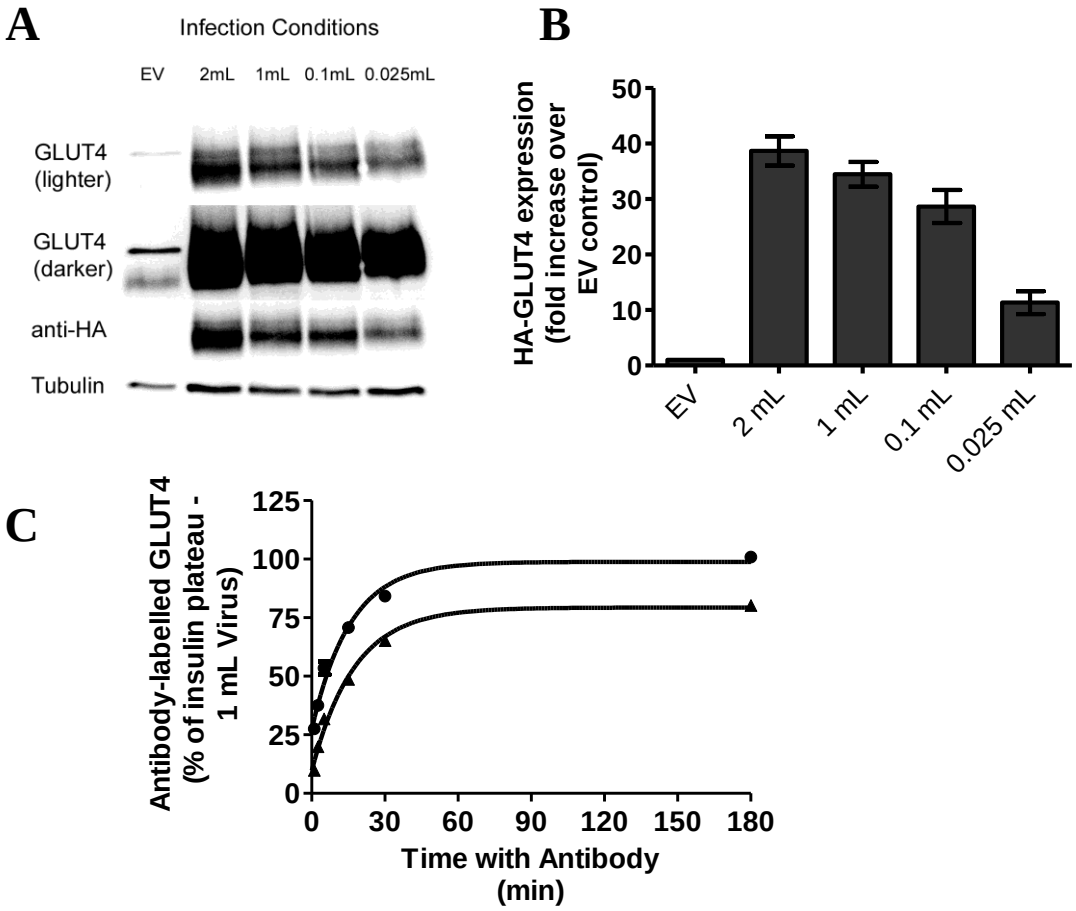
A
Infection Conditions
EV
2mL
1mL
0.1mL
0.025mL
GLUT4 (lighter)
GLUT4 (darker)
anti-HA
Tubulin
B
HA-GLUT4 expression (fold increase over EV control)
EV
2 mL
1 mL
0.1 mL
0.025 mL
C
Antibody-labelled GLUT4 (% of insulin plateau - 1 mL Virus)
Time with Antibody (min)
D
P (% of insulin plateau)
E
T (% of insulin plateau)
F
k_{ex} (min^{-1})
G
k_{in} (min^{-1})
2 mL Virus Basal
2 mL Virus Insulin
1 mL Virus Basal
1 mL Virus Insulin
0.1 mL Virus Basal
0.1 mL Virus Insulin
0.025 mL Virus Basal
0.025 mL Virus insulin

The proportion of cellular GLUT4 recycling with the cell surface is higher than has previously been reported in 3T3-L1 adipocytes (Govers et al., 2004). Therefore, before detailed kinetic analysis of GLUT4 trafficking, it was important to determine whether newly synthesised GLUT4 was contributing to the amount of GLUT4 combining with antibody under basal conditions. For example, it maybe that newly synthesised GLUT4 is trafficked to the endosomal recycling pool or specialised storage compartment via the plasma membrane. Therefore, a high rate of HA-GLUT4 synthesis (which is under the control of a SV40 promoter) may result in a high level of GLUT4 labelling in basal cells. To control for this possibility, L6 cells were incubated with the protein synthesis inhibitor cycloheximide for 60 min before the start of the uptake assay. The uptake of antibody in basal an insulin-stimulated cells was identical in control and cycloheximide-treated myocytes (Figure 4.2 *A* and *B*). The presence of this inhibitor did not affect the rate of antibody uptake or the final plateau level of antibody uptake.

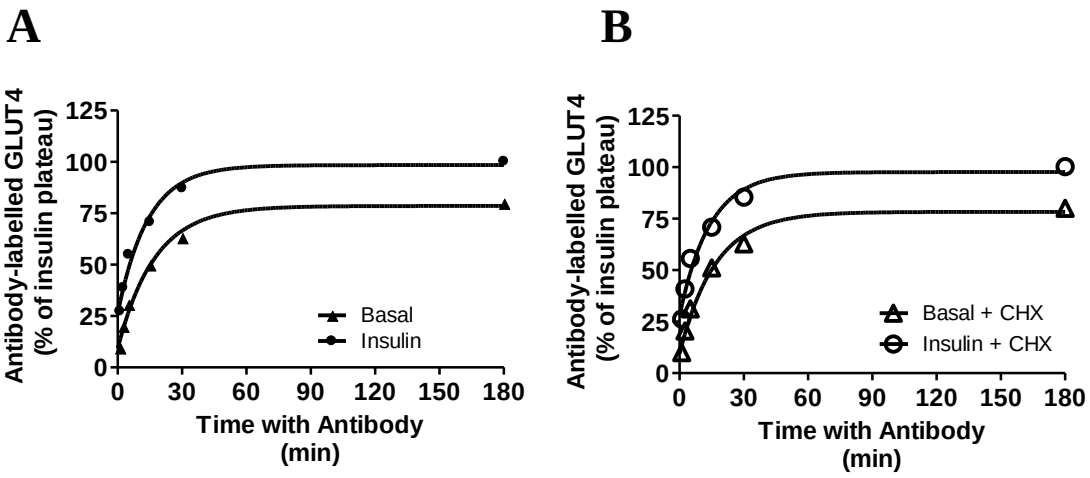

Figure 4.2. Inhibition of protein synthesis does not affect anti-HA antibody uptake into basal and insulin-stimulated L6 myotubes. L6 myotubes expressing HA-GLUT4 were maintained in the basal state (▲ or △) or stimulated to steady-state with 200 nM insulin (• or ○) in the absence (*A* - closed symbols) or presence (*B* - open symbols) of 15 µM cycloheximide (CHX). Anti-HA antibody was then added and the incubations with antibody were continued for the indicated times. Bound antibody was determined by incubation with an Alexa-488-conjugated secondary antibody. Results are the mean and S.E.M from 3-7 experiments. In some cases error bars are smaller than the symbol.

The final validation of this method was to investigate the subcellular localisation of antibody-labelled GLUT4 throughout the antibody uptake procedure. This control was performed

for two principal reasons. Firstly, it is vital to establish that the anti-HA antibody remains bound to HA-GLUT4 within the cell. The anti-HA antibody taken-up into L6 cells colocalises with GLUT4 (Figure 4.3 *A*). Therefore, anti-HA antibody remains bound to HA-GLUT4 throughout its intracellular trafficking route.

Secondly, we investigated whether the binding of a large antibody molecule to the exofacial HA-epitope alters the intracellular trafficking of GLUT4. This has been previously investigated in 3T3-L1 adipocytes. In this cell type GLUT4 trafficking kinetics is unaffected by antibody binding (Martin et al., 2006). L6 myotubes were visualised by confocal microscopy following the antibody uptake assay and colocalisation of the anti-HA signal with different subcellular markers was assessed (Figure 4.3). Antibody-labelled HA-GLUT4 has a punctate distribution throughout the cell interior with a particular concentration in a perinuclear region as is described in cardiomyocytes expressing HA-GLUT4-GFP (Fazakerley et al., 2009) and skeletal muscle expressing GLUT4-GFP (Lauritzen et al., 2006).

The subcellular distribution of antibody-bound GLUT4 in L6 myotubes was interrogated using a series of well characterised subcellular markers (Figure 4.3 *B-F*). Antibody bound HA-GLUT4 partially localises with markers for the Golgi complex (WGA and Syntaxin6) and for early endosomes (EAA1). These are subcellular compartments through which endogenous GLUT4 has been reported to traffic. There is no colocalisation of antibody-bound GLUT4 with a marker for the endoplasmic reticulum (PDI) or lysosomes (LAMP2).

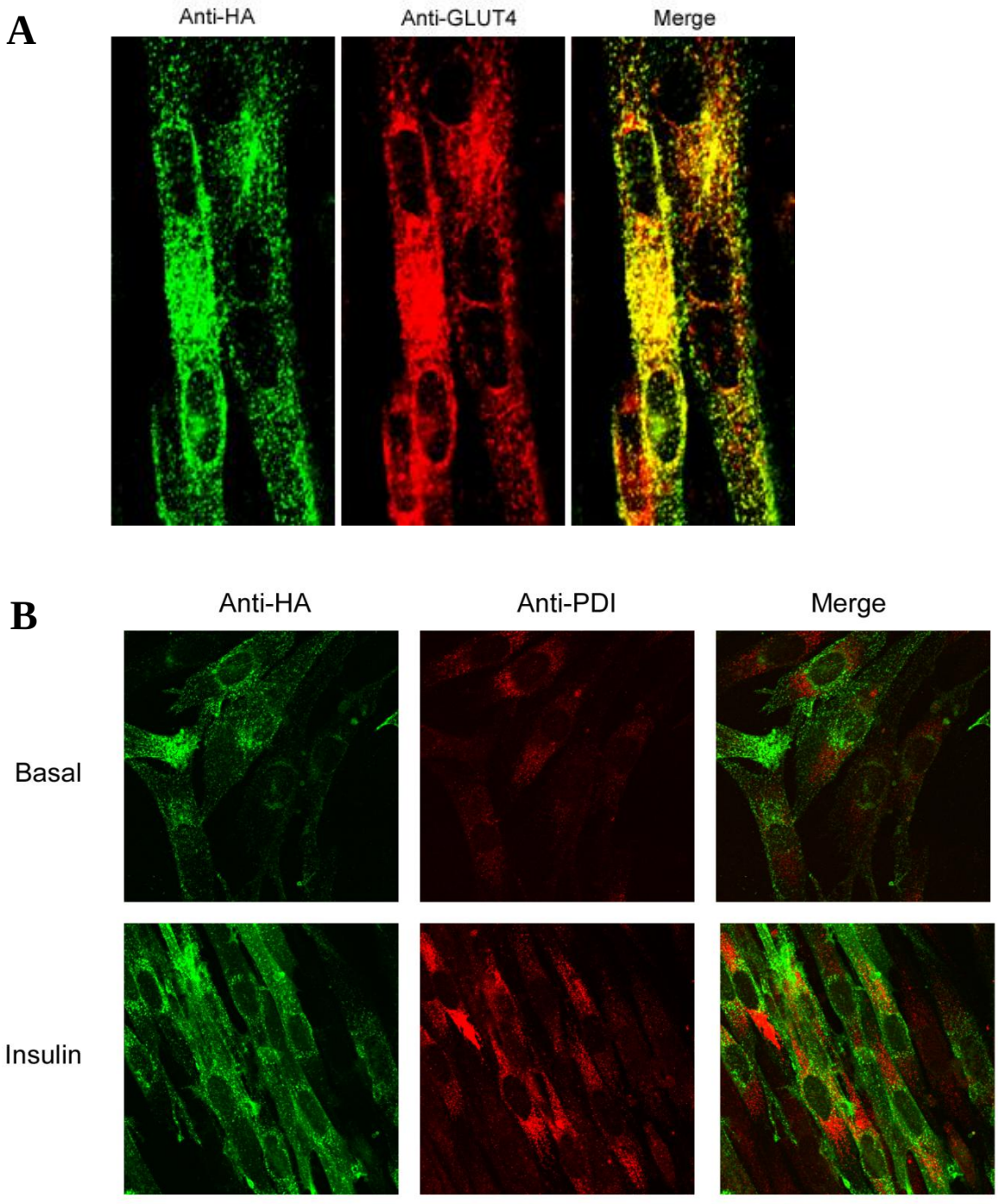
A
Anti-HA
Anti-GLUT4
Merge
B
Anti-HA
Anti-PDI
Merge
Basal
Insulin

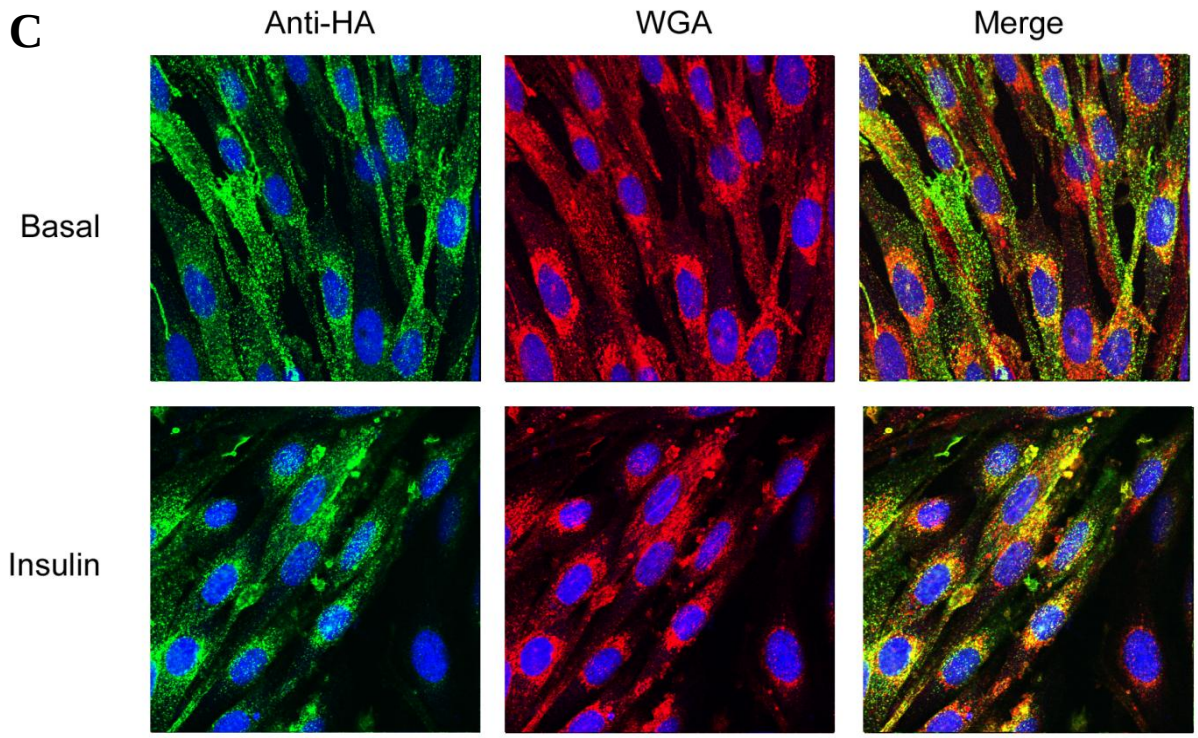
C
Anti-HA
WGA
Merge
Basal
Insulin

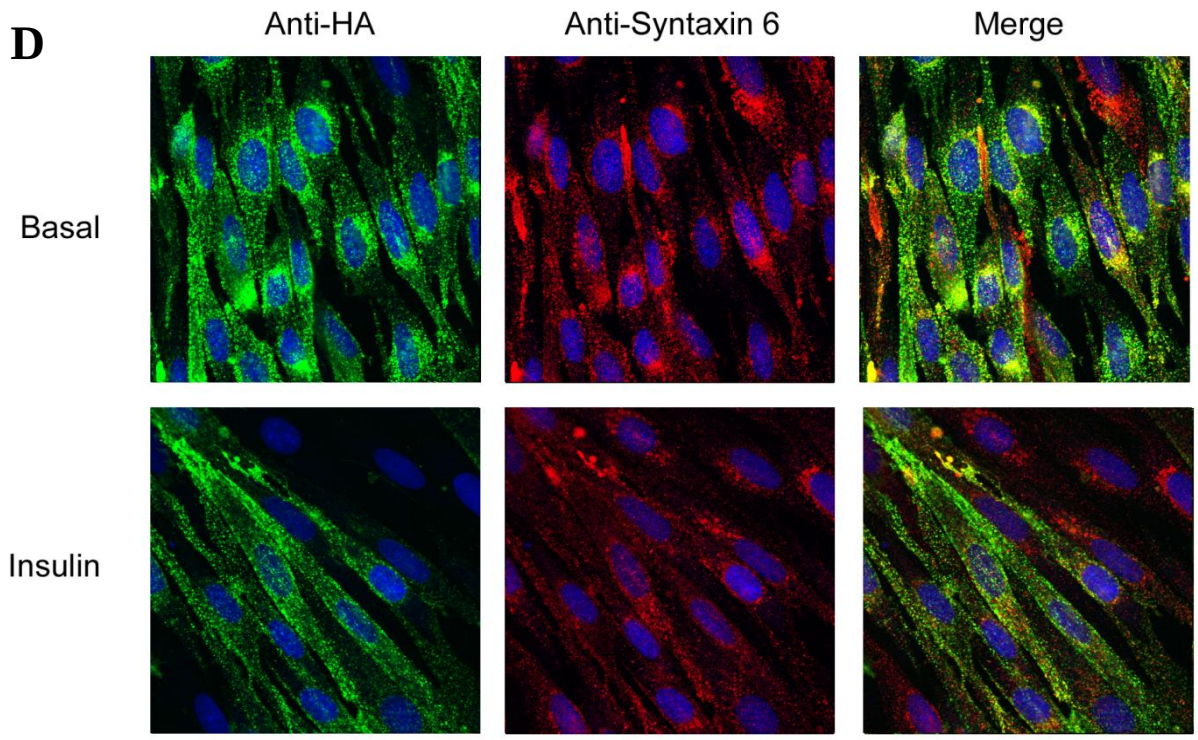
D
Anti-HA
Anti-Syntaxin 6
Merge
Basal
Insulin

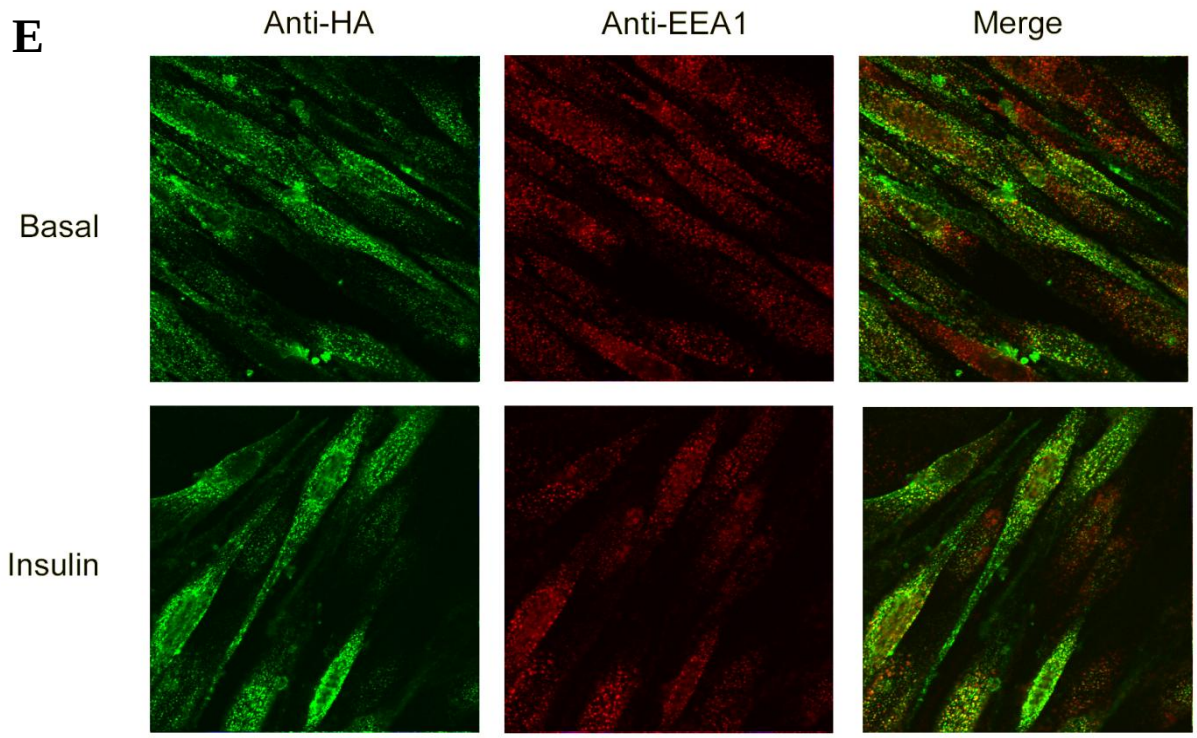
E
Anti-HA
Anti-EEA1
Merge
Basal
Insulin

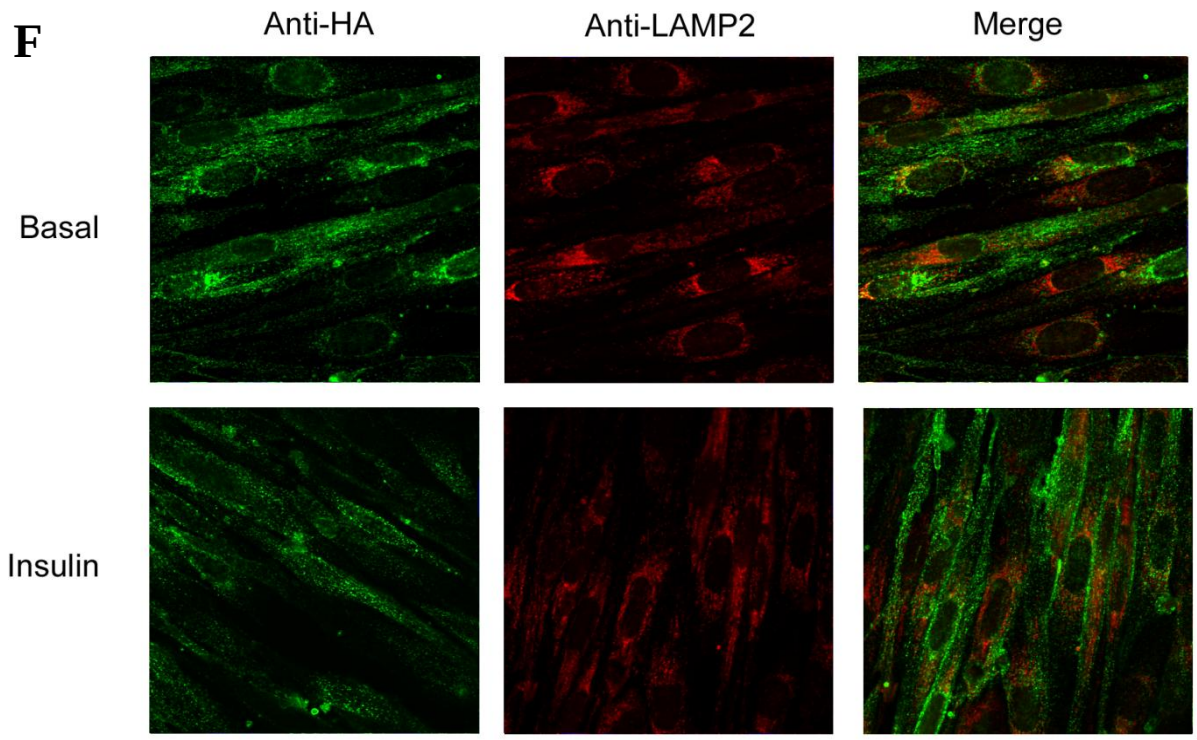
F
Anti-HA
Anti-LAMP2
Merge
Basal
Insulin

Figure 4.3. Subcellular localisation of anti-HA antibody labelled HA-GLUT4. L6 myotubes expressing HA-GLUT4 were maintained in the basal state or stimulated to a steady-state. Anti-HA antibody was then added and the incubations with antibody were continued for 15 minutes. Anti-HA antibody was detected by incubation with an Alexa-488-conjugated secondary antibody (green in all panels). L6 myotubes were also probed for a range of subcellular markers (red in all panels). Cells were visualised by confocal microscopy at 63x magnification. *A,* L6 myotubes were maintained in the basal state and probed for anti-HA antibody and for GLUT4 (C-terminal). *B-F*, L6 myotubes maintained in the basal state or stimulated with insulin were probed for anti-HA antibody and for subcellular markers for the endoplasmic reticulum (*B*, PDI), Golgi complex (*C*, wheat germ agglutinin (WGA) and *D*, syntaxin 6), early endosomes (*E*, EEA1) or lysosomes (*F*, LAMP2). Myotubes probed with Golgi markers were also labelled with a nuclear dye (Hoechst).

4.2 Activation of PKB/Akt and AMPK in L6 cells increases cell surface GLUT4

The activation of PKB/Akt and AMPK in L6 myotubes was assessed by western blot (Figure 4.4*A* and *B*). Insulin-stimulation results in a large increase in phosphorylation of PKB/Akt at serine 473. In L6 cells we observed a small activation of PKB/Akt under basal conditions (Figure 4.4 *A*). Incubation of cells with the AMPK-activators AICAR or A-769622 did not result in increased PKB/Akt phosphorylation at serine 473. PKB/Akt phosphorylation was detected in all samples treated with insulin.

AMPK phosphorylation at threonine 172 was increased in the presence of 2 mM AICAR (Figure 4.4 *A*). This corresponded with increased phosphorylation of ACC, a downstream target of AMPK. AMPK phosphorylation was also detected following incubation with 100 µM A-769622. The increase in phosphorylated AMPK was less than the increase observed following AICAR stimulation. However, stimulation with 100 µM A-769662 resulted in a similar activation of AMPK as 2 mM AICAR as determined by phospho-ACC levels. Insulin-stimulation had no effect on AMPK phosphorylation. AMPK and ACC phosphorylation was detected in L6 myotubes incubated in the presence of AICAR or A-769662 in combination with insulin at a similar level as with AICAR or A-769662 alone.

The time course of PKB/Akt activation following insulin-stimulation was examined by detection of phospho-PKB/Akt by whole-cell fluorescent microscopy (Figure 4.4 *B*). The level of phosphorylated PKB/Akt increased very rapidly, within 1 min of insulin stimulation, and reached

a maximum level between 2.5 and 10 min after stimulation at a level 2.50-times greater than in basal cells. There was a small decrease in the amount of phosphorylated PKB/Akt measured after 15 min so that by 60 min the level of phosphorylated PKB/Akt was 2.0-fold higher than in basal cells.

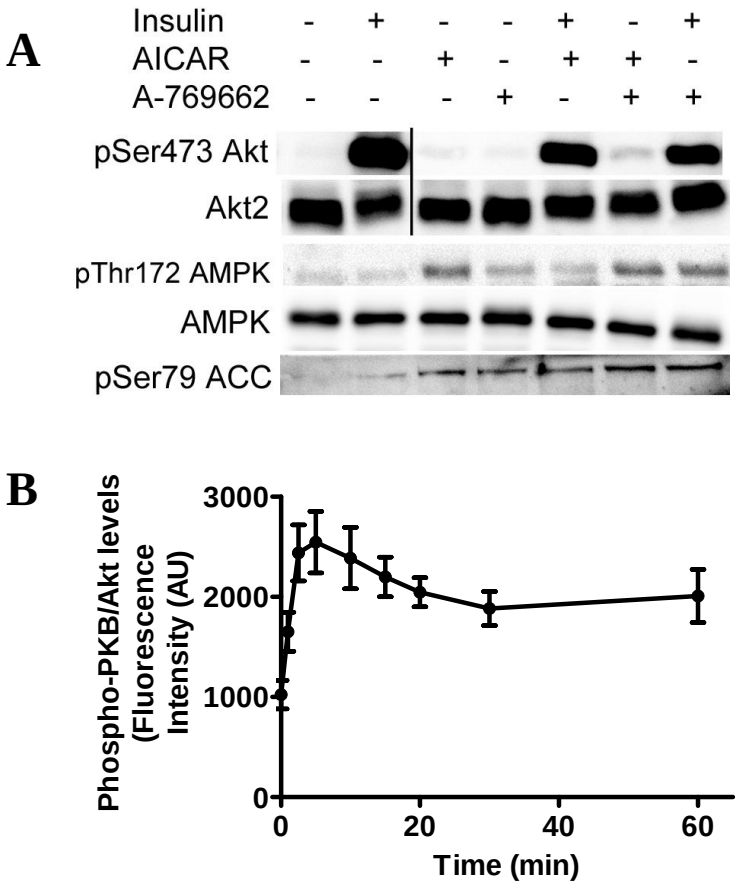

Figure 4.4. Activation of PKB/Akt and AMPK in L6 myotubes. *A,* PKB/Akt activation was determined by western blotting for phospho-serine473 in basal L6 cells and cells treated with 200 nM insulin, 2 mM AICAR and/or 100 µM A-769662, or a combination of these stimuli. PKBβ/Akt2 levels were determined from the same solubilised cell lysates. Membrane was cut on the phospho-PKB/Akt and PKBβ/Akt2 to remove lanes as indicated. Similarly, AMPK activation was determined by blotting for phospho-threonine 172 AMPK and phospho-serine 79 ACC in basal cells and stimulated cells. AMPK (α-subunit) levels were determined from the same solubilised cell lysates. B, The time course of PKB/Akt activation measured by phospho-serine 473 PKB/Akt was followed by immunofluorescence. The level of fluorescence from wide-field epifluorescence images was quantified at specified times after insulin stimulation. Each time point is the average of 4-5 ROIs taken from 3 separate wells from one experiment. Errors bars are ± S.D.

The kinetics of GLUT4 translocation to the plasma membrane were measured during the transition from the basal state to the activated state as demarcated by addition of an agonist of interest (Figure 4.5 *A*). The amount of GLUT4 exposed at the plasma membrane was calculated as a percentage of total GLUT4 levels, which were measured by labelling permeabilised cells with anti-HA antibody (Figure 4.5 *A* and *C*). The increase in cell surface GLUT4 in response to all the agonists was very rapid and was essentially complete within 2-5 min (Figure 4.5 *A*). For insulin this corresponds with the rapid increase in phospho-PKB/Akt (Figure 4.4 *B*). Fits of the transition state data to Eq. 1 determined that the transitions occurred with short half times of 1.21 and 1.27 min for insulin- and AICAR-stimulated cells, respectively (Figure 4.5*B*). A shorter half time (0.62 min) was observed for A-769662-stimulated cells. At approximately 10 min, a new steady-state level of GLUT4 was reached and this was maintained for at least 60 min (Figure 4.5*A*).

Insulin stimulation resulted in a 3.4-fold increase in cell surface GLUT4 levels over basal cells after 30 minutes ($p = 0.0008$) (Figure 4.5 *A*). AICAR and A-769662 both increased cell surface GLUT4 to a lower level than insulin following the same incubation time ($p = <0.005$). Cell surface GLUT4 levels were enhanced by 2.6- and 2.4-fold over basal cells following AICAR stimulation and A-769662 stimulation, respectively.

Figure 4.5. Transition to a steady-state GLUT4 distribution in L6 myotubes. *A*, L6 myotubes expressing HA-GLUT4 were stimulated with 200 nM insulin (•), 2 mM AICAR (■), 100 µM A-769662 (▲) and 200 nM insulin plus 2 mM AICAR (○) for the indicated times and then cells were fixed and the surface GLUT4 level was determined in fixed cells using an anti-HA primary antibody and an Alexa-488-conjugated secondary antibody. Each data point represents the mean and S.E.M from 3 experiments. In some cases the S.E.M bars are smaller than the symbol. *B*, Times for the half maximal increase above basal in cell surface HA-GLUT4 were determined for insulin, AICAR, A-769662 and the combination of insulin and AICAR. *C*, The cell surface levels of GLUT4 reached at 30 min of incubation with the agonists were determined as a percentage of the total cellular GLUT4 available in permeabilised cells. *D*, The plateau levels of antibody labelled-GLUT4 reached following incubation with the anti-HA antibody for 180 min were determined as a percentage of the total cellular GLUT4 available in permeabilised cells. Results are the mean and S.E.M. from 3 experiments. *** p= <0.0005, **p=<0.005 (unpaired t test compared to basal), *** p = <0.005, ** p = <0.05, *p=<0.05 (unpaired t-test double stimulation compared to single stimuli).

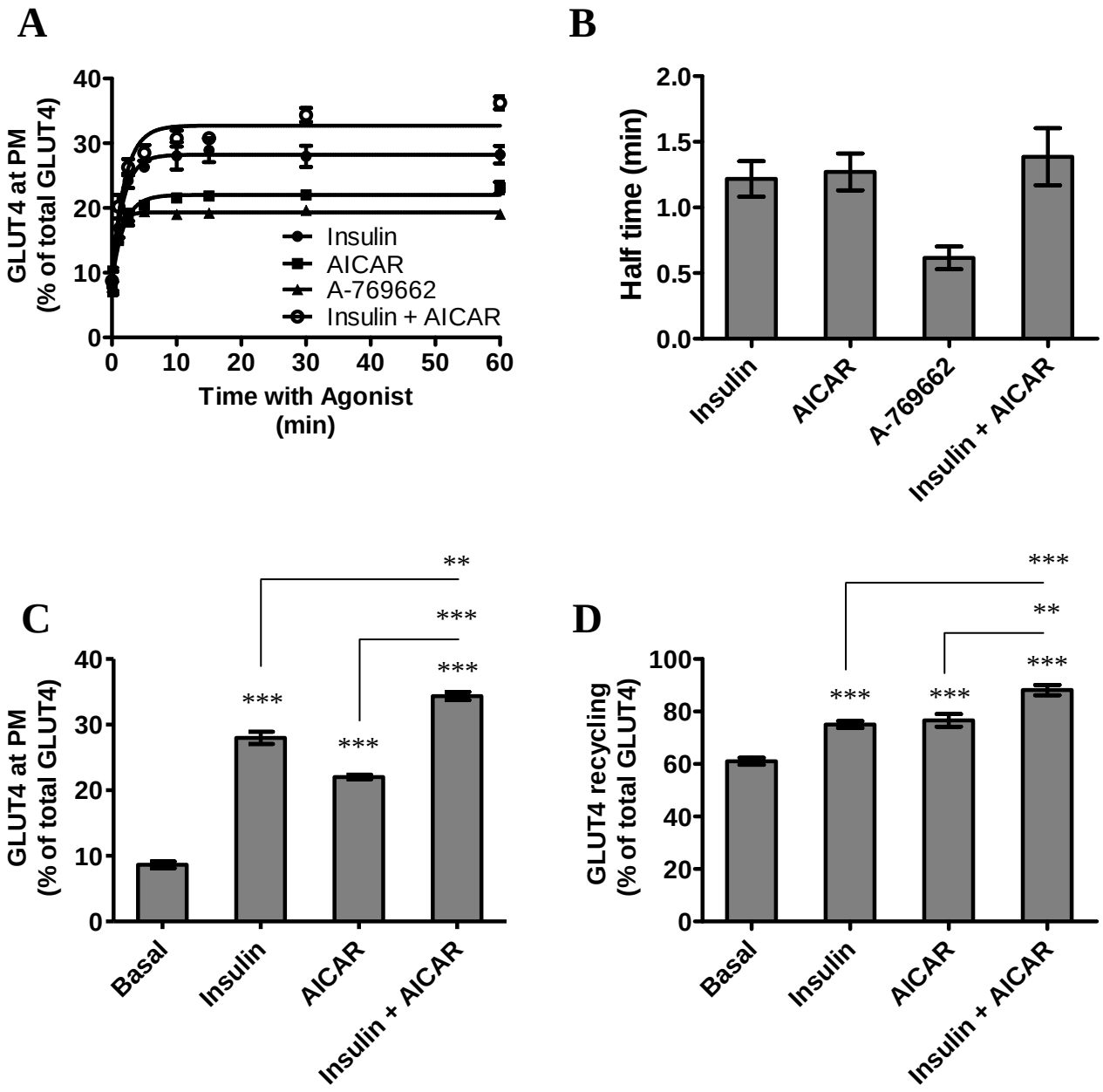

Furthermore, the combined stimulation with insulin and AICAR led to an increase in cell surface GLUT4 to a level that was higher than with either stimulus alone (Figure 4.5 *C*). Stimulation of cells with insulin plus AICAR gave a similar time-course to the individual agonists, with a half time of 1.39 min. The plateau level of GLUT4 is equivalent to a 3.9–fold increase over basal cells (p= <0.005), and is higher than is measured with either agonist alone (p = 0.019 vs. Insulin alone, p = 0.0037 vs, AICAR alone).

4.3 Insulin signalling and AMPK activation increase the amount of GLUT4 in the recycling pool in an additive manner

The amount of GLUT4 recycling with the cell surface under each condition was assessed by an anti-HA antibody uptake assay. Long-term measurements (3 h) in this assay were used to estimate the percentage of the total cellular GLUT4 (as determined in permeabilised cells) that was available for eventual combination with antibody at the surface (Figure 4.5 *D*). All changes in the surface level of GLUT4 were highly correlated with the total amount of GLUT4 present in the recycling system. In basal cells only 61% of the GLUT4 exchanges with the surface at steady-state. This value increased to 75% ($p = 0.0002$) and 77% ($p = 0.0009$) in insulin and AICAR treated cells, respectively. Intriguingly, the amount of GLUT4 in the recycling pathway in the presence of insulin plus AICAR was significantly greater than that observed with either stimulus alone (88%, $p < 0.005$). In addition, these data indicate that residual or latent pools of GLUT4 remain even following prolonged stimulation of trafficking and capture of cell surface GLUT4 with anti-HA antibody.

4.4 GLUT4 steady state recycling assay; anti-HA antibody uptake assay

The kinetics of GLUT4 trafficking under steady-state conditions were investigated in order to more fully understand how insulin and AMPK activators enhance GLUT4 cell surface levels. Once the transition phase is over and a new steady-state is reached, GLUT4 is distributed between the plasma membrane and internal compartments and the rates of traffic into and out of the plasma membrane are equal. We have studied GLUT4 trafficking at steady-state by maintaining L6 myotubes with anti-HA antibody throughout 180 min incubations (Figure 4.6). The assay was developed in a 96 well plate format and the amount of anti-HA antibody uptake determined by quantification of the fluorescent signal by a plate reader. Preliminary experiments determined the validity of this approach in L6 cells using our expressing system and allowed optimisation of time-points of antibody uptake used in the investigation. For example, L6 myotubes were visualised by microscopy following the antibody uptake assay to confirm the data derived from the plate reader (Figure 4.6 *A*). In addition, these experiments highlighted the importance of early time points (between 0 and 15 minutes) so that the initial curvature can be accurately fitted. In order to verify data obtained from this fluorescent based method, the method was

repeated using ^{125}I labelled anti-HA antibody (data not shown, n = 1). The results obtained from these separate methods were very similar.

We have approached the further analysis of the steady-state antibody uptake by assuming that at steady-state only a single intracellular compartment contributes to the recycling. This is an over-simplification and will be discussed in more detail. Furthermore, it is evident that the single intracellular compartment from which GLUT4 is recruited is not the same for all stimuli as there is additivity in the responses to PKB/Akt and to AMPK stimulation. Fitting the uptake assay data to Eq.2 allows calculation of 4 parameters (Figure 4.7). These are the plasma membrane level, P, the final plateau level T and the rate constants k_{ex} and k_{in} for movement out of, and back into, the single intracellular compartment.

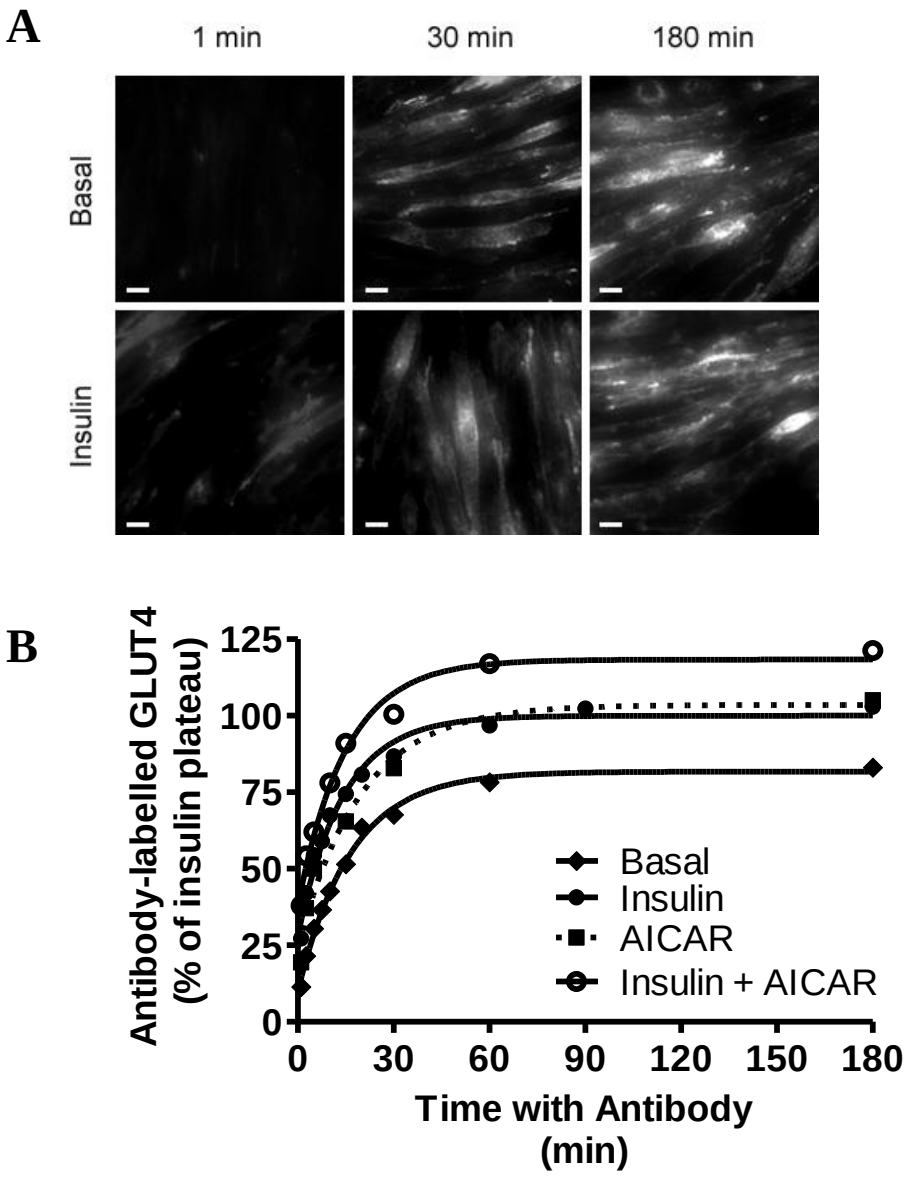

Figure 4.6. Anti-HA antibody uptake reveals GLUT4 steady-state recycling kinetics. L6 myotubes expressing HA-GLUT4 were maintained in the basal state or stimulated to a steady-state. Anti-HA antibody was then added and the incubations with antibody were continued for the indicated times. At indicated times the bound antibody was determined by incubation with an Alexa-488-conjugated secondary antibody. *A,* L6 myotubes were maintained in the basal state or stimulated to steady-state with 200 nM insulin. At indicated times L6 myotubes were visualised by wide-field epifluorescence microscopy at 40x magnification (Scale bar 20 µm). *B*, L6 myotubes were maintained in the basal state (◆) or stimulated to steady-state with 200 nM insulin (•), 2 mM AICAR (■) or 200 nM insulin plus 2mM AICAR (○). Results are the mean and S.E.M. from 3-7 experiments. In some cases error bars are smaller than the symbol.

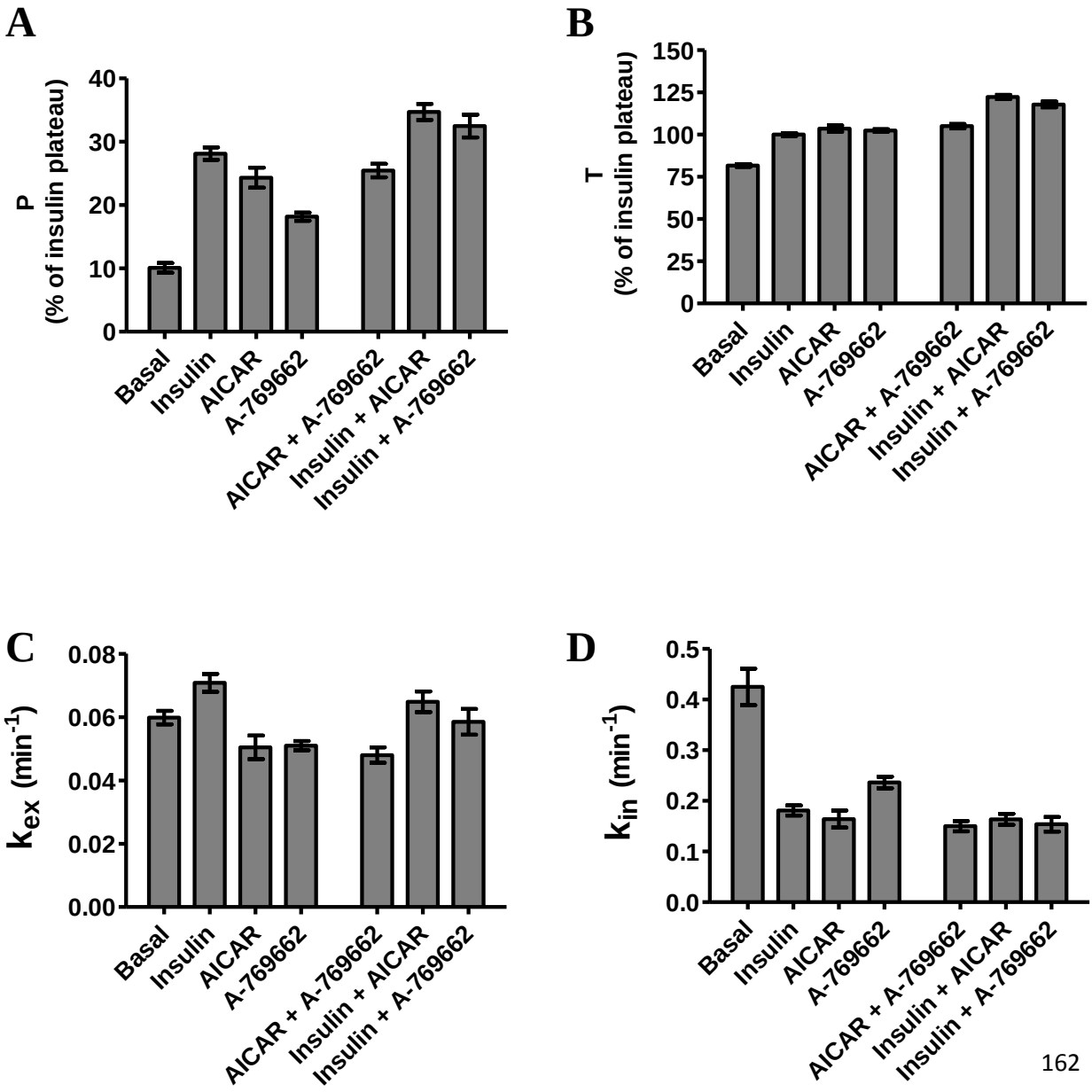

Figure 4.7. Kinetic parameters for GLUT4 recycling at steady-state. The uptake time-courses for the increase in antibody bound to GLUT4 HA were analysed to give *A*, the plasma membrane level of HA-GLUT4 (*P*), *B*, the total available GLUT4 (*T), C*, the k_{ex} rate constant and *D*, the k_{in} rate constant. The analysed data are from 3-7 experiments. S.E.M. calculated from the confidence intervals (see Materials and Experimental Procedures) for the fits are shown.

4.5 Insulin-stimulation and AMPK activation increases the amount of GLUT4 at the plasma membrane and in the recycling pool

As described above, long incubations with antibody permits the measurement of the amount of GLUT4 available to traffic to the plasma membrane under each condition. Note that the final levels of antibody bound to GLUT4 in these incubations are reported relative to the maximum insulin stimulated level, but also correspond to those presented in Figure 4.5. The half time of antibody uptake under all conditions was approximately 10-15 min, which is an order of magnitude slower than the half time for the transition from the basal to the stimulated state (Figure 4.5 *B*). In contrast to the transition from the basal to the stimulated state which was complete within approximately 10 min (Figure 4.5 *A*), the steady-state antibody uptake appeared to reach a plateau level in approximately 60 min (Figure 4.6 *B*). The plasma membrane GLUT4 (P) detected by this assay were similar to those measured by the transition state assay (Figure 4.5 *C* and Figure 4.7 *A*). The 15-20% increase in P following stimulation corresponds to a 15-20% increase in T under the same conditions.

The analysis of P and T values from the steady-state equations confirm the additivity in the responses to insulin and the AMPK stimuli noted in the examination of the transition data (Figure 4.5 *C* and *D*, Figure 4.7 *A* and *B*). Stimulation with insulin plus AICAR and insulin plus A-769662 led to increases in the level of cell surface HA-antibody bound to GLUT4 that was higher than with either stimulus alone (Figure 4.7 *A*). The additivity in the amount of GLUT4 at the cell surface following stimulation of the PKB/Akt and/or AMPK signalling pathways correlate closely with changes in the amount of intracellular GLUT4 that participates in recycling (as revealed by the changes in the parameter T) (Figure 4.7 *B*).

4.6 The steady-state GLUT4 exocytosis rate constant is not a major site of insulin, AICAR or A-769662 action

The analysis of the rate constants for exo- and endocytosis reveals that the rise in P strongly correlates with a reduction in k_{in} rather than to increased k_{ex} (Figure 4.7). There was a relatively small, increase in k_{ex} in response to all concentrations of insulin tested (Figure 4.7 *C* and Figure 4.10 *C*). An increase in k_{ex} was also found in the response to the combined effects of AICAR or A-769662 plus insulin (Figure. 4.7 *C*). However, both AICAR and A-769662 treatments alone led to a slight reduction in k_{ex}. There was no additivity in response to a combination of these AMPK agonists on k_{ex}.

4.7 Insulin, A-769662 and AICAR reduce the rate constant for GLUT4 internalisation

The antibody uptake assay also allowed the derivation of the rate constant for GLUT4 endocytosis (k_{in}) (Eq.3). The basal k_{in} value represented extremely rapid endocytosis of GLUT4 in L6 myoblasts and this was reduced by approximately 50% following treatment with insulin, AICAR or A-769662. There was no additivity in response to combination treatments with insulin plus these AMPK agonists or a combination treatment with both AMPK activators (Figure 4.7 *D*).

To corroborate the steady-state k_{in} values determined from antibody uptake experiments, an alternative experimental protocol was used to determine the same parameter. A more direct method for determination of the rate of loss of cell surface tagged GLUT4 was employed (Figure 4.8), whereby the internalisation of antibody-tagged GLUT4 from the cell surface was measured. The direct internalisation method confirmed a very rapid loss of surface GLUT4 in the basal state. k_{in} values determined by fitting the direct measurements of GLUT4 internalisation to Eq. 5 closely matched those derived from the steady-state antibody uptake (Figure 4.8 *B*).

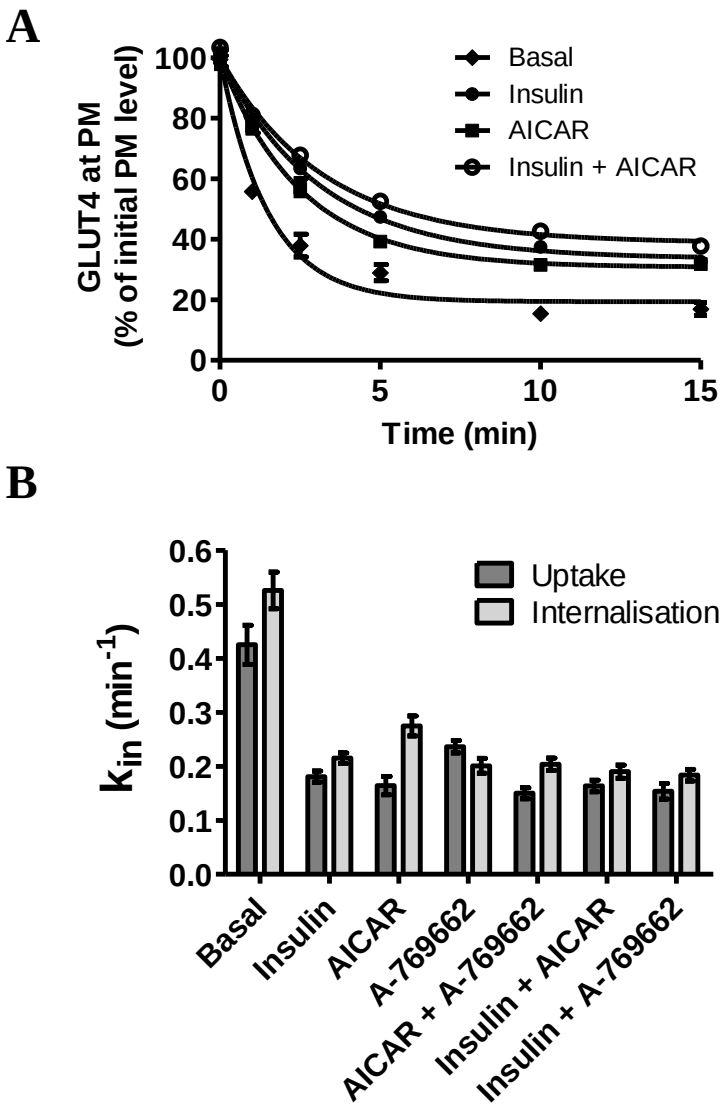

Figure 4.8. Direct measurements of steady-state GLUT4 internalisation. ***A,*** **L6 myotubes expressing HA-GLUT4 were maintained either in the basal steady-state (◆) or stimulated to a new steady-state with 200 nM insulin (•), 2 mM AICAR (■) or 200 nM insulin plus 2 mM AICAR (○). Anti-HA antibody was bound to cell surface GLUT4 at 4° C , excess antibody was removed by washing and then the cells were incubated for the indicated times at 37° C. During this time, surface bound antibody was internalised and the remaining antibody at the cell surface was detected with Alexa-488-conjugated secondary antibody. Results are the mean and SE from 3-5 experiments. In some cases error bars are smaller than the symbols.** ***B*****, Internalisation k_{in} rate constants from steady-state antibody uptake (dark bars) have been compared with the internalisation assay measurements (light bars). S.E.M. calculated from the confidence intervals (see Materials and Experimental Procedures) for the fits are shown.**

4.8 Inhibition of PI-3-K and PKB/Akt in insulin-stimulated cells rapidly reduced GLUT4 plasma membrane levels

To further corroborate the rapid internalisation of GLUT4 measured in L6 myotubes, the internalisation of GLUT4 in L6 myotubes returning to a basal state was investigated. Following insulin-stimulation and progression to the insulin-stimulated steady-state, the reduction in GLUT4 at the cell surface in response to inhibition of PI-3-K using wortmannin was monitored. In addition, this assay enabled a direct comparison between the internalisation of GLUT4 in the presence and absence of antibody. This is an important comparison since it is possible that that antibody-tagged GLUT4 internalises at a different rate to unlabelled GLUT4.

At 37^{o}C the amount of GLUT4 at the plasma membrane is rapidly reduced to a basal level upon addition of wortmannin. This transition occurred with a half-time of 1.0-1.1 min (Figure 4.9 *A* and *B*). The internalisation of GLUT4 was not affected by the binding of antibody to the exofacial tag (Pre-fix labelling, Figure 4.9 *B*). The transition from a stimulated to a basal level of cell surface GLUT4 was slowed by performing the assay at 25^{o}C. As at 37^{o}C the half time of transition (3.6-3.8 min) was unchanged by labelling the GLUT4 with antibody pre-fixation

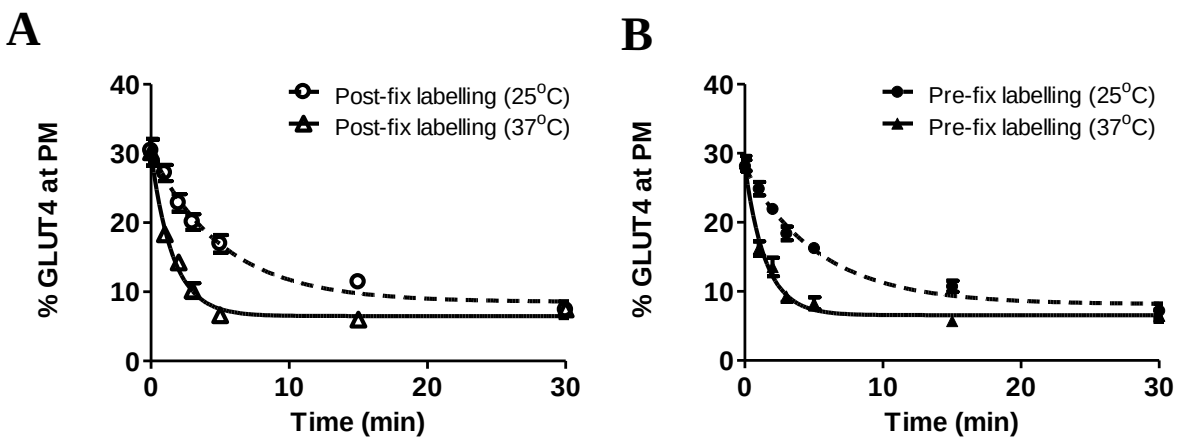

Figure 4.9. Wortmannin treatment causes a rapid reversal of insulin-stimulated GLUT4 translocation in L6 myotubes. L6 myotubes were stimulated to the steady-state with 200 nM insulin and returned to a basal state by the addition of 100 nM wortmannin. The amount of HA-GLUT4 at the cell surface was determined at specified times after wortmannin addition. Anti-HA labelling of cell surface HA-GLUT4 was performed after fixation (*A* - open symbols) or before fixation (*B* - closed symbols). Furthermore, this assay was performed at both 25°C (•, ○) and 37°C (△, ▲). The analysed data are from 3 experiments. Error bars are ± S.E.M.

4.9 Insulin-stimulation increases the amount of GLUT4 at the plasma membrane and in the recycling pool in a dose-dependent manner

It has previously been reported that GLUT4 is released from sequestration into the recycling pool in response to insulin stimulation in a dose-dependent manner in 3T3-L1 adipocytes (Coster et al., 2004). To investigate whether the same quantal release mechanism is present in L6 myotubes, antibody uptake assays were performed at increasing concentrations of insulin.

Cell-surface GLUT4 (P) was increased in a dose dependent manner, with maximal stimulation reached between 10 nM and 200 nM insulin. The increase in P correlated with the increase in the amount of GLUT4 in the recycling pathway (T) (Figure 4.10 *A* and *B*).

As noted previously (Figure 4.7), although the increase in k_{ex} is small there is a consistent enhancement by insulin-stimulation and at higher concentrations of insulin, there is a trend towards a larger stimulation of k_{ex} (Figure 4.10 *C*). Despite this, enhanced cell surface GLUT4 under steady-state conditions is more strongly correlated to k_{in} (Figure 4.10 *D*). The

maximal reduction in k_{in} is observed at a lower concentration (10 nM) than maximal stimulation of GLUT4 translocation to the plasma membrane (between 10 nM and 200 nM).

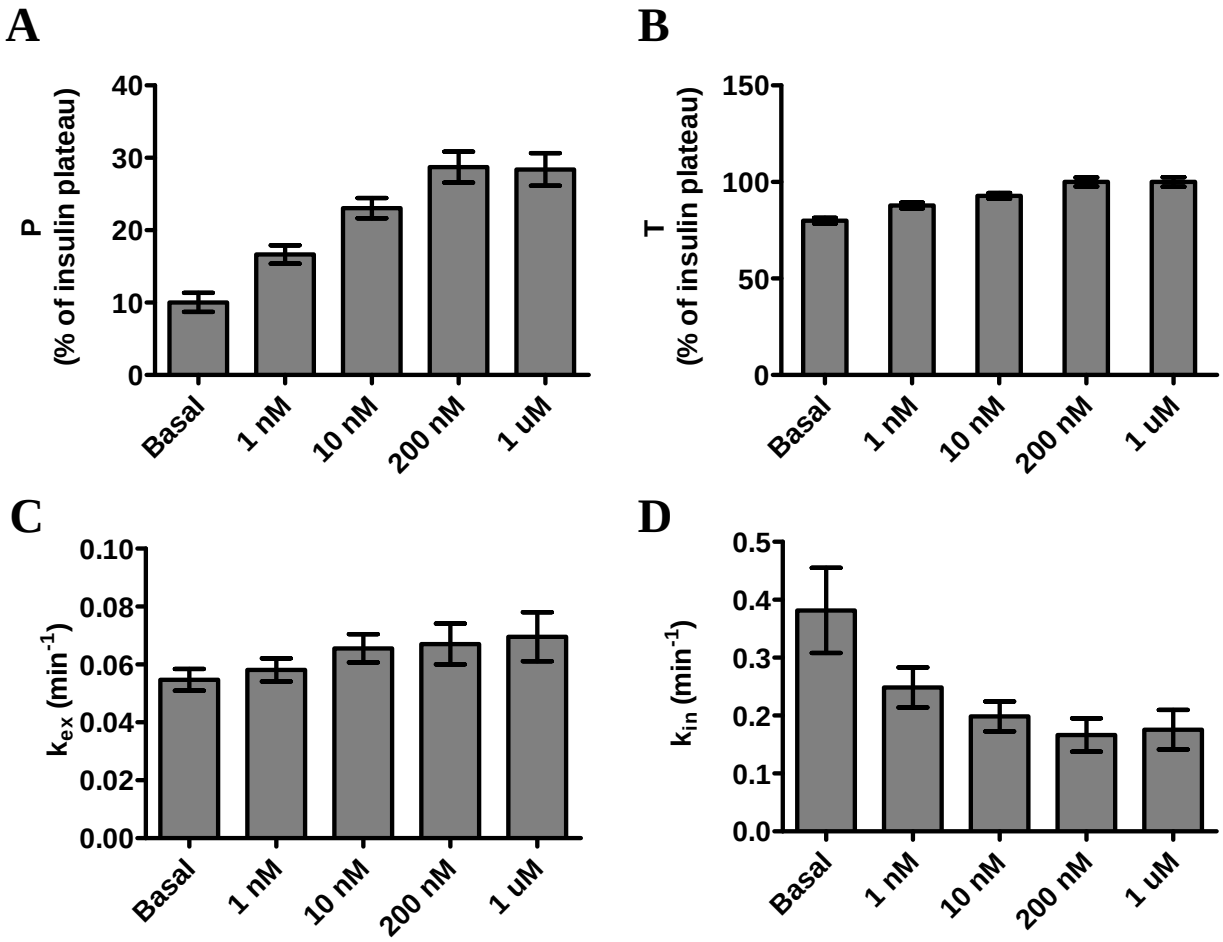

Figure 4.10. Kinetic parameters for GLUT4 recycling at steady-state following stimulation with increasing concentrations with insulin. The uptake time-courses for the increase in antibody bound to HA-GLUT4 were analysed to give *A*, the plasma membrane level of HA-GLUT4 (*P*), *B*, the total available GLUT4 (*T*), *C*, the k_{ex} rate constant and *D*, the k_{in} rate constant. The analysed data are from 3 experiments. S.E.M. calculated from the confidence intervals (see Materials and Experimental Procedures) for the fits are shown.

4.10 The rate of GLUT4 trafficking

We have also examined whether the amount of GLUT4 that is moved to and from the cell surface becomes limiting during responses to agonists. The transport rate (R) is a parameter that reflects the dependence of GLUT4 traffic on the GLUT4 mass that moves as well as the time constant for movement. This parameter was calculated from the kinetic parameters measured in the antibody uptake assay (Eq.4). Interestingly no major difference in GLUT4 traffic rates were apparent for any of the conditions studied (Figure 4.11), despite there being a range of values observed for T, P, k_{ex} and k_{in}.

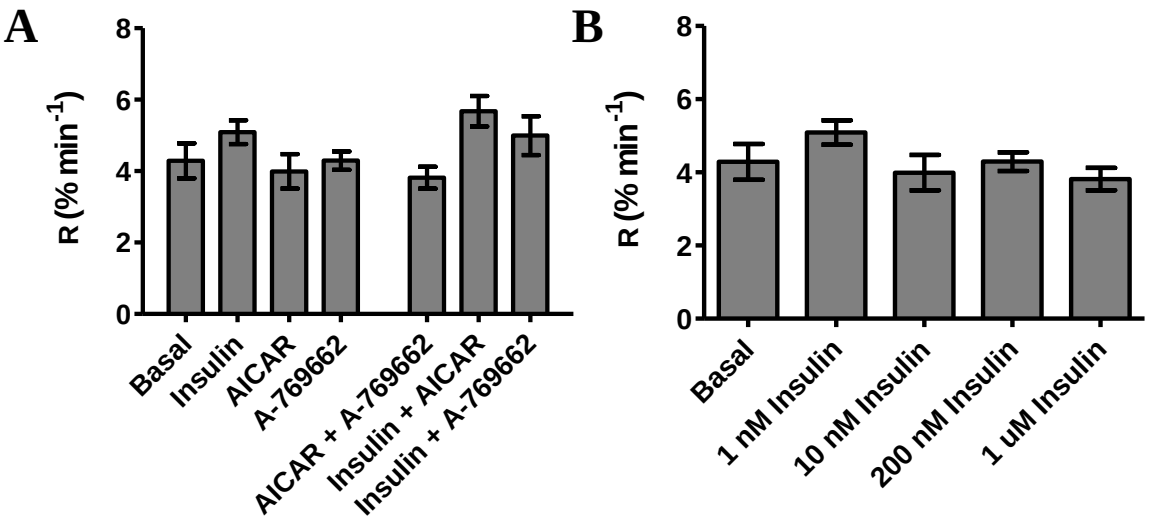

Figure 4.11. GLUT4 transport rates under steady-state conditions. The steady-state GLUT4 transport rates ($R = k_{in}P$) following stimulation with the maximal dose of different agonists (*A*) or increasing doses of insulin (*B*). All data presented in A and B are means values from 3-7 experiments. S.E.M. calculated from the confidence intervals (Materials and Experimental Procedures) for the fits are shown.

4.11 Wortmannin and Akti inhibit insulin-induced PKB/Akt phosphorylation and GLUT4 translocation

We next aimed to dissect out the roles of PI-3-K and PKB/Akt in insulin-induced changes in GLUT4 trafficking. DMSO control assays were performed in all cases and showed no significant difference from non-treated cells. The PI-3-K inhibitor wortmannin and PKB/Akt inhibitor Akti

were incubated with L6 myotubes in the absence and presence of insulin. Insulin caused an increase in PKB/Akt phosphorylation in L6 cells. Wortmannin treatment resulted in a complete inhibition of insulin-stimulated PKB/Akt activation whereas the specific PKB/Akt inhibitor Akti only reduced PKB/Akt phosphorylation to the level observed in basal cells (Figure 4.12 *A*). These data are similar to those previously reported for 3T3-L1 adipocytes (Gonzalez and McGraw, 2006). These inhibitors did not result in inhibition of AMPK activation by AICAR or A-769662 as measured by phosphorylation of AMPK and phosphorylation of its downstream substrate ACC (Figure 4.12 *B*). There was a notable decrease in AICAR-stimulated AMPK phosphorylation following the presence of Akti. However, this did not translate to a decrease in AMPK activity as measured by ACC phosphorylation.

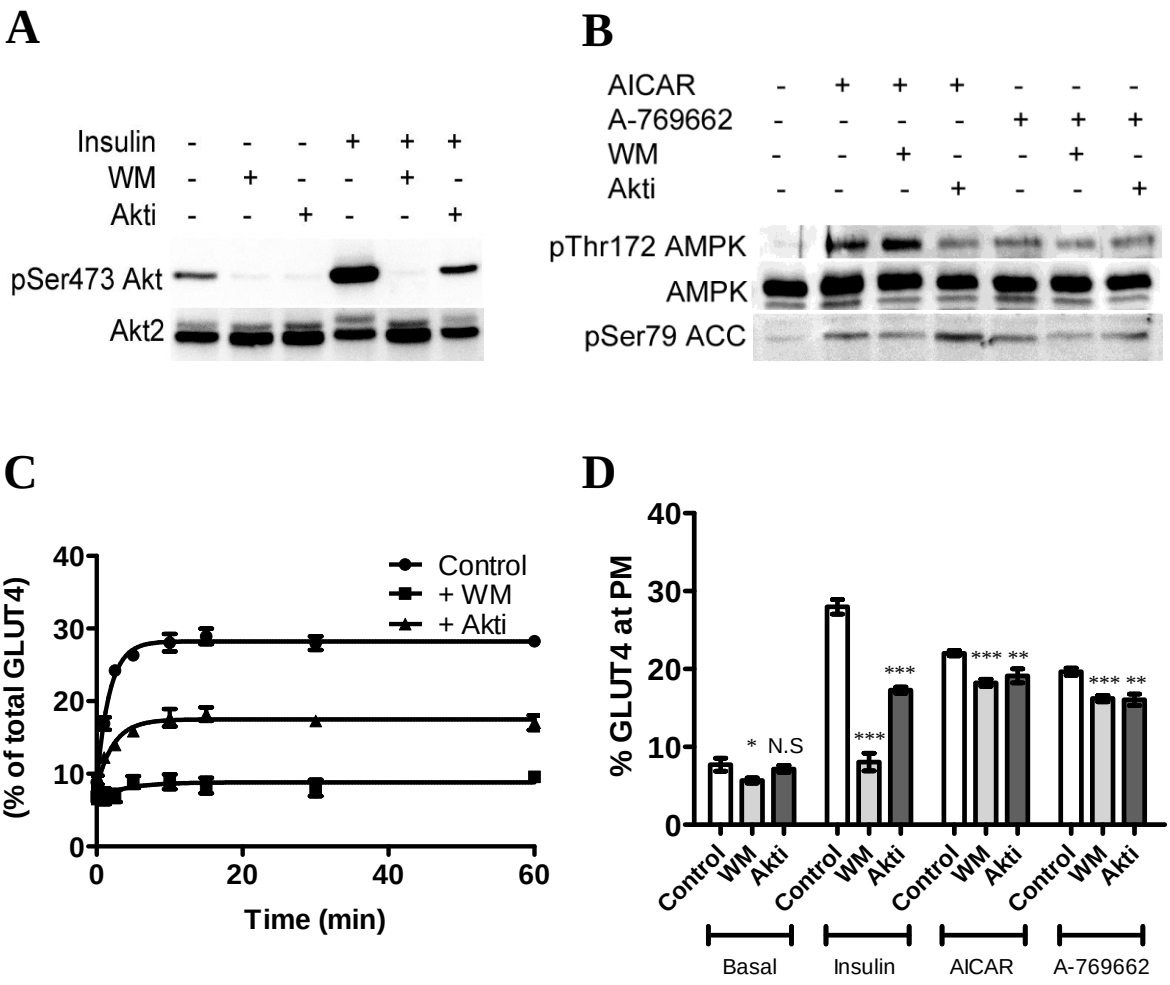

Figure 4.12. PKB/Akt controls of the transition from basal to insulin-stimulated state. *A*, PKB/Akt activation was determined by blotting for phospho-serine473 in basal cells and cells treated with 200 nM insulin (upper panels). Both basal and insulin-treated cells were also treated with 100 nM wortmannin and 10 μM Akti as indicated. PKBβ/Akt2 levels were determined from the same solubilised cell lysates (bottom panels). *B*, AMPK activation was determined by blotting for phospho-threonine 172 AMPK and phospho-serine 79 of ACC. AMPK levels were determined from the same solubilised cell lysates. *C*, The rate of transition from the basal to the insulin-stimulated state in the absence (•) and presence of wortmannin (■) and Akti (▲) was determined in fixed cells using anti-HA antibody and an Alexa-488-conjugated secondary antibody. Each point represents the mean and S.E.M. from 3 experiments. In some cases error bars are smaller than the symbol. *D*, The cell surface levels of GLUT4 reached at 30 min of incubation with the agonists with or without inhibitors were determined as a percentage of the total cellular GLUT4 available in permeabilised cells. Each data set represents the mean and S.E.M from 3 experiments. *** p = <0.001, ** p = <0.01, *p=<0.05 (unpaired t-test inhibitor-treated compared to control).

Correspondingly, the transition from the basal to the insulin-stimulated state was completely blocked by wortmannin (p = <0.0001) but was not completely blocked by Akti (p = <0.0001) (Figure 4.12 *C*). The half time for the transition was increased by 25% and the final plasma membrane level of GLUT4 was reduced by approximately 50% in the presence of Akti. Wortmannin and Akti marginally inhibited AICAR- and A-769662-induced increased cell surface levels of GLUT4 (Figure 4.12 *D*). This small effect was significant in each case (p = <0.07). There is a reduction in basal cell surface GLUT4 levels in the presence of wortmannin (p = 0.0163). Therefore, the percentage increase in cell surface GLUT4 following AICAR- and A-769662-stimulation in control (AICAR = 14.3%, A-769662 = 11.9%) and wortmannin-treated cells (AICAR = 12.5%, A-769662 = 10.5%) remained similar.

4.12 Inhibition of PI-3–K or PKB/Akt differently inhibit insulin-modulated GLUT4 trafficking parameters

We next examined the effects of wortmannin and Akti on the steady-state trafficking of GLUT4 (Figure 4.13). The antibody uptake experiments are carried out over an extended time course. Therefore, it was important to ascertain whether wortmannin and Akti effectively inhibited the

activation of PKB/Akt in the presence of insulin over this time course. Wortmannin completely inhibited insulin-induced phosphorylation of PKB/Akt after incubation with insulin for 30 min and 180 min. As reported above (Figure 4.12 *A*), Akti only reduced PKB/Akt phosphorylation to the level observed in basal cells after a 30 min incubation with insulin. In contrast, Akti completely inhibited PKB/Akt phosphorylation in cells incubated with insulin for 180 min.

Wortmannin completely inhibited the insulin-dependent increment in surface levels of GLUT4 (P). By contrast, and as evident in the transition experiments (Figure 4.12 *C* and *D*), Akti did not completely inhibit the insulin effect on the initial cell surface levels (P) (Figure 4.13 *B*) The wortmannin and Akti effects on the available GLUT4 level (the steady-state parameter T) also differed. Whereas wortmannin reduced T values obtained from insulin-treated cells to those obtained from basal cells (~80%), Akti reduced both basal and insulin-stimulated levels of T (~65%). At these reduced levels of available GLUT4 any insulin dependent increase in T was completely inhibited.

Wortmannin did not inhibit the increase in cell surface GLUT4 levels (P) following activation of AMPK by AICAR and A-769662 (Figure 4.13 *G*). This is inconsistent with the data obtained from transition state experiments (Figure 4.12 *D*), although the inhibition observed by this method was very marginal. AICAR-stimulated GLUT4 translocation was not inhibited by Akti (Figure 4.13 *G*). In contrast, Akti did partially inhibit A-769662-stimulated GLUT4 translocation as measured by the uptake assay (Figure 4.13 *G*). Furthermore, both AICAR- and A-769622-stimulation resulted in increased levels of T in the presence of wortmannin and Akti compared to basal cells under the same treatment. Incubation with Akti resulted in reduced GLUT4 recycling levels (~80%) in AICAR and A-769622 stimulated cells when compared to control cells (100%). However, these stimuli still resulted in ~15-20% increase in the size of the GLUT4 recycling pool when compared to basal or insulin-stimulated cells treated with Akti. This results in a similar fold-increase in T over basal cells treated with Akti as observed between appropriate control cells (Figure 4.13 *G*).

Both wortmannin and Akti both markedly reduced steady-state k_{ex} values, although the basal k_{ex} was reduced to a lower level following wortmannin treatment (Figure 4.13 *D*). In addition, the overall transport rate of GLUT4 was slowed following incubation with wortmannin or Akti (Figure 4.13 *F*). Both basal and stimulated values of k_{ex} were reduced. The inhibitory

effect of Akti was less pronounced than that which occurred following the wortmannin treatment (Figure 4.13 *D*).

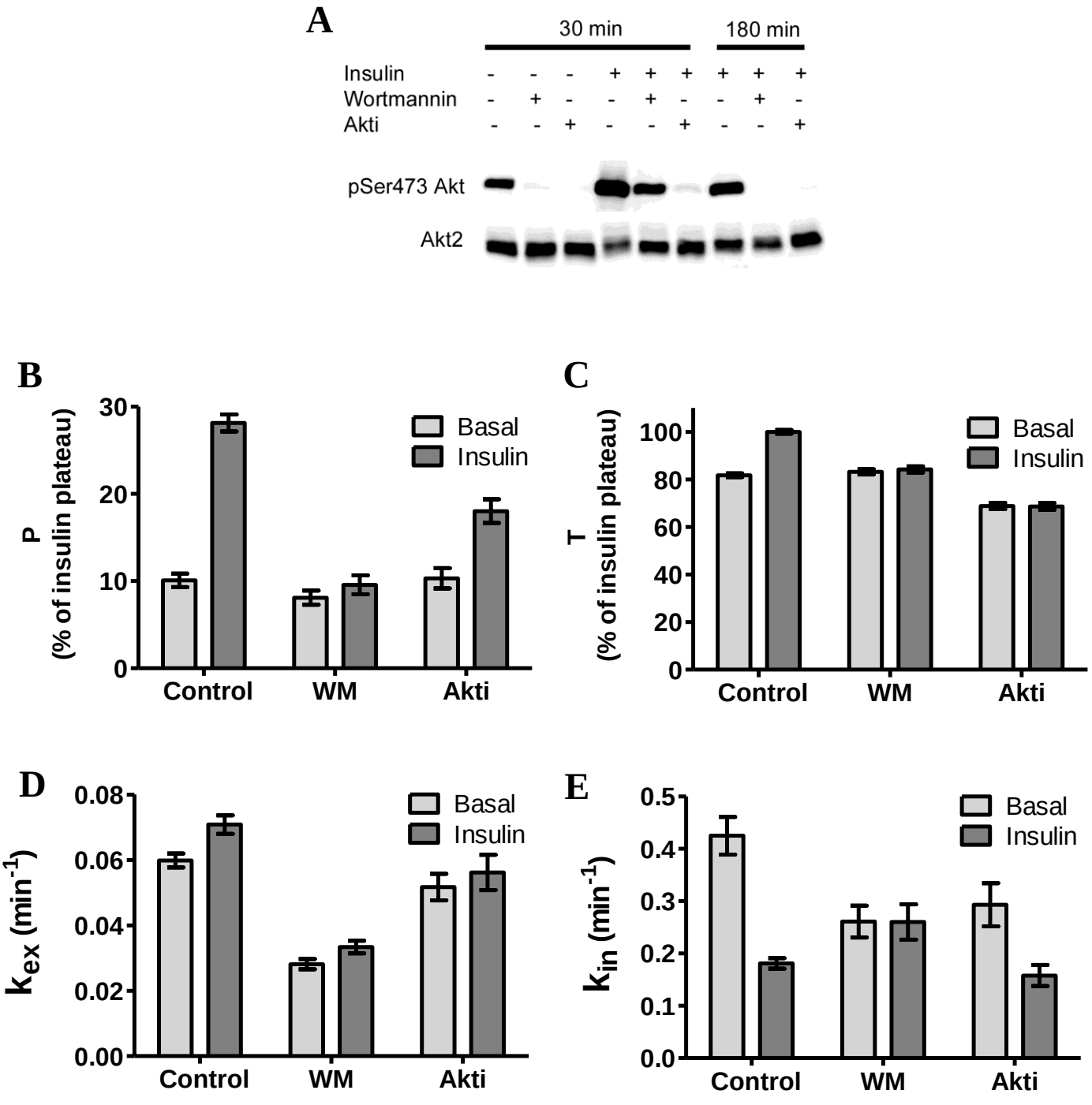

F

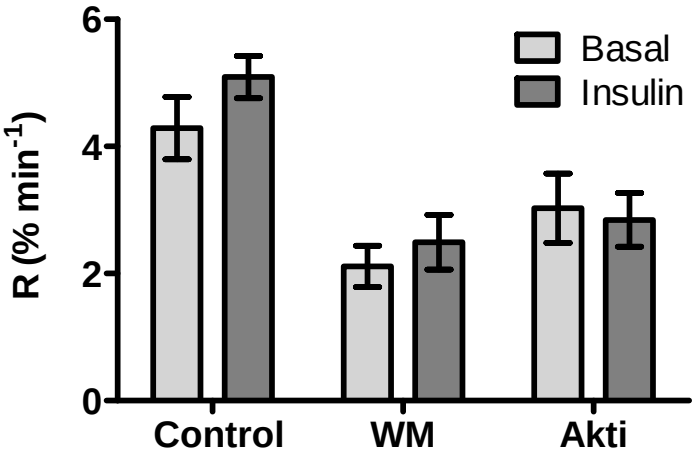
6
4
2
0
R (% min-1)
Basal
Insulin
Control
WM
Akti

G

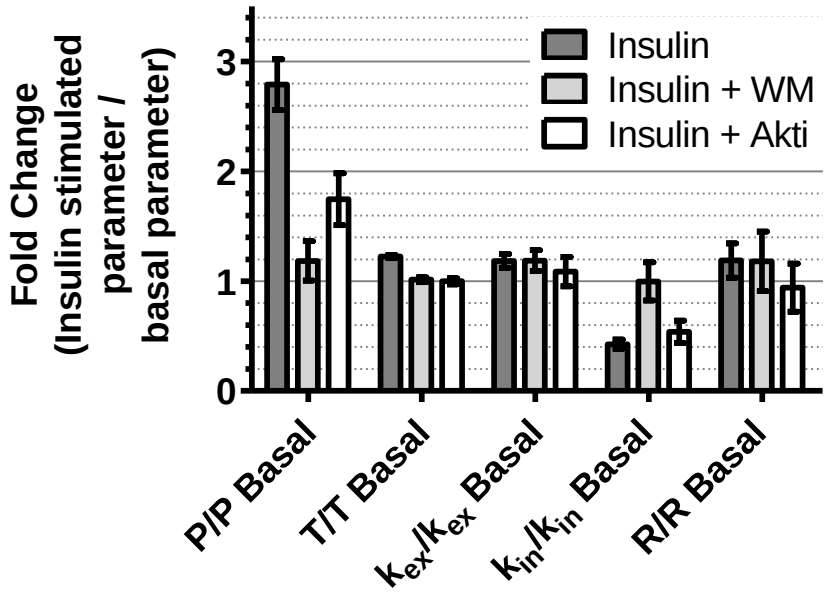
Fold Change (Insulin stimulated parameter / basal parameter)
3
2
1
0
Insulin
Insulin + WM
Insulin + Akti
P/P Basal
T/T Basal
Kex/Kex Basal
Kin/Kin Basal
R/R Basal

H

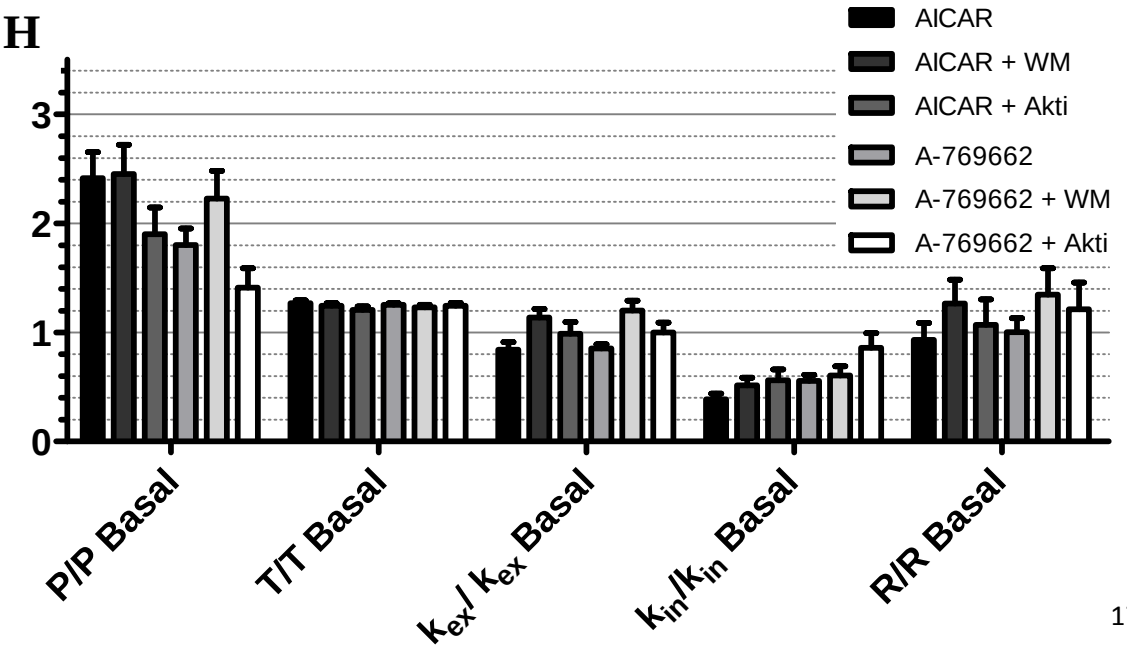
3
2
1
0
AICAR
AICAR + WM
AICAR + Akti
A-769662
A-769662 + WM
A-769662 + Akti
P/P Basal
T/T Basal
Kex/ Kex Basal
Kin/Kin Basal
R/R Basal

Figure 4.13. Inhibition of steady-state GLUT4 recycling by wortmannin and Akti. *A*, PKB/Akt activation was determined by blotting for phospho-serine473 in basal cells and cells treated with 200 nM insulin for 30 min and 180 min (upper panels). Both basal and insulin-treated cells were also treated with 100 nM wortmannin or 10 μM Akti for 15 min before stimulation as indicated. PKBβ/Akt2 levels were determined from the same solubilised cell lysates (bottom panels). Steady-state kinetic plots without inhibitor (Control) or following treatment with wortmannin (WM) or the PKB/Akt inhibitor (Akti) were analysed to give *B*, the plasma membrane level of HA-GLUT4 (*P*), *C*, the total available GLUT4 (*T*), *B*, the k_{ex} rate constant, *E*, the k_{in} rate constant and *F*, the transport rate (R). The analysed data are from 3 experiments. S.E.M. calculated from the confidence intervals (see Methods) for the fits are shown. *G* and *H*, To isolate effects associated with inhibitor action on kinetic parameters in the stimulated states the fold changes over basal levels were determined.

4.13 Insulin-stimulation inhibits GLUT4 internalisation in the presence of an PKB/Akt inhibitor

Treatment with wortmannin and Akti reduced basal k_{in} values to a similar level (Figure 4.12 *E*). However, wortmannin and Akti had differing effects on insulin-induced changes in k_{in}. Wortmannin completely inhibited insulin-induced reduction in k_{in}. However, the insulin-dependent reduction in k_{in} was mostly retained in the presence of Akti. This PKB/Akt-independent step may explain why Akti is not able to completely inhibit insulin-induced GLUT4 increases at the cell surface, as is seen with wortmannin.

The inhibitory effects of wortmannin and Akti on basal GLUT4 trafficking complicate the analysis and interpretation of whether these reagents have inhibitory effects on agonist-stimulated trafficking. In an attempt to separate out the inhibitory effects on basal trafficking from those on insulin-stimulated trafficking, all the basal and insulin-stimulated steady-state parameters were calculated as a fold-change (Figure 4.12 *G*). The clearest effect of insulin was to increase P by 2.8-fold. The effects on P were highly correlated with insulin-associated changes in k_{in}. The insulin-dependent reduction (reduction of 0.244 min^{-1} (57.4%) compared to corresponding basal k_{in}) in k_{in} was completely reversed by wortmannin treatment but only

partially reversed by Akti treatment (reduction of 0.135 min^{-1} (46.2%) compared to corresponding basal k_{in}).

AICAR- and A-769662-stimulated cells all exhibit a similar fold-decrease in k_{in} in the presence and absence of inhibitors, except for A-769662-stimulated cells treated with Akti (Figure 4.13 *H*). This corresponds with the partial inhibition of the A-769662-stimulated increase in plasma membrane GLUT4 by Akti.

4.14 Discussion

The development and validation of antibody uptake and internalisation assays in the L6 cell culture model expressing HA-epitope tagged GLUT4 has permitted detailed analysis of GLUT4 trafficking responses to insulin and AMPK activators. It has been previously reported that antibody-bound GLUT4 traffics in a similar manner to unlabelled GLUT4 (Martin et al., 2006). In support of this finding, GLUT4 internalisation in L6 cells is not changed by the binding of antibody to HA-GLUT4. We have investigated the subcellular localisation of antibody-bound GLUT4 to ascertain whether the antibody remains bound to GLUT4 and whether it is present in expected locations. These studies have indicated that the anti-HA antibody remains bound to GLUT4 while trafficking through L6 myotubes since internalised antibody colocalised with GLUT4. Furthermore, tagged GLUT4 localises to the TGN and early endosomes which have been reported to form part of the GLUT4 intracellular trafficking itinerary (Lampson et al., 2001; Shewan et al., 2003; Ploug et al., 1998). A more extensive characterisation of the route of GLUT4 trafficking could be performed using antibody uptake or pulse-chase protocols and subcellular markers of GSVs (e.g. VAMP2 and IRAP).

The expression level of HA-GLUT4 induced by the retroviral expression system utilised in this study does not interfere with GLUT4 trafficking parameters. This is an important finding since it has been reported that over expression of GLUT4 in adipocytes can inhibit insulin-stimulated GLUT4 translocation (Al Hasani et al., 1999). The viral amount with which L6 cells were infected resulted in a uniform expression in L6 myotubes at a level (3.5 ρmoles/mg of protein) similar to endogenous GLUT4 in rat epitrochlearis muscle (calculated from unpublished data from a previous study (Karlsson et al., 2009)). Uninfected L6 myotubes express very little GLUT4 as compared to 3T3-L1 adipocytes, primary adipocytes and primary muscle tissue. This may mean that L6 myotubes have an under-developed GSV compartment. If this is the case, then GLUT4 would be forced into the constitutively recycling system. However, reduced HA-GLUT4 expression did not increase the proportion of total cellular GLUT4 within the sequestered GSV compartment.

The transitions from a basal state GLUT4 distribution to a fully stimulated distribution are extremely rapid in L6 myotubes. The increases occur with half times of less than 1.5 min and would be expected to closely match the half time for internalisation at steady-state as both time courses, in a simple analysis, are dependent on a rate constant that is the sum of k_{ex} and k_{in}.

Previous studies have noted differences between the transition and steady-state kinetics of GLUT4 translocation that are inconsistent with a single intracellular pool which is stimulated and maintained in the stimulated state (Coster et al., 2004; Holman et al., 1994). There are several possibilities that could account for the rapid transition. There may be a direct release of GLUT4 to the plasma membrane from a kinetically separate pool. This pool could be a specialised GSV compartment that translocates to the cell surface very slowly, or not at all, in the basal state but rapidly translocates, and undergoes fusion with the plasma membrane when stimulated. Alternatively, a single kinetic pool could be stimulated in a rapid transitory manner with a subsequent relaxation to a steady-state in which GLUT4 recycles much more slowly. Some combination of these two possibilities may also account for the rapid transition-phase kinetics. For example GLUT4 could be released from a specialised GSV compartment as a pulse into the plasma membrane and from there into the endosomal recycling pool. The possibility that GLUT4 is released directly into an unstimulated endosomal recycling pool seems to be unlikely, as the additional GLUT4 that is released would not reach the plasma membrane as rapidly as observed in the transition phase kinetic experiments.

In this study we have identified several novel aspects of membrane protein trafficking. We have found that GLUT4 recycling is considerably faster in the muscle cell line L6 than in adipocytes (Jhun et al., 1992; Yang and Holman, 1993; Satoh et al., 1993; Karylowski et al., 2004; Govers et al., 2004). Despite this, relatively low cell surface levels of GLUT4 are maintained in the basal state due to a very rapid endocytic rate. In contrast to adipocytes, where the predominant effect of insulin action is on GLUT4 exocytosis, in L6 cells insulin and AMPK agonists maintain enhanced plasma membrane GLUT4 levels largely by inhibiting GLUT4 endocytosis. This inhibition of endocytosis was independent of the PKB/Akt pathway. These data indicate that different cell types can co-ordinate a similar transient change in cell surface GLUT4 by targeting discrete limbs of the GLUT4 trafficking pathway. Although we did not measure a significant increase in the overall k_{ex}, an insulin effect on GLUT4 exocytosis from the specialised storage pool might be masked by the high basal recycling that occurs in L6 cells. Indeed, in all insulin-stimulated conditions tested there was a trend towards an enhancement of the rate constant for exocytosis. An increase in k_{ex} was not noted in response to AMPK activation by AICAR or A-769662. In fact, the calculated k_{ex} in cells stimulated with AICAR or A-769622 was lower than the k_{ex} for GLUT4 in untreated cells.

The trafficking of GLUT4 in L6 cells differs from that in adipocytes in two major respects. First, in the basal state the endocytosis rate constant is 2-3-times faster than in 3T3-L1 adipocytes. This suggests that different aspects of the GLUT4 trafficking itinerary can be discretely regulated in different cell types resulting in essentially the same outcome, which in this case is low expression of the transporter on the plasma membrane in the absence of insulin. The basal recycling rate of GLUT4 is faster in L6 than in 3T3-L1 adipocytes (Govers et al., 2004; Karylowski et al., 2004; Jhun et al., 1992; Yang and Holman, 1993). If the basal endocytosis rate was similar in both cell types a greater proportion of GLUT4 would be found at the plasma membrane in the basal state in L6 cells. However, L6 cells seem to have adapted to this situation by increasing the internalisation of GLUT4. Thus while it is uncertain if this situation mimics GLUT4 trafficking in skeletal muscle *in vivo*, particularly since we are using an artificial over-expression system, these studies highlight the enormous plasticity of the endosomal recycling system.

The second unique feature of GLUT4 trafficking in L6 cells is that agonists including insulin and AMPK activators maintain enhanced surface levels of GLUT4 in the steady-state in large part by inhibiting endocytosis. By investigating GLUT4 trafficking at different concentrations of insulin, these studies have revealed that maximal inhibition of k_{in} in response to insulin-stimulation occurs at 10 nM. This is a lower concentration than the concentration of insulin that induces a maximal increase in cell surface GLUT4, implying that insulin-regulated GLUT4 internalisation is more sensitive to insulin than changes in other trafficking parameters such as the insulin-induced mobilisation of GLUT4. It will be of interest to explore the mechanism for regulated endocytosis of GLUT4.

The regulation of GLUT4 internalisation following insulin-stimulation described here could be explained by at least two models. First, the inhibition of endocytosis may be 'signal' mediated. So far an insulin-regulated signalling pathway that specifically targets GLUT4 endocytosis has not been reported. It does not appear to be dependent on the PKB/Akt pathway because Akti only partially overcame this inhibitory effect, consistent with previous studies in adipocytes (Gonzalez and McGraw, 2006). However, the effect was blocked by wortmannin. Therefore, it would be of interest to specifically inhibit other insulin-regulated kinases such as aPKC and MAP kinase to try and ascertain which signalling pathway is responsible for insulin-regulated inhibition of GLUT4 internalisation.

One potential caveat of this signalling model is that wortmannin-treatment also slowed GLUT4 exocytosis. This leads to the second potential model, which is that slowing of endocytosis in response to insulin or other agonists may be a mass action, non signal mediated, phenomenon. This is supported by the steady-state transport rates (R), which were approximately the same in all conditions studied. In this model the endocytosis rate may be operating close to its maximum capacity in the basal state. The delivery of previously sequestered GLUT4 to the plasma membrane that occurs in response to insulin and the other agonists may saturate this step causing accumulation of GLUT4 at this site. As such, the rate of GLUT4 transport (R) from the plasma membrane (as opposed to the rate constant) remains the same in basal and stimulated cells. Consistent with this notion, it has been reported that GLUT4 possesses an N-terminal endocytosis motif (FQQI) that is homologous to, but far less efficient than, similar motifs found in other proteins such as the transferrin receptor (YXRF). Substitution of the phenylalanine for tyrosine in the GLUT4 endocytosis motif markedly improves its trafficking efficiency (Piper et al., 1993; Garippa et al., 1994). Hence, it is conceivable that GLUT4 evolved with a relatively weak endocytosis motif in this position to accommodate the capacity for saturable regulation under certain circumstances such as those described here.

This observation does not overshadow the fact that L6 cells have adapted novel mechanisms to regulate surface levels of GLUT4 despite an elevated basal recycling rate. In the absence of insulin or other agonists L6 cells maintain relatively low cell surface levels of GLUT4, somewhat analogous to 3T3-L1 adipocytes, not by slowing exocytosis but rather by rapid endocytosis of GLUT4 under basal conditions. This endocytosis rate affords these cells greater flexibility in modulating surface levels of GLUT4 simply by slowing endocytosis. This mechanism, which also exists in adipocytes (Blot and McGraw, 2006; Jhun et al., 1992; Karylowski et al., 2004), likely plays a much greater role in L6 cells due to the relative basal recycling kinetics. These observations raise several questions that will serve as the basis for future studies; is there a physiological advantage to the muscle cell in regulating surface levels of GLUT4 in this manner as opposed to a more active intracellular retention mechanism; is GLUT4 trafficking similarly regulated in skeletal muscle *in vivo*; and what is the mechanism by which GLUT4 undergoes endocytosis in these cells? In regard to this final question studies in cardiomyocytes, skeletal muscle and adipocytes have reported localisation of GLUT4 to clathrin coated vesicles in basal and stimulated cells (Fazakerley et al., 2009; Vassilopoulos et al., 2009; Slot et al., 1991b; Robinson et al., 1992; Huang et al., 2007). GLUT4 internalisation has been reported to occur by

both clathrin-mediated and clathrin-independent routes in both 3T3-L1 adipocytes and L6 myoblasts (Blot and McGraw, 2006; Antonescu et al., 2008). The basal internalisation rate constant for GLUT4 in basal myotubes (0.43 min^{-1}) is similar to the rate constant for the TfR internalisation (0.44 min^{-1}) (calculated in (Muretta and Mastick, 2009) from (Tanner and Lienhard, 1987)). This implies that GLUT4 may traffic with TfR in basal myotubes. TfR has been reported to internalise via a clathrin-mediated mechanism (Antonescu et al., 2008). The reduction in k_{in} following stimulation may therefore be a result of an inhibition of this mechanism or a re-routing GLUT4 through a different internalisation mechanism.

Recent studies have attempted to identify changes in these different endocytic processes in response to insulin and other stimuli. In 3T3-L1 adipocytes, insulin reportedly inhibits GLUT4 internalisation via a cholesterol-dependent route, which is the dominant route in basal cells. GLUT4 is therefore thought to internalise via the clathrin-dependent pathway in stimulated cells (Blot and McGraw, 2006). In L6 myoblasts, DNP treatment inhibited the clathrin-dependent pathway to slow GLUT4 internalisation. We have not addressed the mechanism by which insulin and AMPK activation led to inhibition of GLUT4 endocytosis in this study. These published data imply insulin and AMPK activation may inhibit different endocytic processes. It should be noted that the DNP-mediated effect on GLUT4 endocytosis has been reported to be dependent on PKC and not AMPK (Thong et al., 2007). Therefore, the findings from this study may not be applicable to our data. However, it is unlikely that different agonists regulate GLUT4 endocytosis via independent mechanisms because we failed to observe additivity between different agonists. By extending our trafficking studies to include other recycling proteins such as the TfR, it will be possible to determine whether modulation of GLUT4 trafficking by agonists is specific to GLUT4.

The reduction in GLUT4 endocytosis measured under insulin-stimulation contrasts with previous studies where no insulin effect on GLUT4 internalisation was reported in L6 myoblasts (Wijesekara et al., 2006; Antonescu et al., 2008). While we cannot be certain of the nature of this discrepancy between the previously published data in L6 cells, one major difference is that in the previous study a 37^{o}C wash step was used between incubation with the GLUT4 labelling antibody at 4^{o}C and commencement of the internalisation assay. In our study we initiated internalisation by immediate substitution of the cold wash buffer with pre-warmed buffer followed by continuous incubation at 37^{o}C. In view of the greater difference between the initial data points in

the internalisation experiment in these cells, omitting just 1-2 min of the initial internalisation experiment, as is likely the case in the previous study (Antonescu et al., 2008), may bias the fitting of the data and reduce the difference in the rate constants obtained. In addition, these studies were principally confined to non-differentiated myoblasts. Although the same results have been found in myotubes, this is perhaps surprising given that it is known that GLUT4 trafficking in pre-adipocytes is vastly different to that in mature cells (Govers et al., 2004). The finding of an inhibitory effect with both insulin and AMPK agonists were verified using two different methods for measuring endocytosis. In both cases we observed a similar degree of inhibition of GLUT4 endocytosis with insulin and AICAR. Furthermore, the capacity for rapid endocytosis is supported by the very fast return to a basal level of GLUT4 at the plasma membrane following treatment of insulin-stimulated cells with wortmannin.

There are at least two ways in which the delivery of GLUT4 to the plasma membrane may be increased; either by increasing the rate of exocytosis and/or by increasing the amount of GLUT4 located in the recycling system. In adipocytes both of these parameters are regulated by insulin (Govers et al., 2004; Muretta et al., 2008) while in L6 cells insulin has little effect on the exocytic rate as analysed with a two-compartmental model. Regardless we clearly observed an increase in the total recycling pool of GLUT4 in response to both insulin and AMPK agonists. Partial or incomplete mobilisation of GLUT4 has been reported in 3T3-L1 cells (Govers et al., 2004). Similarly in L6 cells, incubated under basal conditions, the entire cellular pool of GLUT4 does not reach the cell surface even over time courses extending to several hours. This data is inconsistent with data previously in reported in L6 myotubes (Wijesekara et al., 2006). The data presented in this study are very similar to the data presented in this thesis, where in basal cells approximately 60% of the total cellular GLUT4 recycled with the plasma membrane over a time course of 4 h. However, the authors comment that all of the cellular GLUT4 reaches the cell surface if the assay is performed for longer times. We have performed our assay for 5 hours and not noticed any increase in the amount of GLUT4 trafficking with the cell surface in basal cells. The reason for the discrepancy between these studies is not clear.

The size of the basal recycling pool is much more considerable in L6 cells (61%) compared to basal 3T3-L1 adipocytes (≈ 10%) (Govers et al., 2004). While some studies have reported higher basal rates of GLUT4 recycling in adipocytes, even here this pool was smaller than we observe in L6 cells in the present study (Muretta et al., 2008). In contrast to these observations, McGraw's and Klip's groups have reported that the whole cellular pool of GLUT4

recycles with the cell surface under basal conditions in 3T3-L1 adipocytes and L6 myotubes, respectively (Karylowski et al., 2004; Wijesekara et al., 2006). However, the complete mobilisation of GLUT4 that occurred in the studies performed by McGraw's group has recently been attributed to the cell culture conditions, particularly the replating of differentiated adipocytes following electroporation (Muretta et al., 2008). As described in 3T3-L1 adipocytes, insulin-stimulation results in a dose-dependent release of GLUT4 from sequestration into the recycling pathway in L6 cells (Govers et al., 2004; Coster et al., 2004). Insulin-induced mobilisation of GLUT4 is inhibited by wortmannin and Akti and therefore is a PKB/Akt-dependent event. The mechanism for this release has not been investigated in this study but may be regulated by PKB/Akt-mediated phosphorylation and inhibition of the Rab-GAPs TBC1D4/AS160 and/or TBC1D1.

One of the key features of GLUT4 traffic in L6 myotubes revealed by our kinetic study is the additivity observed in the response to combined stimulation with insulin and AMPK agonists. This is apparent by the relative pool size of GLUT4 that can be mobilised in response to these stimuli. The recycling GLUT4 pool in the presence of the AMPK activators and insulin is much greater than each agonist alone, indicating that these agonists do not use a convergent signalling mechanism to mobilise GLUT4. Additivity in glucose transport responses to insulin and AMPK have been reported in a range of muscle types (Hayashi et al., 1998; Bergeron et al., 1999; Yang and Holman, 2005; Fisher et al., 2002; Gao et al., 1994; Rodnick et al., 1992a) and our current studies suggest that part of this effect could be associated with different processes that regulate GLUT4 retention that are downstream of the insulin and AMPK signalling systems. This could involve physically distinct pools of GLUT4 as reported previously (Ploug et al., 1998; Lemieux et al., 2000), although our studies in cardiomyocytes have been unable to replicate these findings (Fazakerley et al., 2009). Alternatively, GLUT4 may be retained in a similar location but regulated by separate molecular mechanisms possibly involving effectors such as the TBC proteins TBC1D1 and TBC1D4/AS160, which may uniquely respond to either AMPK or insulin, respectively (Chen et al., 2008).

One of the control experiments performed for validation of the antibody uptake assay has also revealed some information on the route of GLUT4 trafficking. Insulin-stimulated myotubes were returned to a basal state through the addition of wortmannin. This resulted in a very rapid decrease in plasma membrane GLUT4 levels (Figure 4.9). The return to a basal level of GLUT4 at the cell surface is dependent on both a reversal in the trafficking rate constants and

resequestration of GLUT4. Given the speed of the reversal to basal cell surface GLUT4 levels, it seems likely that GLUT4 traffics through the GSV compartment under stimulated conditions and does not simply recycle via the endosomal compartment. In this way, the release or exocytosis of GSVs from this compartment can be rapidly halted upon addition of wortmannin and GLUT4 sequestered from the cell surface. If the GLUT4 was released from the GSV compartment and subsequently trafficked solely through the endosomal system, it would more challenging to resequester GLUT4 on such a rapid time-scale. If GLUT4 is continually recycling through the GSV compartment, it is very likely that the k_{ex} calculated by our two-compartment model is a composite of at least two exocytic rates. These are the rate of exocytosis from the endosomal recycling pathway and from the GSV compartment. Attempts to dissect out each of these constants by using a double exponential fit to our uptake data have been unsuccessful, perhaps due to the fact that the k_{ex} for GSV to plasma membrane trafficking only accounts for a very small proportion of the total cellular GLUT4 (~15%).

As described, the inhibitors wortmannin and Akti have enabled the determination of PI-3-kinase and PKB/Akt-dependent steps in insulin-mediated changes in GLUT4 trafficking. Interestingly, this study also revealed that basal GLUT4 trafficking is modified by these inhibitors. For example, incubation of the cells with Akti reduced the GLUT4 recycling pool in basal cells. This may have been due to the inhibition of the small amount of activated PKB/Akt in basal cells. However, wortmannin does not have this effect despite being a more potent inhibitor of PKB/Akt activation. In addition, there was a significant slowing of GLUT4 recycling in wortmannin treated cells and to a lesser extent in Akti treated cells. The reason for these changes in response to inhibitors requires further investigation.

Since GLUT4 exocytosis in basal cells is inhibited by wortmannin, a high intrinsic PI-3-kinase activity may form part of the explanation for the higher basal exocytosis rate constant for GLUT4 in L6 cells compared to 3T3-L1 adipocytes. Activation of PI-3-K has been implicated in enhancing GSV fusion with the plasma membrane (Bai et al., 2007; Koumanov et al., 2005). However, measured k_{ex} in the presence of wortmannin was still higher than the k_{ex} reported for GLUT4 in 3T3-L1 adipocytes (Govers et al., 2004; Karylowski et al., 2004; Martin et al., 2006; Muretta et al., 2008). The high basal k_{ex} in L6 myotubes may mask or prevent an increase in GLUT4 exocytosis in stimulated cells, or mask a difference between the effect of insulin-stimulation and AMPK-activation on this parameter. For example, if insulin-stimulation is able to

enhance k_{ex} but AMPK-activation is not, as has been described in skeletal muscle tissue (Karlsson et al., 2009), then this difference would not be observed in these cells. This may offer an explanation as to why all stimulation with all agonists results in such a rapid and similar increase in cell surface GLUT4 as measured by the transition state assay.

Compared to untreated basal cells, both wortmannin and Akti inhibited GLUT4 internalisation. Since the mechanism for signal-mediated inhibition of GLUT4 internalisation is less well defined than the mechanisms for modulating GSV exocytosis, the explanation for this observation is less obvious. In addition, the inhibition of GLUT4 internalisation by wortmannin and Akti appears to be incompatible with our findings that insulin-stimulation (and activation of the PI-3-K-PKB/Akt signalling pathway) inhibits GLUT4 internalisation. Therefore, the reduction in k_{in} following treatment with these inhibitors may be a result of a slower exocytosis of GLUT4. This explanation is analogous to the mass action hypothesis described above and is supported by the reduction in the rate of GLUT4 transport rates (R) in treated cells (Figure 4.13 *F*). Since the rate constant for GLUT4 exocytosis is reduced in wortmannin-treated cells, GLUT4 is delivered to the cell surface at a slower rate than in control cells. Akti does not inhibit the k_{ex} for GLUT4 to the same extent as wortmannin. However, Akti reduced the amount of GLUT4 recycling with the cell surface compared to control cells so that the rate of GLUT4 transport to the cell surface is also reduced in these cells. Consequently, in cells treated with wither wortmannin or Akti a lower k_{in} can maintain basal levels of GLUT4 at the cell surface.

The incomplete inhibition of PKB/Akt phosphorylation by Akti (Figure 4.12 *A* and Figure 4.13 *A*) correlates with the incomplete inhibition of insulin-stimulation GLUT4 translocation. However, incubation of myotubes with Akti resulted in a reduction in the amount of GLUT4 recycling in basal and insulin-stimulated cells to a level below basal control cells. This indicates that Akti was having a significant inhibitory effect. This could be explained by two possibilities. Firstly, Akti is inhibiting all PKB/Akt activity, and this is uncoupled from some residual phosphorylation. Another possibility is that a longer incubation with Akti is required for full inhibition of PKB/Akt activity as supported by the western blot data (Figure 4.13 *A*). However, the amount of GLUT4 at the cell surface in cell treated with insulin and Akti is stable out to at least 60 min (Figure 4.12 *C*). Therefore, it is unlikely that over this time period further inhibition of PKB/Akt is occurring. A more accurate determination of PKB/Akt inhibition by the Akti molecule used in this study using PKB/Akt activity assays may resolve this issue.

Wortmannin and Akti slightly inhibited GLUT4 translocation stimulated by AICAR and A-769662. This inhibition was very moderate compared to the inhibition of insulin-stimulated GLUT4 translocation by wortmannin and Akti as determined by the transition state data. This is expected given the distinct pathways activated by insulin and these AMPK-activators. The reason for the inhibition of increased cell surface GLUT4 levels in response to AICAR and A-769662 is different for wortmannin and Akti.

Wortmannin reduces the cell surface GLUT4 in basal cells. This small reduction matches the difference in cell surface GLUT4 between AICAR- and A-769662-stimulated control and wortmannin-treated cells. Therefore, the overall increase in cell surface GLUT4 is almost the same in control and wortmannin-treated cells. The data obtained from the transition state assay is similar to the plasma membrane GLUT4 levels obtained from the antibody uptake assay (Figure 4.13 *G*).

Akti reduces the amount of GLUT4 recycling in basal cells as explained above. Incubation with AICAR and A-769662 still enhances the size of the recycling pool by a similar 15-20% as observed in control cells. However, stimulated Akti-treated cells still have less GLUT4 recycling than in stimulated control cells. This reduction in the amount of GLUT4 explains the small inhibition on AICAR- and A-769662-mediated increase in cell surface GLUT4 observed in the transition state assay (Figure 4.12 *D*). The plasma membrane levels obtained from the uptake assay for AICAR-stimulated myotubes is similar to the transition state data. However, we calculated a more significant inhibition of A-769622-stimulated increase in cell surface GLUT4 by Akti from the uptake assay. The reason for the difference in cell surface GLUT4 levels obtained from these different assays is unclear.

Considerable evidence points to an important role for AMPK in contraction-induced glucose transport in muscle. However, the evidence for this is somewhat indirect being based on the observation that contraction leads to AMPK activation and the AMPK agonist AICAR stimulates glucose transport. A major problem with this logic is that AICAR is not specific for AMPK. Thus the development of more specific AMPK agonists such as that used here (A-769662) provides a more definitive method for examining AMPK-mediated changes in GLUT4 trafficking. Consistent with one recent study investigating glucose uptake in L6 cells (Guigas et al., 2009), A-769662 was found to stimulate GLUT4 translocation to the plasma membrane. This provides definitive evidence for a role for the AMPK pathway in this process. We selected doses of A-

769662 and AICAR that achieved a similar degree of AMPK activity as judged by ACC phosphorylation and found that at these doses A-769662 led to a more rapid half-time for transition from the basal to the stimulated steady-state than AICAR. It also resulted in a lower level of GLUT4 at the plasma membrane after 30 min of stimulation and a faster k_{in} value. Both AMPK activators targeted a similarly regulated and sized pool of GLUT4 into the recycling pathway. As such. the total amount of GLUT4 recycling under each stimulus was similar, and was non-additive when cells were stimulated with AICAR and A-769662. Therefore, the additional effect of AICAR in enhancing cell surface GLUT4 over A-769662 can be attributed to a greater inhibition of GLUT4 internalisation. This difference may highlight the lack of specificity of AICAR as an AMPK agonist. Nevertheless it is clear, assuming that A-769662 is a specific AMPK activator, that AMPK has a stimulatory effect on GLUT4 trafficking in myotubes.

4.15 Conclusions

Studies on a wide range of kinetic parameters for GLUT4 traffic in muscle are essential as stimulatory agonists have multiple effects. From our studies into the L6 cell line, muscle cells appear to have developed mechanisms for mobilisation of intracellular GLUT4 and for slowing GLUT4 internalisation. Through these mechanisms, muscle cells are able to respond to both hormonal signallng and metabolic changes. However, it is not clear whether L6 cells offer a realistic reflection of GLUT4 trafficking in muscle tissue. Our data contrasts to previously published data in L6 cells (Antonescu et al., 2008; Wijesekara et al., 2006). Furthermore, our studies have revealed a rapid exocytosis of GLUT4 and high level of basal recycling in basal L6 cells. The relatively small amount of GLUT4 sequestered in these cells compared to 3T3-L1 adipocytes raises the question as to whether L6 cells have a fully developed GSV compartment as would be present in muscle tissue *in vivo*. These points taken together suggest that L6 myotubes may not represent an exact replicate of muscle tissue *in vivo*. This is perhaps not surprising given that these cells do not have important architectural features of muscle such as transverse tubules.

Regardless, L6 myotubes offer a convenient cell model for investigating certain aspects of GLUT4 trafficking in response to a range of stimuli. L6 cells may represent an appropriate system for dissecting the mechanism of regulated GLUT4 endocytosis and studying the mechanism by which distinct signalling pathways differentially mobilise GLUT4. As such, it will be important to extend these trafficking studies to include other stimuli such as contraction, which can be mimicked by incubating L6 cells with K^+ ions. In addition, the incorporation of TIRF microscopy into these studies would allow the comparison of GSV trafficking in muscle cells, and in particularly the trafficking of GSVs in response to insulin-independent signalling pathways. Any findings from these studies could be integrated into more focussed investigations in skeletal muscle tissue to ascertain whether the mechanisms present in L6 cells are relevant to GLUT4 trafficking *in vivo*.

Recent studies suggest that most of the stimuli that increase glucose transport in muscle do so by converging upon a common signalling step involving Rab-GAP proteins (Kramer et al., 2007; Kramer et al., 2006a; Cartee and Wojtaszewski, 2007). An implication of this hypothesis is that once the common intermediate is targeted the changes in GLUT4 traffic that occur should be identical and non-additive for all the initiating stimuli. This has not previously been examined

in muscle. These studies in L6 muscle cells have revealed features of GLUT4 traffic that suggest some clear differences in the mechanism for regulating GLUT4 trafficking following PKB/Akt or AMPK activation. For example, insulin-stimulation and AMPK-activation appear to mobilise differentially regulated pools of GLUT4. Considering this difference, and other agonist-induced effects on GLUT4 trafficking that have been reported here, and in other studies, it seems unlikely that a single convergent step can account for the range of GLUT4 trafficking changes observed.

The diversity in end-point mechanisms for increasing cell surface GLUT4 has implications in the design of appropriate therapies for treatment of insulin-resistance. It may be possible to bypass a step in signal and traffic coupling that has become insulin resistant by activating an alternative stimulatory pathway.

5 Characterising TBC1D1 antibodies and investigating AMPK-induced phosphorylation of serine 231

The Rab-GAP proteins TBC1D4/AS160 and TBC1D1 have been identified as potential points of convergence for distinct signalling pathways leading to GLUT4 translocation. TBC1D4/AS160 has been more extensively studied and has been reported to be phosphorylated in response to insulin, contraction and AMPK activation. TBC1D1 has also been reported to be phosphorylated in response to these agonists. Although TBC1D4/AS160 contains several predicted and experimentally confirmed PKB/Akt phosphorylation motifs (Chen et al., 2008; Kane et al., 2002), it does not contain a predicted high-stringency AMPK phosphorylation motif. In contrast, TBC1D1 does contain such an AMPK motif at serine 237 (serine 231 in rat). We have studied the phosphorylation of serine 231 by AMPK using of an *in vitro* AMPK phosphorylation assay and novel TBC1D1 antibodies,

5.1 Mutation of serine 231 to alanine abolishes AMPK induced phosphorylation of TBC1D1 PTB domains *in vitro*

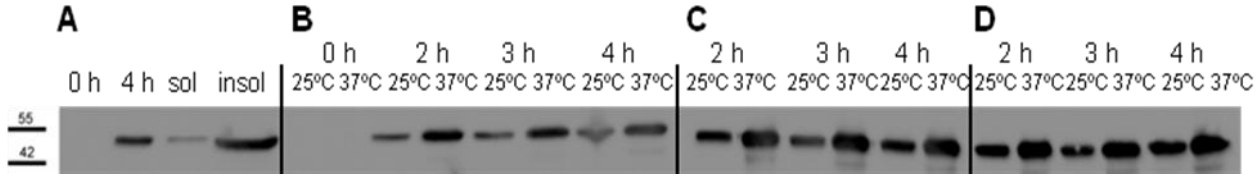

Figure 5.1. Expression of recombinant truncated TBC1D1 (PTB domains, amino acids 12-393). His-tagged truncated TBC1D1 was purified from the Rosetta-Gami *E.coli* strain in which recombinant TBC1D1 expression had been induced with 0.1 mM (*A* and *B*), 0.5 mM (*C*) and 1.0 mM (*D*) IPTG for different times (0, 2, 3 and 4 h) at either 25°C or 37°C. The solubility of recombinant truncated TBC1D1 was assessed after induction of expression with 0.1 mM IPTG for 4 h at 25°C (A). Expressed TBC1D1 was detected with an anti-His antibody.

Truncated TBC1D1 containing the PTB domains (amino acids 12-393) was cloned from a skeletal muscle cDNA library. The conditions for the expression and purification of recombinant His-tagged truncated TBC1D1 from Rosetta-Gami *E.coli* cells were optimised (Figure 5.1).

A series of degradation products were observed when truncated TBC1D1 was expressed at 37^{o}C and subsequently purified. This degradation was not observed or was present at a much lower level if protein expression was induced and carried out at 25^{o}C. Therefore, expression of TBC1D1 (PTB domains) was subsequently carried out at 25^{o}C. The majority of truncated TBC1D1 expressed using this expression system and protocol remains insoluble following a limited sonication protocol (8 x 15 sec at 20 microns) (Figure 5.1 *A*). In subsequent purifications of recombinant TBC1D1 an extended sonication protocol was used (16 x 15 sec at 20 microns). This resulted in a higher proportion of soluble protein without increasing the amount of degradation products purified (data not shown).

TBC1D1 contains a high-stringency predicted AMPK phosphorylation motif at serine 237 (serine 231 in rat) as determined by the web-based sequence scanning programmes Expasy-Prosite (*www.expasy.ch/prosite/*) and Scansite (www.*scansite.mit.edu/*). AMPK-mediated phosphorylation of this predicted site was experimentally tested using an *in vitro* AMPK assay to determine whether it is a *bone fide* AMPK phosphorylation site. Serine 231 was mutated to alanine by site directed mutagenesis. His-tagged recombinant wild-type (WT) and serine 231 to alanine (S231A) truncated TBC1D1 were incubated with rat liver AMPK in the presence of ^{32}P labelled ATP.

AMPK phosphorylated both WT and S231A mutant TBC1D1 proteins (Figure 5.2 *A* and *B*) in this *in vitro* kinase assay. There was no intrinsic incorporation of ^{32}P labelled ATP into the WT or S231A TBC1D1 proteins. Phosphorylation by AMPK of WT protein was 4.4–fold higher than in the S231A mutant protein ($p = 0.0015$) (Figure 5.2 *B*).

The presence of phosphorylation in the SA mutant could be attributed to a threonine rich motif at the C-terminus of the recombinant proteins (Figure 5.4). This sequence was presumably added during the cloning process. The non-specific phosphorylation of this motif by AMPK is confirmed by western blots using a phospho-specific TBC1D1 antibody (Figure 5.4).

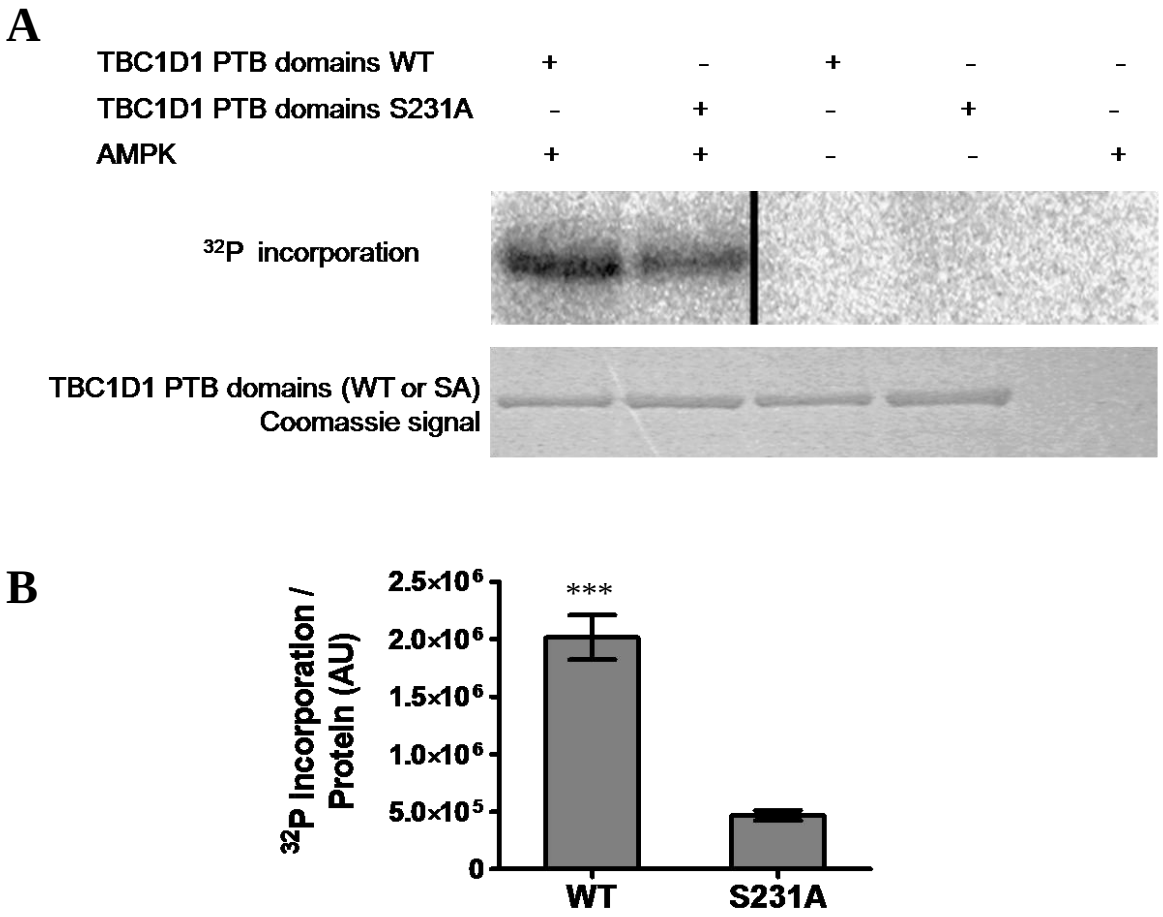

Figure 5.2. ***In vitro*** **phosphorylation of recombinant truncated TBC1D1 at serine 231. Recombinant TBC1D1 (WT and S231A) was incubated with rat liver AMPK in an** ***in vitro*** **kinase assay in the presence of radiolabelled ATP.** ***A*****, The incorporation of ^{32}P Into TBC1D1 was assessed by imaging of a phospho-imaging plate and the amount of truncated TBC1D1 (WT or S231A) present determined by coomassie staining. Lanes have been removed from the image where indicated.** ***B*****, The level of phosphorylation (^{32}P incorporation) of truncated TBC1D1 was quantified. Results are the mean and S.E.M. from 3 experiments. *** p= <0.0005 (unpaired t test).**

5.2 A novel TBC1D1 antibody is specific for TBC1D1 over TBC1D4/AS160

In order to more fully investigate serine 231 phosphorylation, antibodies were generated to recognise either TBC1D1 or TBC1D1 phosphorylated at serine 231. Three separate peptides were used to generate a TBC1D1-specific antibody. Three to four animals were used per peptide resulting in 10 terminal bleeds to test for specificity. An initial test of the antibodies generated to TBC1D1 was performed on over-expressed full-length Flag-tagged TBC1D1 and TBC1D4/AS160. The recognition of these proteins by each of the TBC1D1 antibody bleeds was determined by western blot (Figure 5.3).

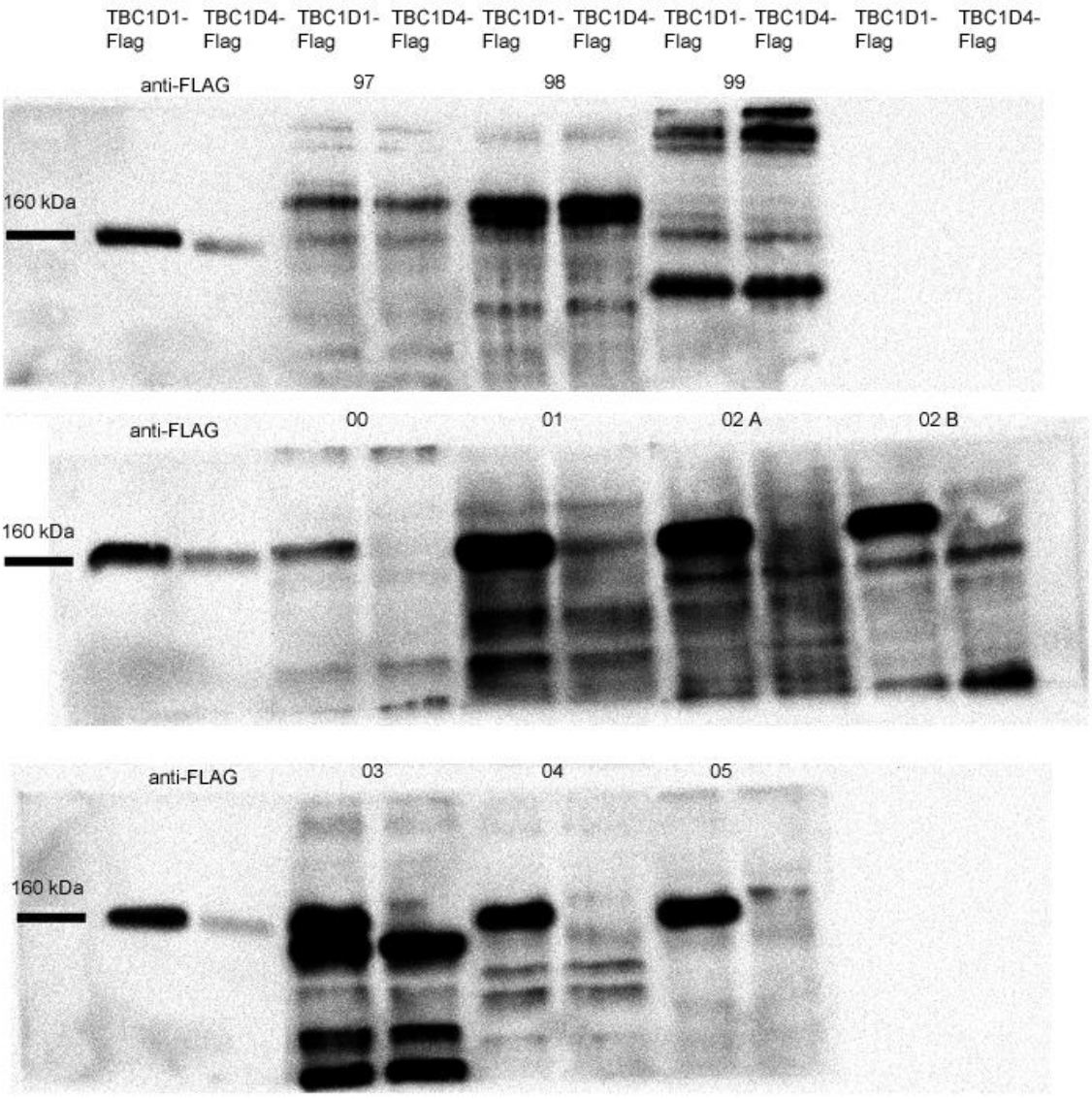

Figure 5.3. Selectivity of TBC1D1 antibodies. Whole cell lysates from HEK-293 cells expressing Flag-tagged TBC1D1 and Flag-tagged TBC1D4/AS160 were probed with 1ten different TBC1D1 antibodies generated from three peptides. Antibodies 97, 98 and 99 were raised towards the peptide (ID. 3001724) Glu-Pro-Asp-Leu-Arg-Lys-Ser-Gln-Pro-Trp, antibodies 00, 01, 02A and 02B were raised towards the peptide (ID. 3001725) Asp-Ser-Pro-Ser-Arg-Tyr-Glu-Asp-Tyr-Ser-Glu and antibodies 03, 04 and 05 were raised towards the peptide (ID. 3001726) Gln-Lys-Leu-Arg-Pro-Arg-Asn-Glu-Gln-Arg-Glu-Asn.

Flag-tagged TBC1D1 was expressed at a higher level than Flag-tagged TBC1D4/AS160. Despite this, it was possible to assess the selective binding of TBC1D1 antibody bleeds to TBC1D1 over TBC1D4/AS160. Both tagged TBC1D1 and TBC1D4 were detected at approximately 160 kDa by the anti-Flag antibody.

Antibodies 97, 98 and 99 exhibit no specificity in binding TBC1D1 over TBC1D4/AS160. These antibodies also strongly bind to other proteins present in the HEK-293 whole-cell lysates, further confirming the lack of specificity of these antibodies. In contrast, the remaining antibody bleeds preferentially recognise TBC1D1 over TBC1D4/AS160, even taking into account the difference in expression levels of the two Rab-GAP proteins. In particular, antibodies 00, 04 and 05 strongly recognise TBC1D1, without recognising TBC1D4/AS160 and without significantly binding to other proteins in the HEK-293 cell lysate. Antibodies 01, 02A, 02B and 03 specifically recognise TBC1D1 (over TBC1D4/AS160), but also recognise a number of other proteins in the HEK-293 cell lysate.

5.3 A novel phospho-specific TBC1D1 antibody recognises TBC1D1 phosphorylated at serine 231 by AMPK

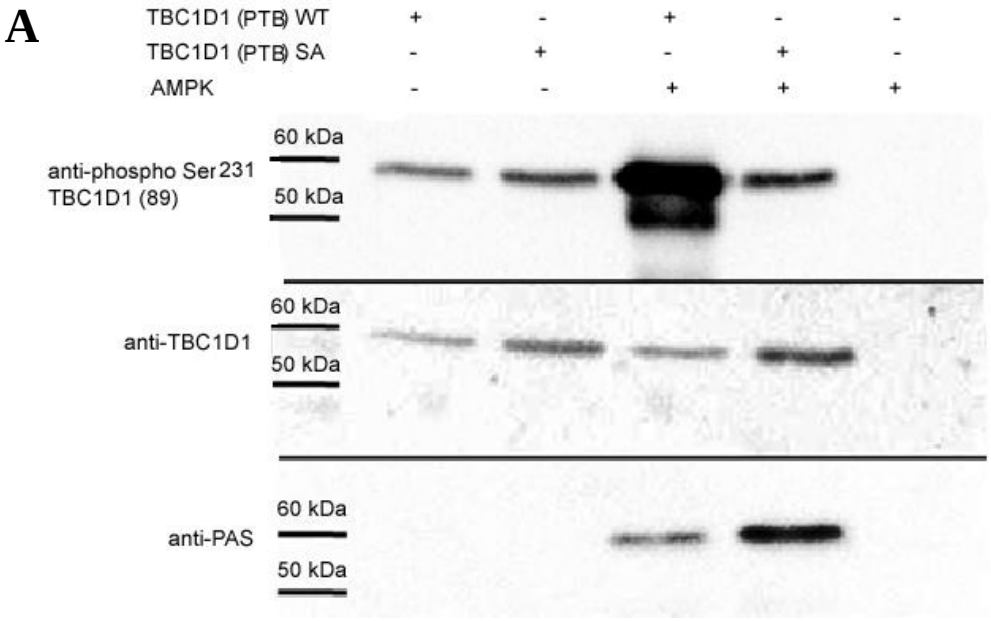

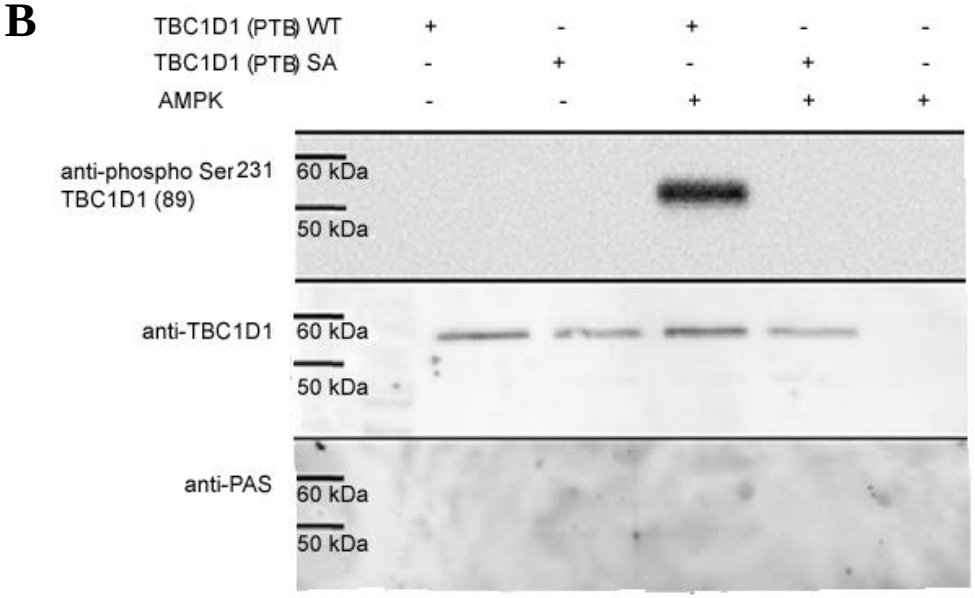

Figure 5.4. Recognition of phosphorylated truncated TBC1D1 by a phospho-specific TBC1D1 antibody (phospho-serine 231). An *in vitro* AMPK kinase assay was performed with both WT and S231A truncated TBC1D1 (spanning PTB domains, amino acids 12-393). The phosphorylation of TBC1D1 proteins was detected by an antibody specific to TBC1D1 phosphorylated at serine 231. Truncated TBC1D1 was detected with an anti-TBC1D1 antibody (antibody 97). In addition, the immuno-reactivity of the PAS antibody with phosphorylated serine 231 was determined (lower panels). This assay was performed with two versions of the TBC1D1 truncated protein. *A*, Recombinant TBC1D1 containing an additional C-terminal sequence containing a poly-threonine sequence added during the cloning process. B, Recombinant TBC1D1 protein without the additional C-terminal sequence.

Of the peptides chosen for the generation of antibodies to TBC1D1, only one peptide (ID. 3001724), corresponding to bleeds 97, 98 and 99 fell within the 12-393 amino acids of the truncated TBC1D1. The other peptides used for TBC1D1 antibody generation were outside of this region and therefore would not be expected to recognise the recombinant protein. As such, antibody 97 was used to detect the recombinant truncated TBC1D1 protein (WT and S231A) (Figure 5.4 *middle panel*s).

A peptide corresponding to the region surrounding serine 231 (Pro-Met-Arg-Lys-Ser-Phe-Ser(phospho)-Gln-Pro-Gly-Leu-Arg-Ser) was used to generate antibodies that recognise TBC1D1 phosphorylated at serine 231. Three separate antibodies were generated, and further purified on a peptide column to deplete any antibody species that recognise non-phosphorylated peptides.

The specificity of these purified bleeds was determined by western blot. Recombinant TBC1D1 PTB domains (WT and S231A) were phosphorylated *in vitro* by purified AMPK. Detection of phosphorylated TBC1D1 following this *in vitro* kinase assay was performed using a serine 231 phospho-specific antibody (bleed 89 in Figure 5.4). The same results were obtained using the other phospho-specific antibodies (90 and 91) (data not shown). The initial characterisation of the phospho-specific antibodies was performed using recombinant truncated TBC1D1 (WT and SA) with an aberrant C-terminal sequence containing multiple threonine residues (Figure 5.4 *A*). The TBC1D1 phospho-specific antibody recognised both WT and SA TBC1D1 not incubated with AMPK. Therefore, this antibody recognised TBC1D1 not phosphorylated at serine 231. However, the phospho-specific antibody had a higher reactivity with WT TBC1D1 protein phosphorylated by AMPK in this assay. In addition, mutation of serine 231 to alanine abolished the increase

phospho-specific antibody reactivity with TBC1D1 following incubation with AMPK. This implies that the phospho-specific antibody does recognise TBC1D1 phosphorylated at serine 231. In addition, incubation of both the WT and S231A TBC1D1 protein with AMPK increased reactivity with the PAS antibody (Figure 5.4 *A*).

This experiment was repeated following the removal of the C-terminal threonine-rich sequence in order to determine whether the reactivity with the PAS antibody was due to a non-specific interaction with phosphorylated residues in the C-terminal sequence. The results obtained from this experiment contrasted with previous results (Figure 5.4 *B*). The removal of this sequence resulted in a complete loss of PAS-antibody binding to this truncated TBC1D1 protein. In addition, the phospho-specific antibody only recognises the WT TBC1D1 phosphorylated at serine 231 following incubation with AMPK.

Following characterisation of the specificity of phospho-specific antibodies to phosphorylated TBC1D1, the phosphorylation status of endogenous TBC1D1 at serine 231 was examined in L6 myotubes (Figure 5.5). Activation of AMPK by AICAR, A-769662 and phenformin increased phosphorylation of TBC1D1 at serine 231. The phosho-TBC1D1 (89) antibody recognised a doublet at approximately 160 kDa. This does not exactly correspond to the size of the TBC1D1 band detected in L6 myotubes. Although the anti-TBC1D1 antibody (04) appeared to detect a specific band, this is at a slightly lower molecular weight than the phospho-TBC1D1 that was detected. The activation of AMPK by these stimuli was confirmed by monitoring phosphorylation of AMPKs downstream substrate ACC. Only stimulation with insulin resulted in activation of PKB/Akt, as determined by phosphorylation of PKB/Akt at serine 473. This activation did not coincide with increased phosphorylation of TBC1D1 at serine 231.

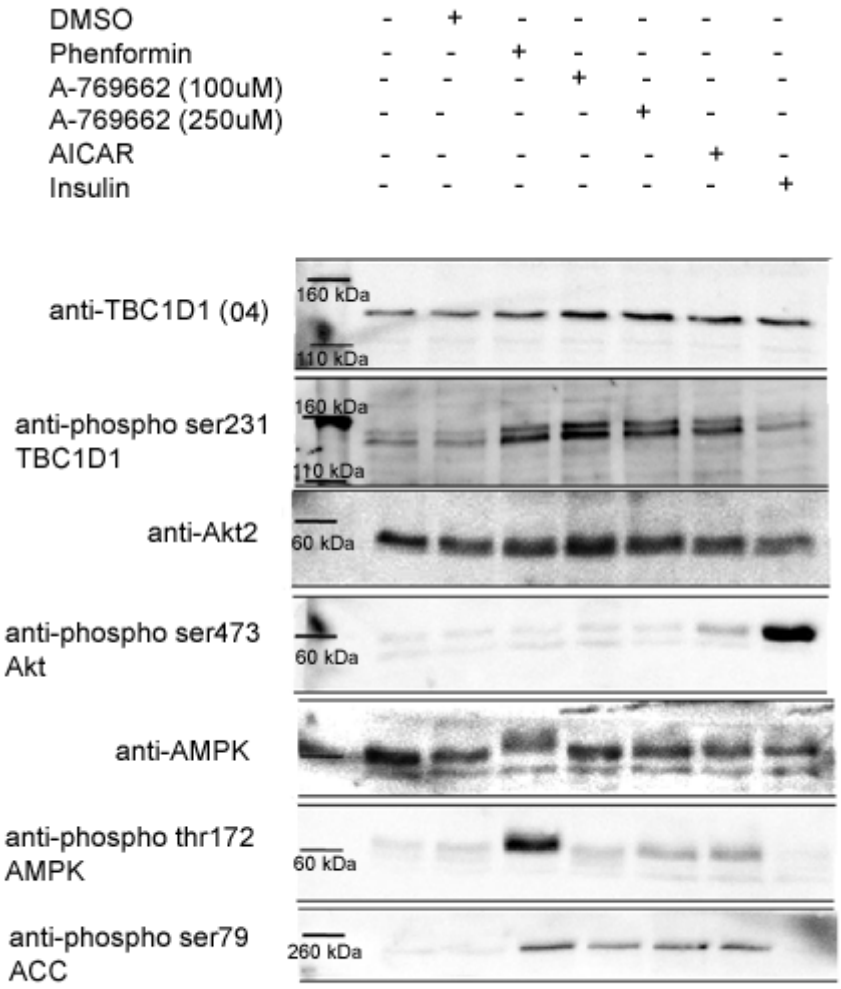

Figure 5.5. Phosphorylation of serine 231 of TBC1D1 following AMPK activation in L6 myotubes. Cells were serum-starved for 16 hrs and maintained in the basal state or incubated for 30 min with 2 mM phenformin, 100 µM or 250 µM A-769662, 2 mM AICAR or 200 nM insulin. A DMSO control was conducted at the same concentration of DMSO was as present for the addition of 250 µM A-769662. The phosphorylation of TBC1D1 at serine 231 was detected with an antibody specific to TBC1D1 phosphorylated at this site. Total TBC1D1 within lysates was detected with an anti-TBC1D1 antibody. PKB/Akt activation was determined by blotting for phospho-serine 473. PKBβ/Akt2 levels were determined from the same solubilised cell lysates (bottom panels). AMPK activation was determined by blotting for phospho-threonine 172 and phospho-serine 79 of ACC. Total AMPK levels were determined from the same solubilised cell lysates.

5.4 Discussion

TBC1D1 and the closely related Rab-GAP TBC1D1/AS160 have been implicated in regulating GLUT4 translocation in response to a range of stimuli in muscle. These include insulin, contraction and AMPK activation (Funai and Cartee, 2009; Kramer et al., 2006a; Taylor et al., 2008; Roach et al., 2007; Peck et al., 2009).

The studies described here outline the preliminary characterisation of antibodies raised to detect TBC1D1. We have generated and characterised antibodies that specifically recognise TBC1D1 without also detecting TBC1D4/AS160. Using these antibodies, endogenous TBC1D1 can be detected in L6 myotubes. However, the specific band detected by the antibodies raised to the peptide Gln-Lys-Leu-Arg-Pro-Arg-Asn-Glu-Gln-Arg-Glu-Asn (amino acids 428-439 of TBC1D1) is at a slightly lower molecular weight than would be expected for TBC1D1 (Figure 5.5). In addition, this band is at a lower molecular weight than phosphorylated TBC1D1 detected by the phospho-specific antibody. It will be important to confirm that these antibodies are specifically recognising TBC1D1 using immunoprecipitation protocols.

The use of antibodies to detect specific phosphorylation sites on TBC1D1 are vital in trying to ascertain the involvement of different phosphorylation sites in signalling leading to GLUT4 translocation. We have confirmed the AMPK-mediated phosphorylation of TBC1D1 at serine 231 (237 in humans) using an *in vitro* kinase assay. To perform this assay, a WT and S231A truncated version of recombinant TBC1D1 was cloned, expressed and purified. Mutation of serine 231 to alanine significantly reduced AMPK-induced phosphorylation of a truncated version of recombinant TBC1D1 (amino acids 12-393). The identification of serine 231 as a *bone fide* AMPK phosphorylation site supports data generated from mass spectrometry studies (Peck et al., 2009; Chen et al., 2008; Taylor et al., 2008).

The initial characterisation of antibodies which specifically recognise TBC1D1 phosphorylated at serine 231 was hampered by the presence of a threonine-rich C-terminal threonine-rich sequence in the recombinant TBC1D1 used in the *in vitro* kinase assay. This sequence was accidently added to the C-terminus of truncated TBC1D1 using the cloning procedure. The presence of this sequence resulted in detection of the non-phosphorylated recombinant TBC1D1 by the phospho-specific antibody. Furthermore, the WT and S231A mutant

TBC1D1 were detected by the PAS antibody following phosphorylation of these proteins by AMPK.

Removal of this C-terminal sequence caused a loss of all phospho-TBC1D1-specific antibody binding except the binding to wild-type TBC1D1 phosphorylated by AMPK. Therefore, this phospho-specific antibody specifically recognised TBC1D1 when phosphorylated at serine 231. Interestingly, the immuno-reactivity of WT and S231A truncated TBC1D1 with the anti-PAS antibody was completely abolished in proteins without the threonine rich C-terminal sequence. This supports a recent study that phosphorylation of TBC1D1 by AMPK at serine 231 does not correlate with immuno-reactivity with the PAS antibody (Pehmoller et al., 2009; Chen et al., 2008). In addition, the small amount AMPK-mediated ^{32}P incorporation into S231A TBC1D1 during the *in vitro* kinase assay can likely be attributed to this C-terminal threonine rich sequence.

Phosphorylation of TBC1D1 in response to AMPK activation occurs in L6 myotubes. The AMPK-activators A-769662 and AICAR have been reported to enhance glucose uptake. This therefore provides a correlative link between TBC1D1 phosphorylation at serine 231 and GLUT4 translocation (Guigas et al., 2009; Jorgensen et al., 2009). It will be important to determine whether there is a causal link between TBC1D1 phosphorylation at serine 231 and glucose uptake.

Given the high stringency of the AMPK consensus site surrounding serine 231, it may be that the anti-phospho-TBC1D1 specific antibody will recognise other phosphorylated AMPK substrates. As such, it would be desirable to perform an immunoprecipitation of TBC1D1 prior to blotting with the phospho-specific antibody to ensure that the band at 160 kDa is a phosphorylated form of TBC1D1.

5.5 Conclusions

Despite the large number of studies conducted into the role of TBC1D4/AS160 and TBC1D1 it is as yet unclear what role the phosphorylation of these Rab-GAPs plays in GLUT4 trafficking. The development of TBC1D1 antibodies, specifically phospho-specific antibodies, will be important tools in investigating the role for TBC1D1 in regulating GLUT4 translocation. In particular, it will be important to move away from using the anti-PAS antibody to probe the phosphorylation status of TBC1D4/AS160 and TBC1D1 and to use a more directed approach. By using antibodies directed toward specific phosphorylation sites, it will be possible to dissect the requirement for TBC1D1 phosphorylation at distinct sites in insulin-, contraction- or AMPK-stimulated GLUT4 translocation. Given the large number of phosphorylation sites that have been identified in both TBC1D4/AS160 and TBC1D1, it is likely that there is a complex regulation of these proteins (Taylor et al., 2008; Peck et al., 2009; Kane et al., 2002; Chen et al., 2008). Furthermore, there is significant variation in TBC1D1 and TBC1D4/AS160 expression in different muscle fibre-types (Taylor et al., 2008). It remains to be determined to what extent each Rab-GAP is involved in insulin and contraction-mediated GLUT4 translocation.

6 Overall Discussion

Significant progress has been made in unravelling how insulin signalling modulates GLUT4 trafficking to invoke its translocation in adipocytes. GLUT4 trafficking has been less studied in muscle because of the technical challenges associated with isolating muscle strips and carrying out subfractionation protocols in this tissue. The investigations detailed in this thesis have taken advantage of epitope-tagged GLUT4 constructs to interrogate GLUT4 trafficking in muscle cells and have revealed features of GLUT4 trafficking in muscle that are altered following insulin-stimulation or following the activation of other signalling pathways which bring about GLUT4 translocation in muscle. Activation of the insulin and AMPK signalling pathways in L6 cells resulted in a similar inhibition of GLUT4 internalisation. In contrast, the other trafficking parameters that have been studied were differently modified by these signalling cascades. This included enhanced GSV fusion at the sarcolemma of cardiomyocytes in response to insulin- and contraction-simulation, but not AMPK-activation, and additive mobilisation GLUT4 from GSVs following insulin-stimulation and AMPK-activation in L6 cells. These distinct effects on GLUT4 trafficking indicates that insulin and AMPK activators stimulate non-convergent signalling pathways.

Insulin-stimulation and AMPK-activation additively mobilise GLUT4 in L6 myotubes. Therefore, it appears that these stimuli target separate pools of GLUT4. These mobilised pools could be physically distinct and/or differentially regulated. We observed no difference in the overall trafficking route of GLUT4 labelled with antibody at the sarcolemma in cardiomyocytes returning to a basal state following the stimulation of GLUT4 translocation by insulin, contraction and AMPK-activation. Although not definitive evidence, these data imply that these stimuli mobilise GLUT4 from a similar intracellular location. However, the experiments performed here did not have sufficient resolution to ascertain whether the intimate details of these trafficking routes were identical.

The specificity of targeting distinct GLUT4 pools by insulin and AMPK signalling may be conferred by the Rab-GAPs TBC1D4/AS160 and TBC1D1. Several studies have identified that TBC1D4/AS160 is primarily phosphorylated by the insulin stimulated kinase PKB/Akt (Sano et al., 2003; Chen et al., 2008; Geraghty et al., 2007). PKB/Akt-mediated phosphorylation of TBC1D4/AS160 is thought to release GLUT4 from sequestration by inactivating TBC1D4/AS160 GAP activity. Although TBC1D1 GAP activity is proposed to be similarly controlled by

phosphorylation, the presence of multiple AMPK phosphorylation sites implies that it is predominantly an AMPK substrate. Experimental data presented in this thesis have confirmed serine 237 (serine 231 in rat) as a *bone fide* AMPK phosphorylation site and that this site is phosphorylated in L6 cells following exposure to AMPK activators. This data is supported by data presented in other studies (Peck et al., 2009; Pehmoller et al., 2009; Taylor et al., 2008; Roach et al., 2007; Chen et al., 2008). In addition, mass spectrometry has identified other AMPK phosphorylation sites in TBC1D1. Although PKB/Akt can also phosphorylate TBC1D1 at threonine 596, phosphorylation at this site may be insufficient to inactivate TBC1D1 GAP activity. For example, phosphorylation of threonine 596 is insufficient to induce 14-3-3 binding (Pehmoller et al., 2009; Chen et al., 2008). Similarly, AMPK activation does not induce 14-3-3 binding in TBC1D4/AS160 (Chen et al., 2008). Therefore, GSVs retained through the Rab-GAP activity of TBC1D1 may not be mobilised following insulin-stimulation. In contrast, AMPK phosphorylated TBC1D1 binds to 14-3-3 and inhibition of TBC1D1 GAP-activity mobilises GSVs regulated by this Rab-GAP.

It may be that insulin-induced activation of PKB/Akt results in the phosphorylation of TBC1D4/AS160 and release of GSVs associated with this Rab-GAP. However, there is a proportion of GLUT4 that is retained through the action of TBC1D1. The additive release of GLUT4 from sequestration can therefore be explained by the release of both TBC1D4/AS160- and TBC1D1-regulated GSVs following insulin-stimulation and AMPK-activation. The hypothesis that insulin-stimulation and AMPK-activation mobilise distinct pools of GLUT4 by targeting different Rab-GAP proteins is inconsistent with the proposal that TBC1D4/AS160 and TBC1D1 act as points of convergence between the insulin- and AMPK-signalling pathways. Detailed studies into the phosphorylation status of TBC1D4/AS160 and TBC1D1 in the L6 cell line will be required to further investigate this hypothesis.

In different muscle fibres the amount of GLUT4 partitioned into TBC1D4/AS160- and TBC1D1-regulated compartments likely depends on the relative expression level of each Rab-GAP. The expression of TBC1D4/AS160 and TBC1D1 has been reported to be muscle-type and fibre-type specific. These differences in Rab-GAP expression levels in muscle subtypes may represent the difference in metabolic demands of these fibres. For example, glycolytic fibres, which have a high level of TBC1D1 expression, may fatigue more rapidly in response to contraction than oxidative fibres and therefore require a Rab-GAP more sensitive to changes in the cellular energy levels.

In furthering our studies into GLUT4 trafficking kinetics, it will of interest to investigate the role for Ca^{2+}/calmodulin in the regulation of TBC1D4/AS160 and TBC1D1 activity during muscle contraction. Both TBC1D4/AS160 and TBC1D1 contain a calmodulin-binding domain (CBD) (Kane and Lienhard, 2005; Kramer et al., 2007; Roach et al., 2007). This interaction domain may provide a mechanism by which both oxidative (highly express TBC1D4/AS160) and glycolytic (highly express TBC1D1) fibres increase glucose uptake in response to contraction (Taylor et al., 2008). Therefore, we would expect a contraction stimulus (or appropriate mimic) to mobilise a similar amount of GLUT4 in L6 cells as observed following stimulation with insulin plus an AMPK-activator. In addition, by crossing a GLUT4 reporter transgenic mouse, such as described here, with the TBC1D1 mutant mice previously described (Chadt et al., 2008), it may be possible to ascertain the extent to which GLUT4 trafficking in different muscle types is controlled by this Rab-GAP *in vivo*.

It has been reported that the amount of fatty acid transporters (e.g. CD36) at the cell surface of cardiomyocytes is enhanced following activation of AMPK (Habets et al., 2009; van Oort et al., 2009). This raises the question as to whether the trafficking of these transporters is regulated in a manner analogous GLUT4. The co-trafficking of glucose and fatty acid transporters to the cell surface would be an appropriate response to a change in the cellular energy status. In this way, AMPK-mediated phosphorylation and inactivation of TBC1D1 could enhance the transport of both glucose and fatty acids into the cell. These substrates could then be metabolised to generate ATP. The hypothesis that TBC1D1 regulates the trafficking of both GLUT4 and fatty acid transporters requires further investigation.

GLUT4 translocation was stimulated by insulin and AMPK-activation to a similar extent in isolated cardiomyocytes and the L6 cell line. The increase in cell surface GLUT4 compared to basal cells was larger in the cardiomyocyte cell model. This was most likely due to the lower amount of GLUT4 at the external membrane in basal cardiomyocytes than observed in basal L6 myotubes. The higher levels in cell surface GLUT4 of unstimulated L6 cells may be due to the large proportion of GLUT4 that recycles with the cell surface under basal conditions. Although not explicitly studied in the cardiomyocyte model, the very low level of anti-HA antibody uptake over a 15 min time period in basal cardiomyocytes in experiments investigating GLUT4 trafficking in cells returning to a basal state indicates that GLUT4 is effectively retained at intracellular sites in basal cardiomyocytes. Since the whole anti-HA antibody was used in this study this conclusion is specific to the retention of GLUT4 from the sarcolemma membrane. Therefore, the high level

of GLUT4 recycling in basal L6 myotubes probably does not represent the recycling of GLUT4 to the sarcolemma in muscle *in vivo*. L6 myotubes may have a limited GSV compartment or lack a retention mechanism present in fully differentiated muscle.

In addition to the changes in the amount of GLUT4 recycling, our studies in cardiomyocytes and L6 cells have identified other changes in GLUT4 trafficking parameters in response to insulin-stimulation, contraction-stimulation and AMPK-activation. Given the putative role for TBC1D4/AS160 and TBC1D1 in mediating GSV retention, it is likely that these additional effects on trafficking are independent of these Rab-GAPs (Deshmukh et al., 2009). We observed a difference in the effect of insulin-stimulation on the exocytosis of GLUT4 between these cell types. By comparing the anti-HA and GFP signals, it was possible to identify that insulin- and contraction- stimulation enhanced GSV fusion at the sarcolemma. However, insulin-stimulation did not significantly enhance the steady-state rate constant for GLUT4 exocytosis in L6 cells. As discussed, there was a trend towards an increase in k_{ex} following insulin-stimulation in L6 cells. Potential reasons that an insulin effect might not be observed in the L6 myotubes model include the high level of basal recycling, the fact that only a small proportion of cellular GLUT4 is localised to GSVs and a high intrinsic PI-3-K activity. Therefore, it is likely that insulin signalling enhances GLUT4 exocytosis or GSV fusion with the sarcolemma in muscle *in vivo* as reported in other studies (Karlsson et al., 2009; Yang and Holman, 2006; Yang and Holman, 2005; Wijesekara et al., 2006).

There was a similarity in the features of trafficking of GLUT4 to the transverse tubule membrane in cardiomyocytes in response to insulin-, contraction- and hypoxia-stimulation. The reason for this may be that these stimuli are unable to enhance GSV fusion at this site, and that GLUT4 translocation to this membrane is primarily mediated by an inhibition of GLUT4 endocytosis. This hypothesis is consistent with the kinetic data obtained from insulin-, AICAR- and A-769662-stimulated L6 cells. Therefore, it may be that the plasma membrane of the L6 cells used for this study more closely mimics the transverse tubule membrane of fully differentiated muscle. We observe different GLUT4 trafficking kinetics in basal and stimulated L6 myotubes to those reported by Klip's laboratory (Wijesekara et al., 2006; Randhawa et al., 2008; Antonescu et al., 2008). The reason for this discrepancy may be that the L6 cell clones used in these studies exhibit GLUT4 trafficking behaviours specific to the different limiting membranes in muscle tissue *in vivo*.

Insulin-stimulation maintains enhanced levels of cell surface GLUT4 by inhibiting GLUT4 endocytosis in L6 cells. However, whether insulin has a similar effect in adipocytes is controversial (Jhun et al., 1992; Yang and Holman, 1993; Yang and Holman, 2005; Govers et al., 2004; Blot and McGraw, 2006; Karylowski et al., 2004; Muretta et al., 2008). This controversy likely stems from the difficulty in directly measuring GLUT4 internalisation and from the different cell models used in investigations. It has been reported that the endocytosis of GLUT4 is accelerated in insulin-resistant primary adipocytes compared to control cells. In these insulin-resistant cells, the AMPK activator metformin inhibits GLUT4 internalisation (Pryor et al., 2000). In contrast, metformin is unable to inhibit GLUT4 internalisation in control cells. This implies that enhanced GLUT4 endocytosis is a feature of compromised systems, such as insulin-resistant adipocytes. Under these conditions, an AMPK activator can reduce the internalisation of GLUT4 and thereby increase cell surface GLUT4 levels. This is therapeutically intriguing since metformin is partly overcoming the defect in GLUT4 internalisation in insulin-resistant cells. However, these data may also provide an explanation as to why some studies have identified an insulin effect on GLUT4 internalisation. If the cell model being used is compromised in any way, for example due to the technicalities of the methods used or during the production of an immortalised cell culture line, then GLUT4 internalisation may be accelerated. Under these specific conditions, insulin may signal to slow GLUT4 endocytosis. This effect would not have been measured had GLUT4 internalisation not been modulated. This hypothesis would require that GLUT4 internalisation under basal conditions *in vivo* is slow and therefore is not a point at which signalling pathways can impinge upon GLUT4 trafficking. Although this hypothesis may explain the inconsistencies between studies into GLUT4 trafficking in adipocytes, it may not apply to muscle tissue because a number of studies have identified GLUT4 endocytosis as a site at which signalling pathways can modulate GLUT4 trafficking in muscle cells (Yang and Holman, 2006; Yang and Holman, 2005; Karlsson et al., 2009; Antonescu et al., 2008; Wijesekara et al., 2006).

The kinetic data presented in this thesis were obtained from the L6 cell line. As discussed, these cells are unlikely to be completely representative of skeletal muscle *in vivo*. Nevertheless, the data obtained from these studies indicate that this cell model is of use to investigate certain aspects if GLUT4 trafficking in muscle. These include the regulation of GLUT4 endocytosis and mobilisation of GLUT4 from differentially regulated GSVs by distinct signalling pathways. However, in order to fully understand GLUT4 trafficking and how this is modulated in response to stimuli that invoke GLUT4 translocation in muscle it will be necessary to perform

similar kinetic analyses *in vivo*, or in a model system that more closely resembles skeletal muscle cells *in vivo*. Primary cardiomyocytes isolated from the HA-GLUT4-GFP transgenic mouse line represent one such cell model, but these cells were not considered for this analysis due to technical difficulties. Although glucose uptake and GLUT4 translocation into cardiomyocytes is of interest in itself, these isolated cardiomyocytes again are a representative model system for studying GLUT4 trafficking in skeletal muscle. Therefore, any findings in these cells would only permit tentative conclusions to be made on GLUT4 trafficking in skeletal muscle *in vivo*.

One problem associated with monitoring GLUT4 trafficking in fully differentiated muscle fibres through the uptake of an extracellular label, such as an anti-HA antibody or photolabel, is that these reagents may have limited accessibility to GLUT4 present in the transverse tubule membrane. This is due to the spatial restriction within these tubules. In our studies into GLUT4 trafficking in cardiomyocytes, we observed that GLUT4 in the transverse tubule membrane of cardiomyocytes is not labelled with whole anti-HA antibody. Therefore, for studying the trafficking kinetics of HA-epitope tagged GLUT4 to both the sarcolemma and the transverse tubules it would be necessary to use an anti-HA Fab fragment. However, it is still likely that Fab fragments will have differential access to HA-epitope exposed at the sarcolemma and transverse tubule membranes. The differential access of whole anti-HA antibody and anti-HA Fab fragments may be of use in order to separately measure the kinetics of GLUT4 trafficking to the sarcolemma and transverse tubule membrane.

The methods described in this thesis to interrogate GLUT4 trafficking in cardiomyocytes and L6 cells offer an advantage over the method described by Lauritzen *et al.* for tracking GLUT4-GFP trafficking *in vivo* (Lauritzen et al., 2002) as we can distinguish between GLUT4 in close proximity to the external membrane and GLUT4 within the external membrane. Furthermore, exofacial epitopes can be labelled to determine whether agonists enhance the GLUT4 recycling pool. This is specifically relevant when investigating the mobilisation of GLUT4 in muscle cells. By monitoring GLUT4-GFP it is difficult to determine whether GLUT4 at the cell surface in stimulated cells is part of a constitutively recycling pool of GLUT4 or was mobilised from a GSV compartment. The release of GLUT4 from sequestration likely represents an important site of agonist action. In addition, it may be that different muscle fibres have more or less GLUT4 partitioned into TBC1D4/AS160- or TBC1D1-regulated GSVs. Therefore, investigating the mobilisation of GLUT4 in different fibre types will allow a comparison between Rab-GAP expression levels and the release of GLUT4 from GSVs in response to the activation of distinct

signalling pathways. The development of a combined approach where GLUT4 trafficking, GSV fusion and GLUT4 mobilisation can be monitored and quantified *in vivo* would significantly advance our understanding of GLUT4 trafficking in muscle.

By studying changes in GLUT4 trafficking it has been possible to determine the point at which different agonists impinge upon GLUT4 trafficking. However, these studies could be furthered by investigating the molecular mechanisms by which these effects on trafficking are mediated. For example, by performing the kinetic assays in cells expressing GLUT4 with mutated targeting motifs (FQQI / LL / TELEY) may reveal whether these motifs are important for the inhibition of GLUT4 endocytosis in stimulated L6 cells (Blot and McGraw, 2008; Shewan et al., 2003; Bernhardt et al., 2009). Furthermore, by using similar methods to those described by Antonescu *et al.* and Blot *et al.* such as the use of inhibitors of endocytosis (e.g. β-cyclodextrin, nystatin, dynamin inhibitors), it may be possible to identify the mechanism by which GLUT4 is internalised in basal and stimulated cells (Antonescu et al., 2008; Blot and McGraw, 2006). Even with these additional studies, the downstream effectors of signalling pathways that mediate these changes may not have been revealed. This is of particular interest in L6 cells since the rate constant for GLUT4 internalisation was not additively reduced in cells stimulated with both insulin and an AMPK activator. Therefore, these signalling pathways may affect GLUT4 endocytosis via a similar mechanism in this cell model, for example by targeting the same downstream effector. Trying to identify these downstream effectors will be an important next step in these studies.

The additivity between insulin-stimulation and AMPK-activation in enhancing cell surface GLUT4 levels in L6 myotubes supports previous findings that these stimuli additively enhance glucose transport into muscle (Hayashi et al., 1998; Bergeron et al., 1999). This additivity can be explained by our findings that, with the exception of their effect on GLUT4 internalisation in L6 myotubes, the insulin and AMPK signalling pathways have distinct effects on GLUT4 trafficking parameters. This includes differential modulation of GLUT4 exocytosis in cardiomyocytes and mobilisation of GLUT4 in L6 myotubes. These data indicate that the signalling pathways activated following incubation with insulin or an AMPK-activator are primarily non-convergent; the AMPK-signalling pathway does not target the same downstream effectors as the insulin-signalling pathway. This may explain how activation of AMPK is still able to enhance glucose uptake in insulin-resistant cells in which the insulin-signalling pathway is compromised.

Activation of AMPK by hypoxia, AICAR and A-769662 enhanced cell surface GLUT4 in cardiomyocytes and L6 myotubes. The data obtained from these different activation methods and cell models support a model whereby AMPK enhances and maintains enhanced levels of cell surface GLUT4 by increasing the size of the GLUT4 recycling pool and by inhibiting GLUT4 internalisation. This role for AMPK in modulating GLUT4 endocytosis is supported by data from earlier studies (Yang and Holman, 2005; Karlsson et al., 2009). Hypoxia and AICAR are indirect activators of AMPK. Therefore, these stimuli are likely to have off-target effects. The use of a more direct and specific AMPK activator, A-769662, allows more definitive conclusions to be drawn on the involvement of AMPK in modulating GLUT4 trafficking. Furthermore, A-769662 specifically activates AMPK trimers containing the β1 subunit (Scott et al., 2008), implicating this subunit in the regulation of GLUT4 translocation in L6 myotubes. Since distinct isoforms of the three AMPK subunits are more highly expressed in different tissues and different muscle fibre-types (Treebak et al., 2009a), the identification and use of activators that target specific isoforms of AMPK in future experiments may permit the identification of an isoform-specific effect on GLUT4 trafficking.

Understanding how AMPK-activation modulates GLUT4 trafficking and furthering these studies to identify the downstream effectors of this signalling pathway is of therapeutic value given that there is hope for the use of novel AMPK activators to treat metabolic disorders such as type 2 diabetes. In addition to stimulating glucose transport in muscle, a further advantage of targeting AMPK is that this kinase is also able to activate glucose metabolism (Marsin et al., 2000). However, AMPK-activators may cause side effects. For example, increased glycolytic flux may result in increased cellular reactive oxygen species. Furthermore, systemic AMPK activation may negatively impact cardiac tissue as mutations in the AMPKγ2 subunit have been identified in a small percentage of patients with Wolff-Parkinson-White syndrome (Arad et al., 2007). This syndrome is manifested mainly as a cardiac conduction system defect. The work presented in this thesis supports the targeting of AMPK for enhancing glucose uptake in muscle cells in type 2 diabetic patients. As discussed above, such therapies may specifically or more potently enhance glucose transport into muscle fibre-types that highly express TBC1D1. Metformin, a commonly prescribed drug to type 2 diabetics, is thought to act by activating AMPK. However, the beneficial effects of metformin can be primarily attributed to its inhibition of gluconeogensis in the liver (Shaw et al., 2005; Owen et al., 2000). Therefore, by additionally activating AMPK at peripheral sites, such as in muscle tissue, AMPK-activators may provide further beneficial effects. Due to

the potential side effects of systemic AMPK activation, the development of skeletal muscle-specific AMPK-activators is likely to be required in order to fully realise the therapeutic potential of AMPK.

7 Overall Conclusions

Multiple signalling inputs impinge upon GLUT4 traffic in muscle. This allows muscle to increase glucose transport in response to insulin, to contraction and to the changes in energy demand that occur during exercise. The signalling pathways leading to enhanced glucose transport in response to exercise, such as the AMPK signalling pathway, remain intact in insulin-resistant individuals. Therefore, these signalling pathways represent a current, in the form of metformin, and future target for treatments of type 2 diabetes. Since AMPK also modulates glucose and lipid metabolism, AMPK-activation is an appealing approach for treating patients with type 2 diabetes and other metabolic disorders.

Accordingly, it is important to investigate how insulin and insulin-independent signalling pathways invoke GLUT4 translocation. The studies presented in this thesis are primarily concerned with effect of activating these signalling pathways on GLUT4 trafficking in muscle cells. This is an important area of research as these studies identify the site at which stimuli impinge upon in GLUT4 trafficking to maintain enhanced cell surface levels. These findings can be used to refine searches for the downstream effectors of these signalling pathways. For example, our finding that insulin and contraction signalling enhance GSV fusion at the sarcolemma and not the transverse tubules implies that a downstream target of these signalling pathways is present specifically at the sarcolemma. By combining data obtained from trafficking studies with data from studies focussed on signalling molecules it will be possible to more fully characterise the molecular mechanism by which stimuli invoke GLUT4 translocation. Recent advancements in proteomic techniques, particularly those concerned with identifying phosphorylated proteins, are likely to aid the identification of these effector molecules. The identification of these downstream substrates is of therapeutic importance since these effectors may represent novel drug targets for treating type 2 diabetes.

Just as identifying changes in GLUT4 trafficking parameters can reveal the site at which signalling pathways induce GLUT4 translocation, this approach could be used to identify abnormalities in GLUT4 trafficking in insulin-resistant cells. By comparing GLUT4 trafficking in insulin-responsive and insulin-resistant cells, it will be possible to identify whether abrogated insulin-stimulated GLUT4 translocation in insulin-resistant cells is due to changes in basal GLUT4 recycling or due to a signalling defect. Indeed, the point at which insulin signalling or GLUT4 trafficking is disrupted in insulin-resistant cells is not clear. Furthermore, the defect may be

different depending on the insult that has induced insulin-resistance (Hoehn et al., 2008). By integrating signalling and trafficking data from insulin-resistant cells, it may be possible to reveal the mechanism for insulin-resistance.

8 References

Abel,E.D., Peroni,O., Kim,J.K., Kim,Y.B., Boss,O., Hadro,E., Minnemann,T., Shulman,G.I., and Kahn,B.B. (2001). Adipose-selective targeting of the GLUT4 gene impairs insulin action in muscle and liver. Nature *409*, 729-733.

Abramson,J., Smirnova,I., Kasho,V., Verner,G., Kaback,H.R., and Iwata,S. (2003). Structure and mechanism of the lactose permease of Escherichia coli. Science *301*, 610-615.

Ahn,M.Y., Katsanakis,K.D., Bheda,F., and Pillay,T.S. (2004). Primary and Essential Role of the Adaptor Protein APS for Recruitment of Both c-Cbl and Its Associated Protein CAP in Insulin Signaling. J. Biol. Chem. *279*, 21526-21532.

Al Hasani,H., Hinck,C.S., and Cushman,S.W. (1998). Endocytosis of the glucose transporter GLUT4 is mediated by the GTPase dynamin. J Biol. Chem. *273*, 17504-17510.

Al Hasani,H., Kunamneni,R.K., Dawson,K., Hinck,C.S., Muller-Wieland,D., and Cushman,S.W. (2002). Roles of the N- and C-termini of GLUT4 in endocytosis. J Cell Sci. *115*, 131-140.

Al Hasani,H., Yver,D.R., and Cushman,S.W. (1999). Overexpression of the glucose transporter GLUT4 in adipose cells interferes with insulin-stimulated translocation. FEBS Lett. *460*, 338-342.

Aledo,J.C., Darakhshan,F., and Hundal,H.S. (1995). Rab4, but not the transferrin receptor, is colocalized with GLUT4 in an insulin-sensitive intracellular compartment in rat skeletal muscle. Biochem. Biophys. Res. Commun. *215*, 321-328.

Alessi,D.R., Caudwell,F.B., Andjelkovic,M., Hemmings,B.A., and Cohen,P. (1996). Molecular basis for the substrate specificity of protein kinase B; comparison with MAPKAP kinase-1 and p70 S6 kinase. FEBS Lett. *399*, 333-338.

Alessi,D.R., James,S.R., Downes,C.P., Holmes,A.B., Gaffney,P.R., Reese,C.B., and Cohen,P. (1997). Characterization of a 3-phosphoinositide-dependent protein kinase which phosphorylates and activates protein kinase Balpha. Curr. Biol. *7*, 261-269.

Antonescu,C.N., Diaz,M., Femia,G., Planas,J.V., and Klip,A. (2008). Clathrin-dependent and independent endocytosis of glucose transporter 4 (GLUT4) in myoblasts: regulation by mitochondrial uncoupling. Traffic. *9*, 1173-1190.

Arad,M., Seidman,C.E., and Seidman,J.G. (2007). AMP-activated protein kinase in the heart: role during health and disease. Circ. Res. *100*, 474-488.

Asano,T., Kanda,A., Katagiri,H., Nawano,M., Ogihara,T., Inukai,K., Anai,M., Fukushima,Y., Yazaki,Y., Kikuchi,M., Hooshmand-Rad,R., Heldin,C.H., Oka,Y., and Funaki,M. (2000). p110beta is up-regulated during differentiation of 3T3-L1 cells and contributes to the highly insulin-responsive glucose transport activity. J Biol. Chem. *275*, 17671-17676.

Axelrod,J.D. and Pilch,P.F. (1983). Unique cytochalasin B binding characteristics of the hepatic glucose carrier. Biochemistry *22*, 2222-2227.

Azevedo,J.L., Jr., Carey,J.O., Pories,W.J., Morris,P.G., and Dohm,G.L. (1995). Hypoxia stimulates glucose transport in insulin-resistant human skeletal muscle. Diabetes *44*, 695-698.

Bae,S.S., Cho,H., Mu,J., and Birnbaum,M.J. (2003). Isoform-specific Regulation of Insulin-dependent Glucose Uptake by Akt/Protein Kinase B. J. Biol. Chem. *278*, 49530-49536.

Bai,L., Wang,Y., Fan,J., Chen,Y., Ji,W., Qu,A., Xu,P., James,D.E., and Xu,T. (2007). Dissecting multiple steps of GLUT4 trafficking and identifying the sites of insulin action. Cell Metab *5*, 47-57.

Bandyopadhyay,G., Kanoh,Y., Sajan,M.P., Standaert,M.L., and Farese,R.V. (2000). Effects of adenoviral gene transfer of wild-type, constitutively active, and kinase-defective protein kinase C-lambda on insulin-stimulated glucose transport in L6 myotubes. Endocrinology *141*, 4120-4127.

Bandyopadhyay,G., Standaert,M.L., Galloway,L., Moscat,J., and Farese,R.V. (1997). Evidence for involvement of protein kinase C (PKC)-zeta and noninvolvement of diacylglycerol-sensitive PKCs in insulin-stimulated glucose transport in L6 myotubes. Endocrinology *138*, 4721-4731.

Barnes,B.R., Marklund,S., Steiler,T.L., Walter,M., Hjalm,G., Amarger,V., Mahlapuu,M., Leng,Y., Johansson,C., Galuska,D., Lindgren,K., Abrink,M., Stapleton,D., Zierath,J.R., and Andersson,L. (2004). The 5'-AMP-activated protein kinase gamma3 isoform has a key role in carbohydrate and lipid metabolism in glycolytic skeletal muscle. J Biol. Chem. *279*, 38441-38447.

Baumann,C.A., Ribon,V., Kanzaki,M., Thurmond,D.C., Mora,S., Shigematsu,S., Bickel,P.E., Pessin,J.E., and Saltiel,A.R. (2000). CAP defines a second signalling pathway required for insulin-stimulated glucose transport. Nature *407*, 202-207.

Beeson,M., Sajan,M.P., Dizon,M., Grebenev,D., Gomez-Daspet,J., Miura,A., Kanoh,Y., Powe,J., Bandyopadhyay,G., Standaert,M.L., and Farese,R.V. (2003). Activation of protein kinase C-zeta by insulin and phosphatidylinositol-3,4,5-(PO4)3 is defective in muscle in type 2 diabetes and impaired glucose tolerance: amelioration by rosiglitazone and exercise. Diabetes *52*, 1926-1934.

Bergeron,R., Previs,S.F., Cline,G.W., Perret,P., Russell,R.R., III, Young,L.H., and Shulman,G.I. (2001). Effect of 5-aminoimidazole-4-carboxamide-1-beta-D-ribofuranoside infusion on in vivo glucose and lipid metabolism in lean and obese Zucker rats. Diabetes *50*, 1076-1082.

Bergeron,R., Russell,R.R., III, Young,L.H., Ren,J.M., Marcucci,M., Lee,A., and Shulman,G.I. (1999). Effect of AMPK activation on muscle glucose metabolism in conscious rats. Am J Physiol *276*, E938-E944.

Bernhardt,U., Carlotti,F., Hoeben,R.C., Joost,H.G., and Al Hasani,H. (2009). A dual role of the N-terminal FQQI motif in GLUT4 trafficking. Biol. Chem. *390*, 883-892.

Berwick,D.C., Dell,G.C., Welsh,G.I., Heesom,K.J., Hers,I., Fletcher,L.M., Cooke,F.T., and Tavare,J.M. (2004). Protein kinase B phosphorylation of PIKfyve regulates the trafficking of GLUT4 vesicles. J Cell Sci. *117*, 5985-5993.

Birk,J.B. and Wojtaszewski,J.F. (2006). Predominant alpha2/beta2/gamma3 AMPK activation during exercise in human skeletal muscle. J Physiol *577*, 1021-1032.

Birnbaum,M.J. (1989). Identification of a novel gene encoding an insulin-responsive glucose transporter protein. Cell *57*, 305-315.

Bjornholm,M., Al Khalili,L., Dicker,A., Naslund,E., Rossner,S., Zierath,J.R., and Arner,P. (2002). Insulin signal transduction and glucose transport in human adipocytes: effects of obesity and low calorie diet. Diabetologia *45*, 1128-1135.

Bjornholm,M. and Zierath,J.R. (2005). Insulin signal transduction in human skeletal muscle: identifying the defects in Type II diabetes. Biochem. Soc. Trans. *33*, 354-357.

Blot,V. and McGraw,T.E. (2006). GLUT4 is internalized by a cholesterol-dependent nystatin-sensitive mechanism inhibited by insulin. EMBO J *25*, 5648-5658.

Blot,V. and McGraw,T.E. (2008). Molecular mechanisms controlling GLUT4 intracellular retention. Mol. Biol. Cell *19*, 3477-3487.

Bogan,J.S., Hendon,N., McKee,A.E., Tsao,T.S., and Lodish,H.F. (2003). Functional cloning of TUG as a regulator of GLUT4 glucose transporter trafficking. Nature *425*, 727-733.

Bose,A., Guilherme,A., Robida,S.I., Nicoloro,S.M., Zhou,Q.L., Jiang,Z.Y., Pomerleau,D.P., and Czech,M.P. (2002). Glucose transporter recycling in response to insulin is facilitated by myosin Myo1c. Nature *420*, 821-824.

Boura-Halfon,S. and Zick,Y. (2009). Phosphorylation of IRS proteins, insulin action, and insulin resistance. Am J Physiol Endocrinol. Metab *296*, E581-E591.

Braiman,L., Alt,A., Kuroki,T., Ohba,M., Bak,A., Tennenbaum,T., and Sampson,S.R. (2001). Activation of protein kinase C zeta induces serine phosphorylation of VAMP2 in the GLUT4 compartment and increases glucose transport in skeletal muscle. Mol. Cell Biol. *21*, 7852-7861.

Brooks,C.C., Scherer,P.E., Cleveland,K., Whittemore,J.L., Lodish,H.F., and Cheatham,B. (2000). Pantophysin is a phosphoprotein component of adipocyte transport vesicles and associates with GLUT4-containing vesicles. J Biol. Chem. *275*, 2029-2036.

Brozinick,J.T., Jr., Hawkins,E.D., Strawbridge,A.B., and Elmendorf,J.S. (2004). Disruption of cortical actin in skeletal muscle demonstrates an essential role of the cytoskeleton in glucose transporter 4 translocation in insulin-sensitive tissues. J Biol. Chem. *279*, 40699-40706.

Bruning,J.C., Michael,M.D., Winnay,J.N., Hayashi,T., Horsch,D., Accili,D., Goodyear,L.J., and Kahn,C.R. (1998). A muscle-specific insulin receptor knockout exhibits features of the metabolic syndrome of NIDDM without altering glucose tolerance. Mol. Cell *2*, 559-569.

Bruss,M.D., Arias,E.B., Lienhard,G.E., and Cartee,G.D. (2005). Increased phosphorylation of Akt substrate of 160 kDa (AS160) in rat skeletal muscle in response to insulin or contractile activity. Diabetes *54*, 41-50.

Bruton,J.D., Katz,A., and Westerblad,H. (2001). The role of Ca2+ and calmodulin in insulin signalling in mammalian skeletal muscle. Acta Physiol Scand. *171*, 259-265.

Bryant,N.J., Govers,R., and James,D.E. (2002). Regulated transport of the glucose transporter GLUT4. Nat. Rev. Mol. Cell Biol. *3*, 267-277.

Cai,D., Dhe-Paganon,S., Melendez,P.A., Lee,J., and Shoelson,S.E. (2003). Two new substrates in insulin signaling, IRS5/DOK4 and IRS6/DOK5. J Biol. Chem. *278*, 25323-25330.

Cain,C.C., Trimble,W.S., and Lienhard,G.E. (1992). Members of the VAMP family of synaptic vesicle proteins are components of glucose transporter-containing vesicles from rat adipocytes. J Biol. Chem. *267*, 11681-11684.

Calderhead,D.M. and Lienhard,G.E. (1988). Labeling of glucose transporters at the cell surface in 3T3-L1 adipocytes. Evidence for both translocation and a second mechanism in the insulin stimulation of transport. J Biol. Chem. *263*, 12171-12174.

Calera,M.R., Martinez,C., Liu,H., Jack,A.K., Birnbaum,M.J., and Pilch,P.F. (1998). Insulin increases the association of Akt-2 with Glut4-containing vesicles. J Biol. Chem. *273*, 7201-7204.

Canto,C., Chibalin,A.V., Barnes,B.R., Glund,S., Suarez,E., Ryder,J.W., Palacin,M., Zierath,J.R., Zorzano,A., and Guma,A. (2006). Neuregulins mediate calcium-induced glucose transport during muscle contraction. J Biol. Chem. *281*, 21690-21697.

Canto,C., Suarez,E., Lizcano,J.M., Grino,E., Shepherd,P.R., Fryer,L.G., Carling,D., Bertran,J., Palacin,M., Zorzano,A., and Guma,A. (2004). Neuregulin signaling on glucose transport in muscle cells. J Biol. Chem. *279*, 12260-12268.

Carling,D. (2004). The AMP-activated protein kinase cascade--a unifying system for energy control. Trends Biochem. Sci. *29*, 18-24.

Cartee,G.D., Douen,A.G., Ramlal,T., Klip,A., and Holloszy,J.O. (1991). Stimulation of glucose transport in skeletal muscle by hypoxia. J Appl. Physiol *70*, 1593-1600.

Cartee,G.D. and Wojtaszewski,J.F. (2007). Role of Akt substrate of 160 kDa in insulin-stimulated and contraction-stimulated glucose transport. Appl. Physiol Nutr. Metab *32*, 557-566.

Chadt,A., Leicht,K., Deshmukh,A., Jiang,L.Q., Scherneck,S., Bernhardt,U., Dreja,T., Vogel,H., Schmolz,K., Kluge,R., Zierath,J.R., Hultschig,C., Hoeben,R.C., Schurmann,A., Joost,H.G., and Al Hasani,H. (2008). Tbc1d1 mutation in lean mouse strain confers leanness and protects from diet-induced obesity. Nat. Genet. *40*, 1354-1359.

Chang,L., Adams,R.D., and Saltiel,A.R. (2002). The TC10-interacting protein CIP4/2 is required for insulin-stimulated Glut4 translocation in 3T3L1 adipocytes. Proc. Natl. Acad. Sci. U. S. A *99*, 12835-12840.

Charron,M.J., Brosius,F.C., III, Alper,S.L., and Lodish,H.F. (1989). A glucose transport protein expressed predominately in insulin-responsive tissues. Proc. Natl. Acad. Sci. U. S. A *86*, 2535-2539.

Chavez,J.A., Roach,W.G., Keller,S.R., Lane,W.S., and Lienhard,G.E. (2008). Inhibition of GLUT4 translocation by Tbc1d1, a Rab GTPase-activating protein abundant in skeletal muscle, is partially relieved by AMP-activated protein kinase activation. J Biol. Chem. *283*, 9187-9195.

Cheatham,B., Volchuk,A., Kahn,C.R., Wang,L., Rhodes,C.J., and Klip,A. (1996). Insulin-stimulated translocation of GLUT4 glucose transporters requires SNARE-complex proteins. Proc. Natl. Acad. Sci. U. S. A *93*, 15169-15173.

Chen,H.C., Bandyopadhyay,G., Sajan,M.P., Kanoh,Y., Standaert,M., Farese,R.V., Jr., and Farese,R.V. (2002). Activation of the ERK pathway and atypical protein kinase C isoforms in exercise- and aminoimidazole-4-carboxamide-1-beta-D-riboside (AICAR)-stimulated glucose transport. J Biol. Chem. *277*, 23554-23562.

Chen,S., Murphy,J., Toth,R., Campbell,D.G., Morrice,N.A., and Mackintosh,C. (2008). Complementary regulation of TBC1D1 and AS160 by growth factors, insulin and AMPK activators. Biochem. J *409*, 449-459.

Chen,W.S., Xu,P.Z., Gottlob,K., Chen,M.L., Sokol,K., Shiyanova,T., Roninson,I., Weng,W., Suzuki,R., Tobe,K., Kadowaki,T., and Hay,N. (2001). Growth retardation and increased apoptosis in mice with homozygous disruption of the Akt1 gene. Genes Dev. *15*, 2203-2208.

Chen,X., Al Hasani,H., Olausson,T., Wenthzel,A.M., Smith,U., and Cushman,S.W. (2003). Activity, phosphorylation state and subcellular distribution of GLUT4-targeted Akt2 in rat adipose cells. J Cell Sci. *116*, 3511-3518.

Chen,Z., Heierhorst,J., Mann,R.J., Mitchelhill,K.I., Michell,B.J., Witters,L.A., Lynch,G.S., Kemp,B.E., and Stapleton,D. (1999). Expression of the AMP-activated protein kinase beta1 and beta2 subunits in skeletal muscle. FEBS Lett. *460*, 343-348.

Chiang,S.H., Baumann,C.A., Kanzaki,M., Thurmond,D.C., Watson,R.T., Neudauer,C.L., Macara,I.G., Pessin,J.E., and Saltiel,A.R. (2001). Insulin-stimulated GLUT4 translocation requires the CAP-dependent activation of TC10. Nature *410*, 944-948.

Cho,H., Mu,J., Kim,J.K., Thorvaldsen,J.L., Chu,Q., Crenshaw,E.B., III, Kaestner,K.H., Bartolomei,M.S., Shulman,G.I., and Birnbaum,M.J. (2001). Insulin resistance and a diabetes mellitus-like syndrome in mice lacking the protein kinase Akt2 (PKB beta). Science *292*, 1728-1731.

Citri,A., Skaria,K.B., and Yarden,Y. (2003). The deaf and the dumb: the biology of ErbB-2 and ErbB-3. Exp. Cell Res. *284*, 54-65.

Clark,R.B., Tremblay,A., Melnyk,P., Allen,B.G., Giles,W.R., and Fiset,C. (2001). T-tubule localization of the inward-rectifier K(+) channel in mouse ventricular myocytes: a role in K(+) accumulation. J Physiol *537*, 979-992.

Clarke,J.F., Young,P.W., Yonezawa,K., Kasuga,M., and Holman,G.D. (1994). Inhibition of the translocation of GLUT1 and GLUT4 in 3T3-L1 cells by the phosphatidylinositol 3-kinase inhibitor, wortmannin. Biochem. J *300 (Pt 3)*, 631-635.

Coderre,L., Kandror,K.V., Vallega,G., and Pilch,P.F. (1995). Identification and characterization of an exercise-sensitive pool of glucose transporters in skeletal muscle. J Biol. Chem. *270*, 27584-27588.

Colville,C.A., Seatter,M.J., Jess,T.J., Gould,G.W., and Thomas,H.M. (1993). Kinetic analysis of the liver-type (GLUT2) and brain-type (GLUT3) glucose transporters in Xenopus oocytes: substrate specificities and effects of transport inhibitors. Biochem. J *290 (Pt 3)*, 701-706.

Cool,B., Zinker,B., Chiou,W., Kifle,L., Cao,N., Perham,M., Dickinson,R., Adler,A., Gagne,G., Iyengar,R., Zhao,G., Marsh,K., Kym,P., Jung,P., Camp,H.S., and Frevert,E. (2006). Identification and characterization of a small molecule AMPK activator that treats key components of type 2 diabetes and the metabolic syndrome. Cell Metab *3*, 403-416.

Coster,A.C., Govers,R., and James,D.E. (2004). Insulin stimulates the entry of GLUT4 into the endosomal recycling pathway by a quantal mechanism. Traffic. *5*, 763-771.

Cushman,S.W. and Wardzala,L.J. (1980). Potential mechanism of insulin action on glucose transport in the isolated rat adipose cell. Apparent translocation of intracellular transport systems to the plasma membrane. J Biol. Chem. *255*, 4758-4762.

Dawson,K., Aviles-Hernandez,A., Cushman,S.W., and Malide,D. (2001). Insulin-regulated trafficking of dual-labeled glucose transporter 4 in primary rat adipose cells. Biochem. Biophys. Res. Commun. *287*, 445-454.

DeFronzo,R.A., Ferrannini,E., Sato,Y., Felig,P., and Wahren,J. (1981). Synergistic interaction between exercise and insulin on peripheral glucose uptake. J Clin. Invest *68*, 1468-1474.

Deshmukh,A.S., Glund,S., Tom,R., and Zierath,J.R. (2009). Role of the AMPK{gamma}3 isoform in hypoxia-stimulated glucose transport in glycolytic skeletal muscle. Am J Physiol Endocrinol. Metab.

Doehner,W., Anker,S.D., and Godsland,I.F. (2005). Optimizing insulin sensitivity assessment using the minimal model in chronic heart failure. Horm. Metab Res. *37*, 106-110.

Doehner,W., Gathercole,D., Cicoira,M., Krack,A., Coats,A.J., Camici,P.G., and Anker,S.D. (2008). Reduced glucose transporter GLUT4 in skeletal muscle predicts insulin resistance in non-diabetic chronic heart failure patients independently of body composition. Int. J Cardiol.

Dohm,G.L., Dolan,P.L., Frisell,W.R., and Dudek,R.W. (1993). Role of transverse tubules in insulin stimulated muscle glucose transport. J Cell Biochem. *52*, 1-7.

Dohm,G.L. and Dudek,R.W. (1998). Role of transverse tubules (T-tubules) in muscle glucose transport. Adv. Exp. Med. Biol. *441*, 27-34.

Ducluzeau,P.H., Fletcher,L.M., Welsh,G.I., and Tavare,J.M. (2002). Functional consequence of targeting protein kinase B/Akt to GLUT4 vesicles. J Cell Sci. *115*, 2857-2866.

Dugani,C.B. and Klip,A. (2005). Glucose transporter 4: cycling, compartments and controversies. EMBO Rep. *6*, 1137-1142.

Easton,R.M., Cho,H., Roovers,K., Shineman,D.W., Mizrahi,M., Forman,M.S., Lee,V.M., Szabolcs,M., de Jong,R., Oltersdorf,T., Ludwig,T., Efstratiadis,A., and Birnbaum,M.J. (2005). Role for Akt3/protein kinase Bgamma in attainment of normal brain size. Mol. Cell Biol. *25*, 1869-1878.

Eckel,J. and Reinauer,H. (1980). Characteristics of insulin receptors in the heart muscle: binding of insulin to isolated muscle cells from adult rat heart. Biochim. Biophys. Acta *629*, 510-521.

Eguez,L., Lee,A., Chavez,J.A., Miinea,C.P., Kane,S., Lienhard,G.E., and McGraw,T.E. (2005). Full intracellular retention of GLUT4 requires AS160 Rab GTPase activating protein. Cell Metab *2*, 263-272.

El Mir,M.Y., Nogueira,V., Fontaine,E., Averet,N., Rigoulet,M., and Leverve,X. (2000). Dimethylbiguanide inhibits cell respiration via an indirect effect targeted on the respiratory chain complex I. J Biol. Chem. *275*, 223-228.

Elchebly,M., Payette,P., Michaliszyn,E., Cromlish,W., Collins,S., Loy,A.L., Normandin,D., Cheng,A., Himms-Hagen,J., Chan,C.C., Ramachandran,C., Gresser,M.J., Tremblay,M.L., and Kennedy,B.P. (1999). Increased insulin sensitivity and obesity resistance in mice lacking the protein tyrosine phosphatase-1B gene. Science *283*, 1544-1548.

Emanuelli,B., Peraldi,P., Filloux,C., Chavey,C., Freidinger,K., Hilton,D.J., Hotamisligil,G.S., and van Obberghen,E. (2001). SOCS-3 inhibits insulin signaling and is up-regulated in response to tumor necrosis factor-alpha in the adipose tissue of obese mice. J Biol. Chem. *276*, 47944-47949.

Emoto,M., Langille,S.E., and Czech,M.P. (2001). A role for kinesin in insulin-stimulated GLUT4 glucose transporter translocation in 3T3-L1 adipocytes. J Biol. Chem. *276*, 10677-10682.

Ewart,M.A., Clarke,M., Kane,S., Chamberlain,L.H., and Gould,G.W. (2005). Evidence for a role of the exocyst in insulin-stimulated Glut4 trafficking in 3T3-L1 adipocytes. J Biol. Chem. *280*, 3812-3816.

Farese,R.V. (2002). Function and dysfunction of aPKC isoforms for glucose transport in insulin-sensitive and insulin-resistant states. Am J Physiol Endocrinol. Metab *283*, E1-11.

Fazakerley,D.J., Lawrence,S.P., Lizunov,V.A., Cushman,S.W., and Holman,G.D. (2009). A common trafficking route for GLUT4 in cardiomyocytes in response to insulin, contraction and energy-status signalling. J Cell Sci. *122*, 727-734.

Feng,Y., Hartig,S.M., Bechill,J.E., Blanchard,E.G., Caudell,E., and Corey,S.J. (2009). The Cdc42 interacting protein 4 (CIP4) gene knockout mouse reveals delayed and decreased endocytosis. J Biol. Chem.

Fischer,Y., Thomas,J., Holman,G.D., Rose,H., and Kammermeier,H. (1996). Contraction-independent effects of catecholamines on glucose transport in isolated rat cardiomyocytes. Am J Physiol *270*, C1204-C1210.

Fisher,J.S., Gao,J., Han,D.H., Holloszy,J.O., and Nolte,L.A. (2002). Activation of AMP kinase enhances sensitivity of muscle glucose transport to insulin. Am J Physiol Endocrinol. Metab *282*, E18-E23.

Fletcher,L.M., Welsh,G.I., Oatey,P.B., and Tavare,J.M. (2000). Role for the microtubule cytoskeleton in GLUT4 vesicle trafficking and in the regulation of insulin-stimulated glucose uptake. Biochem. J *352 Pt 2*, 267-276.

Flier,J.S., Mueckler,M., McCall,A.L., and Lodish,H.F. (1987). Distribution of glucose transporter messenger RNA transcripts in tissues of rat and man. J Clin. Invest *79*, 657-661.

Foran,P.G., Fletcher,L.M., Oatey,P.B., Mohammed,N., Dolly,J.O., and Tavare,J.M. (1999). Protein kinase B stimulates the translocation of GLUT4 but not GLUT1 or transferrin receptors in 3T3-L1 adipocytes by a pathway involving SNAP-23, synaptobrevin-2, and/or cellubrevin. J Biol. Chem. *274*, 28087-28095.

Friedman,J.E., Dudek,R.W., Whitehead,D.S., Downes,D.L., Frisell,W.R., Caro,J.F., and Dohm,G.L. (1991). Immunolocalization of glucose transporter GLUT4 within human skeletal muscle. Diabetes *40*, 150-154.

Fujii,N., Hirshman,M.F., Kane,E.M., Ho,R.C., Peter,L.E., Seifert,M.M., and Goodyear,L.J. (2005). AMP-activated protein kinase alpha2 activity is not essential for contraction- and hyperosmolarity-induced glucose transport in skeletal muscle. J Biol. Chem. *280*, 39033-39041.

Fukuda,N., Emoto,M., Nakamori,Y., Taguchi,A., Miyamoto,S., Uraki,S., Oka,Y., and Tanizawa,Y. (2009). DOC2B: a novel syntaxin-4 binding protein mediating insulin-regulated GLUT4 vesicle fusion in adipocytes. Diabetes *58*, 377-384.

Fukumoto,H., Seino,S., Imura,H., Seino,Y., Eddy,R.L., Fukushima,Y., Byers,M.G., Shows,T.B., and Bell,G.I. (1988). Sequence, tissue distribution, and chromosomal localization of mRNA encoding a human glucose transporter-like protein. Proc. Natl. Acad. Sci. U. S. A *85*, 5434-5438.

Funai,K. and Cartee,G.D. (2008). Contraction-stimulated glucose transport in rat skeletal muscle is sustained despite reversal of increased PAS-phosphorylation of AS160 and TBC1D1. J Appl. Physiol *105*, 1788-1795.

Funai,K. and Cartee,G.D. (2009). Inhibition of contraction-stimulated AMP-activated protein kinase inhibits contraction-stimulated increases in PAS-TBC1D1 and glucose transport without altering PAS-AS160 in rat skeletal muscle. Diabetes *58*, 1096-1104.

Funai,K., Schweitzer,G.G., Sharma,N., Kanzaki,M., and Cartee,G.D. (2009). Increased AS160 phosphorylation, but not TBC1D1 phosphorylation, with increased postexercise insulin sensitivity in rat skeletal muscle. Am J Physiol Endocrinol. Metab *297*, E242-E251.

Gao,J., Ren,J., Gulve,E.A., and Holloszy,J.O. (1994). Additive effect of contractions and insulin on GLUT-4 translocation into the sarcolemma. J Appl. Physiol *77*, 1597-1601.

Garippa,R.J., Judge,T.W., James,D.E., and McGraw,T.E. (1994). The amino terminus of GLUT4 functions as an internalization motif but not an intracellular retention signal when substituted for the transferrin receptor cytoplasmic domain. J Cell Biol. *124*, 705-715.

Geraghty,K.M., Chen,S., Harthill,J.E., Ibrahim,A.F., Toth,R., Morrice,N.A., Vandermoere,F., Moorhead,G.B., Hardie,D.G., and Mackintosh,C. (2007). Regulation of multisite phosphorylation and 14-3-3 binding of AS160 in response to IGF-1, EGF, PMA and AICAR. Biochem. J *407*, 231-241.

Gillingham,A.K., Koumanov,F., Pryor,P.R., Reaves,B.J., and Holman,G.D. (1999). Association of AP1 adaptor complexes with GLUT4 vesicles. J Cell Sci. *112 (Pt 24)*, 4793-4800.

Gonzalez,E. and McGraw,T.E. (2006). Insulin signaling diverges into Akt-dependent and -independent signals to regulate the recruitment/docking and the fusion of GLUT4 vesicles to the plasma membrane. Mol. Biol. Cell *17*, 4484-4493.

Gonzalez,E. and McGraw,T.E. (2009). Insulin-modulated Akt subcellular localization determines Akt isoform-specific signaling. Proc. Natl. Acad. Sci. U. S. A *106*, 7004-7009.

Goransson,O., McBride,A., Hawley,S.A., Ross,F.A., Shpiro,N., Foretz,M., Viollet,B., Hardie,D.G., and Sakamoto,K. (2007). Mechanism of action of A-769662, a valuable tool for activation of AMP-activated protein kinase. J Biol. Chem. *282*, 32549-32560.

Gould,G.W. and Holman,G.D. (1993). The glucose transporter family: structure, function and tissue-specific expression. Biochem. J *295 (Pt 2)*, 329-341.

Gould,G.W., Thomas,H.M., Jess,T.J., and Bell,G.I. (1991). Expression of human glucose transporters in Xenopus oocytes: kinetic characterization and substrate specificities of the erythrocyte, liver, and brain isoforms. Biochemistry *30*, 5139-5145.

Govers,R., Coster,A.C., and James,D.E. (2004). Insulin increases cell surface GLUT4 levels by dose dependently discharging GLUT4 into a cell surface recycling pathway. Mol. Cell Biol. *24*, 6456-6466.

Green,C.J., Goransson,O., Kular,G.S., Leslie,N.R., Gray,A., Alessi,D.R., Sakamoto,K., and Hundal,H.S. (2008). Use of Akt inhibitor and a drug-resistant mutant validates a critical role for protein kinase B/Akt in the insulin-dependent regulation of glucose and system A amino acid uptake. J Biol. Chem. *283*, 27653-27667.

Gual,P., Marchand-Brustel,Y., and Tanti,J.F. (2005). Positive and negative regulation of insulin signaling through IRS-1 phosphorylation. Biochimie *87*, 99-109.

Guigas,B., Sakamoto,K., Taleux,N., Reyna,S.M., Musi,N., Viollet,B., and Hue,L. (2009). Beyond AICA riboside: in search of new specific AMP-activated protein kinase activators. IUBMB. Life *61*, 18-26.

Guilherme,A. and Czech,M.P. (1998). Stimulation of IRS-1-associated phosphatidylinositol 3-kinase and Akt/protein kinase B but not glucose transport by beta1-integrin signaling in rat adipocytes. J Biol. Chem. *273*, 33119-33122.

Guilherme,A., Emoto,M., Buxton,J.M., Bose,S., Sabini,R., Theurkauf,W.E., Leszyk,J., and Czech,M.P. (2000). Perinuclear localization and insulin responsiveness of GLUT4 requires cytoskeletal integrity in 3T3-L1 adipocytes. J Biol. Chem. *275*, 38151-38159.

Guilherme,A., Soriano,N.A., Furcinitti,P.S., and Czech,M.P. (2004). Role of EHD1 and EHBP1 in perinuclear sorting and insulin-regulated GLUT4 recycling in 3T3-L1 adipocytes. J Biol. Chem. *279*, 40062-40075.

Habets,D.D., Coumans,W.A., El Hasnaoui,M., Zarrinpashneh,E., Bertrand,L., Viollet,B., Kiens,B., Jensen,T.E., Richter,E.A., Bonen,A., Glatz,J.F., and Luiken,J.J. (2009). Crucial role for LKB1 to AMPKalpha2 axis in the regulation of CD36-mediated long-chain fatty acid uptake into cardiomyocytes. Biochim. Biophys. Acta *1791*, 212-219.

Habets,D.D., Coumans,W.A., Voshol,P.J., den Boer,M.A., Febbraio,M., Bonen,A., Glatz,J.F., and Luiken,J.J. (2007). AMPK-mediated increase in myocardial long-chain fatty acid uptake critically depends on sarcolemmal CD36. Biochem. Biophys. Res. Commun. *355*, 204-210.

Hartig,S.M., Ishikura,S., Hicklen,R.S., Feng,Y., Blanchard,E.G., Voelker,K.A., Pichot,C.S., Grange,R.W., Raphael,R.M., Klip,A., and Corey,S.J. (2009). The F-BAR protein CIP4 promotes GLUT4 endocytosis through bidirectional interactions with N-WASp and Dynamin-2. J Cell Sci. *122*, 2283-2291.

Hashiramoto,M. and James,D.E. (2000). Characterization of insulin-responsive GLUT4 storage vesicles isolated from 3T3-L1 adipocytes. Mol. Cell Biol. *20*, 416-427.

Hawley,S.A., Boudeau,J., Reid,J.L., Mustard,K.J., Udd,L., Makela,T.P., Alessi,D.R., and Hardie,D.G. (2003). Complexes between the LKB1 tumor suppressor, STRAD alpha/beta and MO25 alpha/beta are upstream kinases in the AMP-activated protein kinase cascade. J Biol. *2*, 28.

Hawley,S.A., Pan,D.A., Mustard,K.J., Ross,L., Bain,J., Edelman,A.M., Frenguelli,B.G., and Hardie,D.G. (2005). Calmodulin-dependent protein kinase kinase-beta is an alternative upstream kinase for AMP-activated protein kinase. Cell Metab *2*, 9-19.

Hayashi,T., Hirshman,M.F., Kurth,E.J., Winder,W.W., and Goodyear,L.J. (1998). Evidence for 5' AMP-activated protein kinase mediation of the effect of muscle contraction on glucose transport. Diabetes *47*, 1369-1373.

He,W., O'Neill,T.J., and Gustafson,T.A. (1995). Distinct modes of interaction of SHC and insulin receptor substrate-1 with the insulin receptor NPEY region via non-SH2 domains. J Biol. Chem. *270*, 23258-23262.

Henriksen,E.J., Rodnick,K.J., Mondon,C.E., James,D.E., and Holloszy,J.O. (1991). Effect of denervation or unweighting on GLUT-4 protein in rat soleus muscle. J Appl. Physiol *70*, 2322-2327.

Henriques,R. and Mhlanga,M.M. (2009). PALM and STORM: what hides beyond the Rayleigh limit? Biotechnol. J *4*, 846-857.

Hoehn,K.L., Hohnen-Behrens,C., Cederberg,A., Wu,L.E., Turner,N., Yuasa,T., Ebina,Y., and James,D.E. (2008). IRS1-independent defects define major nodes of insulin resistance. Cell Metab *7*, 421-433.

Holman,G.D. and Cushman,S.W. (1994). Subcellular localization and trafficking of the GLUT4 glucose transporter isoform in insulin-responsive cells. Bioessays *16*, 753-759.

Holman,G.D., Kozka,I.J., Clark,A.E., Flower,C.J., Saltis,J., Habberfield,A.D., Simpson,I.A., and Cushman,S.W. (1990). Cell surface labeling of glucose transporter isoform GLUT4 by bis-mannose

photolabel. Correlation with stimulation of glucose transport in rat adipose cells by insulin and phorbol ester. J Biol. Chem. *265*, 18172-18179.

Holman,G.D., Lo,L.L., and Cushman,S.W. (1994). Insulin-stimulated GLUT4 glucose transporter recycling. A problem in membrane protein subcellular trafficking through multiple pools. J Biol. Chem. *269*, 17516-17524.

Hosaka,T., Brooks,C.C., Presman,E., Kim,S.K., Zhang,Z., Breen,M., Gross,D.N., Sztul,E., and Pilch,P.F. (2005). p115 Interacts with the GLUT4 vesicle protein, IRAP, and plays a critical role in insulin-stimulated GLUT4 translocation. Mol. Biol. Cell *16*, 2882-2890.

Hresko,R.C. and Mueckler,M. (2005). mTOR.RICTOR is the Ser473 kinase for Akt/protein kinase B in 3T3-L1 adipocytes. J Biol. Chem. *280*, 40406-40416.

Huang,C., Thirone,A.C., Huang,X., and Klip,A. (2005). Differential contribution of insulin receptor substrates 1 versus 2 to insulin signaling and glucose uptake in l6 myotubes. J Biol. Chem. *280*, 19426-19435.

Huang,J., Imamura,T., and Olefsky,J.M. (2001). Insulin can regulate GLUT4 internalization by signaling to Rab5 and the motor protein dynein. Proc. Natl. Acad. Sci. U. S. A *98*, 13084-13089.

Huang,J. and Manning,B.D. (2008). The TSC1-TSC2 complex: a molecular switchboard controlling cell growth. Biochem. J *412*, 179-190.

Huang,S., Lifshitz,L.M., Jones,C., Bellve,K.D., Standley,C., Fonseca,S., Corvera,S., Fogarty,K.E., and Czech,M.P. (2007). Insulin stimulates membrane fusion and GLUT4 accumulation in clathrin coats on adipocyte plasma membranes. Mol. Cell Biol. *27*, 3456-3469.

Hurley,R.L., Anderson,K.A., Franzone,J.M., Kemp,B.E., Means,A.R., and Witters,L.A. (2005). The Ca2+/calmodulin-dependent protein kinase kinases are AMP-activated protein kinase kinases. J Biol. Chem. *280*, 29060-29066.

Iglesias,M.A., Ye,J.M., Frangioudakis,G., Saha,A.K., Tomas,E., Ruderman,N.B., Cooney,G.J., and Kraegen,E.W. (2002). AICAR administration causes an apparent enhancement of muscle and liver insulin action in insulin-resistant high-fat-fed rats. Diabetes *51*, 2886-2894.

Ikonomov,O.C., Sbrissa,D., Dondapati,R., and Shisheva,A. (2007). ArPIKfyve-PIKfyve interaction and role in insulin-regulated GLUT4 translocation and glucose transport in 3T3-L1 adipocytes. Exp. Cell Res. *313*, 2404-2416.

Ikonomov,O.C., Sbrissa,D., Mlak,K., and Shisheva,A. (2002). Requirement for PIKfyve enzymatic activity in acute and long-term insulin cellular effects. Endocrinology *143*, 4742-4754.

Inoue,M., Chang,L., Hwang,J., Chiang,S.H., and Saltiel,A.R. (2003). The exocyst complex is required for targeting of Glut4 to the plasma membrane by insulin. Nature *422*, 629-633.

Inoue,M., Chiang,S.H., Chang,L., Chen,X.W., and Saltiel,A.R. (2006). Compartmentalization of the exocyst complex in lipid rafts controls Glut4 vesicle tethering. Mol. Biol. Cell *17*, 2303-2311.

Isakoff,S.J., Taha,C., Rose,E., Marcusohn,J., Klip,A., and Skolnik,E.Y. (1995). The inability of phosphatidylinositol 3-kinase activation to stimulate GLUT4 translocation indicates additional signaling pathways are required for insulin-stimulated glucose uptake. Proc. Natl. Acad. Sci. U. S. A *92*, 10247-10251.

James,D.E., Strube,M., and Mueckler,M. (1989). Molecular cloning and characterization of an insulin-regulatable glucose transporter. Nature *338*, 83-87.

JeBailey,L., Rudich,A., Huang,X., Ciano-Oliveira,C., Kapus,A., and Klip,A. (2004). Skeletal muscle cells and adipocytes differ in their reliance on TC10 and Rac for insulin-induced actin remodeling. Mol. Endocrinol. *18*, 359-372.

Jedrychowski,M.P., Gartner,C.A., Gygi,S.P., Zhou,L., Herz,J., Kandror,K.V., and Pilch,P.F. (2009). Proteomic analysis of GLUT4 storage vesicles (GSVS) reveals low-density lipoprotein receptor-related protein 1 (LRP1) to be an important vesicle component and target of insulin signaling. J Biol. Chem.

Jefferies,H.B., Cooke,F.T., Jat,P., Boucheron,C., Koizumi,T., Hayakawa,M., Kaizawa,H., Ohishi,T., Workman,P., Waterfield,M.D., and Parker,P.J. (2008). A selective PIKfyve inhibitor blocks PtdIns(3,5)P(2) production and disrupts endomembrane transport and retroviral budding. EMBO Rep. *9*, 164-170.

Jensen,T.E., Maarbjerg,S.J., Rose,A.J., Leitges,M., and Richter,E.A. (2009). Knockout of the predominant conventional PKC isoform, PKCalpha, in mouse skeletal muscle does not affect contraction-stimulated glucose uptake. Am J Physiol Endocrinol. Metab *297*, E340-E348.

Jensen,T.E., Rose,A.J., Jorgensen,S.B., Brandt,N., Schjerling,P., Wojtaszewski,J.F., and Richter,E.A. (2007). Possible CaMKK-dependent regulation of AMPK phosphorylation and glucose uptake at the onset of mild tetanic skeletal muscle contraction. Am J Physiol Endocrinol. Metab *292*, E1308-E1317.

Jessen,N. and Goodyear,L.J. (2005). Contraction signaling to glucose transport in skeletal muscle. J Appl. Physiol *99*, 330-337.

Jewell,J.L., Oh,E., Bennett,S.M., Meroueh,S.O., and Thurmond,D.C. (2008). The tyrosine phosphorylation of Munc18c induces a switch in binding specificity from syntaxin 4 to Doc2beta. J Biol. Chem. *283*, 21734-21746.

Jhun,B.H., Rampal,A.L., Liu,H., Lachaal,M., and Jung,C.Y. (1992). Effects of insulin on steady state kinetics of GLUT4 subcellular distribution in rat adipocytes. Evidence of constitutive GLUT4 recycling. J Biol. Chem. *267*, 17710-17715.

Jiang,L., Fan,J., Bai,L., Wang,Y., Chen,Y., Yang,L., Chen,L., and Xu,T. (2008). Direct quantification of fusion rate reveals a distal role for AS160 in insulin-stimulated fusion of GLUT4 storage vesicles. J Biol. Chem. *283*, 8508-8516.

Jiang,Z.Y., Chawla,A., Bose,A., Way,M., and Czech,M.P. (2002). A phosphatidylinositol 3-kinase-independent insulin signaling pathway to N-WASP/Arp2/3/F-actin required for GLUT4 glucose transporter recycling. J Biol. Chem. *277*, 509-515.

Jiang,Z.Y., Zhou,Q.L., Coleman,K.A., Chouinard,M., Boese,Q., and Czech,M.P. (2003). Insulin signaling through Akt/protein kinase B analyzed by small interfering RNA-mediated gene silencing. Proc. Natl. Acad. Sci. U. S. A *100*, 7569-7574.

Joost,H.G. and Thorens,B. (2001). The extended GLUT-family of sugar/polyol transport facilitators: nomenclature, sequence characteristics, and potential function of its novel members (review). Mol. Membr. Biol. *18*, 247-256.

Joost,H.G., Weber,T.M., and Cushman,S.W. (1988). Qualitative and quantitative comparison of glucose transport activity and glucose transporter concentration in plasma membranes from basal and insulin-stimulated rat adipose cells. Biochem. J *249*, 155-161.

Jorgensen,S.B., Honeyman,J., Oakhill,J.S., Fazakerley,D., Stockli,J., Kemp,B.E., and Steinberg,G.R. (2009). Oligomeric resistin impairs insulin and AICAR-stimulated glucose uptake in mouse skeletal muscle by inhibiting GLUT4 translocation. Am J Physiol Endocrinol. Metab *297*, E57-E66.

Jorgensen,S.B., Viollet,B., Andreelli,F., Frosig,C., Birk,J.B., Schjerling,P., Vaulont,S., Richter,E.A., and Wojtaszewski,J.F. (2004). Knockout of the alpha2 but not alpha1 5'-AMP-activated protein kinase isoform abolishes 5-aminoimidazole-4-carboxamide-1-beta-4-ribofuranosidebut not contraction-induced glucose uptake in skeletal muscle. J Biol. Chem. *279*, 1070-1079.

Kaburagi,Y., Satoh,S., Tamemoto,H., Yamamoto-Honda,R., Tobe,K., Veki,K., Yamauchi,T., Kono-Sugita,E., Sekihara,H., Aizawa,S., Cushman,S.W., Akanuma,Y., Yazaki,Y., and Kadowaki,T. (1997). Role of insulin receptor substrate-1 and pp60 in the regulation of insulin-induced glucose transport and GLUT4 translocation in primary adipocytes. J Biol. Chem. *272*, 25839-25844.

Kaestner,K.H., Christy,R.J., McLenithan,J.C., Braiterman,L.T., Cornelius,P., Pekala,P.H., and Lane,M.D. (1989). Sequence, tissue distribution, and differential expression of mRNA for a putative insulin-responsive glucose transporter in mouse 3T3-L1 adipocytes. Proc. Natl. Acad. Sci. U. S. A *86*, 3150-3154.

Kahn,B.B., Alquier,T., Carling,D., and Hardie,D.G. (2005). AMP-activated protein kinase: ancient energy gauge provides clues to modern understanding of metabolism. Cell Metab *1*, 15-25.

Kanai,F., Ito,K., Todaka,M., Hayashi,H., Kamohara,S., Ishii,K., Okada,T., Hazeki,O., Ui,M., and Ebina,Y. (1993). Insulin-stimulated GLUT4 translocation is relevant to the phosphorylation of IRS-1 and the activity of PI3-kinase. Biochem. Biophys. Res. Commun. *195*, 762-768.

Kandror,K.V. (1999). Insulin regulation of protein traffic in rat adipose cells. J Biol. Chem. *274*, 25210-25217.

Kandror,K.V. and Pilch,P.F. (1996). The insulin-like growth factor II/mannose 6-phosphate receptor utilizes the same membrane compartments as GLUT4 for insulin-dependent trafficking to and from the rat adipocyte cell surface. J Biol. Chem. *271*, 21703-21708.

Kandror,K.V. and Pilch,P.F. (1998). Multiple endosomal recycling pathways in rat adipose cells. Biochem. J *331 (Pt 3)*, 829-835.

Kane,S. and Lienhard,G.E. (2005). Calmodulin binds to the Rab GTPase activating protein required for insulin-stimulated GLUT4 translocation. Biochem. Biophys. Res. Commun. *335*, 175-180.

Kane,S., Sano,H., Liu,S.C., Asara,J.M., Lane,W.S., Garner,C.C., and Lienhard,G.E. (2002). A method to identify serine kinase substrates. Akt phosphorylates a novel adipocyte protein with a Rab GTPase-activating protein (GAP) domain. J Biol. Chem. *277*, 22115-22118.

Kanoh,Y., Sajan,M.P., Bandyopadhyay,G., Miura,A., Standaert,M.L., and Farese,R.V. (2003). Defective activation of atypical protein kinase C zeta and lambda by insulin and phosphatidylinositol-3,4,5-(PO4)(3) in skeletal muscle of rats following high-fat feeding and streptozotocin-induced diabetes. Endocrinology *144*, 947-954.

Kao,A.W., Ceresa,B.P., Santeler,S.R., and Pessin,J.E. (1998). Expression of a dominant interfering dynamin mutant in 3T3L1 adipocytes inhibits GLUT4 endocytosis without affecting insulin signaling. J Biol. Chem. *273*, 25450-25457.

Karlsson,H.K., Chibalin,A.V., Koistinen,H.A., Yang,J., Koumanov,F., Wallberg-Henriksson,H., Zierath,J.R., and Holman,G.D. (2009). Kinetics of GLUT4 trafficking in rat and human skeletal muscle. Diabetes *58*, 847-854.

Karlsson,M., Thorn,H., Parpal,S., Stralfors,P., and Gustavsson,J. (2002). Insulin induces translocation of glucose transporter GLUT4 to plasma membrane caveolae in adipocytes. FASEB J *16*, 249-251.

Karylowski,O., Zeigerer,A., Cohen,A., and McGraw,T.E. (2004). GLUT4 is retained by an intracellular cycle of vesicle formation and fusion with endosomes. Mol. Biol. Cell *15*, 870-882.

Kasuga,M., Hedo,J.A., Yamada,K.M., and Kahn,C.R. (1982a). The structure of insulin receptor and its subunits. Evidence for multiple nonreduced forms and a 210,000 possible proreceptor. J Biol. Chem. *257*, 10392-10399.

Kasuga,M., Karlsson,F.A., and Kahn,C.R. (1982b). Insulin stimulates the phosphorylation of the 95,000-dalton subunit of its own receptor. Science *215*, 185-187.

Kasuga,M., Zick,Y., Blithe,D.L., Crettaz,M., and Kahn,C.R. (1982c). Insulin stimulates tyrosine phosphorylation of the insulin receptor in a cell-free system. Nature *298*, 667-669.

Kawaguchi,T., Tamori,Y., Yoshikawa,M., Kanda,H., and Kasuga,M. (2008). Insulin-stimulated fusion of GLUT4 vesicles to plasma membrane is dependent on wortmannin-sensitive insulin signaling pathway in 3T3-L1 adipocytes. Kobe J Med. Sci. *54*, E209-E216.

Ke,B., Oh,E., and Thurmond,D.C. (2007). Doc2beta is a novel Munc18c-interacting partner and positive effector of syntaxin 4-mediated exocytosis. J Biol. Chem. *282*, 21786-21797.

Keller,S.R., Davis,A.C., and Clairmont,K.B. (2002). Mice deficient in the insulin-regulated membrane aminopeptidase show substantial decreases in glucose transporter GLUT4 levels but maintain normal glucose homeostasis. J Biol. Chem. *277*, 17677-17686.

Kennedy,J.W., Hirshman,M.F., Gervino,E.V., Ocel,J.V., Forse,R.A., Hoenig,S.J., Aronson,D., Goodyear,L.J., and Horton,E.S. (1999). Acute exercise induces GLUT4 translocation in skeletal muscle of normal human subjects and subjects with type 2 diabetes. Diabetes *48*, 1192-1197.

Kessler,A., Tomas,E., Immler,D., Meyer,H.E., Zorzano,A., and Eckel,J. (2000). Rab11 is associated with GLUT4-containing vesicles and redistributes in response to insulin. Diabetologia *43*, 1518-1527.

Kim,J.K., Zisman,A., Fillmore,J.J., Peroni,O.D., Kotani,K., Perret,P., Zong,H., Dong,J., Kahn,C.R., Kahn,B.B., and Shulman,G.I. (2001). Glucose toxicity and the development of diabetes in mice with muscle-specific inactivation of GLUT4. J Clin. Invest *108*, 153-160.

Kim,M.S. and Lee,K.U. (2005). Role of hypothalamic 5'-AMP-activated protein kinase in the regulation of food intake and energy homeostasis. J Mol. Med. *83*, 514-520.

Kimura,A., Baumann,C.A., Chiang,S.H., and Saltiel,A.R. (2001). The sorbin homology domain: a motif for the targeting of proteins to lipid rafts. Proc. Natl. Acad. Sci. U. S. A *98*, 9098-9103.

Knudson,C.M. and Campbell,K.P. (1989). Albumin is a major protein component of transverse tubule vesicles isolated from skeletal muscle. J Biol. Chem. *264*, 10795-10798.

Kohn,A.D., Barthel,A., Kovacina,K.S., Boge,A., Wallach,B., Summers,S.A., Birnbaum,M.J., Scott,P.H., Lawrence,J.C., Jr., and Roth,R.A. (1998). Construction and characterization of a conditionally active version of the serine/threonine kinase Akt. J Biol. Chem. *273*, 11937-11943.

Koistinen,H.A., Galuska,D., Chibalin,A.V., Yang,J., Zierath,J.R., Holman,G.D., and Wallberg-Henriksson,H. (2003). 5-amino-imidazole carboxamide riboside increases glucose transport and cell-surface GLUT4 content in skeletal muscle from subjects with type 2 diabetes. Diabetes *52*, 1066-1072.

Kojima,T., Fukuda,M., Aruga,J., and Mikoshiba,K. (1996). Calcium-dependent phospholipid binding to the C2A domain of a ubiquitous form of double C2 protein (Doc2 beta). J Biochem. *120*, 671-676.

Kolter,T., Uphues,I., Wichelhaus,A., Reinauer,H., and Eckel,J. (1992). Contraction-induced translocation of the glucose transporter Glut4 in isolated ventricular cardiomyocytes. Biochem. Biophys. Res. Commun. *189*, 1207-1214.

Koumanov,F., Jin,B., Yang,J., and Holman,G.D. (2005). Insulin signaling meets vesicle traffic of GLUT4 at a plasma-membrane-activated fusion step. Cell Metab *2*, 179-189.

Kramer,H.F., Taylor,E.B., Witczak,C.A., Fujii,N., Hirshman,M.F., and Goodyear,L.J. (2007). Calmodulin-binding domain of AS160 regulates contraction- but not insulin-stimulated glucose uptake in skeletal muscle. Diabetes *56*, 2854-2862.

Kramer,H.F., Witczak,C.A., Fujii,N., Jessen,N., Taylor,E.B., Arnolds,D.E., Sakamoto,K., Hirshman,M.F., and Goodyear,L.J. (2006a). Distinct signals regulate AS160 phosphorylation in response to insulin, AICAR, and contraction in mouse skeletal muscle. Diabetes *55*, 2067-2076.

Kramer,H.F., Witczak,C.A., Taylor,E.B., Fujii,N., Hirshman,M.F., and Goodyear,L.J. (2006b). AS160 regulates insulin- and contraction-stimulated glucose uptake in mouse skeletal muscle. J Biol. Chem. *281*, 31478-31485.

Kupriyanova,T.A. and Kandror,K.V. (1999). Akt-2 binds to Glut4-containing vesicles and phosphorylates their component proteins in response to insulin. J Biol. Chem. *274*, 1458-1464.

Kupriyanova,T.A. and Kandror,K.V. (2000). Cellugyrin is a marker for a distinct population of intracellular Glut4-containing vesicles. J Biol. Chem. *275*, 36263-36268.

Kupriyanova,T.A., Kandror,V., and Kandror,K.V. (2002). Isolation and characterization of the two major intracellular Glut4 storage compartments. J Biol. Chem. *277*, 9133-9138.

Laemmli,U.K. (1970). Cleavage of structural proteins during the assembly of the head of bacteriophage T4. Nature *227*, 680-685.

Lamaze,C., Dujeancourt,A., Baba,T., Lo,C.G., Benmerah,A., and Dautry-Varsat,A. (2001). Interleukin 2 receptors and detergent-resistant membrane domains define a clathrin-independent endocytic pathway. Mol. Cell *7*, 661-671.

Lampson,M.A., Racz,A., Cushman,S.W., and McGraw,T.E. (2000). Demonstration of insulin-responsive trafficking of GLUT4 and vpTR in fibroblasts. J Cell Sci. *113 (Pt 22)*, 4065-4076.

Lampson,M.A., Schmoranzer,J., Zeigerer,A., Simon,S.M., and McGraw,T.E. (2001). Insulin-regulated release from the endosomal recycling compartment is regulated by budding of specialized vesicles. Mol. Biol. Cell *12*, 3489-3501.

Lanner,J.T., Bruton,J.D., Katz,A., and Westerblad,H. (2008). Ca(2+) and insulin-mediated glucose uptake. Curr. Opin. Pharmacol. *8*, 339-345.

Larance,M., Ramm,G., and James,D.E. (2008). The GLUT4 code. Mol. Endocrinol. *22*, 226-233.

Larance,M., Ramm,G., Stockli,J., van Dam,E.M., Winata,S., Wasinger,V., Simpson,F., Graham,M., Junutula,J.R., Guilhaus,M., and James,D.E. (2005). Characterization of the role of the Rab GTPase-activating protein AS160 in insulin-regulated GLUT4 trafficking. J Biol. Chem. *280*, 37803-37813.

Lauritzen,H.P. (2009). In vivo imaging of GLUT4 translocation. Appl. Physiol Nutr. Metab *34*, 420-423.

Lauritzen,H.P., Galbo,H., Brandauer,J., Goodyear,L.J., and Ploug,T. (2008a). Large GLUT4 vesicles are stationary while locally and reversibly depleted during transient insulin stimulation of skeletal muscle of living mice: imaging analysis of GLUT4-enhanced green fluorescent protein vesicle dynamics. Diabetes *57*, 315-324.

Lauritzen,H.P., Ploug,T., Ai,H., Donsmark,M., Prats,C., and Galbo,H. (2008b). Denervation and high-fat diet reduce insulin signaling in T-tubules in skeletal muscle of living mice. Diabetes *57*, 13-23.

Lauritzen,H.P., Ploug,T., Prats,C., Tavare,J.M., and Galbo,H. (2006). Imaging of insulin signaling in skeletal muscle of living mice shows major role of T-tubules. Diabetes *55*, 1300-1306.

Lauritzen,H.P., Reynet,C., Schjerling,P., Ralston,E., Thomas,S., Galbo,H., and Ploug,T. (2002). Gene gun bombardment-mediated expression and translocation of EGFP-tagged GLUT4 in skeletal muscle fibres in vivo. Pflugers Arch. *444*, 710-721.

Lee,J. and Pilch,P.F. (1994). The insulin receptor: structure, function, and signaling. Am J Physiol *266*, C319-C334.

Lee-Young,R.S., Canny,B.J., Myers,D.E., and McConell,G.K. (2009). AMPK activation is fiber type specific in human skeletal muscle: effects of exercise and short-term exercise training. J Appl. Physiol *107*, 283-289.

Leff,T. (2003). AMP-activated protein kinase regulates gene expression by direct phosphorylation of nuclear proteins. Biochem. Soc. Trans. *31*, 224-227.

Leloup,C., Arluison,M., Kassis,N., Lepetit,N., Cartier,N., Ferre,P., and Penicaud,L. (1996). Discrete brain areas express the insulin-responsive glucose transporter GLUT4. Brain Res. Mol. Brain Res. *38*, 45-53.

Lemieux,K., Han,X.X., Dombrowski,L., Bonen,A., and Marette,A. (2000). The transferrin receptor defines two distinct contraction-responsive GLUT4 vesicle populations in skeletal muscle. Diabetes *49*, 183-189.

Lemieux,M.J., Song,J., Kim,M.J., Huang,Y., Villa,A., Auer,M., Li,X.D., and Wang,D.N. (2003). Three-dimensional crystallization of the Escherichia coli glycerol-3-phosphate transporter: a member of the major facilitator superfamily. Protein Sci. *12*, 2748-2756.

Leney,S.E. and Tavare,J.M. (2009). The molecular basis of insulin-stimulated glucose uptake: signalling, trafficking and potential drug targets. J Endocrinol. *203*, 1-18.

Li,J., Houseknecht,K.L., Stenbit,A.E., Katz,E.B., and Charron,M.J. (2000). Reduced glucose uptake precedes insulin signaling defects in adipocytes from heterozygous GLUT4 knockout mice. FASEB J *14*, 1117-1125.

Li,Y., Wang,P., Xu,J., Gorelick,F., Yamazaki,H., Andrews,N., and Desir,G.V. (2007). Regulation of insulin secretion and GLUT4 trafficking by the calcium sensor synaptotagmin VII. Biochem. Biophys. Res. Commun. *362*, 658-664.

Lindsay,A.J. and McCaffrey,M.W. (2004). The C2 domains of the class I Rab11 family of interacting proteins target recycling vesicles to the plasma membrane. J Cell Sci. *117*, 4365-4375.

Lindsley,C.W., Barnett,S.F., Layton,M.E., and Bilodeau,M.T. (2008). The PI3K/Akt pathway: recent progress in the development of ATP-competitive and allosteric Akt kinase inhibitors. Curr. Cancer Drug Targets. *8*, 7-18.

Lindsley,C.W., Zhao,Z., Leister,W.H., Robinson,R.G., Barnett,S.F., Defeo-Jones,D., Jones,R.E., Hartman,G.D., Huff,J.R., Huber,H.E., and Duggan,M.E. (2005). Allosteric Akt (PKB) inhibitors: discovery and SAR of isozyme selective inhibitors. Bioorg. Med. Chem. Lett. *15*, 761-764.

Liu,L.Z., Zhao,H.L., Zuo,J., Ho,S.K., Chan,J.C., Meng,Y., Fang,F.D., and Tong,P.C. (2006). Protein kinase Czeta mediates insulin-induced glucose transport through actin remodeling in L6 muscle cells. Mol. Biol. Cell *17*, 2322-2330.

Liu,S.C., Wang,Q., Lienhard,G.E., and Keller,S.R. (1999). Insulin receptor substrate 3 is not essential for growth or glucose homeostasis. J Biol. Chem. *274*, 18093-18099.

Livingstone,C., James,D.E., Rice,J.E., Hanpeter,D., and Gould,G.W. (1996). Compartment ablation analysis of the insulin-responsive glucose transporter (GLUT4) in 3T3-L1 adipocytes. Biochem. J *315 (Pt 2)*, 487-495.

Lizunov,V.A., Lisinski,I., Stenkula,K., Zimmerberg,J., and Cushman,S.W. (2009). Insulin regulates fusion of GLUT4 vesicles independent of Exo70-mediated tethering. J Biol. Chem. *284*, 7914-7919.

Lizunov,V.A., Matsumoto,H., Zimmerberg,J., Cushman,S.W., and Frolov,V.A. (2005). Insulin stimulates the halting, tethering, and fusion of mobile GLUT4 vesicles in rat adipose cells. J Cell Biol. *169*, 481-489.

Lodhi,I.J., Chiang,S.H., Chang,L., Vollenweider,D., Watson,R.T., Inoue,M., Pessin,J.E., and Saltiel,A.R. (2007). Gapex-5, a Rab31 guanine nucleotide exchange factor that regulates Glut4 trafficking in adipocytes. Cell Metab *5*, 59-72.

Longnus,S.L., Wambolt,R.B., Parsons,H.L., Brownsey,R.W., and Allard,M.F. (2003). 5-Aminoimidazole-4-carboxamide 1-beta -D-ribofuranoside (AICAR) stimulates myocardial glycogenolysis by allosteric mechanisms. Am J Physiol Regul. Integr. Comp Physiol *284*, R936-R944.

Lopez,J.A., Burchfield,J.G., Blair,D.H., Mele,K., Ng,Y., Vallotton,P., James,D.E., and Hughes,W.E. (2009). Identification of a distal GLUT4 trafficking event controlled by actin polymerization. Mol. Biol. Cell *20*, 3918-3929.

Luiken,J.J., Ouwens,D.M., Habets,D.D., van der Zon,G.C., Coumans,W.A., Schwenk,R.W., Bonen,A., and Glatz,J.F. (2009). Permissive action of protein kinase C-zeta in insulin-induced CD36- and GLUT4 translocation in cardiac myocytes. J Endocrinol. *201*, 199-209.

Luiken,J.J., Vertommen,D., Coort,S.L., Habets,D.D., El Hasnaoui,M., Pelsers,M.M., Viollet,B., Bonen,A., Hue,L., Rider,M.H., and Glatz,J.F. (2008). Identification of protein kinase D as a novel contraction-activated kinase linked to GLUT4-mediated glucose uptake, independent of AMPK. Cell Signal. *20*, 543-556.

Lund,S., Holman,G.D., Schmitz,O., and Pedersen,O. (1995). Contraction stimulates translocation of glucose transporter GLUT4 in skeletal muscle through a mechanism distinct from that of insulin. Proc. Natl. Acad. Sci. U. S. A *92*, 5817-5821.

Mahlapuu,M., Johansson,C., Lindgren,K., Hjalm,G., Barnes,B.R., Krook,A., Zierath,J.R., Andersson,L., and Marklund,S. (2004). Expression profiling of the gamma-subunit isoforms of AMP-activated protein kinase suggests a major role for gamma3 in white skeletal muscle. Am J Physiol Endocrinol. Metab *286*, E194-E200.

Malide,D., Dwyer,N.K., Blanchette-Mackie,E.J., and Cushman,S.W. (1997). Immunocytochemical evidence that GLUT4 resides in a specialized translocation post-endosomal VAMP2-positive compartment in rat adipose cells in the absence of insulin. J Histochem. Cytochem. *45*, 1083-1096.

Malide,D., Ramm,G., Cushman,S.W., and Slot,J.W. (2000). Immunoelectron microscopic evidence that GLUT4 translocation explains the stimulation of glucose transport in isolated rat white adipose cells. J Cell Sci. *113 Pt 23*, 4203-4210.

Manning,B.D. and Cantley,L.C. (2007). AKT/PKB signaling: navigating downstream. Cell *129*, 1261-1274.

Marcusohn,J., Isakoff,S.J., Rose,E., Symons,M., and Skolnik,E.Y. (1995). The GTP-binding protein Rac does not couple PI 3-kinase to insulin-stimulated glucose transport in adipocytes. Curr. Biol. *5*, 1296-1302.

Marsin,A.S., Bertrand,L., Rider,M.H., Deprez,J., Beauloye,C., Vincent,M.F., Van den,B.G., Carling,D., and Hue,L. (2000). Phosphorylation and activation of heart PFK-2 by AMPK has a role in the stimulation of glycolysis during ischaemia. Curr. Biol. *10*, 1247-1255.

Martin,O.J., Lee,A., and McGraw,T.E. (2006). GLUT4 distribution between the plasma membrane and the intracellular compartments is maintained by an insulin-modulated bipartite dynamic mechanism. J Biol. Chem. *281*, 484-490.

Martin,S., Ramm,G., Lyttle,C.T., Meerloo,T., Stoorvogel,W., and James,D.E. (2000). Biogenesis of insulin-responsive GLUT4 vesicles is independent of brefeldin A-sensitive trafficking. Traffic. *1*, 652-660.

Martin,S., Reaves,B., Banting,G., and Gould,G.W. (1994). Analysis of the co-localization of the insulin-responsive glucose transporter (GLUT4) and the trans Golgi network marker TGN38 within 3T3-L1 adipocytes. Biochem. J *300 (Pt 3)*, 743-749.

Martin,S., Tellam,J., Livingstone,C., Slot,J.W., Gould,G.W., and James,D.E. (1996). The glucose transporter (GLUT-4) and vesicle-associated membrane protein-2 (VAMP-2) are segregated from recycling endosomes in insulin-sensitive cells. J Cell Biol. *134*, 625-635.

Masure,S., Haefner,B., Wesselink,J.J., Hoefnagel,E., Mortier,E., Verhasselt,P., Tuytelaars,A., Gordon,R., and Richardson,A. (1999). Molecular cloning, expression and characterization of the human serine/threonine kinase Akt-3. Eur. J Biochem. *265*, 353-360.

McCarthy,A.M., Spisak,K.O., Brozinick,J.T., and Elmendorf,J.S. (2006). Loss of cortical actin filaments in insulin-resistant skeletal muscle cells impairs GLUT4 vesicle trafficking and glucose transport. Am J Physiol Cell Physiol *291*, C860-C868.

McDonough,A.A., Zhang,Y., Shin,V., and Frank,J.S. (1996). Subcellular distribution of sodium pump isoform subunits in mammalian cardiac myocytes. Am J Physiol *270*, C1221-C1227.

Merrall,N.W., Plevin,R., and Gould,G.W. (1993a). Growth factors, mitogens, oncogenes and the regulation of glucose transport. Cell Signal. *5*, 667-675.

Merrall,N.W., Wakelam,M.J., Plevin,R., and Gould,G.W. (1993b). Insulin and platelet-derived growth factor acutely stimulate glucose transport in 3T3-L1 fibroblasts independently of protein kinase C. Biochim. Biophys. Acta *1177*, 191-198.

Meyre,D., Farge,M., Lecoeur,C., Proenca,C., Durand,E., Allegaert,F., Tichet,J., Marre,M., Balkau,B., Weill,J., Delplanque,J., and Froguel,P. (2008). R125W coding variant in TBC1D1 confers risk for familial obesity and contributes to linkage on chromosome 4p14 in the French population. Hum. Mol. Genet. *17*, 1798-1802.

Miinea,C.P., Sano,H., Kane,S., Sano,E., Fukuda,M., Peranen,J., Lane,W.S., and Lienhard,G.E. (2005). AS160, the Akt substrate regulating GLUT4 translocation, has a functional Rab GTPase-activating protein domain. Biochem. J *391*, 87-93.

Mitcheson,J.S., Hancox,J.C., and Levi,A.J. (1996). Action potentials, ion channel currents and transverse tubule density in adult rabbit ventricular myocytes maintained for 6 days in cell culture. Pflugers Arch. *431*, 814-827.

Mitra,P., Zheng,X., and Czech,M.P. (2004). RNAi-based analysis of CAP, Cbl, and CrkII function in the regulation of GLUT4 by insulin. J Biol. Chem. *279*, 37431-37435.

Molero,J.C., Whitehead,J.P., Meerloo,T., and James,D.E. (2001). Nocodazole inhibits insulin-stimulated glucose transport in 3T3-L1 adipocytes via a microtubule-independent mechanism. J Biol. Chem. *276*, 43829-43835.

Momcilovic,M., Hong,S.P., and Carlson,M. (2006). Mammalian TAK1 activates Snf1 protein kinase in yeast and phosphorylates AMP-activated protein kinase in vitro. J Biol. Chem. *281*, 25336-25343.

Mora,A., Lipina,C., Tronche,F., Sutherland,C., and Alessi,D.R. (2005a). Deficiency of PDK1 in liver results in glucose intolerance, impairment of insulin-regulated gene expression and liver failure. Biochem. J *385*, 639-648.

Mora,A., Sakamoto,K., McManus,E.J., and Alessi,D.R. (2005b). Role of the PDK1-PKB-GSK3 pathway in regulating glycogen synthase and glucose uptake in the heart. FEBS Lett. *579*, 3632-3638.

Morita,S., Kojima,T., and Kitamura,T. (2000). Plat-E: an efficient and stable system for transient packaging of retroviruses. Gene Ther. *7*, 1063-1066.

Mu,J., Brozinick,J.T., Jr., Valladares,O., Bucan,M., and Birnbaum,M.J. (2001). A role for AMP-activated protein kinase in contraction- and hypoxia-regulated glucose transport in skeletal muscle. Mol. Cell *7*, 1085-1094.

Mueckler,M., Caruso,C., Baldwin,S.A., Panico,M., Blench,I., Morris,H.R., Allard,W.J., Lienhard,G.E., and Lodish,H.F. (1985). Sequence and structure of a human glucose transporter. Science *229*, 941-945.

Muretta,J.M. and Mastick,C.C. (2009). How insulin regulates glucose transport in adipocytes. Vitam. Horm. *80*, 245-286.

Muretta,J.M., Romenskaia,I., and Mastick,C.C. (2008). Insulin releases Glut4 from static storage compartments into cycling endosomes and increases the rate constant for Glut4 exocytosis. J Biol. Chem. *283*, 311-323.

Myers,M.G., Jr., Wang,L.M., Sun,X.J., Zhang,Y., Yenush,L., Schlessinger,J., Pierce,J.H., and White,M.F. (1994). Role of IRS-1-GRB-2 complexes in insulin signaling. Mol. Cell Biol. *14*, 3577-3587.

Naslavsky,N. and Caplan,S. (2005). C-terminal EH-domain-containing proteins: consensus for a role in endocytic trafficking, EH? J Cell Sci. *118*, 4093-4101.

Naslavsky,N., Rahajeng,J., Sharma,M., Jovic,M., and Caplan,S. (2006). Interactions between EHD proteins and Rab11-FIP2: a role for EHD3 in early endosomal transport. Mol. Biol. Cell *17*, 163-177.

Ng,Y., Ramm,G., Burchfield,J.G., Coster,A.C., Stockli,J., and James,D.E. (2009). Cluster analysis of insulin action in adipocytes reveals a key role for Akt at the plasma membrane. J Biol. Chem.

Ng,Y., Ramm,G., Lopez,J.A., and James,D.E. (2008). Rapid activation of Akt2 is sufficient to stimulate GLUT4 translocation in 3T3-L1 adipocytes. Cell Metab *7*, 348-356.

Obata,T., Yaffe,M.B., Leparc,G.G., Piro,E.T., Maegawa,H., Kashiwagi,A., Kikkawa,R., and Cantley,L.C. (2000). Peptide and protein library screening defines optimal substrate motifs for AKT/PKB. J Biol. Chem. *275*, 36108-36115.

Okada,T., Kawano,Y., Sakakibara,T., Hazeki,O., and Ui,M. (1994). Essential role of phosphatidylinositol 3-kinase in insulin-induced glucose transport and antilipolysis in rat adipocytes. Studies with a selective inhibitor wortmannin. J Biol. Chem. *269*, 3568-3573.

Omata,W., Shibata,H., Li,L., Takata,K., and Kojima,I. (2000). Actin filaments play a critical role in insulin-induced exocytotic recruitment but not in endocytosis of GLUT4 in isolated rat adipocytes. Biochem. J *346 Pt 2*, 321-328.

Orci,L., Thorens,B., Ravazzola,M., and Lodish,H.F. (1989). Localization of the pancreatic beta cell glucose transporter to specific plasma membrane domains. Science *245*, 295-297.

Osborne,S.L., Wen,P.J., Boucheron,C., Nguyen,H.N., Hayakawa,M., Kaizawa,H., Parker,P.J., Vitale,N., and Meunier,F.A. (2008). PIKfyve negatively regulates exocytosis in neurosecretory cells. J Biol. Chem. *283*, 2804-2813.

Owen,M.R., Doran,E., and Halestrap,A.P. (2000). Evidence that metformin exerts its anti-diabetic effects through inhibition of complex 1 of the mitochondrial respiratory chain. Biochem. J *348 Pt 3*, 607-614.

Palacios,S., Lalioti,V., Martinez-Arca,S., Chattopadhyay,S., and Sandoval,I.V. (2001). Recycling of the insulin-sensitive glucose transporter GLUT4. Access of surface internalized GLUT4 molecules to the perinuclear storage compartment is mediated by the Phe5-Gln6-Gln7-Ile8 motif. J Biol. Chem. *276*, 3371-3383.

Park,C.R. and Johnson,L.H. (1955). Effect of insulin on transport of glucose and galactose into cells of rat muscle and brain. Am J Physiol *182*, 17-23.

Park,S.Y., Ha,B.G., Choi,G.H., Ryu,J., Kim,B., Jung,C.Y., and Lee,W. (2004). EHD2 interacts with the insulin-responsive glucose transporter (GLUT4) in rat adipocytes and may participate in insulin-induced GLUT4 recruitment. Biochemistry *43*, 7552-7562.

Patel,N., Rudich,A., Khayat,Z.A., Garg,R., and Klip,A. (2003). Intracellular segregation of phosphatidylinositol-3,4,5-trisphosphate by insulin-dependent actin remodeling in L6 skeletal muscle cells. Mol. Cell Biol. *23*, 4611-4626.

Paz,K., Voliovitch,H., Hadari,Y.R., Roberts,C.T., Jr., LeRoith,D., and Zick,Y. (1996). Interaction between the insulin receptor and its downstream effectors. Use of individually expressed receptor domains for structure/function analysis. J Biol. Chem. *271*, 6998-7003.

Peck,G.R., Chavez,J.A., Roach,W.G., Budnik,B.A., Lane,W.S., Karlsson,H.K., Zierath,J.R., and Lienhard,G.E. (2009). Insulin-stimulated phosphorylation of the rab GTPase activating protein TBC1D1 regulates GLUT4 translocation. J Biol. Chem.

Peck,G.R., Ye,S., Pham,V., Fernando,R.N., Macaulay,S.L., Chai,S.Y., and Albiston,A.L. (2006). Interaction of the Akt substrate, AS160, with the glucose transporter 4 vesicle marker protein, insulin-regulated aminopeptidase. Mol. Endocrinol. *20*, 2576-2583.

Pehmoller,C., Treebak,J.T., Birk,J.B., Chen,S., Mackintosh,C., Hardie,D.G., Richter,E.A., and Wojtaszewski,J.F. (2009). Genetic disruption of AMPK signaling abolishes both contraction- and insulin-stimulated TBC1D1 phosphorylation and 14-3-3 binding in mouse skeletal muscle. Am J Physiol Endocrinol. Metab *297*, E665-E675.

Permutt,M.A., Kakita,K., Malinas,P., Karl,I., Bonner-Weir,S., Weir,G., and Giddings,S.J. (1984). An in vivo analysis of pancreatic protein and insulin biosynthesis in a rat model for non-insulin-dependent diabetes. J Clin. Invest *73*, 1344-1350.

Piper,R.C., Tai,C., Kulesza,P., Pang,S., Warnock,D., Baenziger,J., Slot,J.W., Geuze,H.J., Puri,C., and James,D.E. (1993). GLUT-4 NH2 terminus contains a phenylalanine-based targeting motif that regulates intracellular sequestration. J Cell Biol. *121*, 1221-1232.

Ploug,T., van Deurs,B., Ai,H., Cushman,S.W., and Ralston,E. (1998). Analysis of GLUT4 distribution in whole skeletal muscle fibers: identification of distinct storage compartments that are recruited by insulin and muscle contractions. J Cell Biol. *142*, 1429-1446.

Pryor,P.R., Liu,S.C., Clark,A.E., Yang,J., Holman,G.D., and Tosh,D. (2000). Chronic insulin effects on insulin signalling and GLUT4 endocytosis are reversed by metformin. Biochem. J *348 Pt 1*, 83-91.

Ralston,E. and Ploug,T. (1996). GLUT4 in cultured skeletal myotubes is segregated from the transferrin receptor and stored in vesicles associated with TGN. J Cell Sci. *109 (Pt 13)*, 2967-2978.

Ramm,G., Larance,M., Guilhaus,M., and James,D.E. (2006). A role for 14-3-3 in insulin-stimulated GLUT4 translocation through its interaction with the RabGAP AS160. J Biol. Chem. *281*, 29174-29180.

Randhawa,V.K., Bilan,P.J., Khayat,Z.A., Daneman,N., Liu,Z., Ramlal,T., Volchuk,A., Peng,X.R., Coppola,T., Regazzi,R., Trimble,W.S., and Klip,A. (2000). VAMP2, but not VAMP3/cellubrevin, mediates insulin-dependent incorporation of GLUT4 into the plasma membrane of L6 myoblasts. Mol. Biol. Cell *11*, 2403-2417.

Randhawa,V.K., Ishikura,S., Talior-Volodarsky,I., Cheng,A.W., Patel,N., Hartwig,J.H., and Klip,A. (2008). GLUT4 vesicle recruitment and fusion are differentially regulated by Rac, AS160, and Rab8A in muscle cells. J Biol. Chem. *283*, 27208-27219.

Rea,S., Martin,L.B., McIntosh,S., Macaulay,S.L., Ramsdale,T., Baldini,G., and James,D.E. (1998). Syndet, an adipocyte target SNARE involved in the insulin-induced translocation of GLUT4 to the cell surface. J Biol. Chem. *273*, 18784-18792.

Reaven,G.M., Ho,H., and Hoffman,B.B. (1988). Attenuation of fructose-induced hypertension in rats by exercise training. Hypertension *12*, 129-132.

Ribon,V. and Saltiel,A.R. (1997). Insulin stimulates tyrosine phosphorylation of the proto-oncogene product of c-Cbl in 3T3-L1 adipocytes. Biochem. J *324 (Pt 3)*, 839-845.

Roach,W.G., Chavez,J.A., Miinea,C.P., and Lienhard,G.E. (2007). Substrate specificity and effect on GLUT4 translocation of the Rab GTPase-activating protein Tbc1d1. Biochem. J *403*, 353-358.

Robinson,L.J., Pang,S., Harris,D.S., Heuser,J., and James,D.E. (1992). Translocation of the glucose transporter (GLUT4) to the cell surface in permeabilized 3T3-L1 adipocytes: effects of ATP insulin, and GTP gamma S and localization of GLUT4 to clathrin lattices. J Cell Biol. *117*, 1181-1196.

Rodnick,K.J., Henriksen,E.J., James,D.E., and Holloszy,J.O. (1992a). Exercise training, glucose transporters, and glucose transport in rat skeletal muscles. Am J Physiol *262*, C9-14.

Rodnick,K.J., Slot,J.W., Studelska,D.R., Hanpeter,D.E., Robinson,L.J., Geuze,H.J., and James,D.E. (1992b). Immunocytochemical and biochemical studies of GLUT4 in rat skeletal muscle. J Biol. Chem. *267*, 6278-6285.

Rose,A.J., Alsted,T.J., Kobbero,J.B., and Richter,E.A. (2007). Regulation and function of Ca2+-calmodulin-dependent protein kinase II of fast-twitch rat skeletal muscle. J Physiol *580*, 993-1005.

Rose,A.J., Jeppesen,J., Kiens,B., and Richter,E.A. (2009). Effects of contraction on localization of GLUT4 and v-SNARE isoforms in rat skeletal muscle. Am J Physiol Regul. Integr. Comp Physiol.

Ross,S.A., Keller,S.R., and Lienhard,G.E. (1998). Increased intracellular sequestration of the insulin-regulated aminopeptidase upon differentiation of 3T3-L1 cells. Biochem. J *330 (Pt 2)*, 1003-1008.

Rossetti,L., Stenbit,A.E., Chen,W., Hu,M., Barzilai,N., Katz,E.B., and Charron,M.J. (1997). Peripheral but not hepatic insulin resistance in mice with one disrupted allele of the glucose transporter type 4 (GLUT4) gene. J Clin. Invest *100*, 1831-1839.

Rune,A., Osler,M.E., Fritz,T., and Zierath,J.R. (2009). Regulation of skeletal muscle sucrose, non-fermenting 1/AMP-activated protein kinase-related kinase (SNARK) by metabolic stress and diabetes. Diabetologia *52*, 2182-2189.

Rutherford,A.C., Traer,C., Wassmer,T., Pattni,K., Bujny,M.V., Carlton,J.G., Stenmark,H., and Cullen,P.J. (2006). The mammalian phosphatidylinositol 3-phosphate 5-kinase (PIKfyve) regulates endosome-to-TGN retrograde transport. J Cell Sci. *119*, 3944-3957.

Ryder,J.W., Yang,J., Galuska,D., Rincon,J., Bjornholm,M., Krook,A., Lund,S., Pedersen,O., Wallberg-Henriksson,H., Zierath,J.R., and Holman,G.D. (2000). Use of a novel impermeable biotinylated photolabeling reagent to assess insulin- and hypoxia-stimulated cell surface GLUT4 content in skeletal muscle from type 2 diabetic patients. Diabetes *49*, 647-654.

Sakamoto,K. and Holman,G.D. (2008). Emerging role for AS160/TBC1D4 and TBC1D1 in the regulation of GLUT4 traffic. Am J Physiol Endocrinol. Metab *295*, E29-E37.

Sakamoto,K., McCarthy,A., Smith,D., Green,K.A., Grahame,H.D., Ashworth,A., and Alessi,D.R. (2005). Deficiency of LKB1 in skeletal muscle prevents AMPK activation and glucose uptake during contraction. EMBO J *24*, 1810-1820.

Sanders,M.J., Grondin,P.O., Hegarty,B.D., Snowden,M.A., and Carling,D. (2007). Investigating the mechanism for AMP activation of the AMP-activated protein kinase cascade. Biochem. J *403*, 139-148.

Sano,H., Eguez,L., Teruel,M.N., Fukuda,M., Chuang,T.D., Chavez,J.A., Lienhard,G.E., and McGraw,T.E. (2007). Rab10, a target of the AS160 Rab GAP, is required for insulin-stimulated translocation of GLUT4 to the adipocyte plasma membrane. Cell Metab *5*, 293-303.

Sano,H., Kane,S., Sano,E., Miinea,C.P., Asara,J.M., Lane,W.S., Garner,C.W., and Lienhard,G.E. (2003). Insulin-stimulated phosphorylation of a Rab GTPase-activating protein regulates GLUT4 translocation. J Biol. Chem. *278*, 14599-14602.

Sano,H., Roach,W.G., Peck,G.R., Fukuda,M., and Lienhard,G.E. (2008). Rab10 in insulin-stimulated GLUT4 translocation. Biochem. J *411*, 89-95.

Sarbassov,D.D., Guertin,D.A., Ali,S.M., and Sabatini,D.M. (2005). Phosphorylation and regulation of Akt/PKB by the rictor-mTOR complex. Science *307*, 1098-1101.

Sasaoka,T., Fukui,K., Wada,T., Murakami,S., Kawahara,J., Ishihara,H., Funaki,M., Asano,T., and Kobayashi,M. (2005). Inhibition of endogenous SHIP2 ameliorates insulin resistance caused by chronic insulin treatment in 3T3-L1 adipocytes. Diabetologia *48*, 336-344.

Satoh,S., Nishimura,H., Clark,A.E., Kozka,I.J., Vannucci,S.J., Simpson,I.A., Quon,M.J., Cushman,S.W., and Holman,G.D. (1993). Use of bismannose photolabel to elucidate insulin-regulated GLUT4 subcellular trafficking kinetics in rat adipose cells. Evidence that exocytosis is a critical site of hormone action. J Biol. Chem. *268*, 17820-17829.

Scheepers,A., Joost,H.G., and Schurmann,A. (2004). The glucose transporter families SGLT and GLUT: molecular basis of normal and aberrant function. JPEN J Parenter. Enteral Nutr. *28*, 364-371.

Schertzer,J.D., Antonescu,C.N., Bilan,P.J., Jain,S., Huang,X., Liu,Z., Bonen,A., and Klip,A. (2009). A transgenic mouse model to study glucose transporter 4myc regulation in skeletal muscle. Endocrinology *150*, 1935-1940.

Scott,J.W., van Denderen,B.J., Jorgensen,S.B., Honeyman,J.E., Steinberg,G.R., Oakhill,J.S., Iseli,T.J., Koay,A., Gooley,P.R., Stapleton,D., and Kemp,B.E. (2008). Thienopyridone drugs are selective activators of AMP-activated protein kinase beta1-containing complexes. Chem. Biol. *15*, 1220-1230.

Shaw,R.J., Lamia,K.A., Vasquez,D., Koo,S.H., Bardeesy,N., Depinho,R.A., Montminy,M., and Cantley,L.C. (2005). The kinase LKB1 mediates glucose homeostasis in liver and therapeutic effects of metformin. Science *310*, 1642-1646.

Shepherd,P.R., Gnudi,L., Tozzo,E., Yang,H., Leach,F., and Kahn,B.B. (1993). Adipose cell hyperplasia and enhanced glucose disposal in transgenic mice overexpressing GLUT4 selectively in adipose tissue. J Biol. Chem. *268*, 22243-22246.

Shepherd,P.R., Withers,D.J., and Siddle,K. (1998). Phosphoinositide 3-kinase: the key switch mechanism in insulin signalling. Biochem. J *333 (Pt 3)*, 471-490.

Shewan,A.M., Marsh,B.J., Melvin,D.R., Martin,S., Gould,G.W., and James,D.E. (2000). The cytosolic C-terminus of the glucose transporter GLUT4 contains an acidic cluster endosomal targeting motif distal to the dileucine signal. Biochem. J *350 Pt 1*, 99-107.

Shewan,A.M., van Dam,E.M., Martin,S., Luen,T.B., Hong,W., Bryant,N.J., and James,D.E. (2003). GLUT4 recycles via a trans-Golgi network (TGN) subdomain enriched in Syntaxins 6 and 16 but not TGN38: involvement of an acidic targeting motif. Mol. Biol. Cell *14*, 973-986.

Shi,J. and Kandror,K.V. (2007). The luminal Vps10p domain of sortilin plays the predominant role in targeting to insulin-responsive Glut4-containing vesicles. J Biol. Chem. *282*, 9008-9016.

Shiba,T., Takatsu,H., Nogi,T., Matsugaki,N., Kawasaki,M., Igarashi,N., Suzuki,M., Kato,R., Earnest,T., Nakayama,K., and Wakatsuki,S. (2002). Structural basis for recognition of acidic-cluster dileucine sequence by GGA1. Nature *415*, 937-941.

Shigematsu,S., Khan,A.H., Kanzaki,M., and Pessin,J.E. (2002). Intracellular insulin-responsive glucose transporter (GLUT4) distribution but not insulin-stimulated GLUT4 exocytosis and recycling are microtubule dependent. Mol. Endocrinol. *16*, 1060-1068.

Shisheva,A., Rusin,B., Ikonomov,O.C., DeMarco,C., and Sbrissa,D. (2001). Localization and insulin-regulated relocation of phosphoinositide 5-kinase PIKfyve in 3T3-L1 adipocytes. J Biol. Chem. *276*, 11859-11869.

Shoelson,S.E., Chatterjee,S., Chaudhuri,M., and White,M.F. (1992). YMXM motifs of IRS-1 define substrate specificity of the insulin receptor kinase. Proc. Natl. Acad. Sci. U. S. A *89*, 2027-2031.

Shojaiefard,M., Strutz-Seebohm,N., Tavare,J.M., Seebohm,G., and Lang,F. (2007). Regulation of the Na(+), glucose cotransporter by PIKfyve and the serum and glucocorticoid inducible kinase SGK1. Biochem. Biophys. Res. Commun. *359*, 843-847.

Slot,J.W., Garruti,G., Martin,S., Oorschot,V., Posthuma,G., Kraegen,E.W., Laybutt,R., Thibault,G., and James,D.E. (1997). Glucose transporter (GLUT-4) is targeted to secretory granules in rat atrial cardiomyocytes. J Cell Biol. *137*, 1243-1254.

Slot,J.W., Geuze,H.J., Gigengack,S., James,D.E., and Lienhard,G.E. (1991a). Translocation of the glucose transporter GLUT4 in cardiac myocytes of the rat. Proc. Natl. Acad. Sci. U. S. A *88*, 7815-7819.

Slot,J.W., Geuze,H.J., Gigengack,S., Lienhard,G.E., and James,D.E. (1991b). Immuno-localization of the insulin regulatable glucose transporter in brown adipose tissue of the rat. J Cell Biol. *113*, 123-135.

Smith,R.M., Charron,M.J., Shah,N., Lodish,H.F., and Jarett,L. (1991). Immunoelectron microscopic demonstration of insulin-stimulated translocation of glucose transporters to the plasma membrane of isolated rat adipocytes and masking of the carboxyl-terminal epitope of intracellular GLUT4. Proc. Natl. Acad. Sci. U. S. A *88*, 6893-6897.

Soeller,C. and Cannell,M.B. (1999). Examination of the transverse tubular system in living cardiac rat myocytes by 2-photon microscopy and digital image-processing techniques. Circ. Res. *84*, 266-275.

Song,X.M., Fiedler,M., Galuska,D., Ryder,J.W., Fernstrom,M., Chibalin,A.V., Wallberg-Henriksson,H., and Zierath,J.R. (2002). 5-Aminoimidazole-4-carboxamide ribonucleoside treatment improves glucose homeostasis in insulin-resistant diabetic (ob/ob) mice. Diabetologia *45*, 56-65.

Standaert,M.L., Bandyopadhyay,G., Kanoh,Y., Sajan,M.P., and Farese,R.V. (2001). Insulin and PIP3 activate PKC-zeta by mechanisms that are both dependent and independent of phosphorylation of activation loop (T410) and autophosphorylation (T560) sites. Biochemistry *40*, 249-255.

Standaert,M.L., Sajan,M.P., Miura,A., Kanoh,Y., Chen,H.C., Farese,R.V., Jr., and Farese,R.V. (2004). Insulin-induced activation of atypical protein kinase C, but not protein kinase B, is maintained in diabetic (ob/ob and Goto-Kakazaki) liver. Contrasting insulin signaling patterns in liver versus muscle define phenotypes of type 2 diabetic and high fat-induced insulin-resistant states. J Biol. Chem. *279*, 24929-24934.

Stenbit,A.E., Tsao,T.S., Li,J., Burcelin,R., Geenen,D.L., Factor,S.M., Houseknecht,K., Katz,E.B., and Charron,M.J. (1997). GLUT4 heterozygous knockout mice develop muscle insulin resistance and diabetes. Nat. Med. *3*, 1096-1101.

Stockli,J., Davey,J.R., Hohnen-Behrens,C., Xu,A., James,D.E., and Ramm,G. (2008). Regulation of glucose transporter 4 translocation by the Rab guanosine triphosphatase-activating protein AS160/TBC1D4: role of phosphorylation and membrane association. Mol. Endocrinol. *22*, 2703-2715.

Stone,S., Abkevich,V., Russell,D.L., Riley,R., Timms,K., Tran,T., Trem,D., Frank,D., Jammulapati,S., Neff,C.D., Iliev,D., Gress,R., He,G., Frech,G.C., Adams,T.D., Skolnick,M.H., Lanchbury,J.S., Gutin,A., Hunt,S.C., and Shattuck,D. (2006). TBC1D1 is a candidate for a severe obesity gene and evidence for a gene/gene interaction in obesity predisposition. Hum. Mol. Genet. *15*, 2709-2720.

Strutz-Seebohm,N., Shojaiefard,M., Christie,D., Tavare,J., Seebohm,G., and Lang,F. (2007). PIKfyve in the SGK1 mediated regulation of the creatine transporter SLC6A8. Cell Physiol Biochem. *20*, 729-734.

Stuart,C.A., Howell,M.E., Zhang,Y., and Yin,D. (2009). Insulin-stimulated translocation of glucose transporter (GLUT) 12 parallels that of GLUT4 in normal muscle. J Clin. Endocrinol. Metab *94*, 3535-3542.

Stumvoll,M., Nurjhan,N., Perriello,G., Dailey,G., and Gerich,J.E. (1995). Metabolic effects of metformin in non-insulin-dependent diabetes mellitus. N. Engl. J Med. *333*, 550-554.

Sun,X.J., Miralpeix,M., Myers,M.G., Jr., Glasheen,E.M., Backer,J.M., Kahn,C.R., and White,M.F. (1992). Expression and function of IRS-1 in insulin signal transmission. J Biol. Chem. *267*, 22662-22672.

Suter,M., Riek,U., Tuerk,R., Schlattner,U., Wallimann,T., and Neumann,D. (2006). Dissecting the role of 5'-AMP for allosteric stimulation, activation, and deactivation of AMP-activated protein kinase. J Biol. Chem. *281*, 32207-32216.

Suzuki,K. and Kono,T. (1980). Evidence that insulin causes translocation of glucose transport activity to the plasma membrane from an intracellular storage site. Proc. Natl. Acad. Sci. U. S. A *77*, 2542-2545.

Sweeney,G., Garg,R.R., Ceddia,R.B., Li,D., Ishiki,M., Somwar,R., Foster,L.J., Neilsen,P.O., Prestwich,G.D., Rudich,A., and Klip,A. (2004). Intracellular delivery of phosphatidylinositol (3,4,5)-trisphosphate causes incorporation of glucose transporter 4 into the plasma membrane of muscle and fat cells without increasing glucose uptake. J Biol. Chem. *279*, 32233-32242.

Takei,K. and Haucke,V. (2001). Clathrin-mediated endocytosis: membrane factors pull the trigger. Trends Cell Biol. *11*, 385-391.

Talior-Volodarsky,I., Randhawa,V.K., Zaid,H., and Klip,A. (2008). Alpha-actinin-4 is selectively required for insulin-induced GLUT4 translocation. J Biol. Chem. *283*, 25115-25123.

Tamemoto,H., Izumi,T., Kaburagi,Y., Terauchi,Y., Tobe,K., and Kadowaki,T. (1998). [IRS-1 knockout mouse]. Nippon Rinsho *56 Suppl 3*, 738-745.

Tanner,L.I. and Lienhard,G.E. (1987). Insulin elicits a redistribution of transferrin receptors in 3T3-L1 adipocytes through an increase in the rate constant for receptor externalization. J Biol. Chem. *262*, 8975-8980.

Taylor,E.B., An,D., Kramer,H.F., Yu,H., Fujii,N.L., Roeckl,K.S., Bowles,N., Hirshman,M.F., Xie,J., Feener,E.P., and Goodyear,L.J. (2008). Discovery of TBC1D1 as an insulin-, AICAR-, and contraction-stimulated signaling nexus in mouse skeletal muscle. J Biol. Chem. *283*, 9787-9796.

Thong,F.S., Bilan,P.J., and Klip,A. (2007). The Rab GTPase-activating protein AS160 integrates Akt, protein kinase C, and AMP-activated protein kinase signals regulating GLUT4 traffic. Diabetes *56*, 414-423.

Thorell,A., Hirshman,M.F., Nygren,J., Jorfeldt,L., Wojtaszewski,J.F., Dufresne,S.D., Horton,E.S., Ljungqvist,O., and Goodyear,L.J. (1999). Exercise and insulin cause GLUT-4 translocation in human skeletal muscle. Am J Physiol *277*, E733-E741.

Thorens,B., Cheng,Z.Q., Brown,D., and Lodish,H.F. (1990). Liver glucose transporter: a basolateral protein in hepatocytes and intestine and kidney cells. Am J Physiol *259*, C279-C285.

Thorens,B., Gerard,N., and Deriaz,N. (1993). GLUT2 surface expression and intracellular transport via the constitutive pathway in pancreatic beta cells and insulinoma: evidence for a block in trans-Golgi network exit by brefeldin A. J Cell Biol. *123*, 1687-1694.

Thorens,B., Sarkar,H.K., Kaback,H.R., and Lodish,H.F. (1988). Cloning and functional expression in bacteria of a novel glucose transporter present in liver, intestine, kidney, and beta-pancreatic islet cells. Cell *55*, 281-290.

Timmers,K.I., Clark,A.E., Omatsu-Kanbe,M., Whiteheart,S.W., Bennett,M.K., Holman,G.D., and Cushman,S.W. (1996). Identification of SNAP receptors in rat adipose cell membrane fractions and in SNARE complexes co-immunoprecipitated with epitope-tagged N-ethylmaleimide-sensitive fusion protein. Biochem. J *320 (Pt 2)*, 429-436.

Treebak,J.T., Birk,J.B., Hansen,B.F., Olsen,G.S., and Wojtaszewski,J.F. (2009a). A-769662 activates AMPK {beta}1-containing complexes but induces glucose uptake through a PI3 kinase-dependent pathway in mouse skeletal muscle. Am J Physiol Cell Physiol.

Treebak,J.T., Glund,S., Deshmukh,A., Klein,D.K., Long,Y.C., Jensen,T.E., Jorgensen,S.B., Viollet,B., Andersson,L., Neumann,D., Wallimann,T., Richter,E.A., Chibalin,A.V., Zierath,J.R., and Wojtaszewski,J.F. (2006). AMPK-mediated AS160 phosphorylation in skeletal muscle is dependent on AMPK catalytic and regulatory subunits. Diabetes *55*, 2051-2058.

Treebak,J.T., Taylor,E.B., Witczak,C.A., An,D., Toyoda,T., Koh,H.J., Xie,J., Feener,E.P., Wojtaszewski,J.F., Hirshman,M.F., and Goodyear,L.J. (2009b). Identification of a novel phosphorylation site on TBC1D4 regulated by AMP-activated protein kinase in skeletal muscle. Am J Physiol Cell Physiol.

Tsao,T.S., Burcelin,R., Katz,E.B., Huang,L., and Charron,M.J. (1996). Enhanced insulin action due to targeted GLUT4 overexpression exclusively in muscle. Diabetes *45*, 28-36.

Tsao,T.S., Li,J., Chang,K.S., Stenbit,A.E., Galuska,D., Anderson,J.E., Zierath,J.R., McCarter,R.J., and Charron,M.J. (2001). Metabolic adaptations in skeletal muscle overexpressing GLUT4: effects on muscle and physical activity. FASEB J *15*, 958-969.

Tzahar,E., Waterman,H., Chen,X., Levkowitz,G., Karunagaran,D., Lavi,S., Ratzkin,B.J., and Yarden,Y. (1996). A hierarchical network of interreceptor interactions determines signal transduction by Neu differentiation factor/neuregulin and epidermal growth factor. Mol. Cell Biol. *16*, 5276-5287.

Ueki,K., Kondo,T., and Kahn,C.R. (2004). Suppressor of cytokine signaling 1 (SOCS-1) and SOCS-3 cause insulin resistance through inhibition of tyrosine phosphorylation of insulin receptor substrate proteins by discrete mechanisms. Mol. Cell Biol. *24*, 5434-5446.

Usui,I., Imamura,T., Huang,J., Satoh,H., and Olefsky,J.M. (2003). Cdc42 is a Rho GTPase family member that can mediate insulin signaling to glucose transport in 3T3-L1 adipocytes. J Biol. Chem. *278*, 13765-13774.

van Dam,E.M., Govers,R., and James,D.E. (2005). Akt activation is required at a late stage of insulin-induced GLUT4 translocation to the plasma membrane. Mol. Endocrinol. *19*, 1067-1077.

van der Bliek,A.M., Redelmeier,T.E., Damke,H., Tisdale,E.J., Meyerowitz,E.M., and Schmid,S.L. (1993). Mutations in human dynamin block an intermediate stage in coated vesicle formation. J Cell Biol. *122*, 553-563.

van Oort,M.M., van Doorn,J.M., Hasnaoui,M.E., Glatz,J.F., Bonen,A., van der Horst,D.J., Rodenburg,K.W., and JJ,P.L. (2009). Effects of AMPK activators on the sub-cellular distribution of fatty acid transporters CD36 and FABPpm. Arch. Physiol Biochem. *115*, 137-146.

Vanhaesebroeck,B. and Alessi,D.R. (2000). The PI3K-PDK1 connection: more than just a road to PKB. Biochem. J *346 Pt 3*, 561-576.

Vanhaesebroeck,B., Leevers,S.J., Panayotou,G., and Waterfield,M.D. (1997). Phosphoinositide 3-kinases: a conserved family of signal transducers. Trends Biochem. Sci. *22*, 267-272.

Vassilopoulos,S., Esk,C., Hoshino,S., Funke,B.H., Chen,C.Y., Plocik,A.M., Wright,W.E., Kucherlapati,R., and Brodsky,F.M. (2009). A role for the CHC22 clathrin heavy-chain isoform in human glucose metabolism. Science *324*, 1192-1196.

Vatish,M., Yamada,E., Pessin,J.E., and Bastie,C.C. (2009). Fyn kinase function in lipid utilization: a new upstream regulator of AMPK activity? Arch. Physiol Biochem. *115*, 191-198.

Vincent,M.F., Erion,M.D., Gruber,H.E., and Van den,B.G. (1996). Hypoglycaemic effect of AICAriboside in mice. Diabetologia *39*, 1148-1155.

Virkamaki,A., Ueki,K., and Kahn,C.R. (1999). Protein-protein interaction in insulin signaling and the molecular mechanisms of insulin resistance. J Clin. Invest *103*, 931-943.

Volchuk,A., Narine,S., Foster,L.J., Grabs,D., De Camilli,P., and Klip,A. (1998). Perturbation of dynamin II with an amphiphysin SH3 domain increases GLUT4 glucose transporters at the plasma membrane in 3T3-L1 adipocytes. Dynamin II participates in GLUT4 endocytosis. J Biol. Chem. *273*, 8169-8176.

Vollenweider,P., Menard,B., and Nicod,P. (2002). Insulin resistance, defective insulin receptor substrate 2-associated phosphatidylinositol-3' kinase activation, and impaired atypical protein kinase C (zeta/lambda) activation in myotubes from obese patients with impaired glucose tolerance. Diabetes *51*, 1052-1059.

Wang,Q., Khayat,Z., Kishi,K., Ebina,Y., and Klip,A. (1998). GLUT4 translocation by insulin in intact muscle cells: detection by a fast and quantitative assay. FEBS Lett. *427*, 193-197.

Wang,Q., Somwar,R., Bilan,P.J., Liu,Z., Jin,J., Woodgett,J.R., and Klip,A. (1999). Protein kinase B/Akt participates in GLUT4 translocation by insulin in L6 myoblasts. Mol. Cell Biol. *19*, 4008-4018.

Wang,Y., Zhang,J., Chen,Y., Jiang,L., Ji,W., and Xu,T. (2009). Characterization of GLUT4-containing vesicles in 3T3-L1 adipocytes by total internal reflection fluorescence microscopy. Sci. China C. Life Sci. *52*, 665-671.

Warden,S.M., Richardson,C., O'Donnell,J., Jr., Stapleton,D., Kemp,B.E., and Witters,L.A. (2001). Post-translational modifications of the beta-1 subunit of AMP-activated protein kinase affect enzyme activity and cellular localization. Biochem. J *354*, 275-283.

Watson,R.T., Hou,J.C., and Pessin,J.E. (2008). Recycling of IRAP from the plasma membrane back to the insulin-responsive compartment requires the Q-SNARE syntaxin 6 but not the GGA clathrin adaptors. J Cell Sci. *121*, 1243-1251.

Watson,R.T., Khan,A.H., Furukawa,M., Hou,J.C., Li,L., Kanzaki,M., Okada,S., Kandror,K.V., and Pessin,J.E. (2004). Entry of newly synthesized GLUT4 into the insulin-responsive storage compartment is GGA dependent. EMBO J *23*, 2059-2070.

Welsh,G.I., Leney,S.E., Lloyd-Lewis,B., Wherlock,M., Lindsay,A.J., McCaffrey,M.W., and Tavare,J.M. (2007). Rip11 is a Rab11- and AS160-RabGAP-binding protein required for insulin-stimulated glucose uptake in adipocytes. J Cell Sci. *120*, 4197-4208.

White,M.F. and Yenush,L. (1998). The IRS-signaling system: a network of docking proteins that mediate insulin and cytokine action. Curr. Top. Microbiol. Immunol. *228*, 179-208.

Widberg,C.H., Bryant,N.J., Girotti,M., Rea,S., and James,D.E. (2003). Tomosyn interacts with the t-SNAREs syntaxin4 and SNAP23 and plays a role in insulin-stimulated GLUT4 translocation. J Biol. Chem. *278*, 35093-35101.

Wijesekara,N., Konrad,D., Eweida,M., Jefferies,C., Liadis,N., Giacca,A., Crackower,M., Suzuki,A., Mak,T.W., Kahn,C.R., Klip,A., and Woo,M. (2005). Muscle-specific Pten deletion protects against insulin resistance and diabetes. Mol. Cell Biol. *25*, 1135-1145.

Wijesekara,N., Tung,A., Thong,F., and Klip,A. (2006). Muscle cell depolarization induces a gain in surface GLUT4 via reduced endocytosis independently of AMPK. Am J Physiol Endocrinol. Metab *290*, E1276-E1286.

Winder,W.W. and Hardie,D.G. (1999). AMP-activated protein kinase, a metabolic master switch: possible roles in type 2 diabetes. Am J Physiol *277*, E1-10.

Witczak,C.A., Fujii,N., Hirshman,M.F., and Goodyear,L.J. (2007). Ca2+/calmodulin-dependent protein kinase kinase-alpha regulates skeletal muscle glucose uptake independent of AMP-activated protein kinase and Akt activation. Diabetes *56*, 1403-1409.

Withers,D.J., Gutierrez,J.S., Towery,H., Burks,D.J., Ren,J.M., Previs,S., Zhang,Y., Bernal,D., Pons,S., Shulman,G.I., Bonner-Weir,S., and White,M.F. (1998). Disruption of IRS-2 causes type 2 diabetes in mice. Nature *391*, 900-904.

Wojtaszewski,J.F., Hansen,B.F., Urso,B., and Richter,E.A. (1996). Wortmannin inhibits both insulin- and contraction-stimulated glucose uptake and transport in rat skeletal muscle. J Appl. Physiol *81*, 1501-1509.

Wolf,G., Trub,T., Ottinger,E., Groninga,L., Lynch,A., White,M.F., Miyazaki,M., Lee,J., and Shoelson,S.E. (1995). PTB domains of IRS-1 and Shc have distinct but overlapping binding specificities. J Biol. Chem. *270*, 27407-27410.

Woods,A., Dickerson,K., Heath,R., Hong,S.P., Momcilovic,M., Johnstone,S.R., Carlson,M., and Carling,D. (2005). Ca2+/calmodulin-dependent protein kinase kinase-beta acts upstream of AMP-activated protein kinase in mammalian cells. Cell Metab *2*, 21-33.

Woods,A., Johnstone,S.R., Dickerson,K., Leiper,F.C., Fryer,L.G., Neumann,D., Schlattner,U., Wallimann,T., Carlson,M., and Carling,D. (2003a). LKB1 is the upstream kinase in the AMP-activated protein kinase cascade. Curr. Biol. *13*, 2004-2008.

Woods,A., Vertommen,D., Neumann,D., Turk,R., Bayliss,J., Schlattner,U., Wallimann,T., Carling,D., and Rider,M.H. (2003b). Identification of phosphorylation sites in AMP-activated protein kinase (AMPK) for upstream AMPK kinases and study of their roles by site-directed mutagenesis. J Biol. Chem. *278*, 28434-28442.

Wright,D.C., Geiger,P.C., Holloszy,J.O., and Han,D.H. (2005). Contraction- and hypoxia-stimulated glucose transport is mediated by a Ca2+-dependent mechanism in slow-twitch rat soleus muscle. Am J Physiol Endocrinol. Metab *288*, E1062-E1066.

Wright,D.C., Hucker,K.A., Holloszy,J.O., and Han,D.H. (2004). Ca2+ and AMPK both mediate stimulation of glucose transport by muscle contractions. Diabetes *53*, 330-335.

Xu,Y.K., Xu,K.D., Li,J.Y., Feng,L.Q., Lang,D., and Zheng,X.X. (2007). Bi-directional transport of GLUT4 vesicles near the plasma membrane of primary rat adipocytes. Biochem. Biophys. Res. Commun. *359*, 121-128.

Yamada,E., Okada,S., Saito,T., Ohshima,K., Sato,M., Tsuchiya,T., Uehara,Y., Shimizu,H., and Mori,M. (2005). Akt2 phosphorylates Synip to regulate docking and fusion of GLUT4-containing vesicles. J Cell Biol. *168*, 921-928.

Yang,J., Clark,A.E., Harrison,R., Kozka,I.J., and Holman,G.D. (1992). Trafficking of glucose transporters in 3T3-L1 cells. Inhibition of trafficking by phenylarsine oxide implicates a slow dissociation of transporters from trafficking proteins. Biochem. J *281 (Pt 3)*, 809-817.

Yang,J., Gillingham,A.K., Hodel,A., Koumanov,F., Woodward,B., and Holman,G.D. (2002). Insulin-stimulated cytosol alkalinization facilitates optimal activation of glucose transport in cardiomyocytes. Am J Physiol Endocrinol. Metab *283*, E1299-E1307.

Yang,J. and Holman,G.D. (1993). Comparison of GLUT4 and GLUT1 subcellular trafficking in basal and insulin-stimulated 3T3-L1 cells. J Biol. Chem. *268*, 4600-4603.

Yang,J. and Holman,G.D. (2005). Insulin and contraction stimulate exocytosis, but increased AMP-activated protein kinase activity resulting from oxidative metabolism stress slows endocytosis of GLUT4 in cardiomyocytes. J Biol. Chem. *280*, 4070-4078.

Yang,J. and Holman,G.D. (2006). Long-term metformin treatment stimulates cardiomyocyte glucose transport through an AMP-activated protein kinase-dependent reduction in GLUT4 endocytosis. Endocrinology *147*, 2728-2736.

Yeh,T.Y., Sbodio,J.I., Tsun,Z.Y., Luo,B., and Chi,N.W. (2007). Insulin-stimulated exocytosis of GLUT4 is enhanced by IRAP and its partner tankyrase. Biochem. J *402*, 279-290.

Yip,M.F., Ramm,G., Larance,M., Hoehn,K.L., Wagner,M.C., Guilhaus,M., and James,D.E. (2008). CaMKII-mediated phosphorylation of the myosin motor Myo1c is required for insulin-stimulated GLUT4 translocation in adipocytes. Cell Metab *8*, 384-398.

Zeigerer,A., Lampson,M.A., Karylowski,O., Sabatini,D.D., Adesnik,M., Ren,M., and McGraw,T.E. (2002). GLUT4 retention in adipocytes requires two intracellular insulin-regulated transport steps. Mol. Biol. Cell *13*, 2421-2435.

Zhao,P., Yang,L., Lopez,J.A., Fan,J., Burchfield,J.G., Bai,L., Hong,W., Xu,T., and James,D.E. (2009). Variations in the requirement for v-SNAREs in GLUT4 trafficking in adipocytes. J Cell Sci. *122*, 3472-3480.

Zhou,Q.L., Park,J.G., Jiang,Z.Y., Holik,J.J., Mitra,P., Semiz,S., Guilherme,A., Powelka,A.M., Tang,X., Virbasius,J., and Czech,M.P. (2004). Analysis of insulin signalling by RNAi-based gene silencing. Biochem. Soc. Trans. *32*, 817-821.

Zimmet,P. and Alberti,G. (2008). The metabolic syndrome: progress towards one definition for an epidemic of our time. Nat. Clin. Pract. Endocrinol. Metab *4*, 239.